Pollen Tube Reception in the Synergid Cells of *Arabidopsis thaliana* – Novel Players and Old Acquaintances

Dissertation

zur

Erlangung der naturwissenschaftlichen Doktorwürde
(Dr. sc. nat.)

vorgelegt der

Mathematisch-naturwissenschaftlichen Fakultät

der

Universität Zürich

von

Heike Lindner

aus

Deutschland

Promotionskomitee

Prof. Dr. Ueli Grossniklaus (Vorsitz und Leitung der Dissertation)

Prof. Dr. Beat Keller

Prof. Dr. Thomas Dresselhaus

Zürich, 2014

To Doreen

ACKNOWLEDGMENTS

First of all, I would like to thank **Ueli Grossniklaus** for giving me the opportunity to do my PhD in his department and for creating such a nice working atmosphere. I am grateful for his guidance, helpful discussions and great ideas.

Furthermore, I want to thank **Prof. Dr. Beat Keller** (University of Zurich) and **Prof. Dr. Thomas Dresselhaus** (University of Regensburg) for being part of my thesis committee, for reading and evaluating my thesis and for being co-examiners during my PhD defense.

Then, I would like to thank **Sharon Kessler** for being my supervisor, for teaching me basically all the *Arabidopsis* work, and even more importantly, for teaching me being a scientist. I am very grateful for all the scientific discussions, for ideas and suggestions, for encouraging me in frustrating times and last but not least, for becoming such a good friend of mine!

I especially thank **Michael Raissig**. Thank you for believing in me, for encouraging me, for supporting me, for discussing with me and most importantly for loving me and backing me up during rough times.

A special thanks is directed to **Lena Müller** for very helpful discussions, for good ideas, for being a great friend and for being my identical twin ;-).

I would like to thank **Aurelien Boisson-Dernier** for very helpful pollen discussions, for having some brain cramps with me and for being a good friend.

I thank the sex club (**Anna**, **Evelyne**, **Nadine**, **Lena**, **Mo** and **Aurel** (and **Sharon**)) for great scientific discussions every other week and fun times.

Furthermore, I am grateful to **Valeria Gagliardini** for her help during the daily lab business and for always having an open ear in difficult times.

I would like to thank my lab (P2-39: **Mo**, **Polly**, **Nina**, **Joana**, **Nuno**, **Kostas**, **Roger**, **Valeria**, **Fred**, **Alain**, **Sharon**, **Luk**, **Arco**, and last but not least **Marek** and **Johan**) for a great working atmosphere and for fun times!

For technical support I thank **Valeria** for clubbing, **Daniela** for sequencing, **Arturo** for ordering, **Christof** for microscopy and **Peter** for solutions and saving us a lot of time by washing and autoclaving.

Very importantly, I thank a lot of people for their friendship! For chats, for drinks, for parties, for going to the lake and for creating such a great working atmosphere: **Debo** (my Schneeboli and best friend!), **Lena** (Leeenchen!), **Michi**, **Kostas**, **Stefan**, **Daniela**, **Evelyne**, **Mo**, **Aurel**, **Christian S.**, **Milka**, **Sharon**, **Heike W.**, **Johan**, **Marek**, **Anna**, **Valeria**, **Nuno**, **Joana**, **Nina**, **Polly**, **Fred**, **Alain**, **Sam**, **Anja H.**, **Wenjing**, **Quy**, **Mark**, **Anja S.**, **Dima L.**, **Dima S.**, **Bruno**, **Célia**, **Christof**, **Arturo**, **Marian**, **Bobi**, **Christina**, **Afif**, **Hannes**, **Wanhui**, **Stefan W.**, **Guillaume**, **Sibylle**, **Michael**, **Klara**, **Nadine**, **Christian H.**, **Hampe** and **Annegret**.

Furthermore, I would like to thank **my parents** for their love and support. I am also grateful to **Frau Wolf** for everything. A very special thank-you is directed to my sister **Doreen**. I am very grateful for our unique relationship, for your support, for your love, for your guidance and for being the best sister and most importantly best friend!

ABSTRACT

Pollen tube (PT) reception by the synergid cells of the female gametophyte is essential for successful double fertilization of the egg and the central cell. It is controlled by an active signaling pathway in the synergid cells, involving the receptor-like kinase (RLK) FERONIA (FER), the MILDEW RESISTANCE LOCUS O (MLO) family member NORTIA (NTA) and the Glycosyl-phosphatidylinositol (GPI)-anchored protein LORELEI (LRE). Although those proteins were found to mediate PT reception, still little is known about protein interactions and signaling cascades leading to PT growth arrest, PT rupture and sperm release.

Therefore, we conducted a forward genetic screen for the *fer*-like PT overgrowth phenotype, which is characteristic for defects in PT reception. This screen yielded two promising mutant candidates, which were named after two Etruscan goddesses of fertility and fate, namely *turan* (*tun*) and *evan* (*evn*). A newly developed method allowing the mapping of heterozygous mutations by next-generation sequencing identified *TUN* to encode a putative UDP-glycosyltransferase superfamily protein and *EVN* to encode a putative dolichol kinase. Interestingly, both predicted gene functions indicate an involvement during protein N-glycosylation in the endoplasmic reticulum (ER). In addition to the role of *TUN* and *EVN* in mediating PT reception, both proteins play distinct functions in the pollen. Whereas EVN is essential for pollen development, TUN is crucial for PT growth/integrity perhaps by affecting the PT plasma-membrane-localized RLK, ANXUR1 (ANX1), which was shown to prevent early PT rupture.

In addition to the identification of novel members of the PT reception pathway in the synergids, we aimed to find genetic interactors of *FER*. Accordingly, a suppressor screen for *fer*-induced phenotypes was conducted, but unfortunately yielded no promising candidate.

Finally, functional domain analysis of the three *Catharantus roseus* receptor-like Serine/Threonine kinase 1-like subfamily (CrRLK1L) members FERONIA, ANXUR1 and HERCULES1 (HERK1), revealed common downstream targets, but distinct upstream pathways. In addition, we found that the intracellular kinase domain but not kinase activity is required for PT reception.

Together, we indentified two novel members of the PT reception pathway in the synergid cells, which play additional but distinct roles in the pollen. Furthermore, we found functional domain similarities among three CrRLK1L family members potentially sharing downstream factors.

ZUSAMMENFASSUNG

Pollenschlauchempfang durch die Synergidenzellen des weiblichen Gametophyten ist essentiell für die doppelte Befruchtung der Eizelle und der Zentralzelle und somit für erfolgreiche Reproduktion. Pollenschlauchempfang wird durch eine aktive Signalkaskade in den Synergiden kontrolliert, welche die rezeptor-ähnliche Kinase FERONIA (FER), den Mehltauresistenzlokus O (MLO) Faktor NORTIA (NTA) und das Glycosylphosphatidylinositol (GPI)-verankerte Protein LORELEI (LRE) involviert. Die genauen molekularen Mechanismen, wie Proteininteraktionen und Signalkaskaden, die letztendlich zum Wachstumsstopp des Pollen, zum Platzen des Pollenschlauchs und der damit verbundene Spermienabgabe führen, sind jedoch nach wie vor unbekannt.

Aufgrund dessen wurde eine genetische Untersuchung von mutagenisierten Pflanzen durchgeführt und nach Kandidaten gesucht, die kontinuierliches Pollenschlauchwachstum im weiblichen Gametophyten zeigen. Wir konnten zwei vielversprechende Kandidaten identifizieren, welche den entsprechenden Phänotyp zeigen. Beide Mutanten wurden nach zwei etruskischen Fruchtbarkeits- und Schicksalsgöttinen benannt, *turan* (*tun*) and *evan* (*evn*) . Eine neu entwickelte Hochleistungssequenziermethode identifizierte TUN als vermeintliches UDP-Glycosyltransferase Superfamilienprotein and EVN als eine vermeintliche Dolicholkinase. Interessanterweise sind beide Gene potentiell an der N-Glykosylierung von Proteinen im Endoplasmatischen Retikulum (ER) beteiligt. Zusätzlich zu der Funktion beim Pollenschlauchempfang in den Synergiden übernehmen beide Proteine unterschiedliche Aufgaben im Pollen. EVN ist essentiell bei der Pollenentwicklung und TUN ist erforderlich für Pollenschlauchwachstum, womöglich durch einen Effekt auf den Pollen-spezifischen Faktor ANXUR1 (ANX1), der ein zu frühes Platzen des Pollenschlauchs verhindert.

Zusätzlich zu der Identifizierung von neuen Mitgliedern des Pollenschlauchempfangs in den Synergiden, wollten wir genetische Interaktoren von *FER* finden. Eine weitere genetische Untersuchung von mutagenisierten, homozygoten *fer* Pflanzen wurde durchgeführt, um Mutationen zu finden, welche *fer*-induzierte Phänotypen unterdrücken. Leider wurden keine vielversprechenden Kandidaten gefunden.

Schliesslich ergab die Untersuchung vom Austausch funktionaler Domänen der drei Proteine FER, ANX1 und HERCULES 1 (HERK1) Rückschlüsse über gemeinsame nachgeschaltete, aber unterschiedliche voranwirkende Proteine.

Zusammenfassend haben wir zwei neue Mitglieder identifiziert, welche den Pollenschlauchempfang in den Synergiden kontrollieren und zusätzlich unterschiedliche Rollen im Pollen übernehmen. Des Weiteren konnten wir Gemeinamkeiten der funktionalen Domänen von den drei nahe verwandten Proteinen FER, ANX1, HERK1 nachweisen, was auf gemeinsame nachgeschaltete Faktoren hinweist.

CURRICULUM VITAE

Persönliche Daten

Name	LINDNER
Vorname	Heike
Geburtsdatum	26. Juli 1983
Heimatort	Karl-Marx-Stadt, Sachsen, Deutschland

Ausbildung

2000-2003	Gymnasium Johann-Philipp-Bronner-Schule, Wiesloch, Deutschland
Juli 2003	Abitur, Schwerpunktfächer Englisch und Wirtschaft
2003-2008	Diplomstudium der Biologie, Ruprecht-Karls-Universität Heidelberg, Schwerpunkt in Molekularbiologie, Zellbiologie und Botanik
2007-2008	Diplomarbeit am Heidelberger Institut für Pflanzenbiologie (HIP) mit dem Thema „Invertase Inhibitoren in Zuckerrüben“ unter Anleitung von Prof. Thomas Rausch und Dr. Andrea Jansen in enger Kollaboration mit der SÜDZUCKER AG, Deutschland
Nov 2008	Diplomierte Biologin (dipl. biol.) Universtität Heidelberg
2009-heute	Eingeschrieben als Doktorandin MNF an der Universität Zürich

Sonstiges

2006	3-monatiges Laborpraktikum (Hilfswissenschaftlerin) am Deutschen Krebsforschungszentrum (DKFZ), Heidelberg
2010	Mitorganisatorin des Zürich-Basel Plant Science Center PhD Symposium 2010 „Plants Meeting Future Challenges – Food & Energy for the Society in a Changing Environment“

TABLE OF CONTENTS

INTRODUCTION

Scope of the Thesis

Pollen Tube Reception in the Synergid Cells of *Arabidopsis thaliana* – Novel Players and Old Acquaintances

Successful fertilization in flowering plants (angiosperms) depends on several levels of communication between the pollen (male gametophyte) and various female tissues of the flower (reviewed in Beale and Johnson, 2013; Dresselhaus and Franklin-Tong, 2013; Palanivelu and Tsukamoto, 2011). First, the pollen lands on the stigma of the flower and, if compatible, adheres, hydrates and germinates to form a tip growing pollen tube (PT). The PT, which delivers the two immotile sperm cells to the ovule-embedded female gametophyte, penetrates the stigmatic papillae cells and grows through the highly specialized female tissues of the style, the transmitting tract and the ovary, where a complex signaling system is guiding the PT towards the ovule. Once arrived at the micropylar end of the embryo sac (female gametophyte), signaling events in the synergid cells involving the receptor-like kinase *FERONIA* (*FER*), the MILDEW RESISTANCE LOCUS O (MLO) member *NORTIA* (*NTA*) and the glycosyl-phosphatidylinositol (GPI)-anchored protein *LORELEI* (*LRE*) trigger PT growth arrest, PT rupture and sperm release in the receptive synergid cell (Huck et al., 2003; Escobar-Restrepo et al., 2007; Kessler et al., 2010; Capron et al., 2008). The sperm cells finally fuse with the female gametes, the egg cell and the central cell, to form the embryo and the endosperm, respectively.

In this thesis we focus specifically on the process of PT reception in the synergid cells of the model plant *Arabidopsis thaliana* (Figure I1A). As described above, several members of the active signaling cascade during PT reception have been identified, but interactions and upstream or downstream targets remain unknown. To obtain further insights into the molecular mechanisms during PT reception in the synergids, three different questions were addressed in this PhD thesis and different experimental approaches were conducted to answer them:

- What are additional female factors controlling PT reception in the synergid cells?
- What are additional members of the FER-dependent signal transduction mediating PT reception?
- Do three members of the *Catharantus roseus* receptor-like Serine/Threonine kinase 1-like subfamily (*CrRLK1L*) *FERONIA*, *ANXUR1* (*ANX1*) and *HERCULES1* (*HERK1*) share common upstream- or downstream targets?

To address the first question, a forward genetic screen for the *fer*-like PT overgrowth phenotype was conducted and yielded several mutant candidates. The two mutants with the highest phenotypic penetrance, *turan* (*tun*) and *evan (evn)*, were mapped by SNP-ratio mapping (SRM; see Chapter 1; Lindner et al., 2012) a newly developed method that allows the identification of heterozygous mutations by next-generation sequencing. SRM allowed us to quickly identify the causative genes of the *tun* and *evn* mutations, which do not yield in homozygous individuals due to male gametophytic lethality. Interestingly, *TUN* and *EVN* are both involved during PT reception in the synergid cells, but have distinct roles in the male gametophyte (see Chapter 2). The predicted gene functions of both genes indicate an involvement in protein N-glycosylation suggesting this process to be important for successful gametophyte interaction

(see Chapter 2), as it has been described for gamete interaction in mammals (Clark, 2010; 2011).

To identify genetic interactors of *FER*, we applied a suppressor screen in the *fer* homozygous mutant background for suppression of different *fer*-induced phenotypes (see Chapter 3).

Finally, we aimed at investigating functional similarities and thus common upstream- and /or downstream targets of the closely related *CrRLK1L* members *FER*, *ANX1* (Boisson-Dernier et al., 2009; Miyazaki et al., 2009) and *HERK1* (Guo et al., 2009), which are partially expressed in common but also in distinct tissues. To do that, we performed a domain-swap experiment creating chimeric proteins of functional domains of the three proteins and assessed the chimeric constructs for their ability to complement the fertilization phenotype in *fer/FER* plants (see Chapter 4).

In this thesis, published work is inserted with the journal's design and is preceded by a short note indicating Heike Lindner's contribution to the article if she is not first author. Importantly, every chapter – even if it is not published (yet) – is written in the form of a publication including introduction, results, discussion, material and methods and references. Therefore, references might be cited more than once and materials and methods are only specified within the chapters. Supplemental Information to Chapter 1, 2, and 4 can be found in the Appendix.

References:

Beale, K.M. and Johnson, M.A. (2013). Speed dating, rejection, and finding the perfect mate: advice from flowering plants. Curr. Opin. Plant Biol. **16**: 590–597.

Boisson-Dernier, A., Roy, S., Kritsas, K., Grobei, M.A., Jaciubek, M., Schroeder, J.I., and Grossniklaus, U. (2009). Disruption of the pollen-expressed *FERONIA* homologs *ANXUR1* and *ANXUR2* triggers pollen tube discharge. Development **136**: 3279–3288.

Capron, A., Gourgues, M., Neiva, L.S., Faure, J.E., Berger, F., Pagnussat, G., Krishnan, A., Alvarez-Mejia, C., Vielle-Calzada, J.P., Lee, Y.R., Liu, B., and Sundaresan, V. (2008). Maternal Control of Male-Gamete Delivery in *Arabidopsis* Involves a Putative GPI-Anchored Protein Encoded by the *LORELEI* Gene. Plant Cell **20**: 3038–3049.

Clark, G.F. (2011). Molecular models for mouse sperm-oocyte binding. Glycobiology **21**: 3–5.

Clark, G.F. (2010). The Mammalian Zona Pellucida: A Matrix That Mediates Both Gamete Binding and Immune Recognition? Syst Biol Reprod Med **56**: 349–364.

Dresselhaus, T. and Franklin-Tong, N. (2013). Male-Female Crosstalk during Pollen Germination, Tube Growth and Guidance, and Double Fertilization. Mol. Plant **6**: 1018–1036.

Escobar-Restrepo, J.M., Huck, N., Kessler, S., Gagliardini, V., Gheyselinck, J., Yang, W.C., and Grossniklaus, U. (2007). The *FERONIA* Receptor-like Kinase Mediates Male-Female Interactions During Pollen Tube Reception. Science **317**: 656–660.

Guo, H., Li, L., Ye, H., Yu, X., Algreen, A., and Yin, Y. (2009). Three related receptor-like kinases are required for optimal cell elongation in *Arabidopsis thaliana*. Proc. Natl. Acad. Sci. U.S.A.**106**: 7648–7653.

Huck, N., Moore, J.M., Federer, M., and Grossniklaus, U. (2003). The *Arabidopsis* mutant *feronia* disrupts the female gametophytic control of pollen tube reception. Development 130: 2149–2159.

Kessler, S.A., Shimosato-Asano, H., Keinath, N.F., Wuest, S.E., Ingram, G., Panstruga, R., and Grossniklaus, U. (2010). Conserved Molecular Components for Pollen Tube Reception and Fungal Invasion. Science **330**: 968–971.

Lindner, H., Raissig, M.T., Sailer, C., Shimosato-Asano, H., Bruggmann, R., and Grossniklaus, U. (2012). SNP-Ratio Mapping (SRM): identifying lethal alleles and mutations in complex genetic backgrounds by next-generation sequencing. Genetics **191**: 1381–1386.

Miyazaki, S., Murata, T., Sakurai-Ozato, N., Kubo, M., Demura, T., Fukuda, H., and Hasebe, M. (2009). *ANXUR1* and *2*, Sister Genes to *FERONIA/SIRENE*, Are Male Factors for Coordinated Fertilization. Curr. Biol. 19: 1327–1331.

Palanivelu, R. and Tsukamoto, T. (2011). Pathfinding in angiosperm reproduction: pollen tube guidance by pistils ensures successful double fertilization. Wiley Interdiscip. Rev. Dev. Biol.**1**: 96–113.

INTRODUCTION

Fertilization in Flowering Plants

Fertilization in Flowering Plants

In angiosperms, the female gametophyte (embryo sac) is embedded in the ovule, which is enclosed and protected within the ovary of the two carpels. The haploid embryo sac consists of the two female gametes, the egg cell and the central cell, as well as two synergid cells and three antipodal cells. The evolution of highly protected female gametophytes within ovules and carpels caused the emergence of several key aspects of angiosperm sexual reproduction. First, the male gametophyte (pollen), consisting of the vegetative cell and two sperm cells, must be able to reach the female gametophyte. The vegetative cell is required for pollen tube (PT) growth to deliver the two immotile sperm cells to the female gametophyte. The development of accelerated PT growth was required owing to the longer distance to cover and is possible due to the plastic pectic tip and reinforced lateral PT walls with callose plugs in angiosperms (Williams, 2008). Second, complex interaction and communication mechanisms guiding the PT evolved in angiosperms. Accordingly, a set of tissues in the female-reproductive tract, like the stigma, the style, the transmitting tract and the funiculus (Figure I1B), allow specific interaction with the male gametophyte to select suitable and compatible pollen and to guide the PT towards the female gametophyte (Beale and Johnson, 2013; Dresselhaus and Franklin-Tong, 2013; Palanivelu and Tsukamoto, 2011; Chapman and Goring, 2010). Furthermore, the ovules are capable to attract PTs at a short distance with diffusible signals produced by the sporophytic tissue of the ovules or the embryo sac itself (Figure I1C; Beale and Johnson, 2013; Dresselhaus and Franklin-Tong, 2013; Palanivelu and Tsukamoto, 2011; Chapman and Goring, 2010). Once the PT arrives at the female gametophyte, additional communication events take place, to ensure sperm delivery to the female gametes, the egg cell and the central cell, so that another novelty of angiosperms can occur: double fertilization with subsequent embryo and endosperm development (Figure I1C; Friedman, 1992; Beale and Johnson, 2013; Dresselhaus and Franklin-Tong, 2013; Palanivelu and Tsukamoto, 2011; Chapman and Goring, 2010). The following paragraphs highlight the different communication levels between the male gametophyte and the female reproductive tissues: (i) interaction events during the growth of the PT through the female flower tissues, (ii) molecular mechanism during pollen tube reception, and (iii) double fertilization. The following paragraphs only consider communication events between compatible pollen with various female tissues.

Let the Journey Begin: Pollen Adhesion, Hydration and Germination on Stigmatic Papillae Cells

When the pollen grain lands on the dry stigma of *Brassicaceae*, adhesion, hydration and germination follow to form the sperm-cell-transporting pollen tube (PT). In *Arabidopsis thaliana*, pollen adhesion to the stigma is highly selective, occurs within seconds, and is mediated via the outer cell wall of the pollen, the exine, causing surface changes of the stigmatic papillae cells at the interface (Zinkl et al., 1999). Pollen adhesion is followed by pollen hydration; in *Brassica rapa* pollen coat proteins are required for hydration by inducing actin bundling and vacuolar rearrangements in the stigma papilla cells towards the pollen attachment site promoting hydration and germination of compatible pollen (Iwano et al., 2007). Furthermore, pollen coat lipids have been found to control pollen hydration perhaps by regulating the

water flow from the stigma to the pollen (Wolters-Arts et al., 1998; Mayfield and Preuss, 2000; Mayfield et al., 2001). On the female side, the stigmatic papillae plasma membrane (PM) protein Exo70A1, a putative subunit of the plant exocyst complex involved in post-Golgi vesicle tethering to the PM, potentially delivers hydration components of the stigmatic papillae cells to the pollen contact site (Samuel et al., 2009). In addition, stigmas of two mutants deficient in phosphatidylinositol-4-phosphate (PI4P) gradient formation (*root hair defective4-1* (*rhd4-1*) and *PI 4-kinase* β*1/*β*2* (*pi4k*β*1/*β*2*) double mutant) supported slower rates of pollen grain hydration and showed additional maternal fertility defects at a later stage of pollen-pistil interaction (Chapman and Goring, 2011). This suggests that phospoinositides, which are important lipids involved in polarized secretion in general, have a specific role in pollen hydration.

However, an important factor during pollen stigma interaction is calcium (Ca^{2+}): after pollen adhesion, three cytosolic Ca^{2+} peaks have been observed in the apical region of the papillae cells (Iwano et al., 2004): First shortly after pollen hydration, second before pollen germination and third, when the pollen tube penetrates the stigmatic papillae cell wall. In pollen, cytoplasmic Ca^{2+} increased at the potential germination site shortly after hydration and sustained until tube formation (Iwano et al., 2004). This suggests that Ca^{2+} might serve as an intracellular signaling component to coordinate the interaction between the pollen and the stigma from pollen hydration until pollen tube germination. In *Brassica napus*, Exo70A1 was not only important for pollen hydration on the stigma (see above), but also for PT penetration of the stigmatic papillae cuticle or cell wall, probably by delivering enzymes to the penetration point (Samuel et al., 2009). Once the PT emerges at the base of the stigmatic papillae, it grows intercellularly through the style towards the transmitting tract. PT growth through the stigma and style tissues primes the PT for the perception of guidance signals, since *in vitro* grown PTs are more efficient in ovule targeting when they grow through a cut stigma and style (Higashiyama et al., 1998; Palanivelu and Preuss, 2006).

Follow the Signs: Communication Events to Ensure Guided Pollen Tube Growth Through the Female Transmitting Tract

Once the PT has entered the female transmitting tract, a nutrient-rich extracellular matrix (ECM) supports PT growth. In lily and tobacco, Arabinogalactan proteins are expressed in the pistil and transported to the growing PT (Cheung et al., 1995; Wu et al., 1995; Jauh and Lord, 1996). Arabinogalactan proteins are a highly diverse class of cell surface glycoproteins, many of which contain GPI-anchors. They consist of a core-peptide, which is O-glycosylated by one or more complex carbohydrates consisting of galactan and arabinose mainly (Seifert and Roberts, 2007). In *Nicotiana tabacum,* the glycoproteins TRANSMITTING TRACT SPECIFIC 1 (TTS1) and TTS2 belong to the Arabinogalactan protein family and are expressed in the transmitting tract where they promote PT growth (Cheung et al., 1995). They adhere to the PT surface and tip, where they are incorporated and deglycosylated to potentially provide nutrients for PT growth (Wu et al., 1995). Within the transmitting tract they additionally show a gradient of increasing glycosylation towards the ovarian end potentially contributing to PT guidance (Wu et al., 1995). But not only highly glycosylated proteins play a role during PT guidance along the transmitting tract, but also gradients of small cysteine-rich proteins have been observed. In *Arabidopsis*

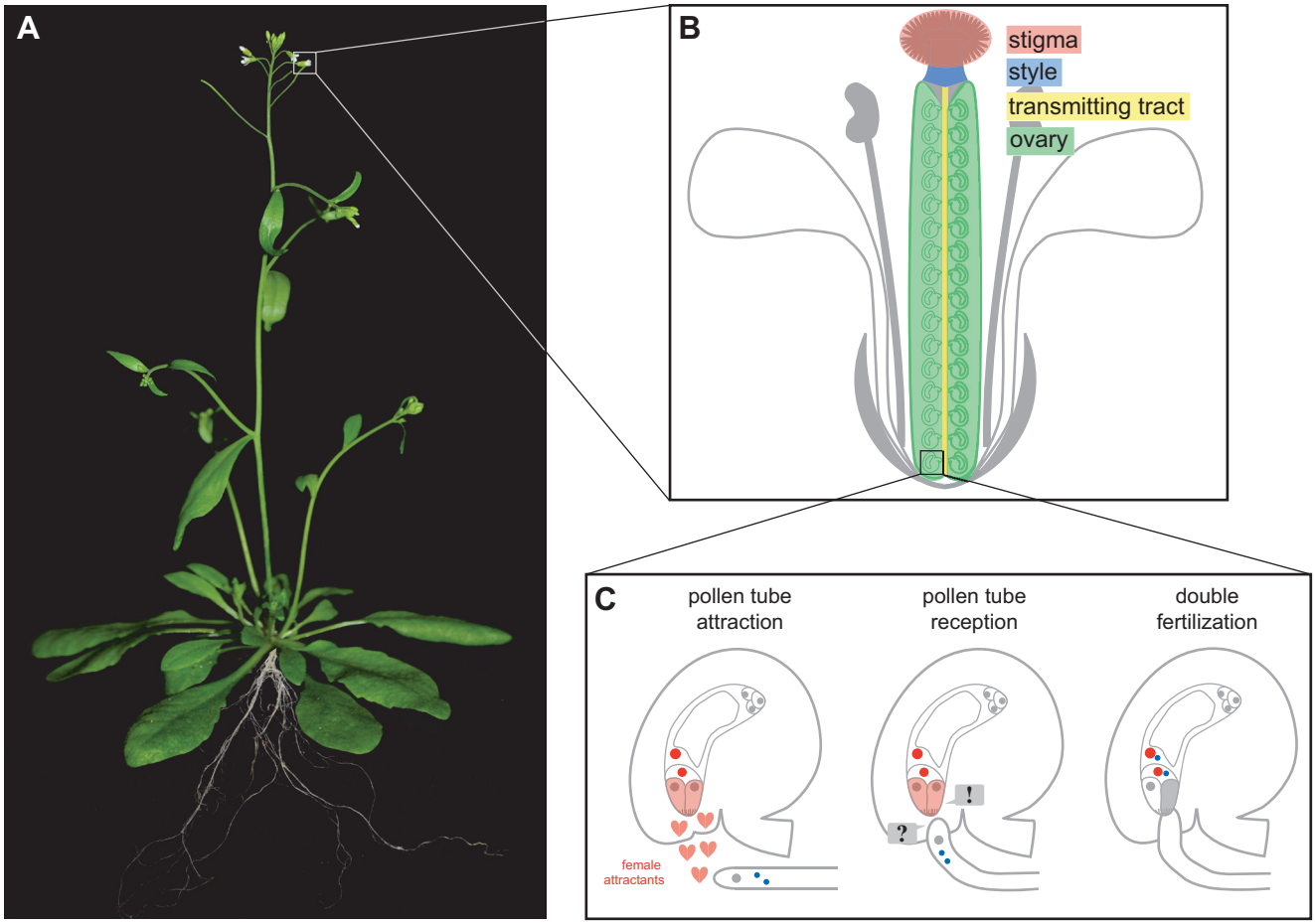

Figure I1. Fertilization in flowering plants.

(A) *Arabidopsis thaliana* ecotype Columbia-0 (Col-0) is our plant model of choice. The picture displays a flowering plant. **(B)** Model of an *Arabidopsis* flower. The colored and highlighted parts are the female tissues of the flower (carpels) containing the ovules and the female gametes. The first site of contact between the male gametophyte (pollen) and the female tissues of the flower is the stigma (colored in red). If the pollen is compatible, then the pollen grain hydrates and germinates and the pollen tube penetrates the stigmatic papillae. Then it grows through the style (colored in blue) towards the transmitting tract (colored in yellow), where a complex system of signals guides the pollen tube towards the ovule-containing ovary (colored in green). **(C)** Pollen tube attraction, pollen tube reception and double fertilization. The pollen tube is attracted to the micropylar end of the ovule by signals (red hearts) mainly secreted by the synergid cells (left panel). After the pollen tube reached the micropyle, an active signaling cascade in the synergid cells (colored in light red) and the pollen is required for pollen tube reception leading to pollen tube growth arrest in the receptive synergid. Finally, upon pollen tube arrival, the receptive synergid degenerates (colored in grey), the pollen tube bursts and releases the immotile sperm cells (blue nuclei), which fertilize egg and central cell (red nuclei, right panel) generating the embryo and the nutritive endosperm, respectively.

thaliana, plantacyanins show a steep gradient from the stigma to the style and ovary and disruption of this expression gradient leads to disrupted PT guidance (Dong et al., 2005). Moreover, in lily a plant lipid transfer protein (LTP), STIGMA/STYLAR CYSTEINE-RICH ADHESIN (SCA) synergistically enhanced the activity of a stigma expressed chemocyanin, which was able to reorient PT growth (Kim et al., 2003). Furthermore, SCA is secreted from the transmitting tract epidermis and is involved in adhesion-mediated PT guidance by the formation of an adhesive matrix with pectin that guides PTs towards the ovule (Mollet et al., 2000; Park et al., 2000). Similarily, the *Arabidopsis* LTP5, an SCA-like LTP, is expressed in PTs and the transmitting tract and plays an important role in PT tip growth and pistil function (Chae et al., 2010). In addition to small cysteine-rich proteins, gradients of small molecules and Ca^{2+} sustain proper PT guidance in the transmitting tract. *POLLEN ON PISTIL 2* (*POP2*) encodes a

γ-aminobutyric acid (GABA) transaminase involved in GABA degradation and its expression and activity leads to increasing GABA concentrations along the PT growth path with highest concentrations at the micropylar end of the ovule (Palanivelu et al., 2003). Furthermore, the rare amino acid D-serine was shown to play a role in PT guidance through the transmitting tract by mediating Ca^{2+}-influx into the PT cytoplasm (Michard et al., 2011).

Recently, a family of 17 transmembrane proteins, the tetraspanins, has been identified in *Arabidopsis* (Boavida et al., 2013). They are expressed in various reproductive tissues where they mainly localize to the PM (Boavida et al., 2013). Several members display an increased expression level in response to pollination, two of them specifically in the transmitting tract. Tetraspanins proteins are conserved among the major eukaryotes (Huang et al., 2005) and are known to act as membrane organizers by recruiting binding partners such as signaling receptors (Hemler, 2005). Therefore, tetraspanins are good candidates to play a role in intercellular communication during PT guidance, but mutant analyses remain to be determined. In the pollen tube, responses and downstream signaling events to transmitting tract components remain largely unknown. However in tomato pollen, two plasma membrane localized receptor-like kinases LePRK1 and LePRK2 form a complex in germinating PTs but dissociate after stylar extract treatment (Wengier et al., 2003). LePRK2 is phosphorylated in germinating PTs and after incubation with a stylar extract LePRK2 is dephosphorylated by STIL (Style Interactor for LePRKs) followed by complex dissociation and PT growth stimulation in a dose-dependent manner (Wengier et al., 2010).

To find additional members of the intercellular communication system during PT growth through the transmitting tract, comparative transcriptome studies (i) between intact ovaries and ovaries with depleted stigma papillae cells and transmitting tracts (Tung et al., 2005), (ii) between *in vitro* grown PTs and PTs grown through pistils (Qin et al., 2009), and (iii) between *in vivo* grown pollen tubes through pistils and unpollinated pistils (Boavida et al., 2011) were conducted. Interestingly, both female and male tissues are enriched in secreted proteins and cell-wall-related proteins potentially involved in extracellular signaling and ECM modifications, respectively. Reverse genetic screens of candidate genes were not conducted thus far but could characterize their role during pollen-pistil interaction and contribute signaling components involved during this intercellular communication process.

Come Closer: Ovular Pollen Tube Attraction

When the PT enters the ovary, it grows almost straight along the funiculus and starts turning when it is in close vicinity to the micropylar end of the ovule (Shimizu and Okada, 2000). Not much is known about the funiculus guidance signal (Fig. I1C), but as mentioned before, the γ-aminobutyric acid (GABA) shows increasing concentration along the PT growth path from the stigma towards the ovule, with highest concentrations at the micropylar end (Palanivelu et al., 2003). There, high GABA concentration seems to arise from the inner integument cells and leads to PT growth reduction to eventually make it stop at the site of reception (Palanivelu et al., 2003). Moreover, in *Arabidopsis thaliana*, the serine-racemase gene (*SR1*) generating active D-serine from inactive L-serine is expressed particularly strong at the micropylar end of the ovules resulting in high D-Serine levels (Michard et al., 2011). D-serine activates PT-tip localized

glutamate-receptor-like channels (GLRs) leading to Ca^{2+}-influx and sustained PT growth (Michard et al., 2011). Also, the small molecule nitric oxide (NO) displays highest concentration levels at the micropyle leading to Ca^{2+}-dependent redirection of the PT and thus proper ovule targeting (Prado et al., 2008). This Ca^{2+}-dependent pollen tube redirection was confirmed by a cytoplasmic Ca^{2+} sensor, revealing Ca^{2+} peaks in the PT tip, when it starts turning towards the micropylar end of the ovule, suggesting that ovular attractants affect Ca^{2+} levels and thus PT growth direction (Iwano et al., 2012). Moreover, in *Arabidopsis* PTs, two cation/proton exchangers (CHX) CHX21 and CHX23 were shown to play a role in ovular PT guidance (Lu et al., 2011). Double mutant PTs grow to the bottom of the the transmitting tract but fail to turn towards the funiculus and, in addition, *semi-in vivo* grown PTs fail to target isolated ovules. CHX23 localizes to the ER and promotes increased K^+ uptake in a pH dependent manner and is proposed to be involved in sensing and/or responding to ovular guidance cues (Lu et al., 2011). Another ER localized protein involved in micropylar PT guidance is POLLEN DEFECTIVE IN GUIDANCE 1 (POD1). It interacts with the ER chaperone CALRETICULIN 3 (CRT3) and is, thus, rather indirectly involved in signal perception, perhaps by protein folding of responsible receptors (Li et al., 2011). In addition, the absence of the PM localized GPI-anchored protein of the COBRA family *COBL10* causes decelerated PT growth in the transmitting tract and hyposensitivity to ovular guidance cues, indicating an important role of *COBL10* in processing female signals in the PT (Li et al., 2013).

In *Arabidopsis*, several mutants deficient in ovule development such as *magatama1* (*maa1*), *maa3*, *protein disulfide isomerase* (*pdi) pdil2-1* and *myb98*, show impaired PT attraction suggesting that mature ovules are essential to control the last steps of PT guidance (Shimizu and Okada, 2000; Kasahara et al., 2005; Punwani et al., 2007; 2008; Shimizu et al., 2008; Wang et al., 2008). Laser ablation analysis in *Torenia fournieri* revealed the synergid cells to be essential for PT attraction, whereas one synergid cell was sufficient, although two were more efficient (Higashiyama et al., 2001; see below). However, not only the synergid cells are important for PT guidance: In *Arabidopsis*, *CENTRAL CELL GUIDANCE* (*CCG*) is expressed in the nucleus of the central cell and might function as a transcriptional regulator mediating PT guidance, since PTs fail to target the micropyle of mutant ovules (Chen et al., 2007). In addition, the egg cell expressed GEX3 protein was shown to play a role in ovular guidance of the PT (Alandete-Saez et al., 2008).

However, the discovery of the first egg apparatus-secreted protein *Zea mays EGG APPARATUS1 (ZmEA1)* in maize (Márton et al., 2005) revealed that not only small, diffusible signals mediate pollen tube attraction, but also small-secreted proteins conduct the last steps of pollen tube attraction. Interestingly, it was shown that ZmEA1 peptides interact with the apex of *in vitro* grown maize PTs in a species-specific manner and that rapid internalization and degradation allow the PT to remain sensitive to the signal (Uebler et al., 2013). After the discovery of *ZmEA1*, further synergid-secreted proteins have been identified: In *Torenia fournieri,* the LUREs (LURE1 (TfCRP1) and LURE2 (TfCRP3)), small cysteine-rich-proteins, mediate pollen tube attraction (Okuda et al., 2009) and just recently, the same type of attractants have been characterized in *Torenia concolor* (TcCRP1; Kanaoka et al., 2011) and in *Arabidopsis thaliana* (*AtLURE1*; Takeuchi and Higashiyama, 2012). AtLURE1 is secreted from mature synergids and attract PTs in a species-preferential manner (Takeuchi and Higashiyama, 2012). In PTs, signal perception involves two plasma membrane localized receptor-like cytoplasmic kinases (RLCKs)

LOST IN POLLEN TUBE GUIDANCE 1 (*LIP1*) and *LIP2,* since *lip1/lip2* double mutants show impaired micropylar guidance and reduced attraction by AtLURE1 (Liu et al., 2013). Since both RLCKs do not have an extracellular domain for ligand activation, they might be part of a receptor complex mediating an AtLURE1-dependent signaling cascade in the pollen tube, leading to proper PT guidance towards the micropylar end of the embryo sac. In *Torenia fournieri* it was additionally shown that PT response to LURE peptides depends on PT growth through the style, indicating that the PT first has to become competent to react on the bound signal (Okuda et al., 2013).

In conclusion, ovular PT attraction depends on normally developed and mature ovules and embryo sacs and is mediated by various attractants.

You Have Reached Your Destination: Pollen Tube Reception at the Synergid Cells

After PT attraction towards the micropylar end of the ovule it slows down its growth (Stewman et al., 2010) so that PT reception can take place at the filiform apparatus, a cell wall- and membrane rich region at the micropylar pole of the synergid cells. Thereafter, the PT grows beyond the filiform apparatus and enters the receptive synergid (Leshem et al., 2013), arrests its growth and ruptures to release the two sperm cells. PT reception is a crucial process depending on communication events between the female- and the male gametophyte resulting in PT growth arrest and PT rupture. The discovery of *FERONIA* (*FER*; Huck et al., 2003) and its allele *SIRÈNE* (*SRN*; Rotman et al., 2003) has shown that PT reception is mediated by an active signaling cascade occuring at the filiform apparatus of the synergids, where the receptor-like Serine/Threonine kinase *FER* is localized (Escobar-Restrepo et al., 2007). *FER* was named after an Etruscan goddess of fertility, because *fer* mutant ovules are impaired in PT reception and, thus, in being fertilized. Fertilization fails, because the PT enters the receptive synergid, but does not stop its growth and does not rupture to release the two sperm cells. Instead, the PT grows continuously leading to the *fer*-like PT overgrowth phenotype (Huck et al., 2003; Escobar-Restrepo et al., 2007). In *fer/FER* mutants pollen and synergid development was normal suggesting that *FER* is a member of an active signaling cascade mediating PT reception at the filiform apparatus of the synergid cells (Huck et al., 2003; Escobar-Restrepo et al., 2007). So far, the ligand of FER, which binds to the extracellular malectin-like domain (Boisson-Dernier et al., 2011) and downstream targets involved in FER-mediated signal transduction remain elusive. To gain more insights into the molecular mechanisms of PT reception a mutant screen was conducted and yielded the mutant *lorelei* (*lre*; Capron et al., 2008). *LRE* encodes a glycosylphosphatidylinositol (GPI)-anchored protein and is predominantly expressed in the synergid cells. Due to its GPI-anchor, LRE was predicted to localize to the plasma membrane and mediate PT reception directly, perhaps as a secreted signal, but translational fusions with GFP yielded no fluorescent signal (Capron et al., 2008). In contrast to *fer/FER* heterozygous mutants, which show a fully penetrant phenotype (50% unfertilized ovules), the *lre/LRE* mutants showed a weaker phenotype with around 30% unfertilized ovules, indicating that *LRE* function is important but not essential for PT reception. A somewhat different mutant in PT reception is the self-sterile *abstinence by mutual consent* (*amc*; Boisson-Dernier et al., 2008). Here, PT reception is only defective, when both, the female gametophyte and the pollen tube, carry the mutated *amc* allele, whereas all the other PT reception members were either

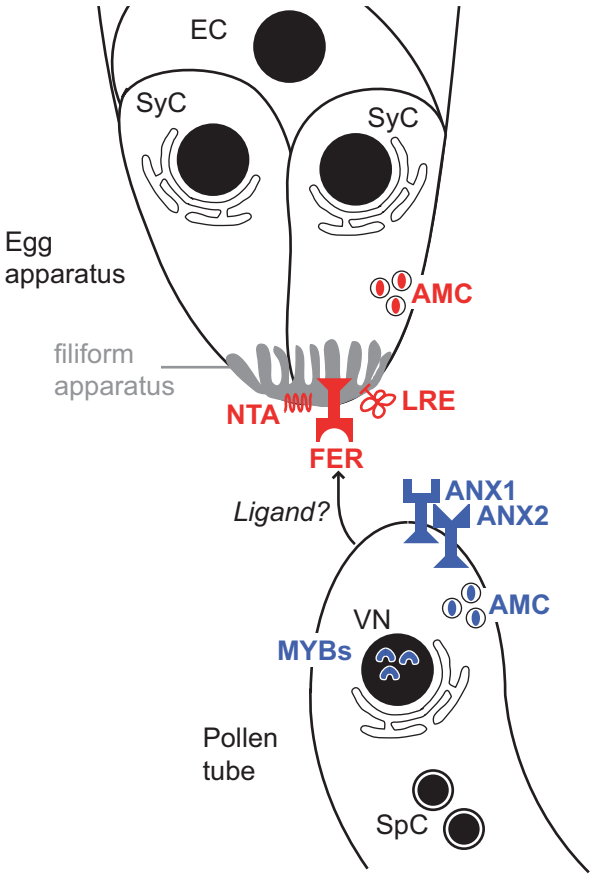

Figure I2. Molecular control of pollen tube reception in *Arabidopsis*.

Pollen tube reception occurs after the pollen tube reached the micropylar end of the ovules. FERONIA (FER), LORELEI (LRE) and NORTIA (NTA) are members of the active signaling cascade in the synergid cells. FER is a receptor-like kinase (RLK), located at the filiform apparatus, that potentially recognizes a yet unknown ligand from the pollen tube. LRE, a glycosylphosphatidylinositol (GPI)-anchored protein, potentially at the synergid surface, and NTA, an MILDEW RESISTANCE O (MLO) member that is relocated towards the filiform apparatus upon pollen tube arrival, are additional synergid-cell-specific factors involved in pollen tube reception. The only male-specific pollen tube reception factors are three nuclear-localized MYB transcription factors (MYB97, MYB101, and MYB120). However, it remains unknown which gene targets downstream of the MYBs are responsible for proper pollen tube reception. Lastly, ABSTINENCE BY MUTUAL CONSENT (AMC), which encodes a peroxine involved in protein import in peroxisomes, is required in both, the pollen tube and the female gametophyte, for normal pollen tube reception. AMC might be involved in the production of peroxisome-derived signals such as reactive oxygen species (ROS) or nitric oxide (NO). In contrast, ANXUR1 (ANX1) and ANX2, two close homologs of FER, are not directly involved in pollen tube reception but have a role in preventing premature pollen tube bursting. A yet unknown signal potentially derived from the female gametophyte might deactivate the ANX-specific signaling cascade, leading to pollen tube rupture and sperm cell release. EC, egg cell; SyC, synergid cell; VN, vegetative nucleus; SpC, sperm cells.

female or male gametophytic (Huck et al., 2003; Capron et al., 2008; Kessler et al., 2010; Lindner et al., 2012; Leydon et al., 2013; Liang et al., 2013). In *amc/AMC* heterozygous individuals, 13.5% of the ovules show the PT overgrowth (Boisson-Dernier et al., 2008). *AMC* encodes a peroxine involved in protein import in peroxisomes, which could be important for the production of small signaling molecule such as ROS or NO (Nyathi and Baker, 2006) to mediate the dialogue between the two gametophytes during PT reception. Another member of the PT reception pathway is *NORTIA* (*NTA*), encoding the *MILDEW RESISTANCE LOCUS O 7* (*MLO7*) gene (Kessler et al., 2010), belonging to the MLO family originally described in barley and associated with powdery mildew susceptibility (Büschges et al., 1997). In *nta/NTA* mutants 12% of the ovules show PT overgrowth indicating that NTA acts in concert with so far unknown proteins to mediate PT reception. *NTA* is expressed specifically in synergids where the protein localized to vesicle-like structures throughout the cytoplasm before fertilization. Upon PT arrival, the protein re-translocated to the plasma membrane of the filiform apparatus in a *FER*-dependent manner (Kessler et al., 2010). The identification of *NTA* created a link between PT reception and fungal invasion at which *FER* seems to be a cofactor. *fer/fer* mutants revealed powdery mildew (*Golovinomyces (syn. Erysiphe) orontii*) resistance and it was speculated that the ubiquitously expressed FER could interact with different MLO members in a tissue-specific manner to mediate similar signaling responses. The last identified female gametophytic member of the PT reception signaling cascade is *TURAN* (*TUN*), encoding an UDP-glycosyltransferase superfamily protein (Lindner et al., 2012). In *tun/TUN* heterozygous mutants 12% of

the ovules remain unfertilized because PT reception fails leading to the *fer*-like PT overgrowth phenotype (further characterization in Chapter 2 of this thesis).

Just recently, the first male gametophytic factors mediating PT reception have been described (Leydon et al., 2013; Liang et al., 2013). A triple mutant of three MYB transcription factors (*myb97, myb101,* and *myb120*) displayed PT overgrowth in around 60% (Liang et al., 2013) and 70% (Leydon et al., 2013) of the ovules. Target gene analysis of MYB97, MYB101 and MYB120 identified mainly transmembrane transporters, carbohydrate-binding proteins and small, secreted peptides (Leydon et al., 2013) including a defensin-like protein (Liang et al., 2013), suggesting that those gene classes might be important male factors for PT reception. However, mutant studies for functional relevance remain to be determined.

After PT arrival in the receptive synergid, additional signaling events ensure PT burst. In maize, the defensin-like proteins Zea mays EMBRYO SAC (ZmES) 1-4 are specifically expressed in the female gametophyte and ZmES4-GFP localizes to vesicles in the secretory zone of the mature synergids (Amien et al., 2010). After PT arrival, ZmES4-GFP is released from the degenerating synergid cell and induces PT rupture by activating a K^+-channel (KZM1) in the PT leading to K^+-influx and subsequent water uptake (Amien et al., 2010). Additionally, ACA9, a Ca2+-pump in the PM of *Arabidopsis* PTs, is involved in PT growth and discharge in the degenerated synergid cell (Schiøtt et al., 2004). *aca9* mutant PTs show reduced growth rates, but once they have reached the ovules, PT growth arrest is unaffected, but discharge fails in around 50% of the targeted ovules, revealing both processes to be independent (Schiøtt et al., 2004). Interestingly, the two closest homologs of *FER* are the pollen-specific genes *ANXUR1* (*ANX1*) and *ANX2*, which seem to prevent early PT rupture (Boisson-Dernier et al., 2009; Miyazaki et al., 2009). Whereas *anx1* and *anx2* single mutants have no phenotype, double mutant pollen tubes burst *in vitro* immediately after germination (Boisson-Dernier et al., 2009; Miyazaki et al., 2009). ANX1 and ANX2 proteins activate two NADPH oxidases leading to ROS production and activation of Ca2+-permeable channels. This fine-tuning of the Ca^{2+}-gradient at the PT tip results in sustained secretion and PT elongation (Boisson-Dernier et al., 2013). Both ANX-YFP fusion proteins localize to the plasma membrane of the growing PT tip (Boisson-Dernier et al., 2009; Miyazaki et al., 2009). Thus, the two ANX receptor-like kinases seem to prevent pollen tube rupture until a yet unknown signal deactivates the ANX-specific signaling cascade, leading to PT rupture and sperm cell release. This deactivation of the ANX-specific signaling cascade in PTs will only happen after the *FER*-dependent PT reception pathway at the filiform apparatus has been activated and signaled the PT to arrest its growth (Boisson-Dernier et al., 2009; Miyazaki et al., 2009). So far, only one female gametophytic mutant leading to aberrant PT rupture has been identified: The *Arabidopsis* gene *VERDANDI* (*VDD*) encodes a putative transcription factor of the plant-specific B3 superfamily and mutant ovules show aberrant antipodal and synergid cell fate and/or differentiation (Matias-Hernandez et al., 2010). In *vdd* mutant ovules, PTs are targeted towards the micropyle and arrest their growth, but fail to rupture and release the sperm cells (Matias-Hernandez et al., 2010).

Finally, the molecular mechanisms leading to synergid cell death after PT arrival remain largely unknown. In *Torenia fournieri* the receptive synergid seems to degenerate due to mechanical breakdown from PT discharge (Higashiyama et al., 2000). In contrast in *Arabidopsis thaliana*, receptive synergid

degeneration occurs after PT arrival, but before PT discharge (Sandaklie-Nikolova et al., 2007) suggesting a PT derived signal to initiate synergid cell degeneration. The communication between the receptive synergid and the PT involves Ca^{2+} oscillations (Iwano et al., 2012). Upon PT arrival Ca^{2+} oscillations in the micropylar pole of the receptive synergid start, spread towards the chalazal end and reach a maximum at PT rupture (Iwano et al., 2012). However it remains to be determined which steps of PT reception are regulated by the arising Ca^{2+} signals.

Only You: Gamete Interaction, Double Fertilization and Polytubey Block

After PT discharge in *Arabidopsis*, the sperm cells rapidly localize between the egg cell and the central cell (within less than 1min) probably by the cytoplasmic flow from PT discharge (Hamamura et al., 2011). The sperm cells stay together and are immobile for around 7.4min at the chalazal end of the degenerated synergid (Hamamura et al., 2011). Upon sperm arrival at the gamete fusion site, the egg cell secretes the small cysteine-rich protein EGG CELL1 (EC1), which mediate gamete interaction by sperm cell activation for gamete fusion (Sprunck et al., 2012). EC1 is stored in vesicles in the egg cell, secreted to the apical region of the degenerating synergid cell leading to fusogen re-localization to the cell surface of the sperm cell. The sperm-cell-specific fusogen GENERATIVE CELL SPECIFIC1 (GCS1)/ HAPLESS2 (HAP2) was previously shown to be required for gamete fusion (Mori et al., 2005; Besser et al., 2006). However, in *semi-in vivo* grown PTs HAP2-YFP localizes to the endomembrane system but not the PM of sperm cells (Mori et al., 2005; Wong and Johnson, 2010). Only after EC1 peptide treatment, HAP2-YFP is re-localized to the sperm PM, suggesting EC1-dependent sperm activation by fusogen re-localization (Sprunck et al., 2012). Subsequently, the sperm cells adhere to the surface of the female gametes with no preferential order regarding their position in the male germ unit and the membranes of both gametophytes fuse (plasmogamy) almost simultaneously (Hamamura et al., 2011). In the central cell the BAHD acyl-transferase has been shown to be essential for sperm fusion, perhaps by providing a signaling molecule, indicating that the central cell actively regulates its own fertilization (Leshem et al., 2012). Furthermore, functional mitochondria are essential to mediate male-female gamete fusion, since gametes deficient in the mitochondrial ankyrin repeat protein ANK6 are incapable in gamete fusion, perhaps by lacking a mitochondrial derived signal (Yu et al., 2010). After PM fusion the cytoplasm and the nucleus of the sperm cell enter the female gamete, whereas the sperm cell PM remains on the surface until finally nuclear fusion (karyogamy) occurs (Igawa et al., 2012).

After plasmogamy it is suggested that a polyspermy block is initiated rapidly in both female gametes (reviewed in Spielman and Scott, 2008). Another strategy to prevent polyspermy is the avoidance of the attraction of more than one PT, a process called polytubey block. In *Arabidopsis*, the arrival of the first PT almost completely prevents the attraction of further PTs (Huck et al., 2003; Beale et al., 2012). If this prevention is ensured by the release of a repulsion signal or by retaining the secretion of attractants remains unclear, although several studies favor the repulsion hypothesis (Shimizu and Okada, 2000; Palanivelu and Preuss, 2006; Tsukamoto et al., 2010; Palanivelu and Tsukamoto, 2011). The origin of the repulsion signal can be the PT, the sporophytic tissue of the ovule and/or the female gametophyte. A first and quick repulsion signal seems to originate when the first PT has successfully targeted the

synergid cells, since ovules of the developmental mutants *maa* and *myb98*, were targeted by multiple PTs at the same time (Shimizu and Okada, 2000; Kasahara et al., 2005). Recently, three independent studies showed that the second and later occurring round of polytubey prevention depends on successful gamete fusion (Beale et al., 2012; Kasahara et al., 2012; Maruyama et al., 2013). However, when gamete fusion does not occur, the second persisting synergid cell attracts further PTs to ensure fertilization success (Beale et al., 2012; Maruyama et al., 2013). Additionally, when ovules were targeted by *cdka;1* pollen, which randomly induces single fertilization of only one gamete, polytubey occurred with a significantly lower frequency (55%), than in ovules targeted by gamete fusion defective *generative cell specific1* (*gcs1)* pollen (89%; Maruyama et al., 2013). This result suggests the existence of a dual-control system in both, the egg cell and the central cell, which act independently and synergistically to induce a polytubey block response. In the central cell this response is presumably regulated by the FERTLIZATION-INDEPENDENT SEED (FIS) class *Polycomb*-Repressive Complex 2 (FIS-PRC2)-mediated H3K27m3 modification, since several mutants of this complex showed impaired polytubey blocks (Maruyama et al., 2013). Interestingly, the polytubey block fails even in *medea (mea)* homozygous mutants, where fertilization seems to occur normally. Therefore and despite of normal fertilization, several PTs are attracted and polytubey is not prevented (Maruyama et al., 2013). Accordingly, all mutants deficient in fertilization, like the female gametophytic PT reception mutants *fer*, *amc*, *nta* and *lre* (Huck et al., 2003; Boisson-Dernier et al., 2008; Kessler et al., 2010; Capron et al., 2008), and mutants impaired in gamete fusion (e.g. *ec1* (Sprunck et al., 2012) or *gcs1/hap2* (Mori et al., 2005; Besser et al., 2006)) attract multiple PTs. However, in wild-type ovules successful gamete fusion initiates programmed cell death in the persisting synergid cell via an ethylene-signaling cascade including the transcription factors *EIN3* and *EIN2* leading to a polytubey block response (Völz et al., 2013).

In conclusion, a complex and intricate system of communication and signaling mechanisms between the male gametophyte and female sporophytic and gametophytic tissues ensure PT guidance and double fertilization and, therefore, reproductive success.

Gamete Interaction in Mammals and Involvement of N-Linked Glycosylation

In mammals, the sperm cells are released in a functionally restricted state and must undergo a process of capacitation within the female reproductive tract to get the ability to fertilize the egg (Austin, 1951; Chang, 1951). Capacitation results in hyperactivation and oriented motility towards chemoattractants to finally undergo the acrosome reaction resulting in PM fusion between the egg cell and the sperm cell (reviewed in Buffone et al., 2011). PM fusion depends on the extracellular matrix of the egg cell, the zona pellucida (ZP). The ZP of the mouse egg cell consists of three cross-linked glycoprotein subunits, mZP1, mZP2 and mZP3 forming filaments and mediating species-specific interaction between the gametes (reviewed in Wassarman and Litscher, 2008). mZP3 acts as a sperm receptor and triggers the acrosome reaction in the sperm cell. The acrosome is the secretory vesicle in the anterior part of the sperm head and exocytosis of its content during early egg-sperm interaction is essential for ZP penetration and subsequent PM fusion (Buffone et al., 2011). Until recently, N-glycosylation of mZP3 proteins was thought to play a major role on egg-sperm binding, because certain oligosaccharides were

able to compete for sperm binding (Clark, 2010; Clark and Dell, 2006) and oocytes of conditional deletion of N-acetylglucosaminyltransferase I (GnT I) in mouse bound 81% fewer sperms (Shi et al., 2004; Hoodbhoy et al., 2005). In contrast, enzymatic de-N-glycosylated mZP3 resulted in equivalent sperm competition compared to intact glycosylated mZP3 (Florman and Wassarman, 1985; Rosiere and Wassarman, 1992) and also site directed mutagenesis of certain N-glycosylation sites resulted in unchanged sperm binding activity of mutated mZP3 proteins (Chen et al., 1998). These contradictory results were combined just recently in a "domain-specific model" (Clark and Dell, 2006; Clark, 2010). In that model, a mouse sperm protein or protein complex interacts with glycans and/or protein backbone of mZP3 depending on its glycosylation state. This dual adhesion model suggests that the sperm factor(s) interacts with both the peptide and the glycans to enhance the probability of sperm-egg binding and, thus, of fertilization (Clark, 2011).

However, as shown in mammals and shown by recent evidence in plants (Lindner et al. 2012, and Chapter 2 of this thesis), protein N-glycosylation seems to play an important role in gamete and gametophyte interaction, respectively. In mammals, the gametes interact directly and glycosylated proteins (like mZP3) mediate and control species-specific interaction of sperm and egg cell (Wassarman and Litscher, 2008). Interestingly, TUN, a UDP-glycosyltransferase superfamily protein with a potential role in protein N-glycosylation, is involved in PT reception (Lindner et al., 2012, and Chapter 2 of this thesis). During PT reception the male and the female gametophyte interact directly for the first time and it is tempting to speculate that glycoproteins might mediate and control the interaction between the gametophytes very similar to the control of gamete interaction in mammals.

Protein N-Glycosylation in the Endoplasmic Reticulum

N-linked glycosylation is an important process that affects protein folding, stability, transport and activity (reviewed in Helenius and Aebi, 2004; Varki, 1993; Skropeta, 2009). Biochemical and genetic analysis in yeast characterized involved enzymes and made it a well-described process (reviewed in Aebi, 2013), whereas in plants relatively little is known since only some enzymes have been characterized so far (reviewed in Pattison and Amtmann, 2009; see Figure I3). In general, N-glycan biosynthesis starts on a phosphorylated dolichol (Dol-P), which is an ER-membrane residing polyisoprenoid lipid of around 20 isoprenoid subunits (Swiezewska and Danikiewicz, 2005). In plants, the *leave wilting1* (*lew1*) mutant is impaired in dolichol biosynthesis and displays several morphological defects such as leaf wilting, decreased stomatal conductance and drought hypersensitivity (Zhang et al., 2009). Assembly of the oligosaccharide starts on the cytosolic site of the ER using UDP-N-acetylglycosamine (UDP-GlcNAc) and GDP-Mannose (GDP-Man) as substrates. Plant mutants defective in formation of nucleotide-activated monosaccharides, *cytokinesis-defective1* (*cyt1*) and *phosphomannomutase1* (*pmm1*), display underglycosylated proteins, deficiencies in N-glycosylation and GPI-anchor formation, altered cell wall composition and even embryo lethality (Conklin et al., 1996; Nickle and Meinke, 1998; Lukowitz et al., 2001; Hoeberichts et al., 2008). On the cytosolic site of the ER two N-acetylglucosamine (GlcNAc) residues and five mannose residues are transferred to the lipid-bound dolichol carrier. This oligosaccharide is then re-oriented towards the ER lumen by a flippase. In the ER lumen four more mannose and three glucose residues are added,

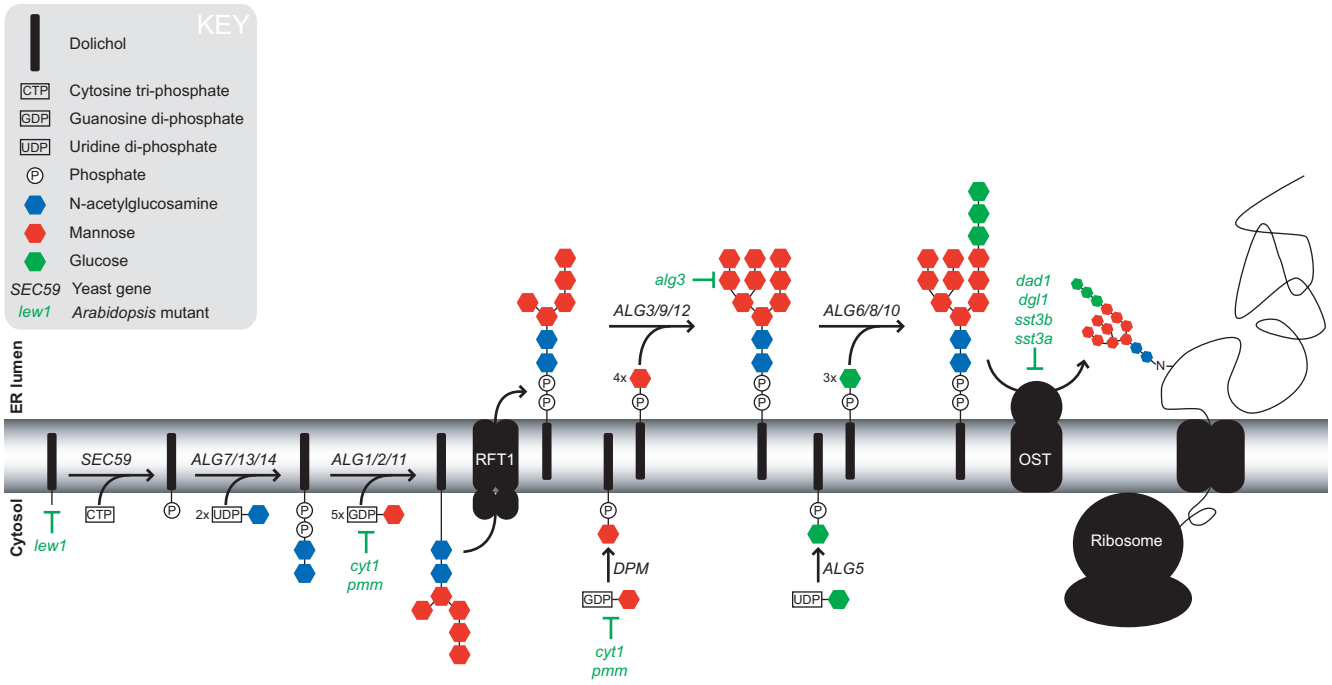

Figure I3. Model of protein N-glycosylation in the ER of yeast.
Dolichol is phosphorylated by the ER-attached dolichol kinase SEC59 using CTP on the cytosolic side of the ER. Two N-Acetylglucosamine (GlcNAc) residues are attached to the phosphorylated Dolichol by ALG7, ALG13, and ALG14 using UDP-GlcNAc. Then ALG1, ALG2 and ALG11 catalyze the connection of five mannose units to the two GlcNAc residues using GDP-mannose. A flippase (RTF1) re-orients the dolichol-oligosaccharide towards the ER lumen, where four additional mannose residues are transferred by ALG3, ALG9, and ALG12 to the oligosaccharide using dolichol-mannose as substrate. Then, ALG6, ALG8 and ALG10 transfer three Glucose units to the oligosaccharide using dolichol-glucose as substrate. Finally, the oligosaccharide is transferred by OST co-translationally to peptide. If the glycoprotein is properly glycosylated and folded, it exits the ER and is transported to the Golgi, where structural diversification of attached N-glycans occurs. Known plant mutants affecting protein N-glycosylation process are indicated in green.

whereas Dol-P-bound mannose and glucose monosaccharides serve as substrates. The plant mutant *asparagine-linked glycosylation 3* (*alg3*) produces oligossaccharides that lack four mannose residues but has no obvious developmental phenotype (Henquet et al., 2008). The end product $Glc_3Man_9GlcNAc_2$ is transferred co-translationally to an asparagin (N) in the N-X-S/T sequon, X being every amino acid except proline (Bause, 1983). The oligosaccharide transfer is catalyzed by the oligosaccharyltransferase (OST) complex. In plants, so far four subunits of the OST complex have been described and mutants show diverse phenotypes. The *defective glycosylation1* (*dgl1*) mutant shows altered cell wall polysaccharide composition and callose accumulation and strong alleles are even embryo and seedling lethal (Lerouxel et al., 2005). Double mutants of another OST subunit *saurosporine and temperature sensitive* (*stt*) 3a and 3b are gametophytic lethal (Kelleher et al., 2003). The fourth mutant, *defender against cell death 1* (*dad1*) shows a reduced rate of secretion of the glycoprotein *PATHOGENESIS RELATED 1* (*PR1*) upon salicylic acid treatment (Wang et al., 2005).

After oligosaccharide transfer the glycoprotein enters the calnexin-calreticulin (CNX-CRT) cycle. CNX and CRT are two lectins residing in the ER ensuring proper folding of glycoproteins. In this cycle, first three Glc residues are removed by the two glucosidases I and II, whereas the UDP-Glc: glycoprotein glucosyltransferase (GT) specifically binds and re-glucosylates misfolded proteins (Helenius

and Aebi, 2001). In plants, mutants in the glucosidase I homolog *glucosidase1 (gcs1*; Boisson et al., 2001) and *knopf* (*knf*; Gillmor et al., 2002) or the glucosidase II homolog *radial swelling3 (rsw3*; Burn et al., 2002) show aberrant cell wall compositions and reduced gametophytic transmission and stronger alleles are embryo lethal. If the glycoprotein is not properly folded a α-mannosidase trims the mannose residues, which provides a glycan signal for ER-associated degredation (ERAD) by the 26S proteasome (reviewed in Hüttner and Strasser, 2012). If the protein is correctly folded it is not re-glucosylated by GT after trimming and thus not bound by the two lectins CNX and CRT. Subsequently, the protein can exit the ER and oligosaccharide processing is continued in the Golgi apparatus where structural diversification of the oligosaccharide takes place.

References:

Aebi, M. (2013). N-linked protein glycosylation in the ER. Biochim. Biophys. Acta **1833**: 2430–2437.

Alandete-Saez, M., Ron, M., and McCormick, S. (2008). *GEX3*, Expressed in the Male Gametophyte and in the Egg Cell of *Arabidopsis thaliana*, Is Essential for Micropylar Pollen Tube Guidance and Plays a Role during Early Embryogenesis. Mol. Plant **1**: 586–598.

Amien, S., Kliwer, I., Márton, M.L., Debener, T., Geiger, D., Becker, D., and Dresselhaus, T. (2010). Defensin-Like ZmES4 Mediates Pollen Tube Burst in Maize via Opening of the Potassium Channel KZM1. PLoS Biol. **8**: e1000388.

Austin, C.R. (1951). Observations on the penetration of the sperm into the mammalian egg. Australian Journal of Biological Sciences **4**: 581-596.

Bause, E. (1983). Structural requirements of N-glycosylation of proteins. Studies with proline peptides as conformational probes. Biochem. J. **209**: 331–336.

Beale, K.M. and Johnson, M.A. (2013). Speed dating, rejection, and finding the perfect mate: advice from flowering plants. Curr. Opin. Plant Biol. **16**: 590–597.

Beale, K.M., Leydon, A.R., and Johnson, M.A. (2012). Gamete Fusion Is Required to Block Multiple Pollen Tubes from Entering an *Arabidopsis* Ovule. Curr. Biol. **22**: 1090–1094.

Besser, von, K., Frank, A.C., Johnson, M.A., and Preuss, D. (2006). *Arabidopsis HAP2* (*GCS1*) is a sperm-specific gene required for pollen tube guidance and fertilization. Development **133**: 4761–4769.

Boavida, L.C., Borges, F., Becker, J.D., and Feijo, J.A. (2011). Whole Genome Analysis of Gene Expression Reveals Coordinated Activation of Signaling and Metabolic Pathways during Pollen-Pistil Interactions in *Arabidopsis*. Plant Phys. **155**: 2066–2080.

Boavida, L.C., Qin, P., Broz, M., Becker, J.D., and McCormick, S. (2013). *Arabidopsis* Tetraspanins Are Confined to Discrete Expression Domains and Cell Types in Reproductive Tissues and Form Homo- and Heterodimers When Expressed in Yeast. Plant Phys. **163**: 696–712.

Boisson, M., Gomord, V., Audran, C., Berger, N., Dubreucq, B., Granier, F., Lerouge, P., Faye, L., Caboche, M., and Lepiniec, L. (2001). *Arabidopsis glucosidase I* mutants reveal a critical role of N-glycan trimming in seed development. EMBO J. **20**: 1010–1019.

Boisson-Dernier, A., Frietsch, S., Kim, T.-H., Dizon, M.B., and Schroeder, J.I. (2008). The peroxin loss-of-function mutation *abstinence by mutual consent* disrupts male-female gametophyte recognition. Curr. Biol. **18**: 63–68.

Boisson-Dernier, A., Kessler, S.A., and Grossniklaus, U. (2011). The walls have ears: the role of plant *CrRLK1Ls* in sensing and transducing extracellular signals. J. Exp. Bot. **62**: 1581–1591.

Boisson-Dernier, A., Lituiev, D.S., Nestorova, A., Franck, C.M., Thirugnanarajah, S., and Grossniklaus, U. (2013). ANXUR Receptor-Like Kinases Coordinate Cell Wall Integrity with Growth at the Pollen Tube Tip Via NADPH Oxidases. PLoS Biol. **11**: e1001719.

Boisson-Dernier, A., Roy, S., Kritsas, K., Grobei, M.A., Jaciubek, M., Schroeder, J.I., and Grossniklaus, U. (2009). Disruption of the pollen-expressed *FERONIA* homologs *ANXUR1* and *ANXUR2* triggers pollen tube discharge. Development **136**: 3279–3288.

Buffone, M.G., Ijiri, T.W., Cao, W., Merdiushev, T., Aghajanian, H.K., and Gerton, G.L. (2011). Heads or tails? Structural events and molecular mechanisms that promote mammalian sperm acrosomal exocytosis and motility. Mol. Reprod. Dev. **79**: 4–18.

Burn, J.E., Hurley, U.A., Birch, R.J., Arioli, T., Cork, A. and Williamson, R.E. (2002). The cellulose-deficient *Arabidopsis* mutant *rsw3* is defective in a gene encoding a putative *glucosidase II*, an enzyme processing N-glycans during ER quality control. Plant J. **32**: 949-960.

Büschges, R., Hollricher, K., Panstruga, R., and Simons, G. et al. (1997). The Barley *Mlo* Gene: A Novel Control Element of Plant Pathogen Resistance. Cell **88**: 695-705.

Capron, A., Gourgues, M., Neiva, L.S., Faure, J.E., Berger, F., Pagnussat, G., Krishnan, A., Alvarez-Mejia, C., Vielle-

Calzada, J.P., Lee, Y.R., Liu, B., and Sundaresan, V. (2008). Maternal Control of Male-Gamete Delivery in *Arabidopsis* Involves a Putative GPI-Anchored Protein Encoded by the *LORELEI* Gene. Plant Cell **20**: 3038–3049.

Chae, K., Kieslich, C.A., Morikis, D., Kim, S.C., and Lord, E.M. (2010). A Gain-of-Function Mutation of *Arabidopsis* Lipid Transfer Protein 5 Disturbs Pollen Tube Tip Growth and Fertilization. Plant Cell **21**: 3902–3914.

Chang, M.C. (1951). Fertilization in relation to the number of spermatozoa in the fallopian tubes of rabbits. Ann. Ostet. Ginecol. **73**: 918–925.

Chapman, L.A. and Goring, D.R. (2011). Misregulation of phosphoinositides in *Arabidopsis thaliana* decreases pollen hydration and maternal fertility. Sex. Plant Reprod. **24**: 319–326.

Chapman, L.A. and Goring, D.R. (2010). Pollen-pistil interactions regulating successful fertilization in the *Brassicaceae*. J. Exp. Bot. **61**: 1987–1999.

Chen, J., Litscher, E.S., and Wassarman, P.M. (1998). Inactivation of the mouse sperm receptor, mZP3, by site-directed mutagenesis of individual serine residues located at the combining site for sperm. Proc. Natl. Acad. Sci. U.S.A. **95**: 6193–6197.

Chen, Y.-H., Li, H.-J., Shi, D.-Q., Yuan, L., Liu, J., Sreenivasan, R., Baskar, R., Grossniklaus, U., and Yang, W.-C. (2007). The central cell plays a critical role in pollen tube guidance in *Arabidopsis*. Plant Cell **19**: 3563–3577.

Cheung, A.Y., Wang, H., and Wu, H.-M. (1995). A floral transmitting tissue-specific glycoprotein attracts pollen tubes and stimulates their growth. Cell **82**: 383–393.

Clark, G.F. (2011). Molecular models for mouse sperm-oocyte binding. Glycobiology **21**: 3–5.

Clark, G.F. (2010). The mammalian zona pellucida: a matrix that mediates both gamete binding and immune recognition? Syst. Biol. Reprod. Med. **56**: 349-364.

Clark, G.F. and Dell, A. (2006). Molecular models for murine sperm-egg binding. J. Biol. Chem. **281**: 13853–13856.

Conklin, P.L., Williams, E.H., and Last, R.L. (1996). Environmental stress sensitivity of an ascorbic acid-deficient *Arabidopsis* mutant. Proc. Natl. Acad. Sci. U.S.A. **93**: 9970–9974.

Danielle Skropeta (2009). The effect of individual N-glycans on enzyme activity. Bioorg. Med. Chem. **17**: 2645–2653.

Dong, J., Kim, S.T., and Lord, E.M. (2005). Plantacyanin plays a role in reproduction in *Arabidopsis*. Plant Phys. **138**: 778–789.

Dresselhaus, T. and Franklin-Tong, N. (2013). Male-Female Crosstalk during Pollen Germination, Tube Growth and Guidance, and Double Fertilization. Mol. Plant **6**: 1018–1036.

Escobar-Restrepo, J.M., Huck, N., Kessler, S., Gagliardini, V., Gheyselinck, J., Yang, W.C., and Grossniklaus, U. (2007). The *FERONIA* Receptor-like Kinase Mediates Male-Female Interactions During Pollen Tube Reception. Science **317**: 656–660.

Florman, H.M. and Wassarman, P.M. (1985). O-linked oligosaccharides of mouse egg ZP3 account for its sperm receptor activity. Cell **41**: 313–324.

Friedman, W.E. (1992). Evidence of a pre-angiosperm origin of endosperm: implications for the evolution of flowering plants. Science **255**: 336–339.

Gillmor, C.S., Poindexter, P., Lorieau, J., Palcic, M.M., and Somerville, C. (2002). *Alpha-glucosidase I* is required for cellulose biosynthesis and morphogenesis in *Arabidopsis*. J. Cell Biol. **156**: 1003–1013.

Hamamura, Y., Saito, C., Awai, C., Kurihara, D., Miyawaki, A., Nakagawa, T., Kanaoka, M.M., Sasaki, N., Nakano, A., Berger, F., and Higashiyama, T. (2011). Live-Cell Imaging Reveals the Dynamics of Two Sperm Cells during Double Fertilization in *Arabidopsis thaliana*. Curr. Biol. **21**: 497–502.

Helenius, A. and Aebi, M. (2001). Intracellular functions of N-linked glycans. Science **291**: 2364–2369.

Helenius, A. and Aebi, M. (2004). Roles of N-Linked Glycans in the Endoplasmic Reticulum. Annu. Rev. Biochem. **73**: 1019–1049.

Hemler, M.E. (2005). Tetraspanin functions and associated microdomains. Nat. Rev. Mol. Cell Biol. **6**: 801-811.

Henquet, M., Lehle, L., Schreuder, M., Rouwendal, G., Molthoff, J., Helsper, J., Van Der Krol, S., and Bosch, D. (2008). Identification of the gene encoding the *alpha1,3-mannosyltransferase* (*ALG3*) in *Arabidopsis* and characterization of downstream n-glycan processing. Plant Cell **20**: 1652–1664.

Higashiyama, T., Kuroiwa, H., Kawano, S., and Kuroiwa, T. (2000). Explosive discharge of pollen tube contents in *Torenia fournieri*. Plant Phys. **122**: 11–14.

Higashiyama, T., Kuroiwa, H., Kawano, S., and Kuroiwa, T. (1998). Guidance *in vitro* of the pollen tube to the naked embryo sac of *torenia fournieri*. Plant Cell **10**: 2019–2032.

Higashiyama, T., Yabe, S., Sasaki, N., and Nishimura, Y. (2001). Pollen tube attraction by the synergid cell. Science **293**: 1480-1483.

Hoeberichts, F.A. et al. (2008). A Temperature-sensitive mutation in the *Arabidopsis thaliana phosphomannomutase* gene disrupts protein glycosylation and triggers cell death. J. Biol. Chem. **283**: 5708–5718.

Hoodbhoy, T., Joshi, S., Boja, E.S., Williams, S.A., Stanley, P., and Dean, J. (2005). Human sperm do not bind to rat zonae pellucidae despite the presence of four homologous glycoproteins. J. Biol. Chem. **280**: 12721–12731.

Huang, S., Yuan, S., Dong, M., Su, J., Yu, C., Shen, Y., and Xie, X. (2005). The phylogenetic analysis of tetraspanins projects the evolution of cell–cell interactions from unicellular to multicellular organisms. Genomics **86**: 674-684.

Huck, N., Moore, J.M., Federer, M., and Grossniklaus, U. (2003). The *Arabidopsis* mutant *feronia* disrupts the female gametophytic control of pollen tube reception. Development **130**: 2149–2159.

Hüttner, S. and Strasser, R. (2012). Endoplasmic reticulum-associated degradation of glycoproteins in plants. Front. Plant Sci. **3**: 67.

Igawa, T., Yanagawa, Y., Miyagishima, S.-Y., and Mori, T. (2012). Analysis of gamete membrane dynamics during double fertilization of *Arabidopsis*. J. Plant Res. **126**: 387–394.

Iwano, M., Ngo, Q.A., Entani, T., Shiba, H., Nagai, T., Miyawaki, A., Isogai, A., Grossniklaus, U., and Takayama, S. (2012). Cytoplasmic Ca^{2+} changes dynamically during the interaction of the pollen tube with synergid cells. Development **139**: 4202–4209.

Iwano, M., Shiba, H., Matoba, K., Miwa, T., Funato, M., Entani, T., Nakayama, P., Shimosato, H., Takaoka, A., Isogai, A., and Takayama, S. (2007). Actin Dynamics in Papilla Cells of *Brassica rapa* during Self- and Cross-Pollination. Plant Phys. **144**: 72–81.

Iwano, M., Shiba, H., Miwa, T., and Che, F.S. (2004). Ca^{2+} dynamics in a pollen grain and papilla cell during pollination of *Arabidopsis*. Plant Phys. **136**: 3562-3571.

Jauh, G.Y. and Lord, E.M. (1996). Localization of pectins and arabinogalactan-proteins in lily (*Lilium longiflorum L.*) pollen tube and style, and their possible roles in pollination. Planta **2**: 251-261.

Kanaoka, M.M., Kawano, N., Matsubara, Y., Susaki, D., Okuda, S., Sasaki, N., and Higashiyama, T. (2011). Identification and characterization of *TcCRP1*, a pollen tube attractant from *Torenia concolor*. Ann. Bot. **108**: 739–747.

Kasahara, R.D., Maruyama, D., Hamamura, Y., Sakakibara, T., Twell, D., and Higashiyama, T. (2012). Fertilization Recovery after Defective Sperm Cell Release in *Arabidopsis*. Curr. Biol. **22**: 1084–1089.

Kasahara, R.D., Portereiko, M.F., Sandaklie-Nikolova, L., Rabiger, D.S., and Drews, G.N. (2005). *MYB98* is required for pollen tube guidance and synergid cell differentiation in *Arabidopsis*. Plant Cell **17**: 2981–2992.

Kelleher, D.J., Karaoglu, D., Mandon, E.C., and Gilmore, R. (2003). Oligosaccharyltransferase isoforms that contain different catalytic STT3 subunits have distinct enzymatic properties. Mol. Cell **12**: 101–111.

Kessler, S.A., Shimosato-Asano, H., Keinath, N.F., Wuest, S.E., Ingram, G., Panstruga, R., and Grossniklaus, U. (2010). Conserved Molecular Components for Pollen Tube Reception and Fungal Invasion. Science **330**: 968–971.

Kim, S., Mollet, J.-C., Dong, J., Zhang, K., Park, S.-Y., and Lord, E.M. (2003). Chemocyanin, a small basic protein from the lily stigma, induces pollen tube chemotropism. Proc. Natl. Acad. Sci. U.S.A. **100**: 16125–16130.

Lerouxel, O., Mouille, G., Andème-Onzighi, C., Bruyant, M.-P., Séveno, M., Loutelier-Bourhis, C., Driouich, A., Höfte, H., and Lerouge, P. (2005). Mutants in *DEFECTIVE GLYCOSYLATION*, an *Arabidopsis* homolog of an oligosaccharyltransferase complex subunit, show protein underglycosylation and defects in cell differentiation and growth. Plant J. **42**: 455–468.

Leshem, Y., Johnson, C., and Sundaresan, V. (2013). Pollen tube entry into the synergid cell of *Arabidopsis* is observed at a site distinct from the filiform apparatus. Plant Reprod. **26**: 93–99.

Leshem, Y., Johnson, C., Wuest, S.E., Song, X., Ngo, Q.A., Grossniklaus, U., and Sundaresan, V. (2012). Molecular characterization of the glauce mutant: a central cell-specific function is required for double fertilization in Arabidopsis. Plant Cell **24**: 3264–3277.

Leydon, A.R., Beale, K.M., Woroniecka, K., Castner, E., Chen, J., Horgan, C., Palanivelu, R., and Johnson, M.A. (2013). Three *MYB* Transcription Factors Control Pollen Tube Differentiation Required for Sperm Release. Curr. Biol. 23: 1209–1214.

Li, H.J., Xue, Y., Jia, D.J., Wang, T., hi, D.Q., Liu, J., Cui, F., Xie, Q., Ye, D., and Yang, W.C. (2011). *POD1* Regulates Pollen Tube Guidance in Response to Micropylar Female Signaling and Acts in Early Embryo Patterning in Arabidopsis. Plant Cell **23**: 3288–3302.

Li, S., Ge, F.-R., Xu, M., Zhao, X.-Y., Huang, G.-Q., Zhou, L.-Z., Wang, J.-G., Kombrink, A., McCormick, S., Zhang, X.S., and Zhang, Y. (2013). *Arabidopsis COBRA-LIKE 10*, a GPI-anchored protein, mediates directional growth of pollen tubes. Plant J. **74**: 486–497.

Liang, Y., Tan, Z.-M., Zhu, L., Niu, Q.-K., Zhou, J.-J., Li, M., Chen, L.-Q., Zhang, X.-Q., and Ye, D. (2013). *MYB97*, *MYB101* and *MYB120* Function as Male Factors That Control Pollen Tube-Synergid Interaction in *Arabidopsis thaliana* Fertilization. PLoS Genet. **9**: e1003933.

Lindner, H., Raissig, M.T., Sailer, C., Shimosato-Asano, H., Bruggmann, R., and Grossniklaus, U. (2012). SNP-Ratio Mapping (SRM): identifying lethal alleles and mutations in complex genetic backgrounds by next-generation sequencing. Genetics **191**: 1381–1386.

Liu, J., Zhong, S., Guo, X., Hao, L., Wei, X., Huang, Q., Hou, Y., Shi, J., Wang, C., Gu, H., and Qu, L.-J. (2013). Membrane-Bound RLCKs LIP1 and LIP2 Are Essential Male Factors Controlling Male-Female Attraction in *Arabidopsis*. Curr. Biol. **23**: 993–998.

Lu, Y., Chanroj, S., Zulkifli, L., Johnson, M.A., Uozumi, N., Cheung, A., and Sze, H. (2011). Pollen Tubes Lacking a Pair of K+ Transporters Fail to Target Ovules in *Arabidopsis*. Plant Cell **23**: 81–93.

Lukowitz, W., Nickle, T.C., Meinke, D.W., Last, R.L., Conklin, P.L., and Somerville, C.R. (2001). *Arabidopsis cyt1* mutants are deficient in a *mannose-1-phosphate guanylyltransferase* and point to a requirement of N-linked glycosylation for cellulose biosynthesis. Proc. Natl. Acad. Sci. U.S.A. **98**: 2262–2267.

Maruyama, D., Hamamura, Y., Takeuchi, H., Susaki, D., Nishimaki, M., Kurihara, D., Kasahara, R.D., and Higashiyama, T. (2013). Independent Control by Each Female Gamete Prevents the Attraction of Multiple Pollen Tubes. Dev. Cell **25**: 317–323.

Matias-Hernandez, L., Battaglia, R., Galbiati, F., Rubes, M., Eichenberger, C., Grossniklaus, U., Kater, M.M., and Colombo, L. (2010). *VERDANDI* is a direct target of the MADS domain ovule identity complex and affects embryo sac differentiation in *Arabidopsis*. Plant Cell **22**: 1702–1715.

Mayfield, J.A. and Preuss, D. (2000). Rapid initiation of *Arabidopsis* pollination requires the oleosin-domain protein GRP17. Nat Cell Biol. **2**: 128–130.

Mayfield, J.A., Fiebig, A., Johnstone, S.E., and Preuss, D. (2001). Gene families from the *Arabidopsis thaliana* pollen coat proteome. Science **292**: 2482–2485.

Márton, M.L., Cordts, S., Broadhvest, J., and Dresselhaus, T. (2005). Micropylar pollen tube guidance by *egg apparatus 1* of maize. Science **307**: 573–576.

Michard, E., Lima, P.T., Borges, F., Silva, A.C., Portes, M.T., Carvalho, J.E., Gilliham, M., Liu, L.H., Obermeyer, G., and Feijo, J.A. (2011). Glutamate Receptor-Like Genes Form Ca2+ Channels in Pollen Tubes and Are Regulated by Pistil D-Serine. Science **332**: 434–437.

Miyazaki, S., Murata, T., Sakurai-Ozato, N., Kubo, M., Demura, T., Fukuda, H., and Hasebe, M. (2009). *ANXUR1* and *2*, Sister Genes to *FERONIA/SIRENE*, Are Male Factors for Coordinated Fertilization. Curr. Biol. **19**: 1327–1331.

Mollet, J.C., Park, S.Y., Nothnagel, E.A., and Lord, E.M. (2000). A lily stylar pectin is necessary for pollen tube adhesion to an in vitro stylar matrix. Plant Cell **12**: 1737–1750.

Mori, T., Kuroiwa, H., Higashiyama, T., and Kuroiwa, T. (2005). *GENERATIVE CELL SPECIFIC 1* is essential for angiosperm fertilization. Nat. Cell Biol. **8**: 64–71.

Nickle, T.C. and Meinke, D.W. (1998). A cytokinesis-defective mutant of *Arabidopsis* (*cyt1*) characterized by embryonic lethality, incomplete cell walls, and excessive callose accumulation. Plant J. **15**: 321-332.

Nyathi, Y. and Baker, A. (2006). Plant peroxisomes as a source of signalling molecules. Biochim. Biophys. Acta **1763**: 1478–1495.

Okuda, S., Suzuki, T., Kanaoka, M.M., Mori, H., Sasaki, N., and Higashiyama, T. (2013). Acquisition of LURE-Binding Activity at the Pollen Tube Tip of *Torenia fournieri*. Mol. Plant **6**: 1074–1090.

Okuda, S., Tsutsui, H., Shiina, K., Sprunck, S., and Takeuchi, H. et al. (2009). Defensin-like polypeptide LUREs are pollen tube attractants secreted from synergid cells. Nature **458**: 357-361.

Palanivelu, R. and Preuss, D. (2006). Distinct short-range ovule signals attract or repel *Arabidopsis thaliana* pollen tubes *in vitro*. BMC Plant Biol. **6**: 7.

Palanivelu, R. and Tsukamoto, T. (2011). Pathfinding in angiosperm reproduction: pollen tube guidance by pistils ensures successful double fertilization. Wiley Interdiscip. Rev. Dev. Biol. **1**: 96–113.

Palanivelu, R., Brass, L., Edlund, A.F., and Preuss, D. (2003). Pollen tube growth and guidance is regulated by *POP2*, an *Arabidopsis* gene that controls GABA levels. Cell **114**: 47–59.

Park, S.Y., Jauh, G.Y., Mollet, J.C., Eckard, K.J., Nothnagel, E.A., Walling, L.L., and Lord, E.M. (2000). A lipid transfer-like protein is necessary for lily pollen tube adhesion to an *in vitro* stylar matrix. Plant Cell **12**: 151–164.

Pattison, R.J. and Amtmann, A. (2009). N-glycan production in the endoplasmic reticulum of plants. Trends Plant Sci. **14**: 92–99.

Prado, A.M., Colaco, R., Moreno, N., Silva, A.C., and Feijo, J.A. (2008). Targeting of Pollen Tubes to Ovules Is Dependent on Nitric Oxide (NO) Signaling. Mol. Plant **1**: 703–714.

Punwani, J.A., Rabiger, D.S., and Drews, G.N. (2007). *MYB98* Positively Regulates a Battery of Synergid-Expressed Genes Encoding Filiform Apparatus Localized Proteins. Plant Cell **19**: 2557–2568.

Punwani, J.A., Rabiger, D.S., Lloyd, A., and Drews, G.N. (2008). The *MYB98* subcircuit of the synergid gene regulatory network includes genes directly and indirectly regulated by *MYB98*. Plant J. 55: 406-414.

Qin, Y., Leydon, A.R., Manziello, A., Pandey, R., Mount, D., Denic, S., Vasic, B., Johnson, M.A., and Palanivelu, R. (2009). Penetration of the Stigma and Style Elicits a Novel Transcriptome in Pollen Tubes, Pointing to Genes Critical for Growth in a Pistil. PLoS Genetics **5**: e1000621.

Rosiere, T.K. and Wassarman, P.M. (1992). Identification of a region of mouse zona pellucida glycoprotein mZP3 that possesses sperm receptor activity. Dev. Biol. **154**: 309–317.

Rotman, N., Rozier, F., Boavida, L., Dumas, C., Berger, F., and Faure, J.-E. (2003). Female control of male gamete delivery during fertilization in *Arabidopsis* thaliana. Curr. Biol. **13**: 432–436.

Samuel, M.A., Chong, Y.T., Haasen, K.E., Aldea-Brydges, M.G., Stone, S.L., and Goring, D.R. (2009). Cellular Pathways

Regulating Responses to Compatible and Self-Incompatible Pollen in *Brassica* and *Arabidopsis* Stigmas Intersect at Exo70A1, a Putative Component of the Exocyst Complex. Plant Cell **21**: 2655–2671.

Sandaklie-Nikolova, L., Palanivelu, R., King, E.J., Copenhaver, G.P., and Drews, G.N. (2007). Synergid Cell Death in *Arabidopsis* Is Triggered following Direct Interaction with the Pollen Tube. Plant Phys. **144**: 1753–1762.

Schiøtt, M., Romanowsky, S.M., Baekgaard, L., Jakobsen, M.K., Palmgren, M.G., and Harper, J.F. (2004). A plant plasma membrane Ca^{2+} pump is required for normal pollen tube growth and fertilization. Proc. Natl. Acad. Sci. U.S.A. **101**: 9502–9507.

Seifert, G.J. and Roberts, K. (2007). The Biology of Arabinogalactan Proteins. Annu. Rev. Plant Biol. **58**: 137–161.

Shi, S., Williams, S.A., Seppo, A., Kurniawan, H., Chen, W., Ye, Z., Marth, J.D., and Stanley, P. (2004). Inactivation of the *Mgat1* gene in oocytes impairs oogenesis, but embryos lacking complex and hybrid N-glycans develop and implant. Mol. Cell. Biol. **24**: 9920–9929.

Shimizu, K.K. and Okada, K. (2000). Attractive and repulsive interactions between female and male gametophytes in *Arabidopsis* pollen tube guidance. Development **127**: 4511–4518.

Shimizu, K.K., Ito, T., Ishiguro, S., and Okada, K. (2008). *MAA3* (*MAGATAMA3*) helicase gene is required for female gametophyte development and pollen tube guidance in *Arabidopsis thaliana*. Plant Cell Physiol. **49**: 1478–1483.

Spielman, M. and Scott, R.J. (2008). Polyspermy barriers in plants: from preventing to promoting fertilization. Sex. Plant Reprod. **21**: 53–65.

Sprunck, S., Rademacher, S., Vogler, F., Gheyselinck, J., Grossniklaus, U., and Dresselhaus, T. (2012). Egg Cell-Secreted EC1 Triggers Sperm Cell Activation During Double Fertilization. Science **338**: 1093–1097.

Stewman, S.F., Jones-Rhoades, M., Bhimalapuram, P., Tchernookov, M., Preuss, D., and Dinner, A.R. (2010). Mechanistic insights from a quantitative analysis of pollen tube guidance. BMC Plant Biol. **10**: 32.

Swiezewska, E. and Danikiewicz, W. (2005). Polyisoprenoids: structure, biosynthesis and function. Prog. Lipid Res. **44**: 235–258.

Takeuchi, H. and Higashiyama, T. (2012). A Species-Specific Cluster of Defensin-Like Genes Encodes Diffusible Pollen Tube Attractants in *Arabidopsis*. PLoS Biol. **10**: e1001449.

Tsukamoto, T., Qin, Y., Huang, Y., Dunatunga, D., and Palanivelu, R. (2010). A role for LORELEI, a putative glycosylphosphatid ylinositol-anchored protein, in *Arabidopsis thaliana* double fertilization and early seed development. Plant J. **62**: 571–588.

Tung, C.-W., Dwyer, K.G., Nasrallah, M.E., and Nasrallah, J.B. (2005). Genome-wide identification of genes expressed in *Arabidopsis* pistils specifically along the path of pollen tube growth. Plant Phys. **138**: 977–989.

Uebler, S., Dresselhaus, T., and Márton, M. (2013). Species-specific interaction of EA1 with the maize pollen tube apex. Plant Signal Behav. **8**: e25682.

Varki, A. (1993). Biological roles of oligosaccharides: all of the theories are correct. Glycobiology **3**: 97–130.

Völz, R., Heydlauff, J., Ripper, D., Lyncker, von, L., and Groß-Hardt, R. (2013). Ethylene Signaling Is Required for Synergid Degeneration and the Establishment of a Pollen Tube Block. Dev. Cell **25**: 310–316.

Wang, D., Weaver, N.D., Kesarwani, M., and Dong, X. (2005). Induction of protein secretory pathway is required for systemic acquired resistance. Science **308**: 1036–1040.

Wang, H., Boavida, L.C., Ron, M., and McCormick, S. (2008). Truncation of a protein disulfide isomerase, PDIL2-1, delays embryo sac maturation and disrupts pollen tube guidance in *Arabidopsis thaliana*. Plant Cell **20**: 3300–3311.

Wassarman, P.M. and Litscher, E.S. (2008). Mammalian fertilization: the egg's multifunctional zona pellucida. Int. J. Dev. Biol. **52**: 665–676.

Wengier, D., Valsecchi, I., Cabanas, M.L., Tang, W.-H., McCormick, S., and Muschietti, J. (2003). The receptor kinases LePRK1 and LePRK2 associate in pollen and when expressed in yeast, but dissociate in the presence of style extract. Proc. Natl. Acad. Sci. U.S.A. **100**: 6860–6865.

Wengier, D.L., Mazzella, M.A., Salem, T.M., McCormick, S., and Muschietti, J.P. (2010). STIL, a peculiar molecule from styles, specifically dephosphorylates the pollen receptor kinase LePRK2 and stimulates pollen tube growth in vitro. BMC Plant Biol. **10**: 33.

Williams, J.H. (2008). Novelties of the flowering plant pollen tube underlie diversification of a key life history stage. Proc. Natl. Acad. Sci. U.S.A. **105**: 11259–11263.

Wolters-Arts, M., Lush, W.M., and Mariani, C. (1998). Lipids are required for directional pollen-tube growth. Nature **392**: 818–821.

Wong, J.L. and Johnson, M.A. (2010). Is HAP2-GCS1 an ancestral gamete fusogen? Trends Cell Biol. **20**: 134–141.

Wu, H., Wang, H., and Cheung, A.Y. (1995). A pollen tube growth stimulatory glycoprotein is deglycosylated by pollen tubes and displays a glycosylation gradient in the flower. Cell **11**: 395-403.

Yu, F. et al. (2010). ANK6, a mitochondrial ankyrin repeat protein, is required for male-female gamete recognition in *Arabidopsis thaliana*. Proc. Natl. Acad. Sci. U.S.A.**107**: 22332–22337.

Zhang, M., Henquet, M., Chen, Z., Zhang, H., Zhang, Y., Ren, X., Van Der Krol, S., Gonneau, M., Bosch, D., and Gong,

Z. (2009) *LEW3*, encoding a putative alpha-1,2-mannosyltransferase (*ALG11*) in N-linked glycoprotein, plays vital roles in cell-wall biosynthesis and the abiotic stress response in *Arabidopsis thaliana*. Plant J. **60**: 983–999.

Zinkl, G.M., Zwiebel, B.I., Grier, D.G., and Preuss, D. (1999). Pollen-stigma adhesion in *Arabidopsis*: a species-specific interaction mediated by lipophilic molecules in the pollen exine. Development **126**: 5431–5440.

INTRODUCTION

CrRLK1L Receptor-Like Kinases

NOTE

The following review is published as Lindner H*, Müller LM*, Boisson-Dernier A, Grossniklaus U: ***CrRLK1L* receptor-like kinases: not just another brick in the wall.** *Curr. Opin. Plant Biol.* 2012, **15**: 659–669.
*these authors contributed equally to this work

HL wrote two chapters and revised the review and conceived and designed Figure 1. LM and ABD each wrote two chapters and designed one figure and revised the review. UG critically read and corrected the review.

Available online at www.sciencedirect.com

SciVerse ScienceDirect

Current Opinion in Plant Biology

CrRLK1L receptor-like kinases: not just another brick in the wall

Heike Lindner[1], Lena Maria Müller[1], Aurélien Boisson-Dernier and Ueli Grossniklaus

In plants, receptor-like kinases regulate many processes during reproductive and vegetative development. The *Arabidopsis* subfamily of *Catharanthus roseus* RLK1-like kinases (CrRLK1Ls) comprises 17 members with a putative extracellular carbohydrate-binding malectin-like domain. Only little is known about the functions of these proteins, although mutant analyses revealed a role during cell elongation, polarized growth, and fertilization. However, the molecular nature of the underlying signal transduction cascades remains largely unknown. CrRLK1L proteins are also involved in biotic and abiotic stress responses. It is likely that carbohydrate-rich ligands transmit a signal, which could originate from cell wall components, an arriving pollen tube, or a pathogen attack. Thus, post-translational modifications could be crucial for CrRLK1L signal transduction and ligand binding.

Address
Institute of Plant Biology & Zürich-Basel Plant Science Center, University of Zürich, Zollikerstrasse 107, 8008 Zürich, Switzerland

Corresponding authors: Boisson-Dernier, Aurélien (aboisson@access.uzh.ch) and Grossniklaus, Ueli (grossnik@botinst.uzh.ch)
[1] These authors contributed equally to this work.

Current Opinion in Plant Biology 2012, **15**:659–669

This review comes from a themed issue on **Cell biology**

Edited by **Keiko U Torii** and **Masao Tasaka**

For a complete overview see the Issue and the Editorial

Available online 10th August 2012

1369-5266/$ – see front matter,

http://dx.doi.org/10.1016/j.pbi.2012.07.003

Introduction

Plant cells are directing the synthesis and deposition of an extracellular matrix known as the cell wall. This rigid yet dynamic cell wall fulfills various functions that are central to plant growth and development, such as withholding positive and negative pressure, providing cell-to-cell adhesion, directing growth, or constituting the first contact barrier between the cell and its neighboring cells, as well as abiotic stresses and invading microorganisms. Despite their diversity between plant species, organs, cell types, or even microdomains [1], all primary cell walls are made of a complex mixture of carbohydrate components. These typically include cellulose, the main load-bearing structure, which is cross-linked with hemicelluloses and embedded in a matrix of pectins and secreted (glyco)proteins. The cells synthesize primary cell walls during growth, which depends on the balance between loosening/deformation of the pre-existing cell wall and addition of new cell wall material at the site of growth [2]. This coordination requires the growing cell to be informed of any perturbations that impact the properties of its cell wall. The latter is therefore able to modulate the cell's activities, such that the cell can adapt during growth. How a plant cell controls the assembly and remodeling of its cell wall during growth while maintaining its mechanical integrity is one of the most fascinating questions in plant biology [3]. In yeasts which also have cell walls, a conserved cell wall integrity (CWI) maintenance system has been characterized in great detail [4,5]. In plants, the existence of cell wall sensing mechanisms was revealed by studies showing that mutations affecting cell wall synthesis resulted in the activation of hormone signaling pathways and increased resistance to pathogens (e.g. [6,7]). The plant receptor-like kinase (RLK) superfamily has been shown to mediate the sensing to many extracellular cues to regulate intracellular activities [8,9]. RLKs are typically composed of an intracellular serine/threonine kinase domain, a transmembrane domain, and a varied extracellular domain (ECD). The functions of a subset of these RLKs, namely the wall-associated kinases (WAKs), Pro-rich extensin-like receptor kinases (PERKs), lectin receptor kinases (LecRKs), and some leucine-rich repeat (LRR) RLKs, appear to be tightly linked to cell wall synthesis, remodeling, and sensing (reviewed in [3,10–12]). Regarding cell wall surveillance mechanisms, the *Catharantus roseus* RLK1-like (*CrRLK1L*) subfamily with its 17 members (At5g38990, At5g39000, At5g39020, At5g39030, *FER* – At3g51550, *ANX2* – At5g28680, *ANX1* – At3g04690, *HERK2* – At1g30570, At4g39110, At2g21480, At5g61350, *THE1* – At5g54380, At2g39360, At5g59700, *HERK1* – At3g46290, At5g24010, At2g23200) has received increasing attention over the past 6 years [13–15]. CrRLK1 proteins have an ECD with two domains showing limited homology to the carbohydrate-binding domain of the animal Malectin protein [16]. Six out of 17 subfamily members have been proposed to function in coordinating cell growth, cell–cell communication, and cell wall remodeling during both vegetative and reproductive development. Here, we review recent findings concerning downstream targets of the CrRLK1Ls and discuss their putative role in responses to abiotic and biotic stresses and the putative importance of post-translational modifications for these RLKs.

Figure 1

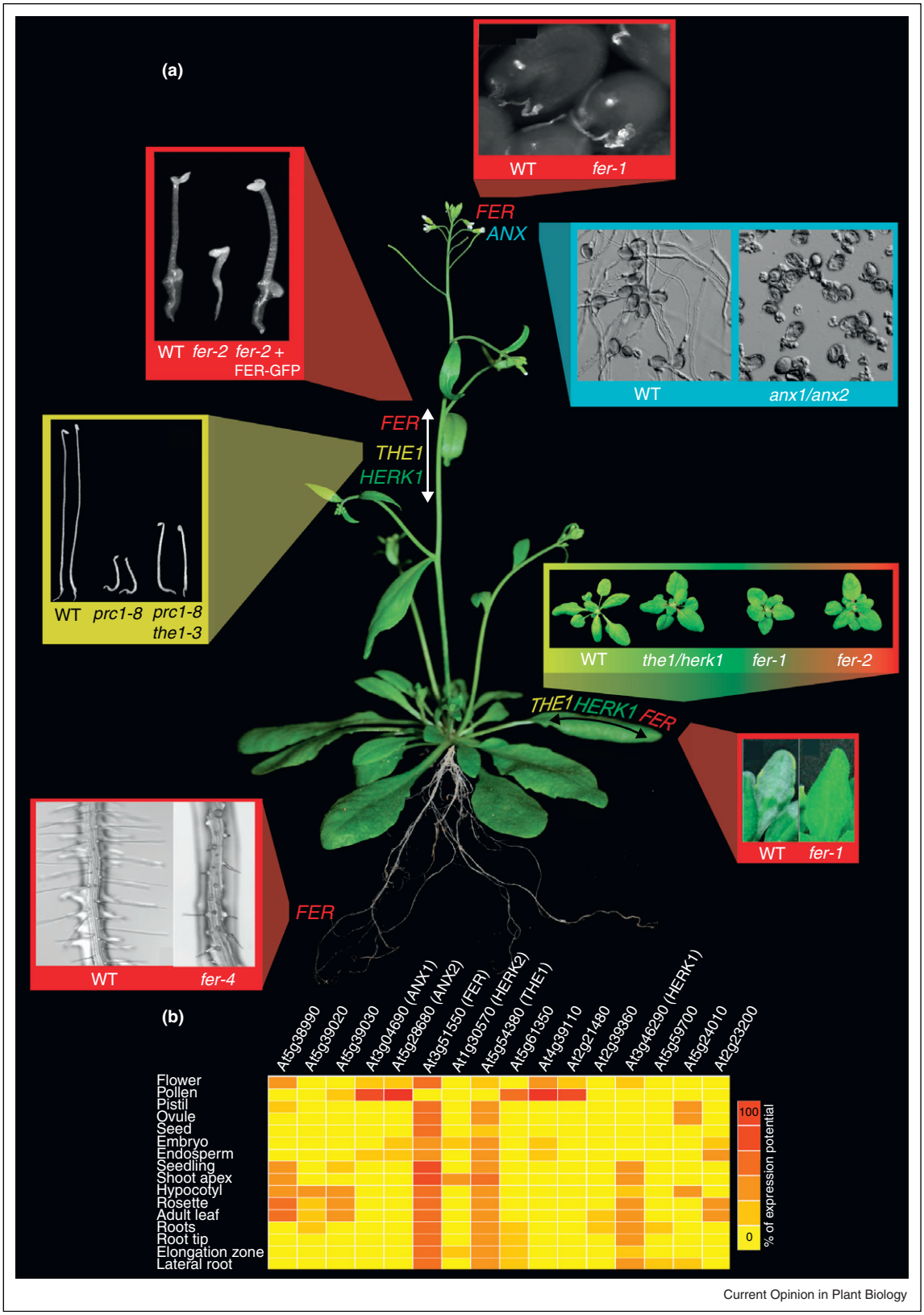
(a)
WT fer-1
FER
ANX
WT fer-2 fer-2 + FER-GFP
WT anx1/anx2
FER
THE1
HERK1
WT prc1-8 prc1-8 the1-3
WT the1/herk1 fer-1 fer-2
THE1 HERK1 FER
WT fer-1
WT fer-4
FER
(b)
At5g38990
At5g39020
At5g39030
At3g04690 (ANX1)
At5g28680 (ANX2)
At3g51550 (FER)
At1g30570 (HERK2)
At5g54380 (THE1)
At5g61350
At4g39110
At2g21480
At2g39360
At3g46290 (HERK1)
At5g59700
At5g24010
At2g23200
Flower
Pollen
Pistil
Ovule
Seed
Embryo
Endosperm
Seedling
Shoot apex
Hypocotyl
Rosette
Adult leaf
Roots
Root tip
Elongation zone
Lateral root
100
0
% of expression potential
Current Opinion in Plant Biology

The role of CrRLK1Ls in cell elongation

FERONIA, *HERCULES1* and *THESEUS1* control cell elongation during vegetative development

Three members of the CrRLK1L subfamily, encoded by *THESEUS1* (*THE1*) and *HERCULES1* (*HERK1*), both named after Greek mythological figures, and *FERONIA* (*FER*), named after an Etruscan goddess of fertility, are plasma membrane-localized receptor-like Ser/Thr-kinases [17••,18••,19•] with some common but also distinct functions during plant development.

THE1 was discovered as suppressor of the cellulose synthase-deficient mutant *procuste1* (*cesA6*$^{prc1\text{-}1}$), partially rescuing its short hypocotyl phenotype when grown in the dark (Figure 1a) [18••]. This suppression is not due to a recovery of cellulose biosynthesis in the *prc1*/*the1* double mutant. Rather, sensing of perturbations in cell wall composition seems affected since the *the1* mutation has no apparent phenotype in a context with intact cell walls. This was the first evidence that a defect in cellulose synthesis did not restrict cell growth physically, but that cell elongation is actively inhibited by *THE1*-dependent sensing of cell wall perturbations. Moreover, *THE1* is required for lignin accumulation that is either caused by mutations in the cellulose-synthase complex [18••] or by the cellulose synthesis inhibitor isoxaben [20•]. Isoxaben treatment also induces the accumulation of reactive oxygen species (ROS) in wild-type seedlings, but this happens neither in *the1* nor in *rbohD*/*rbohF* mutants that affect the ROS-producing NADPH oxidase [20•]. These studies indicate that if CWI is not sustained, THE1 activates a signal transduction pathway leading to ROS production, growth inhibition, and lignin accumulation.

In contrast to its inhibitory effect on cellular growth in cell wall damaged contexts, *THE1* was found to be required for cell elongation during vegetative growth together with *HERK1* and *FER* (Figure 1a) [19•]. All three genes were shown to be upregulated after treatment with brassinosteroid (BR) [21], a plant hormone involved in many growth and developmental processes [22]. Additionally, all three genes were shown to be plasma membrane-localized and are widely expressed in most vegetative tissues such as leaves, stems and roots (Figure 1b) [17••,18••,19•], with a stronger expression in regions with elongating cells [19•]. *THE1* and *HERK1* seem to act redundantly since the single null mutants have no obvious vegetative phenotype. However, the *the1*/*herk1* double mutant displays cell elongation defects in leaves and leaf petioles with an even stronger phenotype in the *the1*/*herk1*/*herk2* triple mutant [23]. Homozygous *fer* single mutants show a comparable cell elongation defect, leading to the hypothesis that FER could act as a co-receptor of THE1/HERK RLKs. In addition, similar genes are mis-expressed in the respective mutants, further supporting that *THE1*/*HERK* and *FER* may act in a common pathway [19•].

Despite the transcriptional increase of these three members of the *CrRLK1L* subfamily after BR treatment, the *THE1*/*HERK* pathway regulating cell elongation seems to be largely independent of BRs because only a subset of BR influenced genes are affected in the *the1*/*herk1* mutant [19•]. By contrast, it was shown that *fer* null mutants display an imbalance of endogenous ethylene and BRs [24]. Whereas hypocotyls of light-grown *fer* mutants show an enhanced BR response, dark-grown etiolated *fer* seedlings are partially BR-insensitive and display an enhanced ethylene response, leading to shorter hypocotyls in the mutant (Figure 1a).

FERONIA, *ANXUR1* and *ANXUR2* maintain cell wall integrity to sustain polar growth

In addition to its role during cell elongation in leaves and hypocotyls [19•], Duan *et al.* [25••] revealed an interaction between FER and ROPGEF1 in yeast and root protoplast cells. ROPGEFs belong to the guanine exchange factor family [26,27], activating Rho-like GTPases, monomeric GTP-binding proteins that are known as RAC/ROPs in plants. These RAC/ROPs accomplish various signaling functions that regulate development and polar growth [28].

Interestingly, the disruption of *FER* disturbs the polar growth of root hairs, as *fer* mutant roots carry arrested, collapsed, short, and bursting root hairs (Figure 1a) [25••]. This phenotype is similar to that of the *root hair defective2* (*rhd2*) mutant, in which the ROS-producing NADPH oxidase *RbohC* is affected [29,30•,31]. Reduced levels of activated RAC/ROP in *fer* null mutants support the role of FER as an upstream regulator of ROPs [32]. Furthermore, reduced levels of ROS in *fer* compared to wild-type roots indicate that the interaction of FER and

(Figure 1 Legend) (a) Phenotypes of CrRLK1L subfamily mutants during plant development and reproduction. Explanation in clockwise rotation starting at the flowers: aniline-blue staining of callose in pollen tubes two days after pollination. Fertilized wild-type ovule (left) and *fer* mutant embryo sac (right) with abnormal pollen tube reception (pollen tube overgrowth). In *anx1*/*anx2* double mutants (right) pollen tubes burst directly after germination *in vitro*, whereas wild-type pollen tubes (left) are rapidly growing. During vegetative growth *the1*/*herk1* double mutants show a severe phenotype (short petioles), which is comparable to the dwarf phenotype of homozygous *fer-1* and *fer-2* mutants. Powdery mildew infected plants with fungal mycelium and conidiophores on the wild-type leaf (left), whereas the *fer-1* mutant is resistant (right). Root hairs of 4-day old *fer-4* mutant seedlings display a severe defect with short, collapsing, and bursting root hairs, compared to the wild type (left). The *the1* mutant was found as suppressor of the cellulose synthase-deficient mutant *prc1*, partially rescuing its short-hypocotyl phenotype in 5-day old dark-grown seedlings (right). Dark-grown etiolated *fer-2* seedlings display an enhanced ethylene response after 4 days of growth in ethylene, leading to shorter hypocotyls in the mutant (middle) compared to the wild type (left) and *fer-2* mutants complemented with a FER-GFP construct (right). Figure 1 **(a)** is adapted from [19•,24,25••,45••] **(b)** Relative gene expression of *CrRLK1Ls* in various plant tissues according to Genevestigator microarray database using the Meta-Profile Analysis tool, Anatomy Profile [76].

ROPGEFs, with the subsequent activation of ROPs, result in NADPH oxidase-dependent ROS production.

Intriguingly, *FER*'s two closest homologs in *Arabidopsis* are preferentially expressed in pollen tubes (Figure 1b) – the male gametophytes that, like root hairs, elongate polarly – and are localized to the plasma membrane of the pollen tube tip [33•,34•]. Thus, they were named after the male consort of Feronia, *ANXUR1* (*ANX1*) and *ANXUR2* (*ANX2*). They share 85.6% amino acid level identity and work redundantly since only double mutant plants show a severe male sterility phenotype. Sterility occurs because *anx1/anx2* double mutant pollen tubes lose their cellular integrity and burst during growth between the stigma and the style, preventing them to reach and fertilize the female gametes (Figure 1a) [33•,34•]. Because of the similarity between the *fer* root hair and *anx1/anx2* pollen tube phenotypes, it would be important to investigate whether ANX1/2 regulate NADPH oxidase-dependent ROS production in pollen tubes as FER does in root hairs. Nonetheless, FER and ANX1/2 appear to function at the tip of polarly growing cells to prevent loss of CWI during rapid growth.

CrRLKL1s in cell–cell communication

FERONIA triggers pollen tube discharge during fertilization

Communication between cells is a crucial process in plant development, reproduction, and defense. The communication between male and female tissues is important during every step of pollination and fertilization: communication between stigma cells and pollen grains leads to pollen hydration and germination of the pollen tubes [35]. After growing through the style and transmitting tract, pollen tubes are guided towards the ovules by small cysteine-rich proteins that are secreted by the synergid cells [36,37]. The two female gametes, the egg and central cell, are also involved in this process but their role is less well understood [38,39]. Importantly, cell–cell communication is also required during the final stages of reproduction, when the pollen tube enters the degenerating synergid, ruptures, and releases the two sperm cells to effect double fertilization [17••,40].

The allelic female gametophytic *fer* and *sirène* mutants – hereafter referred to as *fer* – were identified because they disrupt the communication process between male and female cells during pollen tube reception [41,42]. *FER* is – with the exception of mature pollen – expressed throughout the whole plant (Figure 1b) and strongly accumulates in the female gametophyte at the filiform apparatus, a specialized cell wall structure at the basal end of the synergid cells [17••,43]. In *fer* mutant ovules, the pollen tube does not rupture after entering the female gametophyte, but instead continues to grow in the embryo sac, leading to a pollen tube overgrowth phenotype (Figure 1a) [41,42]. Consequently, *fer* mutant embryo sacs remain unfertilized. In addition, *fer* mutant ovules can attract supernumerary pollen tubes. The mutation does not affect the development or identity of female gametophytic cells, thus only the communication process between male and female gametophytes appears impaired. Hypothetically, FER could recognize a ligand secreted or carried by the pollen tube. Alternatively, FER could interact with a ligand originating from female tissues, which could reflect a change or modification of the cell wall structure caused by the arriving pollen tube.

Whereas *ANX1/2* seem to be required to sustain pollen tube growth and prevent bursting within female tissues, *FER* inhibits pollen tube growth and positively regulates pollen tube discharge after pollen tube arrival in the synergid. Therefore, it is possible that upon pollen tube arrival the *ANX1/2*-dependent pathway gets inactivated in pollen, while the *FER* signaling cascade becomes activated in the female gametophyte to prepare pollen tube discharge and fertilization. It has been proposed that during pollen tube reception FER and ANX1/2 could compete for the same ligand, a competition that would result in inactivation of the ANX1/2-dependent pollen tube integrity and the activation of the FER-mediated pollen tube recognition [44].

After the discovery of *FER*, several other mutants displaying a similar pollen tube overgrowth phenotype in the embryo sac have been identified: *nortia* (*nta*), which will be discussed below [45••]; *lorelei* (*lre*), a mutation affecting a glycosylphosphatidylinositol (GPI)-anchored protein expressed in the embryo sac [46]; *scylla* (*syl*), which displays, in addition to pollen tube overgrowth, fertilization-independent endosperm development [47], and the mutant *abstinence by mutual consent* (*amc*) affecting a gene encoding a peroxin, where the failure in pollen tube growth arrest is only observed when both male and female gametophytes carry the mutation [48]. The latest mutant with disrupted pollen tube reception and *fer*-like pollen tube overgrowth is *turan* (*tun*), named after an Etruscan goddess of love and fertility, affecting a gene encoding a UDP-glycosyltransferase superfamily protein [49]. The exact role these genes play in the *FER* signal transduction pathway remains to be elucidated.

Pollen tube reception and fungal invasion recruit the same *FER*-dependent pathway

NTA is a member of the plant-specific MILDEW RESISTANCE LOCUS O (MLO) family of proteins [45••]. The MLO protein family was first identified because it plays a role in powdery mildew resistance and mutations in *MLO* genes confer resistance to powdery mildew, while presence of the wild-type proteins causes susceptibility [50,51]. Fungal invasion is analogous to the fertilization process and strongly relies on cell–cell communication: when a fungal spore lands on an epidermal cell, it hydrates, germinates, and the tip-growing fungal hyphae penetrate

the host cell wall in order to establish feeding structures called haustoria [52]. The host cell reacts with re-organization of the cell polarity, which includes the transport of MLO proteins towards the penetration site [53], and will eventually lead to a reinforcement of the cell wall [52].

NTA is localized throughout the cytoplasm of the synergids before fertilization, and gets polarly localized to the basal part of the synergid cells after arrival of the pollen tube [45••]. However, this does not occur in *fer* mutant embryo sacs, indicating that the re-localization of NTA fully depends on a functional *FER* signaling pathway. Supporting this link between fungal invasion and pollen tube reception, *fer* homozygous mutants are resistant to infection by the powdery mildew *Golovinomyces* (*syn. Erysiphe*) *orontii*, which infects *Arabidopsis* (Figure 1a) [45••]. This suggests that the correct positioning of NTA or other MLO proteins to the filiform apparatus and the fungal penetration site, respectively, are crucial for successful pollen tube reception and fungal invasion. Their re-localization depends on *FER*, which might recognize the cell wall changes caused by either invading pollen tubes or fungal hyphae.

Biotic and abiotic stress responses modulate CrRLK1L transcript levels

As abiotic stresses and microorganisms can deeply impact plant growth and the molecular and mechanical properties of the cell wall, it is not surprising that plants respond to these extracellular challenges by modulating the expression levels of the *CrRLK1L* gene family. Among them, *THE1* is the member whose transcript levels are influenced the most by abiotic stresses, while *At5g39030* transcript levels do not show dramatic changes (Figure 2).

Figure 2

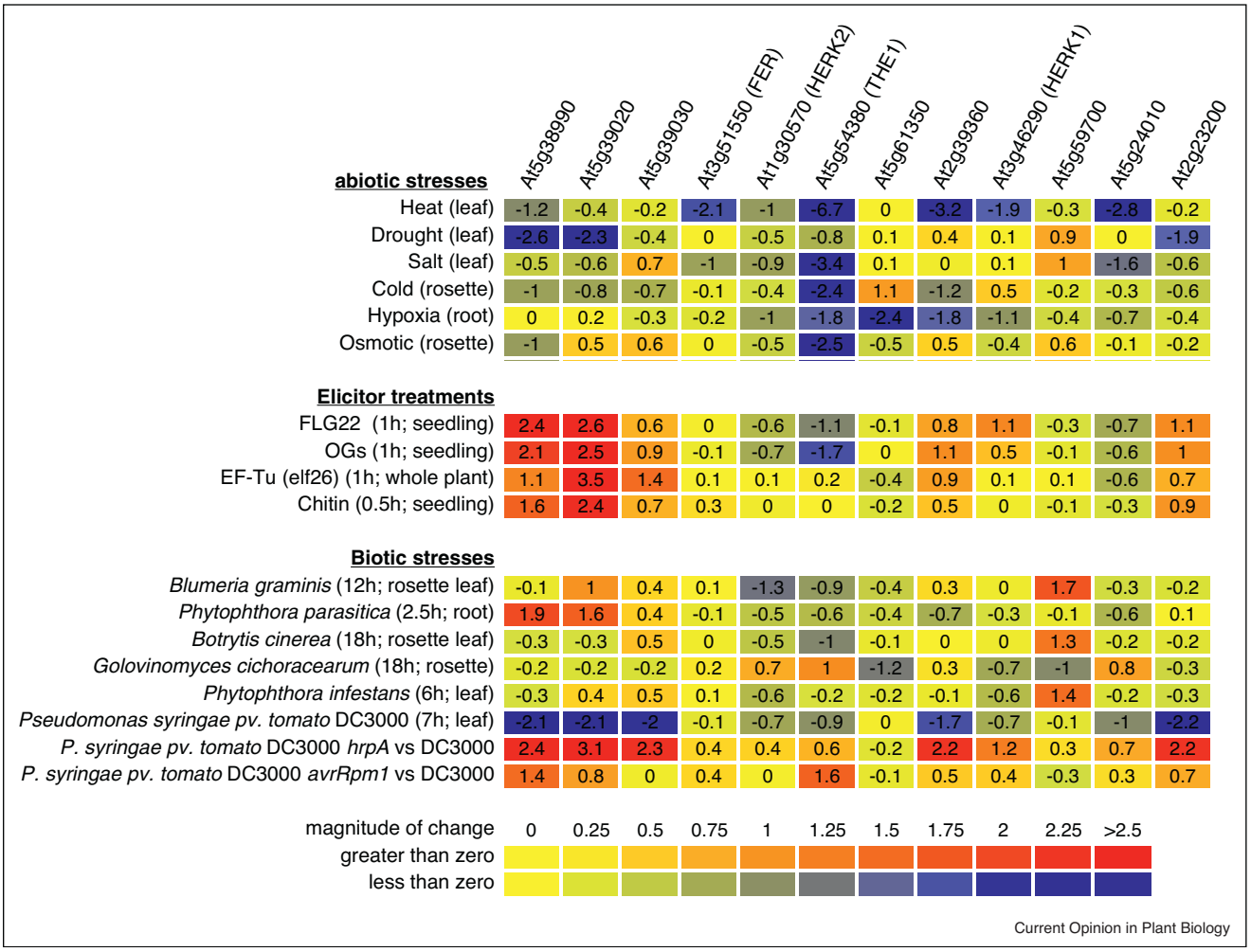

Significant transcript level changes for the *Arabidopsis CrRLK1L* gene subfamily under abiotic, elicitor, and biotic treatments. Changes in steady-state transcript levels for the *CrRLK1Ls* that are not preferentially expressed in pollen were obtained from the Genevestigator microarray database [76]. Data are represented as log(2)-ratio versus mock or untreated control (if not specified), and are filtered via the Genevestigator Perturbations tool for treatments that induce a fold-change >2 (p-value <0.05) for at least one member of the *CrRLK1Ls*. The heat map was generated using the HeatMapper Tool (http://bar.utoronto.ca/ntools/cgi-bin/ntools_heatmapper.cgi). Note that *At5g39000* is represented by the same probe as *At5g38990*.

Figure 3

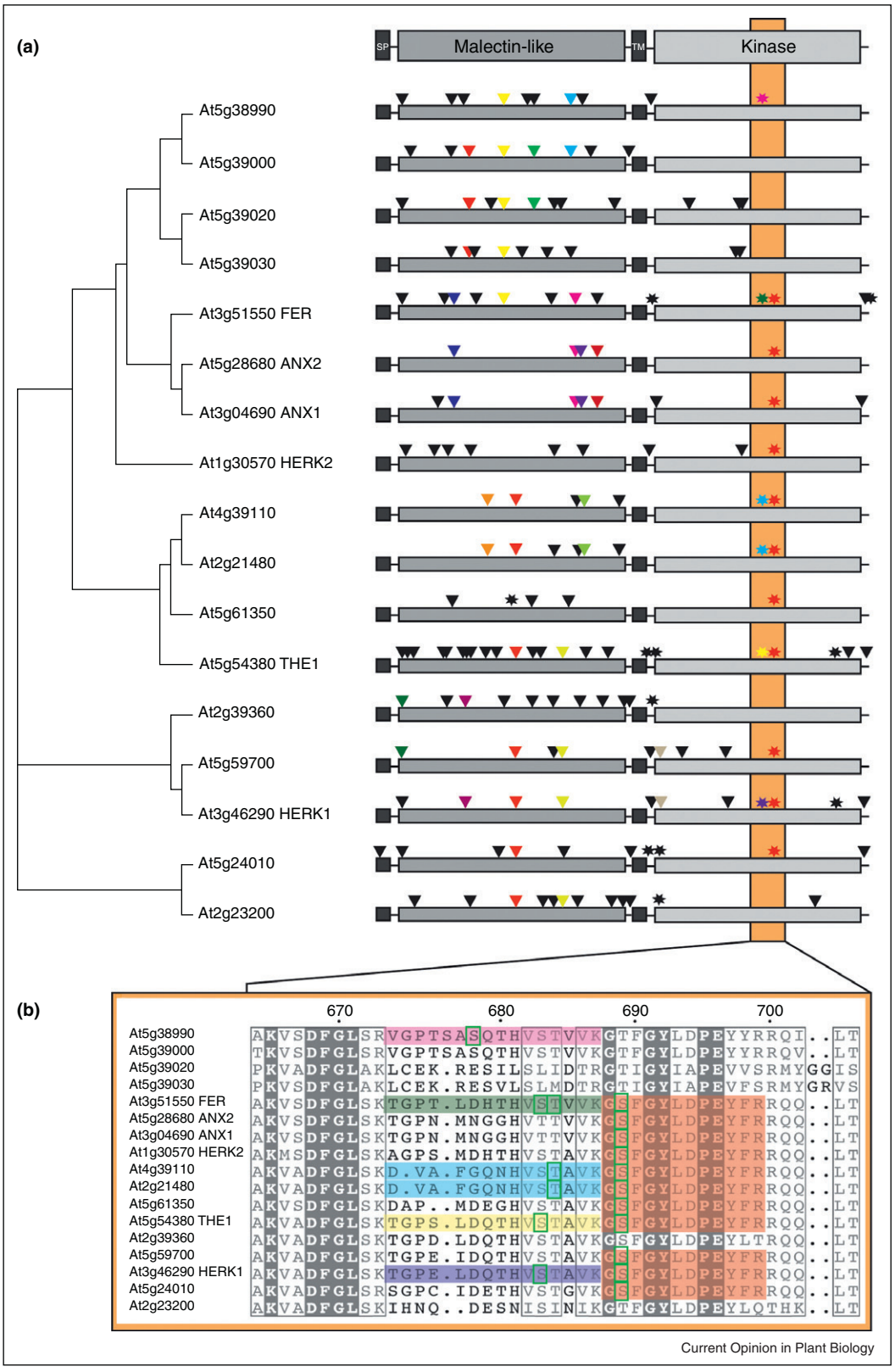

Phylogenetic tree, domain organization, and post-translational modifications of the CrRLK1Ls. **(a)** Phylogenetic tree of the 17 members of the *Arabidopsis* CrRLK1L subfamily with their domain organization and post-translational modifications. Triangles: putative glycosylation sites based on

The global plant response to environmental stresses is complex because plants integrate the environmental challenges at every organization level in both time and space. Abiotic stresses trigger various and numerous effects in plants, and eventually lead to growth inhibition. Besides ion imbalance, one of the consensus stress-induced effects is the enhanced accumulation of ROS, which can become harmful to plant cells by damaging lipids, proteins, DNA, and carbohydrates (e.g. [54]). Therefore, to cope efficiently with surrounding stresses, plants have to shift the balance of ROS detoxification/production towards detoxification. Curiously, little variation in gene expression is observed for the ROS-producing enzymes, the Rboh NADPH-oxidases, under abiotic stresses [55]. However, abiotic stresses result globally in downregulation of *CrRLK1Ls*, with heat treatment and hypoxia being the most effective (Figure 2). Since an emerging role for the *CrRLK1L* subfamily appears to be the regulation of NADPH-oxidase-dependent ROS production [20,25••], downregulation of *CrRLK1L* transcript levels in response to abiotic stress could be a strategy plants have developed to reduce the production of ROS. Although no abiotic stress-related phenotype has been described for any *CrRLK1L* mutants, it would be interesting to test whether some of these mutants, for example, *the1* or *fer*, exhibit impaired an response to abiotic stresses such as heat-shock protein accumulation under heat stress [56].

The functional importance among *CrRLK1Ls* during plant-microorganism interactions has so far only been revealed for *FER*, which mediates susceptibility to *G. orontii* and is affected in FLG22-induced ROS production, MAPK activity, and stomatal closure [45••,57]. To protect themselves from microorganisms, plants are able to sense danger by recognizing conserved pathogen-associated or microbe-associated molecular patterns (PAMPs or MAMPs) through pattern-recognition receptors (PRRs). They also recognize their own molecular patterns, referred to as damage-associated molecular patterns (DAMPs), which appear only when plant tissue is infected or damaged. Those molecular patterns are collectively called elicitors when applied externally. They rapidly induce plant innate immune responses characterized by a quick increase in cytosolic Ca^{2+}, MAPK signaling activation, ROS production, cell wall reinforcements, and defense-related gene expression [58]. Except for *THE1* and *At5g24010*, elicitor treatments result in a rapid increase of *CrRLK1L* transcript levels with *At5g39020* and *At5g38990* being upregulated the most consistently across elicitor treatments, followed by *At3g39030*, *At2g39360* and *At2g23200* (Figure 2). Moreover, the transcript levels of these five *CrRLK1Ls* are highly downregulated in response to inoculation with virulent *Pseudomonas syringae pv. tomato* and this downregulation is completely dependent on the ability of the bacteria to secrete effectors into the plant (Figure 2, see difference with *P. syringae pv. tomato* DC3000 *hrpA* mutant strain vs virulent DC3000 strain). As secreted bacterial effectors suppress PAMP-triggered responses [59], it would be worth to investigate the role of those *CrRLK1Ls* in PAMP-triggered immunity; for example, they could be part of and regulate PAMP RLK complexes. In this respect, the fact that the *P. syringae* effector AvrPto interacts *in vitro* with and inhibits the autophosphorylation of the elicitor-induced CrRLK1L At2g23200 as well as the PRRs FLAGELLLIN-SENSING2 (FLS2) and the EF-Tu receptor (EFR) could be of significant importance [60•].

Post-translational modifications could be crucial for *CrRLK1L* function

Phosphorylation of the kinase domain might be involved in signal transduction

Protein regulation by phosphorylation or dephosphorylation is an important means to modulate cellular processes and is accomplished by protein kinases and phosphatases, respectively. It has been shown *in vitro* that the kinase domains of FER and At2g23200 are active and able to autophosphorylate [17••,60•]; however, the biological relevance of phosphorylation is unknown. Several studies have experimentally assessed the phosphoproteome of various plant tissues under different environmental conditions, discovering several phosphopeptides that could be assigned to various members of the CrRLK1L subfamily (Figure 3) [61,62,63•,64,65]. Only recently, a study investigating the pollen phosphoproteome was published [66]. This is especially interesting because *de novo* transcription is not essential for pollen germination and initial tube growth. Therefore, the cellular machinery leading to pollen germination and rapid tip growth must be regulated at the post-transcriptional level. In their study, Mayank *et al.* identified two different ambiguous phosphopeptides representing the CrRLK1L subfamily [66]. The first phosphopeptide, with a phosphorylated threonine, is only conserved between At2g21480 and

(Figure 3 Legend Continued) prediction by NetNGlyc1.0. Only significant sites are depicted. Black triangles: unique glycosylation sites. Colorful triangles: glycosylation sites that are conserved in their location and sequence between family members. Asterisks: phosphorylation sites. Black asterisks: unique phosphosites. Red asterisks: conserved phosphosite between 11 members of the CrRLK1L subfamily that lies within the activation loop of the kinase domain. Colorful asterisks: phosphosites that are within the activation loop, but not conserved between members or only between two close relatives (blue asterisks). The colors of the asterisks are consistent with the color code in panel **(b)**. **(b)** Multiple sequence alignment of a section of the activation loop of the kinase domain of CrRLK1Ls. Shaded in red: phosphopeptide that is conserved between 11 members. Shaded in colors: phosphopeptides within the activation loop that are not conserved or only conserved between two members (blue). Note that the color code is consistent with the asterisks in panel **(a)**. Green rectangles: experimentally validated/confirmed phosphorylation sites. Phosphorylation sites and phosphopeptides in panels **(a)** and **(b)** are based on [61,62,63•,64–66,77].

At4g39110, which are specifically expressed in pollen (Figure 1) [15]. The second identified phosphopeptide, with a phosphorylated serine, perfectly matches 11 members of the CrRLK1L subfamily, including THE1, HERK1 and FER, but can be assigned to the four representatives that are preferentially expressed in pollen: ANX1 and ANX2 and the above-mentioned At2g21480 and At4g39110 (Figure 3b).

Interestingly, the very same phosphopeptide has been identified before in suspension-cultured cells and lies within the activation loop of the kinase domain of CrRLK1Ls [63•], pointing towards the importance of an active kinase domain in all these proteins. It will be interesting to experimentally verify the biological importance of the phosphorylation sites *in vivo*, for example by direct manipulation of the relevant amino acids and mutant complementation assays. So far the only known interactors of the intracellular domain for CrRLK1L members are ROPGEFs, ROPs and AvrPto [25••,60•]. Further studies addressing whether the CrRLK1Ls are able to directly phosphorylate ROPGEFs/ROPs or if other kinases are involved are awaited for.

Ligand binding may depend on N-linked glycosylation of the extracellular domain

Recently, several studies have proposed a role in pollen tube guidance and fertilization for proteins involved in endoplasmic reticulum (ER) quality control of secreted proteins [67,68] and glycosylation [49], respectively. Whereas the pollen tubes of *pollen defective in guidance1* (*pod1*) and *cation/proton exchanger chx21/chx23* mutants are impaired in targeting embryo sacs, *tun* mutant female gametophytes are defective in pollen tube reception. *POD1* encodes a protein of unknown function, and localizes, like CHX23, to the ER. *TUN* encodes a UDP-glycosyltransferase superfamily protein, which might play a role in glycosylating proteins in the ER. N-linked glycosylation refers to the co-translational and post-translational covalent attachment of an oligosaccharide (Glc_3-Man_9-$GlcNAc_2$ in eukaryotes) in the N-X-S/T context, where X stands for every amino acid except proline [69]. After attachment of the oligosaccharide (glycan) to a protein in the ER, it can be further modified in the secretory pathway. In plants, the glycans on glycoproteins are important for the protein folding process within the ER [70]. Beyond the ER, N-glycans affect catalytic activity, stability, and folding, as well as the subcellular localization and secretion of proteins. Furthermore, N-glycosylation seems to be involved in plant pathogen interactions and in the functional binding of ligands to PRRs belonging to the RLK family [71].

The extracellular region of the 17 members of the *Arabidopsis* CrRLK1L subfamily consists of two domains with limited homology to the carbohydrate-binding domain of Malectin, and is referred as malectin-like domain (Figure 3) [13]. Malectin was found as an ER-membrane localized lectin in *Xenopus laevis* and binds carbohydrates with selectivity for di-glucose-high mannose N-glycan (Glc_2-N-glycan) [16]. More recently, this protein has been found to participate in mammalian ER-quality control for glycoproteins [72]. Although CrRLK1L subfamily members contain a malectin-like domain, they are not thought to be involved in N-glycosylation owing to their plasma membrane localization and the weak conservation of residues mediating the interaction with glucose residues in the original Malectin. Nevertheless, it is interesting to note that all 17 members have several putative N-glycosylation sites (3–16 sites), 43–100% of those lie in the extracellular malectin-like domain (Figure 3a). Proteins with higher identities share several N-glycosylation sites even in the extracellular region, which is less conserved among the CrRLK1L members. The functional importance of the N-glycosylation sites in malectin-like domains is unknown, but Haweker *et al.* [73•] showed that a mutation in a single conserved glycosylation site in the ECD of the EFR–RLK, involved in receptor-mediated immune response, leads to a loss of ligand (elf18) binding ability.

That glycosylation sites can be involved in ligand binding is further encouraged by the role they play during fertilization in animals. There, cross-linked glycoprotein filaments in the extracellular coat of the oocyte, the zona pellucida, mediate species-restricted recognition between the gametes [74]. A mutation in a single glycosylation site of the zona pellucida glycoprotein 3 (ZP3) reduced sperm binding by 80% [75]. One of the known roles of *FER* is to prepare the female gametophyte for fertilization. It is very likely that the ECD of this RLK interacts with signals outside the cell, which are transduced by a signaling cascade inside the synergid cell. The presence of a malectin-like domain in its ECD leads us to speculate that the putative ligand of the CrRLK1L kinases could contain polysaccharides. Whether these putative ligands originate from degraded cell wall components or from secreted glycosylated proteins, and if some glycosylation sites in the malectin-like domain mediate ligand-binding, requires further investigations.

Conclusion

The plant cell wall has to be able to react quickly to external and internal signals. External signals can be abiotic stresses, biotic stresses such as pathogens, or invading pollen tubes. By contrast, internal signals originate from the plant's own tissues, leading to adaptations such as cell elongation during plant growth. Characterized members of the CrRLK1L subfamily seem to play a crucial role in sensing cell wall perturbations. Signal perception and transduction could rely on post-translational modifications such as N-glycosylation and phosphorylation. These modifications can be specific for different cell types, tissues, and species. This could explain, for example, why *FER*, which

is widely expressed throughout the plant, can accomplish diverse functions depending on the tissue or organ it is expressed in. We anticipate that further studies on this subfamily of RLKs will impact many important aspects of plant biology, including cell wall remodeling, glycobiology, cell growth, cell–cell communication, as well as plant responses to abiotic and biotic stresses.

Acknowledgements

We thank Cyril Zipfel, Robert Dudler, and the members of the Grossniklaus group, in particular Sharon Kessler, for enriching discussions, and our esteemed colleagues Kian Hématy, Herman Höfte, Alice Cheung, Yanhai Yin and Paul Larsen for generously providing the original pictures shown in Figure 1. The work on the CrRLK1L family in our lab is supported by the University of Zürich, the Forschungskredit der Universität Zürich and the European Union through a Marie Curie International Reintegration grant to A.B.-D., grants of the Swiss National Science Foundation (31003A-112489) and SystemsX.ch ('Plant Growth') to U.G., and support for H.L. and L.M.M. through Research Modules of the ProDoc Programs 'Molecular Life Sciences' and 'Plant Science and Policy' to U.G.

References and recommended reading

Papers of particular interest, published within the period of review, have been highlighted as:

- • of special interest
- •• of outstanding interest

1. Popper ZA, Michel G, Herve C, Domozych DS, Willats WG, Tuohy MG, Kloareg B, Stengel DB: **Evolution and diversity of plant cell walls: from algae to flowering plants**. *Annu Rev Plant Biol* 2011, **62**:567-590.

2. Cosgrove DJ: **Growth of the plant cell wall**. *Nat Rev Mol Cell Biol* 2005, **6**:850-861.

3. Wolf S, Hématy K, Höfte H: **Growth control and cell wall signaling in plants**. *Annu Rev Plant Biol* 2012, **63**:381-407.

4. Levin DE: **Regulation of cell wall biogenesis in *Saccharomyces cerevisiae*: the cell wall integrity signaling pathway**. *Genetics* 2011, **189**:1145-1175.

5. Ernst JF, Pla J: **Signaling the glycoshield: maintenance of the *Candida albicans* cell wall**. *Int J Med Microbiol* 2011, **301**: 378-383.

6. Ellis C, Karafyllidis I, Wasternack C, Turner JG: **The *Arabidopsis* mutant *cev1* links cell wall signaling to jasmonate and ethylene responses**. *Plant Cell* 2002, **14**:1557-1566.

7. Cano-Delgado A, Penfield S, Smith C, Catley M, Bevan M: **Reduced cellulose synthesis invokes lignification and defense responses in *Arabidopsis thaliana***. *Plant J* 2003, **34**:351-362.

8. Shiu SH, Bleecker AB: **Expansion of the receptor-like kinase/ Pelle gene family and receptor-like proteins in *Arabidopsis***. *Plant Physiol* 2003, **132**:530-543.

9. Gish LA, Clark SE: **The RLK/Pelle family of kinases**. *Plant J* 2011, **66**:117-127.

10. Steinwand BJ, Kieber JJ: **The role of receptor-like kinases in regulating cell wall function**. *Plant Physiol* 2010, **153**:479-484.

11. Seifert GJ, Blaukopf C: **Irritable walls: the plant extracellular matrix and signaling**. *Plant Physiol* 2010, **153**:467-478.

12. Ringli C: **Monitoring the outside: cell wall-sensing mechanisms**. *Plant Physiol* 2010, **153**:1445-1452.

13. Boisson-Dernier A, Kessler SA, Grossniklaus U: **The walls have ears: the role of plant CrRLK1Ls in sensing and transducing extracellular signals**. *J Exp Bot* 2011, **62**:1581-1591.

14. Cheung AY, Wu HM: **THESEUS 1, FERONIA and relatives: a family of cell wall-sensing receptor kinases?** *Curr Opin Plant Biol* 2011, **14**:632-641.

15. Hématy K, Höfte H: **Novel receptor kinases involved in growth regulation**. *Curr Opin Plant Biol* 2008, **11**:321-328.

16. Schallus T, Jaeckh C, Feher K, Palma AS, Liu Y, Simpson JC, Mackeen M, Stier G, Gibson TJ, Feizi T *et al.*: **Malectin: a novel carbohydrate-binding protein of the endoplasmic reticulum and a candidate player in the early steps of protein N-glycosylation**. *Mol Biol Cell* 2008, **19**:3404-3414.

17. •• Escobar-Restrepo JM, Huck N, Kessler S, Gagliardini V, Gheyselinck J, Yang WC, Grossniklaus U: **The FERONIA receptor-like kinase mediates male-female interactions during pollen tube reception**. *Science* 2007, **317**:656-660.
This paper describes the molecular characterization of FERONIA, a receptor-like serine/threonine kinase that is highly expressed in synergid cells. It is shown that the kinase domain is able to autophosphorylate *in vitro*, consistent with a role in cell–cell communication.

18. •• Hématy K, Sado PE, Van Tuinen A, Rochange S, Desnos T, Balzergue S, Pelletier S, Renou JP, Höfte H: **A receptor-like kinase mediates the response of *Arabidopsis* cells to the inhibition of cellulose synthesis**. *Curr Biol* 2007, **17**:922-931.
This paper presents the identification of *theseus1* as a suppressor of the cellulose-deficient mutant *procuste1* (cesA6^{prc1-1}), rescuing the short-hypocotyl phenotype. It is proposed that THE1 senses cell wall perturbations and in turn regulates cell elongation.

19. • Guo H, Li L, Ye H, Yu X, Algreen A, Yin Y: **Three related receptor-like kinases are required for optimal cell elongation in *Arabidopsis thaliana***. *Proc Natl Acad Sci USA* 2009, **106**: 7648-7653.
In this report it is shown that HERK1, another CrRLK1L subfamily member, and THE1 are acting redundantly in cell elongation during vegetative development. *fer* and *herk1/the1* display a dwarf phenotype, indicating a role in cell expansion.

20. • Denness L, McKenna JF, Segonzac C, Wormit A, Madhou P, Bennett M, Mansfield J, Zipfel C, Hamann T: **Cell wall damage-induced lignin biosynthesis is regulated by a reactive oxygen species- and jasmonic acid-dependent process in *Arabidopsis***. *Plant Physiol* 2011, **156**:1364-1374.
This paper shows that cell wall damage-induced lignin deposition requires both THE1 and the ROS-producing NADPH oxidases RbohD and RbohF, further strengthening the link between CrRLK1Ls and control of ROS production.

21. Nemhauser JL, Mockler TC, Chory J: **Interdependency of brassinosteroid and auxin signaling in *Arabidopsis***. *PLoS Biol* 2004, **2**:E258.

22. Kim TW, Wang ZY: **Brassinosteroid signal transduction from receptor kinases to transcription factors**. *Annu Rev Plant Biol* 2010, **61**:681-704.

23. Guo H, Ye H, Li L, Yin Y: **A family of receptor-like kinases are regulated by BES1 and involved in plant growth in *Arabidopsis thaliana***. *Plant Signal Behav* 2009, **4**:784-786.

24. Deslauriers SD, Larsen PB: ***FERONIA* is a key modulator of brassinosteroid and ethylene responsiveness in *Arabidopsis* hypocotyls**. *Mol Plant* 2010, **3**:626-640.

25. •• Duan Q, Kita D, Li C, Cheung AY, Wu HM: **FERONIA receptor-like kinase regulates RHO GTPase signaling of root hair development**. *Proc Natl Acad Sci USA* 2010, **107**:17821-17826.
This is the first discovery of an interactor of FER. FER and ROPGEF1 physically interact, leading to the activation of RAC/ROPs. *fer* mutants have arrested, collapsed, and bursting root hairs.

26. Gu Y, Li S, Lord EM, Yang Z: **Members of a novel class of *Arabidopsis* Rho guanine nucleotide exchange factors control Rho GTPase-dependent polar growth**. *Plant Cell* 2006, **18**: 366-381.

27. Berken A, Thomas C, Wittinghofer A: **A new family of RhoGEFs activates the Rop molecular switch in plants**. *Nature* 2005, **436**:1176-1180.

28. Nibau C, Wu HM, Cheung AY: **RAC/ROP GTPases: 'hubs' for signal integration and diversification in plants**. *Trends Plant Sci* 2006, **11**:309-315.

29. Schiefelbein JW, Somerville C: **Genetic control of root hair development in *Arabidopsis thaliana***. *Plant Cell* 1990, **2**: 235-243.

30. Monshausen GB, Bibikova TN, Messerli MA, Shi C, Gilroy S:
• **Oscillations in extracellular pH and reactive oxygen species modulate tip growth of *Arabidopsis* root hairs**. *Proc Natl Acad Sci USA* 2007, **104**:20996-21001.
The authors provide evidence that the NADPH oxidase RbohC generates ROS oscillations in the lateral walls behind the root hair apex. However, RbohC is not absolutely required to maintain a tip-focused Ca^{2+} gradient, which plays a central role in polar growth.

31. Foreman J, Demidchik V, Bothwell JH, Mylona P, Miedema H, Torres MA, Linstead P, Costa S, Brownlee C, Jones JD *et al.*: **Reactive oxygen species produced by NADPH oxidase regulate plant cell growth**. *Nature* 2003, **422**:442-446.

32. Swanson S, Gilroy S: **ROS in plant development**. *Physiol Plant* 2010, **138**:384-392.

33. Boisson-Dernier A, Roy S, Kritsas K, Grobei MA, Jaciubek M,
• Schroeder JI, Grossniklaus U: **Disruption of the pollen-expressed *FERONIA* homologs *ANXUR1* and *ANXUR2* triggers pollen tube discharge**. *Development* 2009, **136**:3279-3288.
This study describes the two closest homologues of FER, ANX1/2, which are preferentially expressed in pollen tubes. They act redundantly in maintaining the CWI of pollen tubes and anx1/anx2 double mutants are sterile owing to premature pollen tube rupture.

34. Miyazaki S, Murata T, Sakurai-Ozato N, Kubo M, Demura T,
• Fukuda H, Hasebe M: ***ANXUR1* and *2*, sister genes to *FERONIA*/*SIRENE*, are male factors for coordinated fertilization**. *Curr Biol* 2009, **19**:1327-1331.
See [33•].

35. Higashiyama T: **Peptide signaling in pollen-pistil interactions**. *Plant Cell Physiol* 2010, **51**:177-189.

36. Okuda S, Tsutsui H, Shiina K, Sprunck S, Takeuchi H, Yui R, Kasahara RD, Hamamura Y, Mizukami A, Susaki D *et al.*: **Defensin-like polypeptide LUREs are pollen tube attractants secreted from synergid cells**. *Nature* 2009, **458**:357-361.

37. Higashiyama T, Yabe S, Sasaki N, Nishimura Y, Miyagishima S, Kuroiwa H, Kuroiwa T: **Pollen tube attraction by the synergid cell**. *Science* 2001, **293**:1480-1483.

38. Marton ML, Cordts S, Broadhvest J, Dresselhaus T: **Micropylar pollen tube guidance by *egg apparatus 1* of maize**. *Science* 2005, **307**:573-576.

39. Chen YH, Li HJ, Shi DQ, Yuan L, Liu J, Sreenivasan R, Baskar R, Grossniklaus U, Yang WC: **The central cell plays a critical role in pollen tube guidance in *Arabidopsis***. *Plant Cell* 2007, **19**: 3563-3577.

40. Yu F, Shi J, Zhou J, Gu J, Chen Q, Li J, Cheng W, Mao D, Tian L, Buchanan BB *et al.*: **ANK6, a mitochondrial ankyrin repeat protein, is required for male-female gamete recognition in *Arabidopsis thaliana***. *Proc Natl Acad Sci USA* 2010, **107**: 22332-22337.

41. Huck N, Moore JM, Federer M, Grossniklaus U: **The *Arabidopsis* mutant *feronia* disrupts the female gametophytic control of pollen tube reception**. *Development* 2003, **130**:2149-2159.

42. Rotman N, Rozier F, Boavida L, Dumas C, Berger F, Faure JE: **Female control of male gamete delivery during fertilization in *Arabidopsis thaliana***. *Curr Biol* 2003, **13**:432-436.

43. Huang B-Q, Russell SD: **Female germ unit: organization, isolation, and function**. *Int Rev Cytol* 1992, **140**.

44. Kanaoka MM, Torii KU: **FERONIA as an upstream receptor kinase for polar cell growth in plants**. *Proc Natl Acad Sci USA* 2010, **107**:17461-17462.

45. Kessler SA, Shimosato-Asano H, Keinath NF, Wuest SE, Ingram G,
•• Panstruga R, Grossniklaus U: **Conserved molecular components for pollen tube reception and fungal invasion**. *Science* 2010, **330**:968-971.
This study reveals the connection between fertilization and fungal invasion by conserved molecular components. NTA, a MILDEW RESISTANCE LOCUS O (MLO) protein, is involved in pollen tube reception and its proper localization depends on FER activity. Interestingly, homozygous *fer* mutants are powdery mildew resistant, demonstrating a link between pollen tube reception and fungal invasion.

46. Capron A, Gourgues M, Neiva LS, Faure JE, Berger F, Pagnussat G, Krishnan A, Alvarez-Mejia C, Vielle-Calzada JP, Lee YR *et al.*: **Maternal control of male-gamete delivery in *Arabidopsis* involves a putative GPI-anchored protein encoded by the *LORELEI* gene**. *Plant Cell* 2008, **20**:3038-3049.

47. Rotman N, Gourgues M, Guitton AE, Faure JE, Berger F: **A dialogue between the *SIRENE* pathway in synergids and the fertilization independent seed pathway in the central cell controls male gamete release during double fertilization in *Arabidopsis***. *Mol Plant* 2008, **1**:659-666.

48. Boisson-Dernier A, Frietsch S, Kim TH, Dizon MB, Schroeder JI: **The peroxin loss-of-function mutation *abstinence by mutual consent* disrupts male-female gametophyte recognition**. *Curr Biol* 2008, **18**:63-68.

49. Lindner H, Raissig MT, Sailer C, Shimosato-Asano H, Bruggmann R, Grossniklaus U: **SNP-Ratio Mapping (SRM): identifying lethal alleles and mutations in complex genetic backgrounds by Next-Generation Sequencing**. *Genetics* 2012 http://dx.doi.org/10.1534/genetics.112.141341.

50. Consonni C, Humphry ME, Hartmann HA, Livaja M, Durner J, Westphal L, Vogel J, Lipka V, Kemmerling B, Schulze-Lefert P *et al.*: **Conserved requirement for a plant host cell protein in powdery mildew pathogenesis**. *Nat Genet* 2006, **38**:716-720.

51. Buschges R, Hollricher K, Panstruga R, Simons G, Wolter M, Frijters A, van Daelen R, van der Lee T, Diergaarde P, Groenendijk J *et al.*: **The barley *Mlo* gene: a novel control element of plant pathogen resistance**. *Cell* 1997, **88**:695-705.

52. O'Connell RJ, Panstruga R: **Tête-a-tête inside a plant cell: establishing compatibility between plants and biotrophic fungi and oomycetes**. *New Phytol* 2006, **171**:699-718.

53. Bhat RA, Miklis M, Schmelzer E, Schulze-Lefert P, Panstruga R: **Recruitment and interaction dynamics of plant penetration resistance components in a plasma membrane microdomain**. *Proc Natl Acad Sci USA* 2005, **102**:3135-3140.

54. Pucciariello C, Banti V, Perata P: **ROS signaling as common element in low oxygen and heat stresses**. *Plant Physiol Biochem* 2012 http://dx.doi.org/10.1016/j.plaphy.2012.02.016.

55. Suzuki N, Miller G, Morales J, Shulaev V, Torres MA, Mittler R: **Respiratory burst oxidases: the engines of ROS signaling**. *Curr Opin Plant Biol* 2011, **14**:691-699.

56. Saidi Y, Finka A, Goloubinoff P: **Heat perception and signalling in plants: a tortuous path to thermotolerance**. *New Phytol* 2011, **190**:556-565.

57. Keinath NF, Kierszniowska S, Lorek J, Bourdais G, Kessler SA, Shimosato-Asano H, Grossniklaus U, Schulze WX, Robatzek S, Panstruga R: **PAMP (pathogen-associated molecular pattern)-induced changes in plasma membrane compartmentalization reveal novel components of plant immunity**. *J Biol Chem* 2010, **285**:39140-39149.

58. Segonzac C, Zipfel C: **Activation of plant pattern-recognition receptors by bacteria**. *Curr Opin Microbiol* 2011, **14**:54-61.

59. Block A, Alfano JR: **Plant targets for *Pseudomonas syringae* type III effectors: virulence targets or guarded decoys?** *Curr Opin Microbiol* 2011, **14**:39-46.

60. Xiang T, Zong N, Zou Y, Wu Y, Zhang J, Xing W, Li Y, Tang X, Zhu L,
• Chai J *et al.*: ***Pseudomonas syringae* effector AvrPto blocks innate immunity by targeting receptor kinases**. *Curr Biol* 2008, **18**:74-80.
This work demonstrates that the bacterial elicitor AvrPto interacts with the CrRLK1L At2g23200 and inhibits its autophosphorylation ability. This suggests that this protein could be involved PAMP-triggered immunity.

61. Benschop JJ, Mohammed S, O'Flaherty M, Heck AJ, Slijper M, Menke FL: **Quantitative phosphoproteomics of early elicitor signaling in *Arabidopsis***. *Mol Cell Proteomics* 2007, **6**: 1198-1214.

62. Nühse TS, Bottrill AR, Jones AM, Peck SC: **Quantitative phosphoproteomic analysis of plasma membrane proteins reveals regulatory mechanisms of plant innate immune responses**. *Plant J* 2007, **51**:931-940.

63. Nühse TS, Stensballe A, Jensen ON, Peck SC:
• **Phosphoproteomics of the *Arabidopsis* plasma membrane and a new phosphorylation site database**. *Plant Cell* 2004, **16**:2394-2405.
This detailed study of the phosphoproteome of *Arabidopsis* plasma membranes reveals phosphopeptides that can be allocated to members of the CrRLK1L subfamily, amongst them a phosphopeptide in the activation loop that is conserved between 11 members.

64. Engelsberger WR, Schulze WX: **Nitrate and ammonium lead to distinct global dynamic phosphorylation patterns when resupplied to nitrogen-starved *Arabidopsis* seedlings**. *Plant J* 2012, **69**:978-995.

65. Whiteman SA, Serazetdinova L, Jones AM, Sanders D, Rathjen J, Peck SC, Maathuis FJ: **Identification of novel proteins and phosphorylation sites in a tonoplast enriched membrane fraction of *Arabidopsis thaliana***. *Proteomics* 2008, **8**:3536-3547.

66. Mayank P, Grossman J, Wuest S, Boisson-Dernier A, Roschitzki B, Nanni P, Nuhse T, Grossniklaus U: **Characterization of the phosphoproteome of mature *Arabidopsis* pollen**. *Plant J* 2012 http://dx.doi.org/10.1111/j.1365-313X.2012.05061.x.

67. Li HJ, Xue Y, Jia DJ, Wang T, Hi DQ, Liu J, Cui F, Xie Q, Ye D, Yang WC: ***POD1* regulates pollen tube guidance in response to micropylar female signaling and acts in early embryo patterning in *Arabidopsis***. *Plant Cell* 2011, **23**:3288-3302.

68. Lu Y, Chanroj S, Zulkifli L, Johnson MA, Uozumi N, Cheung A, Sze H: **Pollen tubes lacking a pair of K^+ transporters fail to target ovules in *Arabidopsis***. *Plant Cell* 2011, **23**:81-93.

69. Bause E: **Structural requirements of N-glycosylation of proteins. Studies with proline peptides as conformational probes**. *Biochem J* 1983, **209**:331-336.

70. Helenius A, Aebi M: **Roles of N-linked glycans in the endoplasmic reticulum**. *Annu Rev Biochem* 2004, **73**:1019-1049.

71. Song W, Henquet MG, Mentink RA, van Dijk AJ, Cordewener JH, Bosch D, America AH, van der Krol AR: **N-glycoproteomics in plants: perspectives and challenges**. *J Proteomics* 2011, **74**:1463-1474.

72. Galli C, Bernasconi R, Solda T, Calanca V, Molinari M: **Malectin participates in a backup glycoprotein quality control pathway in the mammalian ER**. *PLoS ONE* 2011, **6**:e16304.

73. Haweker H, Rips S, Koiwa H, Salomon S, Saijo Y, Chinchilla D,
• Robatzek S, von Schaewen A: **Pattern recognition receptors require N-glycosylation to mediate plant immunity**. *J Biol Chem* 2010, **285**:4629-4636.
This paper shows that a mutation in a single N-linked glycosylation site of the RLK EF-Tu is sufficient to prevent ligand binding ability.

74. Monne M, Jovine L: **A structural view of egg coat architecture and function in fertilization**. *Biol Reprod* 2011, **85**:661-669.

75. Han L, Monne M, Okumura H, Schwend T, Cherry AL, Flot D, Matsuda T, Jovine L: **Insights into egg coat assembly and egg-sperm interaction from the X-ray structure of full-length ZP3**. *Cell* 2010, **143**:404-415.

76. Hruz T, Laule O, Szabo G, Wessendorp F, Bleuler S, Oertle L, Widmayer P, Gruissem W, Zimmermann P: **Genevestigator v3: a reference expression database for the meta-analysis of transcriptomes**. *Adv Bioinform* 2008, **2008**:420747.

77. Sugiyama N, Nakagami H, Mochida K, Daudi A, Tomita M, Shirasu K, Ishihama Y: **Large-scale phosphorylation mapping reveals the extent of tyrosine phosphorylation in *Arabidopsis***. *Mol Syst Biol* 2008, **4**:193.

RESULTS - CHAPTER 1

SNP-Ratio Mapping (SRM)

NOTE

All of Chapter 1 is published as **Lindner H.*, Raissig M. T.*, Sailer C., Shimosato-Asano H., Bruggmann R., Grossniklaus U**. (2012) SNP-Ratio Mapping (SRM): Identifying Lethal Alleles and Mutations in Complex Genetic Backgrounds by Next-Generation Sequencing. Genetics **191**: 1381–1386.
*these authors contributed equally to this work

HL, MTR and UG developed this method together. It was applied to identify causative mutations from two different forward genetic screens aiming at (i) novel players of the pollen tube reception pathway in the synergid cells (HL) and (ii) regulators of imprinted *MEA* expression (MTR). The development of SRM was essential, since all mutant genotypes only yielded heterozygous individuals. Available mapping by next-generation sequencing approaches rely on homozygous mutant individuals, large numbers of mutant individuals and/or many rounds of backcrossing. The development of SRM allowed the use of heterozygous mutant individuals, with comparatively few mutant individuals after only two rounds of backcrossing, thus representing a time-saving method, which can be applied for various mutant backgrounds. We successfully mapped three mutants of the PT reception pathway (see Chapter 2) by SRM, one of which is described in the following chapter.

Supplementary Information can be found in the Appendix A1.

SNP-Ratio Mapping (SRM): Identifying Lethal Alleles and Mutations in Complex Genetic Backgrounds by Next-Generation Sequencing

Heike Lindner,*,[1] Michael T. Raissig,*,[1] Christian Sailer,* Hiroko Shimosato-Asano,*,[2] Rémy Bruggmann,[†,‡] and Ueli Grossniklaus*,[3]

*Institute of Plant Biology and Zürich-Basel Plant Science Center, University of Zürich, CH-8008 Zürich, Switzerland, [†]Functional Genomics Center Zürich of the Eidgenössische Technische Hochschule and University of Zürich, CH-8057 Zürich, Switzerland, and [‡]Interfacultary Bioinformatics Support, Department of Biology, University of Bern, CH-3012 Bern, Switzerland

ABSTRACT We present a generally applicable method allowing rapid identification of causal alleles in mutagenized genomes by next-generation sequencing. Currently used approaches rely on recovering homozygotes or extensive backcrossing. In contrast, SNP-ratio mapping allows rapid cloning of lethal and/or poorly transmitted mutations and second-site modifiers, which are often in complex genetic/transgenic backgrounds.

FORWARD genetic screens are powerful in uncovering novel gene functions in genetic model organisms. While some mutant screens can be quick to perform, the identification of the causative mutation by map-based cloning is extremely labor-intensive. Large F_2 mapping populations of >1000 mutant individuals are required (Lukowitz *et al.* 2000; Jander *et al.* 2002) to fine-map a chromosomal region harboring a causative mutation. This number of mutant individuals can be difficult to obtain, especially when working with phenotypic traits that (i) are difficult to score, (ii) are weakly transmitted, or (iii) are in organisms that are hard to propagate. The recent development of next-generation sequencing (NGS) platforms has made sequencing of whole genomes quick and affordable. One application of NGS is to replace map-based cloning by the sequencing of mutagenized genomes to quickly identify causative mutations, a method successfully applied in many model organisms (Sarin *et al.* 2008; Smith *et al.* 2008; Srivatsan *et al.* 2008; Blumenstiel *et al.* 2009; Irvine *et al.* 2009; Schneeberger *et al.* 2009; Zuryn *et al.* 2010; Austin *et al.* 2011). However, current methods depend on identifying homozygous mutant individuals in an F_2 mapping population after outcrossing (Schneeberger *et al.* 2009; Austin *et al.* 2011) or require several rounds of backcrossing (Zuryn *et al.* 2010), a time-consuming requirement not easily met in organisms with long generation times.

Here, we describe a generally applicable method, SNP-ratio mapping (SRM), which allows the rapid identification of lethal and/or poorly transmitted mutations and second-site modifiers by NGS. It is based on the distinct segregation ratio of the causative (and linked) single-nucleotide polymorphism(s) (SNPs) from that of unlinked SNPs. SRM allows the mapping of lethal mutations after only two rounds of backcrossing via NGS. After backcrossing twice to the non-mutagenized parent, any unlinked SNP created by ethyl methanesulfonate (EMS) mutagenesis segregates 1:3 in a pool of individuals. By selecting only mutant individuals in the F_1 generation of the second backcross (BC2), the causative SNP is enriched and segregates 1:1 in a pool of mutant BC2 individuals (Figure 1). Thus, calculating the SNP/non-SNP segregation ratio allows the quick identification of the causative mutation. The method is applicable to any model organism and mutagen causing mostly point mutations or small indels. SRM is the method of choice when working with (i) lethal mutations, (ii) hard-to-score phenotypes, (iii) mutations with low transmission, and (iv) second-site modifiers in complex genetic/transgenic backgrounds. Here, we demonstrate the power of

doi: 10.1534/genetics.112.141341
Manuscript received February 9, 2012; accepted for publication May 21, 2012
Supporting information is available online at http://www.genetics.org/content/suppl/2012/05/26/genetics.112.141341.DC1.
[1]These authors contributed equally to this work.
[2]Present address: Graduate School of Biological Sciences, Nara Institute of Science and Technology, Ikoma, Nara 630-0192, Japan.
[3]Corresponding author: Institute of Plant Biology and Zürich-Basel Plant Science Center University of Zürich, Zollikerstrasse 107, CH-8008 Zürich, Switzerland. E-mail: grossnik@botinst.uzh.ch

SRM by cloning a gametophyte lethal mutation in *Arabidopsis thaliana*, for which the recovery of homozygotes is not possible.

As proof of principle, we aimed to map the gene affected in a pollen-tube reception mutant obtained from a forward genetic screen using EMS-treated seeds of *A. thaliana* (Col-0 accession, Supporting Information, File S1). The *turan-1* (*tun-1*) mutant disrupts cell–cell communication between male and female gametophytes, which is indispensable for fertilization. In flowering plants, the gametes are produced by the haploid, multicellular gametophytes. The male gametophyte (pollen tube) delivers two sperm cells to the female gametophyte (embryo sac), harboring two female gametes. Fertilization of the egg and central cell forms the embryo and the endosperm, respectively. In heterozygous *tun-1* mutants, 12% (n = 1318 ovules) of the embryo sacs remain unfertilized, compared to only 1.5% (n = 1389 ovules) in the wild-type control. In *tun-1* mutants, the pollen tube fails to stop growing inside the female gametophyte and does not rupture to release the sperm cells, which leads to a pollen-tube overgrowth phenotype revealed by aniline-blue staining of callose in the pollen tube's cell wall (Figure 2 and File S1). Due to impaired fertilization and an additional effect of the mutant in the pollen, the transmission of the mutation is highly reduced, and homozygous individuals cannot be recovered. Thus, recently published methods for mutant allele identification by NGS (Schneeberger *et al.* 2009; Austin *et al.* 2011) are not applicable to mapping this gametophyte lethal mutation.

To identify the *TUN* gene by SRM, heterozygous mutants were crossed back twice to the wild-type Col-0 parent. By selecting only mutant individuals in the F_1 generation of the BC2, the causative SNP is enriched and segregates 1:1 in a pool of mutant BC2 individuals, whereas any unlinked SNP segregates 1:3 (Figure 1). We simulated a binomial distribution for a 1:1 and a 1:3 segregation to determine the optimal sample size and calculated that a 50-fold sequence coverage of the *Arabidopsis* genome was sufficient to distinguish a SNP segregating 1:1 from a SNP segregating 1:3 ($P < 0.05$, Table S1). Genomic DNA from 53 F_1 individuals of the BC2 generation that displayed the mutant phenotype was pooled for sequencing (File S1). A sequencing library was prepared (File S1) and sequenced on the SOLiD 4 platform, as this method provides an incomparable sequencing accuracy optimal for SNP detection. Reads were mapped to the *A. thaliana* genome assembly and SNPs were called and analyzed (File S1).

We identified 2337 SNPs, of which 521 were homozygous and 1816 were heterozygous with an average sequence coverage of 57 reads (Table S2 and Table S3). The homozygous SNPs were likely due to discrepancies between our lab strain of Col-0 and the published sequence. The homozygous SNPs were discarded, since all relevant SNPs should only be heterozygous (Figure 1). Before plotting the SNP/non-SNP ratios of the heterozygous SNPs, we filtered any SNPs that showed very low or high coverage. Low-coverage SNPs could exhibit a misleading ratio due to small sample size, while very high coverage (>2× average coverage) SNPs often mapped to repetitive and/or transposable element sequences, where mapping quality is usually poor (Figure S1). Thus, we filtered out the lowest (< 19×) and the highest (> 103×) 10% quantiles, leaving 80% of the original data set. The SNP/non-SNP ratio of the remaining 1468 heterozygous SNPs was calculated and plotted against their chromosomal position (Figure 3). Any unlinked SNP should have a SNP/non-SNP ratio of ~ 0.25, whereas a causative SNP is expected to segregate 1:1, *i.e.*, producing a SNP/non-SNP ratio of 0.5. Furthermore, the SNPs surrounding the causative mutation should have segregation ratios > 0.25 since they have been coselected and thus cosegregate due to genetic linkage. Using this method, the causative SNP can be easily identified on the basis of the criteria that it must have a segregation ratio of ~ 0.5, while the flanking, noncausative SNPs should cosegregate and display a ratio between 0.25 and 0.5, depending on the genetic/physical distance. The closer the flanking SNPs are, the higher this ratio will be. On the segregation ratio plot, this results in a rounded, rather flat curve, which can be visually identified without further statistical analyses (Figure 3A, red shading). Noncausative SNPs with a segregation ratio of 0.5 are likely to be surrounded by SNPs with low segregation ratios, leading to sharp drops in the SNP/non-SNP ratios of nearby SNPs (Figure 3). In our analysis of the *tun-1* mutant, the only rounded peak was present in the upper arm of chromosome I (Figure 3A, red shading).

Although the causative SNP could easily be identified in our experiment, we did not want to rely on a visual identification of the rounded peak. Thus, we developed a statistical test based on the expected recombination rate of neighboring SNPs as a function of the genetic distance between the SNPs. For each SNP following the 1:1 binomial distribution (n = 118, coverage ≥ 50), we calculated the expected pattern of cosegregation with the two neighboring SNPs on each side by using the expected recombination rate according to the mean genetic distance of 1 cM/357,042 bp (File S1 and File S2). Using a χ^2 goodness-of-fit test, 108 of 118 1:1 class SNPs did not lie in a linkage group (5 neighboring SNPs) that fit the expected pattern of cosegregation and therefore were discarded. Of the 10 remaining candidate SNPs, 8 reside in recombination-deficient centromeric regions. This is probably due to intrinsic problems in mapping reads to the highly repetitive centromeric sequences, leading to a high SNP density with unusual segregation ratios. Moreover, these eight linkage groups encompass 0.013 cM or less (Table S4), and the probability that 5 random SNPs lie in such close proximity is $P = 1.4 \times 10^{-8}$ (Poisson distribution, $\lambda = 0.071$, $k = 5$). Thus, any 5 SNPs that are in such close vicinity are likely of artificial nature due to mapping errors and should not be considered. In contrast, the linkage groups of the two remaining noncentromeric SNPs cover a genetic distance of 4.7 cM (ratio = 0.49) and 6.8 cM (ratio = 0.44), respectively. Both SNPs lie in the rounded peak that we visually

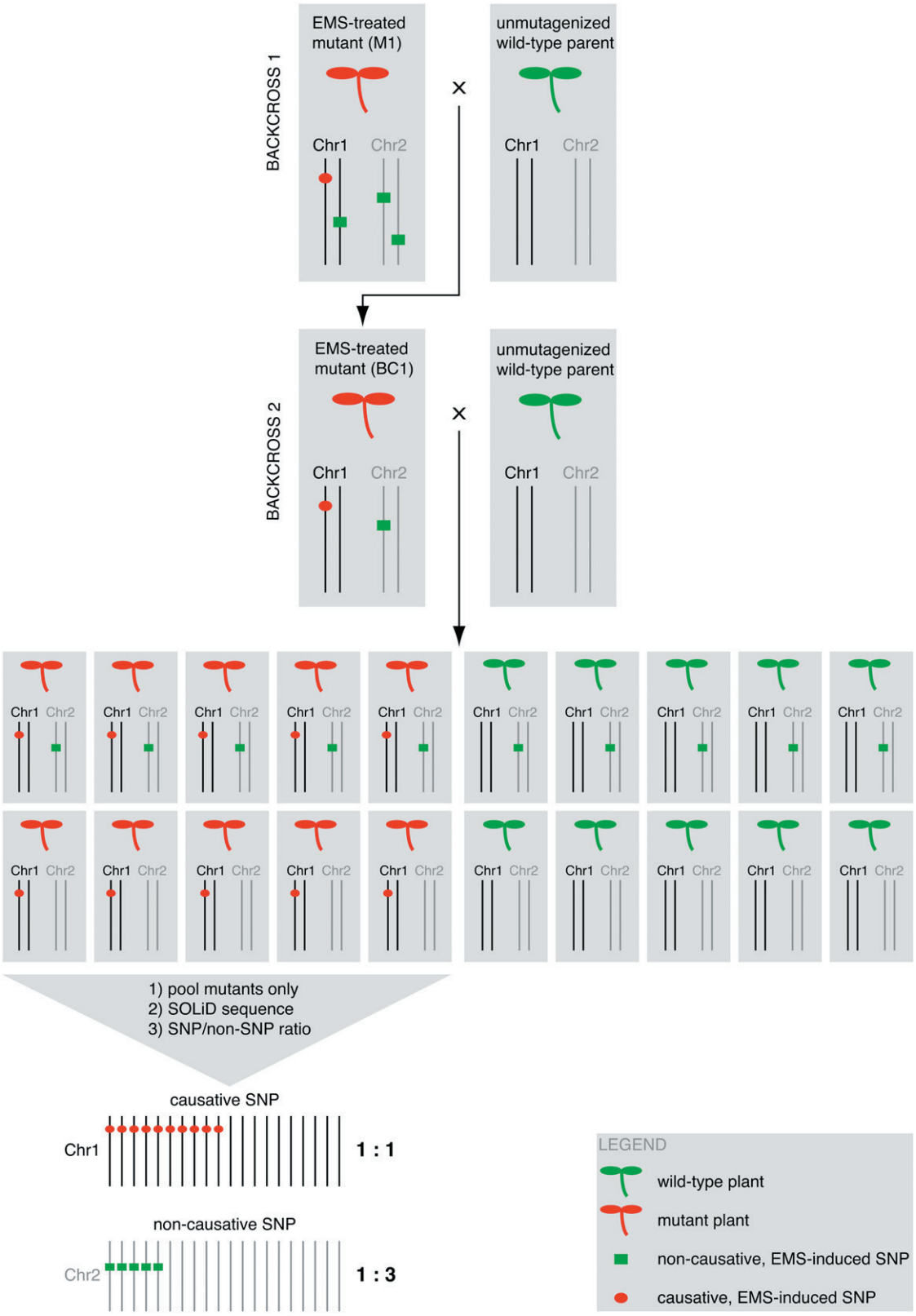

Figure 1 SRM scheme. An EMS-treated mutant (red plant) harboring several EMS-induced SNPs throughout the genome is backcrossed to an unmutagenized wild-type parent (green plant) of the same accession. The first backcross eliminates half of the SNPs. The F_1 generation is phenotyped, and a single mutant individual (red plant, BC1) is backcrossed. The F_1 of the second backcross (BC2) is phenotyped, and genomic DNA of 25–50 mutant individuals is extracted and pooled. The causative SNP (red circle) is present in every mutant individual in a heterozygous state and thus segregates 1:1 in a pool of mutant individuals. Unlinked SNPs (green square) are not selected and thus segregate 1:3. After SOLiD sequencing, SNP calling, and SNP/non-SNP ratio calculation, the two different segregation ratios can be distinguished.

identified on the upper arm of chromosome I and are neighbors (Figure 3, red shading).

Of the two visually and statistically identified 1:1 class SNPs, the SNP with a ratio of 0.44 was intronic whereas the SNP with a segregation ratio of 0.49 (the closest to 0.5 in the whole data set) (Figure 3A, arrow) was a nonsynonymous GC-to-AT nucleotide change, which is characteristic of most EMS-induced SNPs (Sega 1984). This nucleotide change produces a stop codon in the sixth exon of gene *At1g16570*, a putative UDP-glycosyltransferase superfamily protein. To demonstrate that the causative SNP was identified, the *At1g16570* gene was amplified from each of the 53 DNA samples that had been pooled for sequencing (File S1). The PCR products were digested with nucleases cleaving single-base-pair mismatches in heteroduplex DNA (Till *et al.* 2004). Using this method, 52 samples were shown to have a SNP at the indicated position, while one sample was not cut (Figure S2). The progeny of this plant showed no phenotype, indicating that it was a sampling mistake due to wrong phenotyping in the BC2 generation. Finally, T-DNA insertion lines disrupting the identified gene *At1g16570* were tested for a pollen-tube reception phenotype. The line SAIL_400_A01 (*tun-2*), which has an insertion in the fourth exon of *At1g16570*, displays the same pollen-tube overgrowth phenotype as the EMS allele *tun-1* (Figure 2C), indicating that the correct gene has been identified by SRM.

In this example, no further analyses were required to identify the causative SNP. However, if genome coverage or mapping quality of the reads is lower than expected, the application of several filtering strategies could narrow down the list of potential candidate SNPs. First, selecting for exonic SNPs (nonsynonymous, synonymous) removes most of the detected SNPs (Table S2). Second, prioritizing characteristic EMS-induced SNPs (Sega 1984) should unambiguously identify the causative SNP in most cases. If not, then the rare cases where the mutation affects a regulatory region that is not exonic or an atypical EMS-induced nucleotide change have to be considered.

Interestingly, we also observed SNP ratios > 0.5. Since this should not be possible considering our genetic backcrossing strategy (Figure 1), we performed a detailed analysis of all SNPs on chromosome I with ratios > 0.5. All such SNPs display a low coverage (low-sample-size effect) or are covered by reads with low mapping quality (Figure S1). This indicates that such high ratios might be mapping artifacts in repetitive and/or transposable element regions. In addition, any SNPs found in and around the centromere display unusual segregation ratios (Figure 3, gray shading), probably representing an intrinsic problem in mapping sequence reads to highly repetitive centromeric regions.

On the whole, labor-intensive, map-based cloning has been replaced by cloning via NGS in recent years. Until now, this worked only (i) with homozygous viable mutants using the SHOREmap or similar strategies (Schneeberger *et al.* 2009; Austin *et al.* 2011) after outcrossing or (ii) for organisms with a short generation time and an easy-to-score phenotype, where multiple required backcrosses still save time (Zuryn *et al.* 2010). In contrast, SRM enables the mapping of zygotic or even gametophytic lethal mutations after only two rounds of backcrossing. SRM is generally applicable, but the identification of heterozygous mutant individuals may require progeny tests, *e.g.*, scoring for the presence of aborted seeds or defective embryos among the progeny. This might involve some adaptations of the crossing scheme shown in Figure 1, including a combination of inter se crosses and backcrosses if selfing is not possible. In outcrossing species, individual males could first be crossed to siblings to identify the heterozygotes in a progeny test, as well as to wild-type females to generate the backcrossed progeny used for SRM. In fact, SRM could also be used for the cloning of the causative genes on the basis of homozygous mutants in F_2 populations: the expected SNP ratios would be different (1.0 *vs.* 0.5), but the approach would still benefit from the small number of individuals required.

SRM is especially advantageous for (i) lethal mutations, (ii) organisms with a long generation time, (iii) hard-to-score phenotypes, and (iv) mutations with low transmission because only a small number of individuals are needed. Importantly, SRM is the method of choice for second-site modifier screens, in which a mutant with a certain phenotype is mutagenized a second time to identify novel mutant alleles that enhance or suppress this phenotype. Again, classical mapping or the SHOREmap strategy (Schneeberger *et al.* 2009; Austin *et al.* 2011), which rely on outcrossing and an F_2 mapping population, require the original mutation to be present in at least two genetic backgrounds. This is possible only when another allele is available in a different accession or by outcrossing the mutation five to six times to another accession. This procedure is time-consuming and has the disadvantage that, due to a lack of recombination

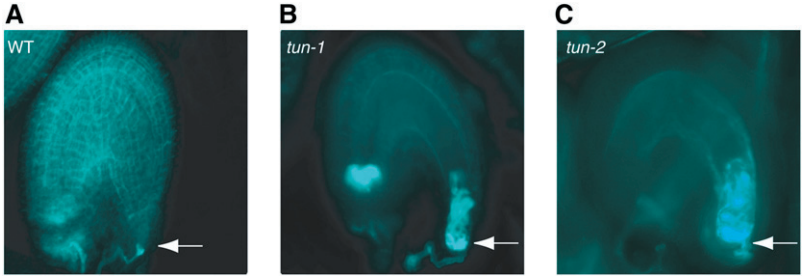

Figure 2 Aniline-blue staining of callose in pollen tubes 2 days after pollination. The arrow indicates the place of pollen-tube arrest. (A) Fertilized wild-type ovule. (B) Ovule harboring a *tun-1* embryo sac with defective pollen-tube reception. The pollen tube continues its growth and does not rupture to release the sperm cells. (C) Pollen-tube overgrowth phenotype in *tun-2*, an independent T-DNA line disrupting the *At1g16570* gene.

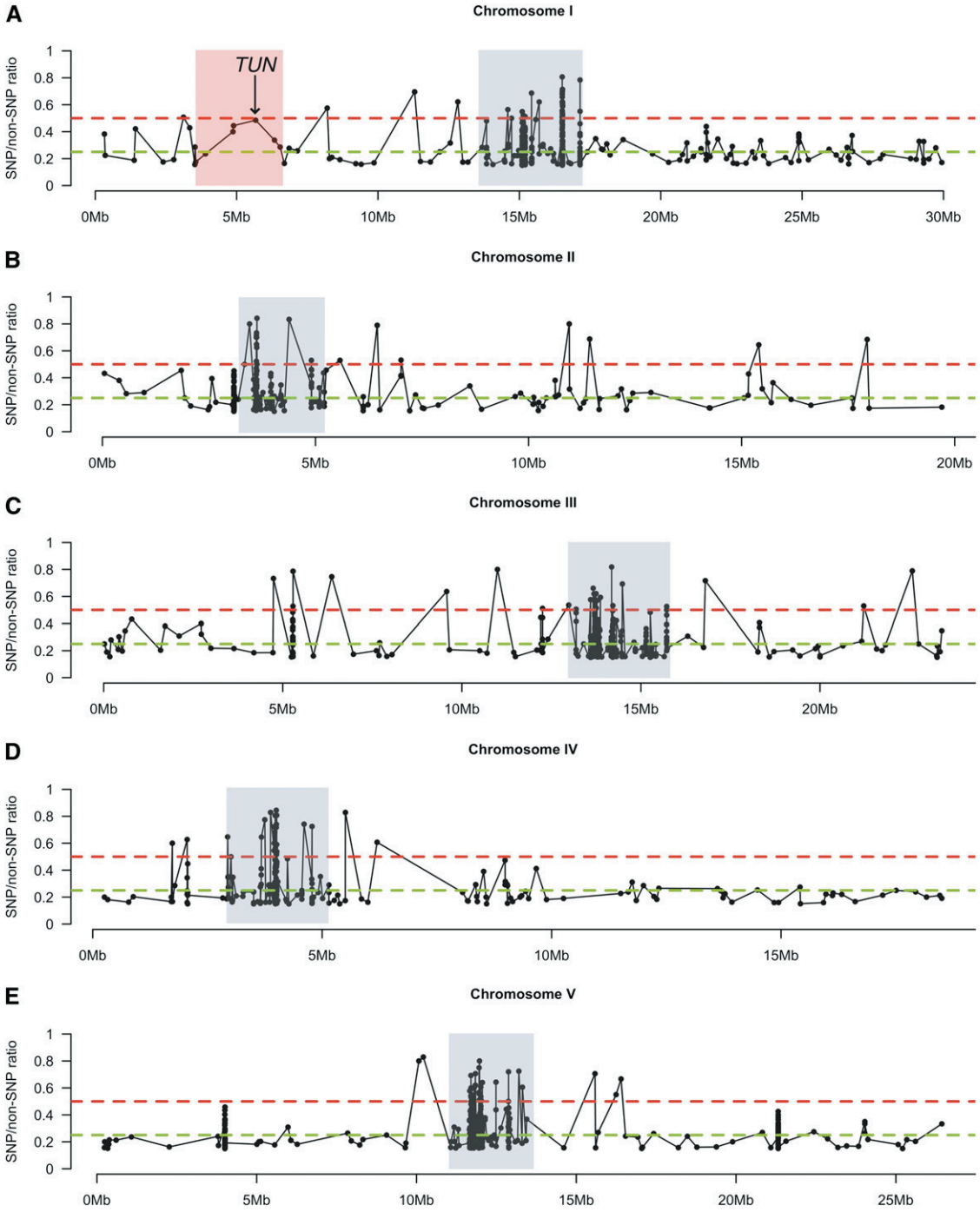

Figure 3 SNP/non-SNP ratio plots. The SNP/non-SNP ratio of all heterozygous SNPs is calculated and plotted against the chromosomal position of the heterozygous SNPs. The red dashed line marks the SNP/non-SNP ratio at 0.5, where the causative SNP should be; the green dashed line marks the SNP/non-SNP ratio at 0.25, where all other SNPs should locate. The red shading marks the genetically linked and selected region on chromosome I with the causative SNP in *At1g16570* (arrow). The gray shading marks the centromeric regions with a high SNP density, likely due to a poor mapping quality in these regions. (A–E) Chromosome I, II, III, IV, and V, respectively.

events close to the mutation, additional enhancer/suppressor mutations in the vicinity of the original mutation cannot be mapped. Furthermore, second-site modifier screens are often performed in complex, tailor-made backgrounds involving several mutants and/or transgenes (Page and Grossniklaus 2002). It is very hard to generate the identical genetic/transgenic constitution in two distinct accessions. By using SRM, the enhancer/suppressor mutant has to be backcrossed only to the original mutant background, no matter how complex it is.

Finally, SRM can be applied to any genetic system. In fact, we expect that SRM can also be applied in organisms without a well-annotated genome. As mentioned above, plotting the

SNP/non-SNP ratio over the chromosomal positions and visually identifying flat curves indicating a region under selection can be statistically tested (File S1 and File S2) and used to identify the causative SNP. This is also possible with partly assembled and poorly annotated genomes.

In conclusion, we successfully identified a gene disrupted in a gametophyte lethal mutant in *A. thaliana* by SRM. The need for relatively few individuals and only two rounds of backcrosses, which are needed in any case to purify the genetic background after mutagenesis, make this a very versatile and useful method for any genetic organism.

Acknowledgment

We thank A. Patrigiani for preparing the library for SOLiD sequencing and R. Schlapbach for access to the facilities of the Functional Genomics Center Zürich. We also thank S. A. Kessler and J. Jaenisch for helpful comments on the manuscript. This work was supported by grants from the European Research Council and the Swiss National Science Foundation to U.G. The costs for next-generation sequencing were covered by a project of the University Research Priority Program in Functional Genomics/System Biology of the University of Zürich.

Note added in proof: While our paper was under review, Abe *et al.* (2012) published a similar method based on the distinct segregation ratios of linked and unlinked SNPs to map homozygous mutants in rice. This shows that SRM can be applied to map homozygous mutants, as we suggested in our manuscript.

Literature Cited

Abe, A., S. Kosugi, K. Yoshida, S. Natsume, H. Takagi *et al.*, 2012 Genome sequencing reveals agronomically important loci in rice using MutMap. Nat. Biotechnol. 30: 174–178.

Austin, R. S., D. Vidaurre, G. Stamatiou, R. Breit, N. J. Provart *et al.*, 2011 Next-generation mapping of *Arabidopsis* genes. Plant J. 67: 715–725.

Blumenstiel, J. P., A. C. Noll, J. A. Griffiths, A. G. Perera, K. N. Walton *et al.*, 2009 Identification of EMS-induced mutations in *Drosophila melanogaster* by whole-genome sequencing. Genetics 182: 25–32.

Irvine, D. V., D. B. Goto, M. W. Vaughn, Y. Nakaseko, W. R. McCombie *et al.*, 2009 Mapping epigenetic mutations in fission yeast using whole-genome next-generation sequencing. Genome Res. 19: 1077–1083.

Jander, G., S. R. Norris, S. D. Rounsley, D. F. Bush, I. M. Levin *et al.*, 2002 *Arabidopsis* map-based cloning in the post-genome era. Plant Physiol. 129: 440–450.

Lukowitz, W., C. S. Gillmor, and W. R. Scheible, 2000 Positional cloning in *Arabidopsis*: Why it feels good to have a genome initiative working for you. Plant Physiol. 123: 795–805.

Page, D., and U. Grossniklaus, 2002 The art and design of genetic screens: *Arabidopsis thaliana*. Nat. Rev. Genet. 3: 124–136.

Sarin, S., S. Prabhu, M. M. O'Meara, I. Pe'er, and O. Hobert, 2008 *Caenorhabditis elegans* mutant allele identification by whole-genome sequencing. Nat. Methods 5: 865–867.

Schneeberger, K., S. Ossowski, C. Lanz, T. Juul, A. H. Petersen *et al.*, 2009 SHOREmap: simultaneous mapping and mutation identification by deep sequencing. Nat. Methods 6: 550–551.

Sega, G. A., 1984 A review of the genetic effects of ethyl methanesulfonate. Mutat. Res. 134: 113–142.

Smith, D. R., A. R. Quinlan, H. E. Peckham, K. Makowsky, W. Tao *et al.*, 2008 Rapid whole-genome mutational profiling using next-generation sequencing technologies. Genome Res. 18: 1638–1642.

Srivatsan, A., Y. Han, J. Peng, A. K. Tehranchi, R. Gibbs *et al.*, 2008 High-precision, whole-genome sequencing of laboratory strains facilitates genetic studies. PLoS Genet. 4: e1000139.

Till, B. J., C. Burtner, L. Comai, and S. Henikoff, 2004 Mismatch cleavage by single-strand specific nucleases. Nucleic Acids Res. 32: 2632–2641.

Zuryn, S., S. Le Gras, K. Jamet, and S. Jarriault, 2010 A strategy for direct mapping and identification of mutations by whole-genome sequencing. Genetics 186: 427–430.

Communicating editor: C. D. Jones

RESULTS - CHAPTER 2

TURAN and *EVAN* Regulate Pollen Tube Reception

NOTE

All of Chapter 2 will be submitted with the title "*TURAN* and *EVAN* Regulate Pollen Tube Reception in the Synergid Cells, but Play Distinct Roles in the Male Gametophyte" and the contributing authors Lindner H, Kessler SA, Müller LM, Shimosato-Asano H, Boisson-Dernier A, and Grossniklaus U.

HL, SAK and UG designed the experiments. HL, LM and HSA performed the experiments. HL, SAK, ABD and UG interpreted the results. HL wrote the manuscript. SAK, LM and UG critically read and corrected the manuscript.

All supplemental data can be found in the Appendix A2.

TURAN and *EVAN* Mediate Pollen Tube Reception in the Synergid Cells but Play Distinct Roles in the Male Gametophyte

Heike Lindner[1], Sharon A. Kessler[1,2], Lena M. Müller[1], Hiroko Shimosato-Asano[1,3], Aurélien Boisson-Dernier[1], and Ueli Grossniklaus[1]*

[1] Institute of Plant Biology & Zürich-Basel Plant Science Center, University of Zürich, CH-8008 Zürich, Switzerland
[2] Department of Microbiology and Plant Biology, University of Oklahoma, 770 Van Vleet Oval, Norman, OK 73019, USA
[3] Graduate School of Biological Sciences, Nara Institute of Science and Technology, Ikoma, Nara 630-0192, Japan

Running title: *TURAN* and *EVAN* Mediate Pollen Tube Reception

*to whom correspondence should be addressed: grossnik@botinst.uzh.ch

ABSTRACT:

Double fertilization in flowering plants requires sperm delivery by the pollen tube (PT) to the embedded female gametophyte. When the PT arrives at the micropylar end of the ovule, PT reception has to take place to ensure PT growth arrest, PT rupture and sperm release for subsequent double fertilization. Although several members of the signaling cascade during PT reception have been described, still relatively little is known about the molecular control of PT reception. Here, we describe *TURAN* (*TUN*) and *EVAN* (*EVN*), two novel members of the PT reception pathway in the synergid cells of the female gametophyte. Mutant ovules show impaired PT reception leading to continuous PT growth in the female gametophyte without PT burst. *TUN* encodes a putative UDP-glycosyltransferase superfamily protein and *EVN* encodes a putative dolichol kinase. Thus, both genes are potentially involved during protein N-glycosylation in the endoplasmic reticulum (ER). In addition to their role during PT reception in the synergids, *TUN* and *EVN* play distinct roles in the pollen. Whereas *EVN* is essential during pollen development, *TUN* mediates PT growth/integrity perhaps by directly targeting the pollen-specific, plasma-membrane-localized receptor-like kinase *ANXUR1*, which has been reported to prevent premature PT rupture. Furthermore, downregulation of *TUN* expression resulted in reduced vegetative growth and dwarf individuals. Taken together, *TUN* and *EVN*, two genes with a potential role in protein N-glycosylation, are involved in mediating PT reception in the synergid cells, are required for PT growth/integrity and pollen development, respectively, and have a role in vegetative growth.

INTRODUCTION:

In angiosperms, both male and female gametes are embedded in spatially separated gametophytes, the pollen and the embryo sac, respectively. A complex series of communication events between the male gametophyte and the female tissues of the flower is required to enable the pollen tube (PT) to deliver the sperm cells to the embryo sac (reviewed in Beale and Johnson, 2013; Dresselhaus and Franklin-Tong, 2013; Palanivelu and Tsukamoto, 2011). Eventually, double fertilization occurs, in which one male gamete, the sperm cell, fuses with the egg cell to form the embryo and a second sperm cell fuses with the central cell to give rise to the embryo-nourishing endosperm. The communication between the pollen and the female tissue starts after pollen landing on the stigma (reviewed in Palanivelu and Tsukamoto, 2011; Dresselhaus and Franklin-Tong, 2013). If the pollen is recognized to be compatible, then the pollen grain hydrates and germinates to form a tip-growing PT. The PT transports the two immobile sperm cells by growing through the stigma and style to reach the transmitting tract. Within the transmitting tract, nutrients as well as short- and long-range signals mediate PT growth and guidance towards the ovules (reviewed in Palanivelu and Tsukamoto, 2011; Dresselhaus and Franklin-Tong, 2013). For instance, gradients of various small molecules like GABA (Palanivelu et al., 2003), D-serine (Michard et al., 2011) and nitric oxide (NO; Prado et al., 2008) along the PT growth path with highest concentrations at the micropylar end of the ovule are thought to play a role in PT guidance partially by modulating Ca^{2+} signaling in the PT. Reception and/or transduction of those ovular signals by the pollen tube were shown to require several ER-localized proteins and GPI-anchored proteins (Lu et al., 2011; Li et al., 2011; 2013). In addition to these gradients of small molecules secreted from the sporophyte and gametophyte, larger, short-range signaling molecules produced by the synergid cells play an essential role in directing PTs to the entrance of the embryo sac. The synergid cells flank the egg cell and are located at the micropylar end of the female gametophyte. In *Torenia fournieri*, the synergid cells were shown to be essential for PT guidance and attraction by secreting *LUREs,* small defensin-like proteins (DEFL), which are part of a subgroup of cysteine-rich polypeptides (CRPs; Okuda et al., 2009). *Arabidopsis thaliana* uses similar LURE peptides as short-range PT attractants (Takeuchi and Higashiyama, 2012). Perception of these female signals in the PT involves two receptor-like cytoplasmic kinases *LOST IN POLLEN TUBE GUIDANCE 1* (*LIP1*) and *LIP2* (Liu et al., 2013). Until recently, it was believed that once the PT has arrived at the micropyle of the ovule, it enters the receptive synergid through the filiform apparatus, a membrane- and cell wall rich structure due to invaginations at the micropylar pole of both synergids. However, a recent study revealed that the PT grows beyond the filiform apparatus at least in some cases and enters at the so-called "synergid hook", a site where the cell wall might be weakened (Leshem et al., 2013). Therefore, interaction between the PT and the synergid cells might consist of two spatially and temporally separable stages. First, PT reception at the filiform apparatus (see below) and second, further growth towards the PT entry site of the receptive synergid, PT growth arrest, degeneration of the receptive synergid, PT rupture and release of the two sperm cells. However, as shown by several PT reception mutants, the second stage of PT entry is not dependent on the first stage of PT reception at the filiform apparatus. FERONIA, a receptor-like kinase of the *Catharantus roseus* receptor-like Serine/Threonine kinase 1-like (*Cr*RLK1L) subfamily is localized at the filiform apparatus of the synergid cells and was the first identified gene of an active signaling process involved in PT reception (Huck et al.,

2003; Escobar-Restrepo et al., 2007). In *fer/FER* and the allelic *sirène* (*srn/SRN*; Rotman et al., 2003) mutants, 50% of the ovules remain unfertilized, although synergid and pollen development are normal. In these unfertilized ovules, the PT enters the receptive synergid, but does not stop its growth to rupture and release the sperm cells. Instead, PT growth continues inside the female gametophyte leading to a PT overgrowth phenotype (Huck et al., 2003; Escobar-Restrepo et al., 2007). The two closest homologs of *FER* are the pollen-specific genes *ANXUR1* (*ANX1*) and *ANX2* (Boisson-Dernier et al., 2009; Miyazaki et al., 2009). *anx1* and *anx2* single mutants have no phenotype, but double mutant pollen tubes burst *in vitro* immediately after germination (Boisson-Dernier et al., 2009; Miyazaki et al., 2009). ANX proteins activate NADPH oxidases leading to fine-tuning of the Ca^{2+}-gradient at the PT tip resulting in sustained secretion and PT elongation (Boisson-Dernier et al., 2013). Both ANX-YFP fusion proteins localize to the plasma membrane of the growing PT tip (Boisson-Dernier et al., 2009; Miyazaki et al., 2009). Thus, the two ANX receptor-like kinases seem to prevent PT rupture until a yet unknown signal deactivates the ANX-specific signaling cascade, leading to PT rupture and sperm cell release. This deactivation of the ANX-specific signaling cascade in PTs will only happen after the *FER*-dependent PT reception pathway at the filiform apparatus of the female gametophyte has been activated (Boisson-Dernier et al., 2009; Miyazaki et al., 2009). After *FERONIA,* other factors were identified to play a role during the PT reception pathway in the synergid cells: LORELEI (LRE), a synergid expressed glycosylphosphatidylin ositol (GPI)-anchored protein (Capron et al., 2008) and NORTIA (NTA), a MILDEW RESISTANCE LOCUS O 7 (MLO7) protein that becomes redistributed from the cytosol to the filiform apparatus in a FER-dependent manner upon PT arrival (Kessler et al., 2010). *lre/LRE* and *nta/NTA* mutants show the *fer*-like PT overgrowth phenotype in about 30% and 12% of the ovules, respectively (Capron et al., 2008; Kessler et al., 2010). In addition, the *abstinence by mutual consent* (*amc*) mutant is disrupted in a peroxin gene responsible for protein import into peroxisomes, and shows the *fer*-like PT overgrowth phenotype only if mutant pollen tubes fertilize mutant ovules (Boisson-Dernier et al., 2008). This particular phenotype suggests disrupted communication between both gametophytes due to missing signaling molecules from the peroxisomes. Recently, the first male gametophytic members of the PT reception pathway were identified (Leydon et al., 2013; Liang et al., 2013). Pollen tubes of a triple mutant of three MYB transcription factors (*myb97, myb101, myb120*) failed to arrest growth, to rupture and to release the sperm cells in 60-70% of targeted ovules (Leydon et al., 2013; Liang et al., 2013). However, the target genes of these transcription factors remain to be identified.

Here we describe two novel mutants impaired in PT reception in the synergids. Like *fer*, both mutants were named after Etruscan goddesses of fertility and fate, namely *turan (tun)* and *evan (evn)*. Interestingly, *tun* and *evn* plants show the same female gametophytic *fer*-like PT overgrowth phenotype in a subset of the mutant ovules, but have different pollen defects. Whereas *evn* mutant pollen grains degenerate before maturation, *tun* mutant grains develop normally, but PTs burst immediately after *in vitro* germination. The molecular identities of *TUN* and *EVN* suggest that both are involved in protein N-glycosylation, since they are coding for a putative UDP-glycosyltransferase superfamily protein and a dolichol kinase, respectively. However, their mutations seem not to affect the three described members of the PT reception pathway FER, NTA and LRE. In contrast, *tun* mutant pollen grains do not express ANX1-YFP, indicating that ANX proteins are potential targets of TUN-dependent glycosylation.

RESULTS:

tun and *evn* Mutants Show a *fer*-Like Pollen Tube Overgrowth Phenotype

To gain more insight into the molecular mechanisms involved in PT reception, a forward genetic ethyl methanesulfunate (EMS)-screen was conducted and yielded several new mutants showing a *fer*-like PT overgrowth phenotype in the female gametophyte. The two mutants with the highest penetrance were chosen for further characterization. Like *fer*, both mutants were named after Etruscan goddesses of fertility and fate, namely *turan (tun)* and *evan (evn)*. 12% (n=1318) and 20% (n=1233) of the ovules remained unfertilized in siliques of *tun-1/TUN* and *evn-1/EVN* heterozygous mutants, respectively, compared to only 1.5% (n=1389) in the wild type control (Table 1). In those unfertilized ovules the PT continued to grow inside the female gametophyte, failed to arrest its growth, and did not rupture to release the sperm cells in order to allow double fertilization (Figure 1A to 1C).

To ensure that the PT overgrowth phenotype was not caused by cell identity defects in the mutants, a β-Glucuronidase (GUS) synergid cell fate marker (ET2634) was analyzed. In both *tun* and *evn* mutant ovules GUS expression was restricted to the synergid cells (Figure 1D to 1F), indicating that the synergid cell identity was not affected. However, some ovules within a mutant silique showed an abnormal structure at the micropylar end of the synergids (Figure 1E). To further investigate this structure, ovule clearings and sections were analyzed 2 days after emasculation (DAE). In cleared ovules of *tun-1/TUN* and *evn-1/EVN* mutants 50% of mature embryo sacs showed the abnormal structure at the site of the filiform apparatus (Figure 1G to 1I). To gain more insight into the composition of this structure, 6μm thin ovule sections were stained for callose by Aniline Blue. In both *tun-1/TUN* and *evn-1/EVN* mutants 50% of the mature embryo sacs showed increased callose levels at the micropylar end (Figure 1J to 1L). However, the increased callose deposition did not influence PT attraction, since all ovules could attract pollen tubes. Additionally, callose deposition seemed not to influence PT reception and double fertilization, since 30% of the mutant ovules were fertilized normally. To investigate, if callose deposition in *tun* and *evn* ovules is an indicator of upregulated defense related response (Nishimura et al., 2003), the expression of several genes of different plant defense pathways were tested in mutant pistils 2DAE, but no upregulation was observed (Figure S1).

Taken together, we identified two novel members of the PT reception pathway in the synergid cells of the ovules. In both mutants, synergid differentiation is normal and increased callose levels accumulate at the micropylar end of the mutant ovules.

tun and *evn* Mutants Show Additional But Distinct Male Gametophytic Defects

Self-pollination of both *tun-1/TUN* and *evn-1/EVN* mutant plants yielded only heterozygous and wild-type offspring. Additionally, attempts to propagate the mutants by crossing wild-type plants with mutant pollen did not yield any mutant progeny. These results led to the hypothesis that not only the female but also the male gametophyte was affected by the *tun* and *evn* mutations. To further investigate this hypothesis, *tun-1/TUN* and *evn-1/EVN* plants were crossed to *quartet* (*qrt/qrt)* mutants (Preuss et al., 1994; Rhee et al., 2003). In the *qrt/qrt* mutant background, microspores fail to separate after meiosis and form tetrads of pollen grains. *qrt/qrt* analysis of heterozygous mutant individuals allows the detection

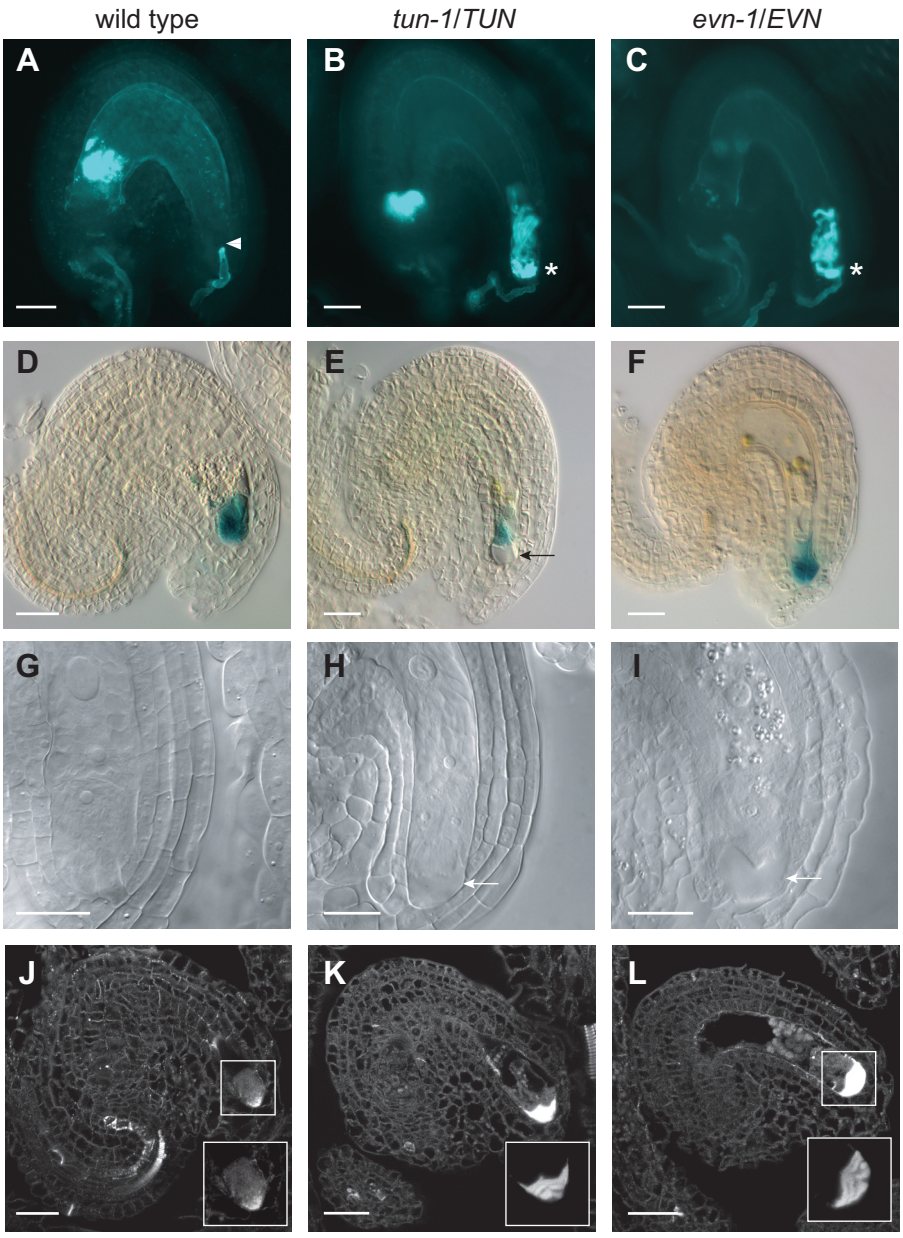

Figure 1. *tun* and *evn* ovules display a pollen tube overgrowth phenotype and increased callose accumulation at the filiform apparatus.

(A) to **(C)** Aniline blue staining of callose in PT cell walls 2 DAP. **(A)** Pollen tube reception in a wild-type ovule. Arrowhead indicates site of pollen tube growth arrest. **(B)** PT overgrowth phenotype in *tun-1* mutant ovules. **(C)** PT overgrowth phenotype in *evn-1* mutant ovules. Asterisks indicate PT overgrowth phenotype.

(D) to **(F)** GUS staining of synergid marker (ET2634) 2DAE **(D)** in wild type, **(E)** in *tun-1* mutant ovules, **(F)** and in *evn-1* mutant ovules. Arrow indicates abnormal structure at the filiform apparatus.

(G) to **(I)** Chloralhydrate clearings of ovules 2 DAE **(G)** in the wild-type control, **(H)** in *tun-1* mutants, and **(I)** *evn-1* mutants. Arrows indicate abnormal structure at the filiform apparatus.

(J) to **(L)** Aniline blue staining of callose in ovule cell walls in 6μm thin ovule sections 2 DAE. **(J)** Wild-type control ovule section. **(K)** Increased micropylar callose deposition in *tun-1* ovule section. **(L)** Increased micropylar callose deposition in *evn-1* ovule section. Boxes represent close-ups of indicated regions, whereas mutant close-ups are captured with reduced exposure time (K) and (L) than the wild type (J).

Scale bars in A-F and J-L = 20μm; scale bars in G-I = 10μm.

Table 1. Overview of the phenotypes in *tun* and *evn* mutant plants.

	pollen tube overgrowth		pollen phenotype		transmission efficiency	
	%	n	%	n	female	male
wild type (Col-0)	1.5%	1389	5% ± 5%[2]	128	NA	NA
tun-1/TUN	12%	1318	63% ± 1.5%[2]	441	74.5	0
tun-2/TUN	15%	513	44% ± 6.5%[2]	404	n.d.	n.d.
evn-1/EVN	20%	1233	54% ± 5%[3]	800	28	0
evn-2/EVN	28%	337	50% ± 0%[3]	495	n.d.	n.d.
evn-3/EVN	22%	320	50% ± 0%[3]	200	n.d.	n.d.
***tun-2/TUN* compl.[1]**	1%	280	1.7% ± 0.5%[2]	509	NA	NA
***TUN/TUN* compl.[1]**	0%	320	3.6% ± 1.6%[2]	620	NA	NA

[1] complementation construct is *pTUN::TUN-GFP* (homozygous)
[2] *anx1/anx2*-like pollen burst phenotype was assessed
[3] *evn*-induced pollen death was assessed
NA, not applicable
n.d., not determined

of pollen defects since within one tetrad, two microspores carry the wild-type allele and two the mutant allele of the gene of interest. *In vitro* pollen germination experiments revealed that in *tun-1/TUN* mutants, pollen development was normal, but 63% ± 1.5% (n=441) of mature pollen tubes burst immediately after germination, compared to 5% ± 5% (n=128) in the wild-type control (Figure 2A to 2C; Table 1). The pollen phenotype of *tun* is, therefore, reminiscent of double mutants affecting *ANX1* and *ANX2*, the pollen-specific homologues of *FER* (Boisson-Dernier et al., 2009; Miyazaki et al., 2009). However, in *evn-1/EVN* mutants 54% ± 5% (n=800) of the pollen grains degenerate before maturation, indicating general defects in pollen development (Figure 2D; Table 1). In the wild-type control all pollen grains were intact at maturity (n=600). DAPI staining of different pollen developmental stages revealed that *evn* mutant pollen degenerates during the early tri-cellular stage (n=2816; Figure 2E; Figure S2). Mutant grains were able to complete the second mitosis to form tri-cellular pollen, but comparison with the wild-type pollen within the same tetrad revealed a minor delay in some cases (Figure S2). Thus, pollen maturation does not occur in *evn* mutant grains.

Both *evn* and *tun* pollen defects were fully penetrant (i.e. male gametophytic lethal) and lead to a male transmission efficiency of 0% (n=96 plants per mutant; Table 1). In contrast the female transmission was reduced to 74.5% (n=96) and 28% (n=96) in *tun-1/TUN* and *evn-1/EVN* mutants, respectively (Table 1).

Reciprocal crosses between *tun-1/TUN* and *evn-1/EVN* mutants with Col-0 wild-type plants showed that the *fer*-like PT overgrowth phenotype was caused by the female gametophytic defect. Whereas mutant ovules fertilized by wild-type pollen showed the *fer*-like PT overgrowth phenotype, wild-type pistils pollinated with pollen from heterozygous mutants showed no phenotype (Figure S3) as expected since no mutant pollen tubes are formed.

Taken together, both *tun* and *evn* mutants display distinct male gametophytic defects, which cause complete loss of male transmission. However, decreased PT reception in mutant ovules is caused by a

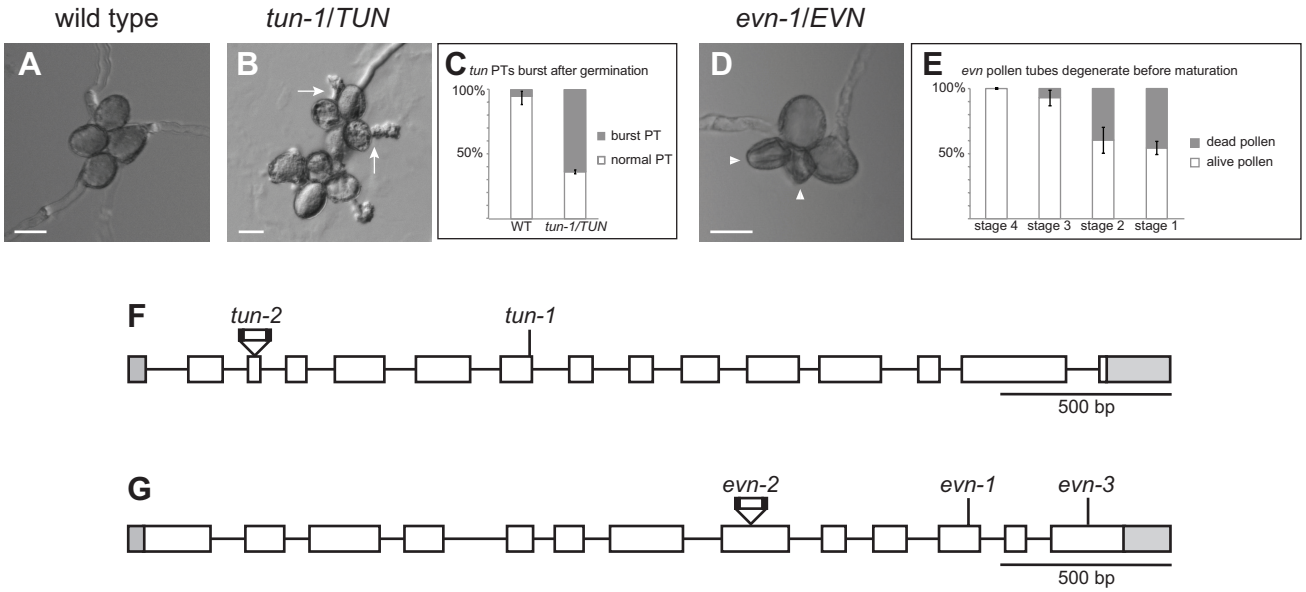

Figure 2. Different pollen defects in *tun* and *evn*.
(A) Pollen *in vitro* germination assay of *qrt/qrt* mutant pollen. **(B)** Pollen *in vitro* germination assay of *tun-1/TUN;qrt/qrt* pollen. Arrows indicate pollen tube bursting. **(C)** Graph of PT bursting counts in *qrt/qrt* and *tun-1/TUN;qrt/qrt* pollen. **(D)** Pollen *in vitro* germination assay of *evn-1/EVN;qrt/qrt* mutant pollen. Arrowheads indicate degenerated pollen grains. **(E)** Graph of counted degenerating pollen grains in different stages of *evn-1/EVN* mutants after DAPI staining. Stage 4 relates to the bi-cellular/early tri-cellular pollen stage. Stage 3 represents tri-cellular pollen stage. Stage 2 refers to late tri-cellular/early mature pollen stage. Stage 1 refers to mature pollen stage. Scale bars: 20μm. **(F)** Gene model of *TUN* with mutant alleles. **(G)** Gene model of *EVN* with mutant alleles. EMS SNPs are indicated by lines, T-DNA insertions by triangles.

female gametophytic defect, which causes decreased female transmission of the mutation.

TUN Encodes a Putative UDP-Glycosyltransferase and *EVN* Encodes a Dolichol-Kinase

In order to identify the two causative mutations in *tun-1/TUN* and *evn-1/EVN* heterozygous mutants, SNP-ratio mapping (SRM) was developed (Lindner et al., 2012b). SRM enables the mapping of heterozygous mutant individuals by next-generation sequencing after only two rounds of backcrossing. Briefly, the segregation ratios of EMS-induced SNPs are used to identify the causative SNP that segregates in a 1:1 ratio in a backcross mutant population versus a 1:3 ratio for unlinked SNPs segregating in the background.

Applying SRM on *tun-1/TUN* mutants revealed a stop codon in the sixth exon of the gene *At1g16570*, which encodes a putative UDP-glycosyltransferase superfamily protein (Figure 2F; Lindner et al., 2012b). In *evn-1/EVN* mutants SRM identified a stop codon in the eleventh exon of the gene *At3g45040* (Figure 2G; Figure S4), which encodes a dolichol-kinase. Interestingly, both TUN and EVN encode proteins that are likely to play roles in protein N-glycosylation.

In order to confirm that the correct genes had been identified, T-DNA insertion lines disrupting the mapped genes were analyzed. As described previously, the T-DNA insertional mutant allele *tun-2* (SAIL_400_A01) has an insertion in the fourth exon of *At1g16570* and displays the same pollen tube overgrowth phenotype (15%; n=513; Figure 2F; Table 1; Figure S5B; Lindner et al., 2012b) as *tun-1*. In addition, *tun-2* also causes premature PT bursting *in vitro* at a rate similar to the EMS allele *tun-1* (44% ± 6.5%; n=404; Table 1; Figure S5F), indicating that the correct gene had been identified by SRM. Furthermore, *evn-2*, which corresponds to the insertion line SAIL_529_E06, disrupts the eighth exon of

At3g45040 and shows the same female (28%; n=337) and male (50% ± 0%; n=495) phenotypes as the EMS mutant *evn-1* (Figure 2G; Table 1; Figure S5C and S5G). Finally, the third allele *evn-3* was found in the same EMS screen and identified by a combination of SRM (Figure S6) and classical map-based cloning (see Material & Methods). This allele has a premature stop codon in the last exon and displays similar female (22%; n= 320) and male (50% ± 0%; n=200) phenotypes to *evn-1* and *evn-2* (Figure 2G; Table 1; Figure S5D and S5H).

In summary, *TUN* and *EVN* encode genes potentially involved in protein N-glycosylation and loss-of-function of those genes cause impaired PT reception in the synergids and additional, but different pollen defects.

ER-Localization of TUN and EVN Supports Their Predicted Roles During Protein N-Glycosylation

N-linked protein glycosylation occurs as proteins transit through the endoplasmic reticulum (ER; reviewed in Aebi, 2013). In order to gain insight into the subcellular localization of the TUN and EVN proteins and to confirm the genes by functional complementation, native promotor-protein-GFP fusions were transformed into mutant plants and analyzed. The *pTUN::TUN-GFP* construct complemented both the female (PT overgrowth: 1%; n=280 *tun-2/TUN* complemented; 0% n=320 wild-type control) and the male (PT bursting: 1.7% ± 0.5%; n=509 *tun-2/TUN* complemented; 3.6% ± 1.6%; n=620 wild-type control) phenotypes (Table 1). In ovules, the strongest GFP signal was observed throughout the synergid cells before and after fertilization and in pollen tubes, where TUN-GFP localized in patchy, vesicle-like structures (Figure S7A to S7C). Co-localization studies of the *p35S::TUN-GFP* fusion with different subcellular marker lines in transiently transformed onion epidermis cells revealed TUN-GFP localization in the ER (Figure S7D). This ER localization supports the hypothesis that TUN might have a role in transferring mannose to the assembled oligosaccharide on the cytosolic site of the ER according to its yeast ortholog *ASPARAGINE-LINKED GLYCOSYLATION 1* (*ALG1*; Huffaker and Robbins, 1982; Couto et al., 1984).

The *pEVN::EVN-GFP* construct neither yielded GFP signal nor complemented the phenotypes, suggesting that the construct was not functional *in planta* potentially due to missing regulatory elements further upstream or downstream of the gene. However, a *p35S::EVN-GFP* construct was used to determine the subcellular localization of EVN-GFP in tobacco leaf epidermal cells, but could not be used for complementation analysis, since this promoter is not expressed in gametophytes. The EVN-GFP protein co-localized with the ER marker (Figure S7E) suggesting that EVN localizes to the expected subcellular compartment for its predicted role in N-glycosylation. In yeast, dolichol kinases like the EVN ortholog SECRETORY 59 (SEC59) are attached to the cytosolic site of the ER-membrane and phosphorylate the membrane-bound lipid carrier dolichol, before oligosaccharide assembly can start (Ferro-Novick et al., 1984; Bernstein et al., 1989; Heller et al., 1992).

In conclusion, TUN and EVN subcellularly localize to the ER and could, therefore, play the same roles during N-linked protein glycosylation as their characterized yeast orthologs.

FER, NTA and LRE Are Not Mis-Localized in *tun* and *evn* Mutant Ovules

Protein N-glycosylation plays important roles in many processes, among these are protein folding, protein stabilization, protein targeting (Helenius and Aebi, 2001), and receptor-ligand interactions (Haweker et al., 2010). Since *tun* and *evn* ovules show the *fer*-like PT overgrowth phenotype, we hypothesized that the stability and/or localization of known PT reception proteins could be compromised in *tun* and *evn* mutants. FER-GFP, NTA-GFP, and LRE-Citrine reporter constructs were introduced into the *tun* and *evn* mutant backgrounds and analyzed for changes in expression level and localization. First, *pFER::FER-GFP* and *pNTA::NTA-GFP* translational fusions were analyzed in *tun-2/TUN* and *evn-2/EVN* mutant siliques 2 DAE. Whereas NTA-GFP was shown to localize in vesicle-like structures throughout the cytoplasm before fertilization (Kessler et al., 2010), FER-GFP is localized at the filiform apparatus of the synergid cells (Escobar-Restrepo et al., 2007). Neither NTA-GFP nor FER-GFP localization was changed in either *tun* or *evn* mutants (Figure 3A to 3F), indicating that the PT overgrowth phenotype in *tun* and *evn* ovules is not caused by mis-localization of FER and NTA.

On the other hand, no reporter gene was available for LRE, which encodes a predicted GPI-anchored protein, but *in situ* hybridization experiments showed *LRE* expression predominantly in both synergid cells before fertilization (Capron et al., 2008). LRE-GFP fusions did not yield fluorescent signal in transient transformations (Capron et al., 2008), possibly due to the exposure of the GFP tag to the acetic pH of the extracellular matrix. However, LRE was a good candidate to be a target of EVN, since its mutant yeast ortholog *sec59,* is depleted in GPI-membrane anchored proteins (Heller et al., 1992). Therefore, we produced a LRE reporter using the pH stable fluorescent protein Citrine (Griesbeck et al., 2001) and cloned it between the predicted signal peptide and GPI-anchor of the LRE gene (Capron et

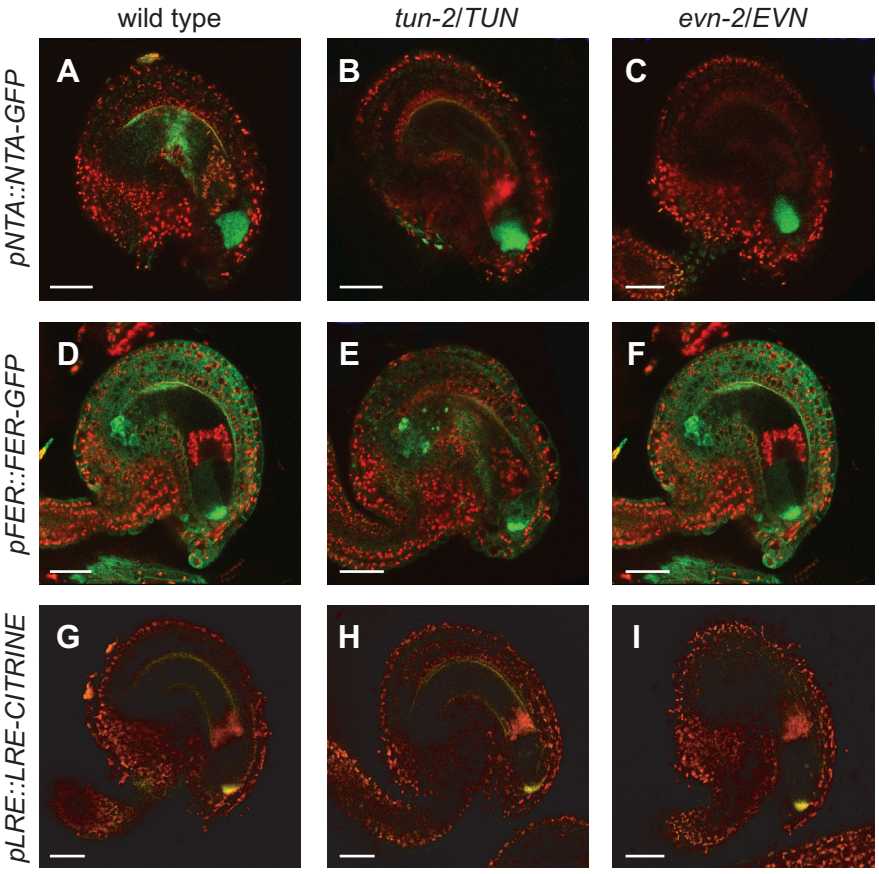

Figure 3. *NTA*, *FER* and *LRE* show proper localization in *tun* and *evn* mutant ovules.

(A) to **(I)** Confocal microscope analysis of fluorescently labeled proteins. **(A)** Cytoplasmic NTA-GFP localization in a wild-type ovule. **(B)** Cytoplasmic NTA-GFP localization in a *tun* mutant ovule. **(C)** Cytoplasmic NTA-GFP localization in a *evn* mutant ovule. **(D)** FER-GFP at the filiform apparatus and in cell membranes of a wild-type ovule. **(E)** FER-GFP at the filiform apparatus and in cell membranes of a *tun* mutant ovule. **(F)** FER-GFP at the filiform apparatus and in cell membranes of an *evn* mutant ovule. **(G)** Extracellular localization of LRE-Citrine in a wild-type ovule. **(H)** Extracellular localization of LRE-Citrine in a *tun* mutant ovule. **(I)** Extracellular localization of LRE-Citrine in an *evn* mutant ovule. Red signal in all panels represents chlorophyll autofluorescence. Scale bars: 20μm.

al., 2008). Interestingly, the LRE-Citrine fusion protein localized specifically to the micropylar end of the synergids (Figure 3G). LRE-Citrine localization appears at the surface of the synergid cells, and seems to be different to the filiform apparatus localization of FER-GFP (Figure 3D to 3F). Therefore LRE-Citrine might face the extracellular space and serve as an extracellular signal for PT reception. However, LRE-Citrine production and localization were unaffected by EVN and TUN loss-of-function mutations in the ovules (Figure 3H and 3I).

The normal localization of the FER, NTA, and LRE reporters in *tun* and *evn* mutant embryo sacs indicates that the synergids differentiate normally, as predicted from our GUS reporter analysis (Figure 1D to 1F). Furthermore, deficient PT reception in part of the mutant ovules is not caused by mis-expression or mis-localization of the characterized members of the PT reception pathway.

Downregulation of *TUN* Causes a Vegetative Growth Phenotype, But N-Glycosylation of FER-GFP Seems Not to Be Affected

In *tun* mutant plants, we observed both the *fer*-like PT overgrowth phenotype and the *anx1/anx2*-like premature PT bursting phenotype. The FER, ANX1 and ANX2 proteins all have multiple predicted N-glycosylation sites (Lindner et al., 2012a), indicating that TUN may be involved in the specific glycosylation of this receptor-like kinase subclass. Although in *tun* synergids FER-GFP localization seemed to be normal, it remained unclear if the protein was properly glycosylated. FER has nine putative N-glycosylation sites, eight of which reside on the extracellular, malectin-like domain (Lindner et al., 2012a). Since homozygous *tun/tun* mutants could not be recovered due to the loss of male transmission, RNA interference (RNAi) was used to knock down the expression of TUN using a constitutively-expressed 35S promoter. *TUN(RNAi)* constructs were cloned and transformed into Col-0 plants expressing a *pFER::FER-GFP* translational fusion. Complete *TUN* knockouts were not retrieved, but four independent *TUN(RNAi)* lines with greatly reduced *TUN* expression (down to 12% of wild-type levels, Figure 4A) were chosen for further analysis. Seedling proteins were isolated from wild type and *TUN(RNAi)* lines and separated by SDS-PAGE. FER-GFP was detected by immunoblot analysis using an anti-GFP antibody. In the case of complete absence of potential N-Glycans attached to FER, due to a defect in the N-glycosylation pathway, we would expect a band shift of the under-glycosylated (and thus smaller) FER protein in mutant *TUN(RNAi)* plants compared to wild-type controls (Farid et al., 2013). However, no obvious band-shift indicating loss of glycosylation was detected between FER-GFP of *TUN* knockdown seedlings and the wild-type control (Figure S8). In contrast, a clear mobility-shift was seen when FER-GFP was deglycosylated by N-glycan-site-deglycosylase Endoglycosidase H (EndoH) treatment *in vitro*. These data suggest that FER-GFP is not under-glycosylated in *TUN(RNAi)* seedlings. However, we cannot exclude the possibility that residual levels of TUN activity in the RNAi lines were able to partially or fully glycosylate FER in leaves or that FER-GFP is mis-glycosylated rather than under-glycosylated.

Nevertheless, *TUN* knockdown plants showed a strong vegetative dwarf phenotype that is reminiscent of the vegetative phenotype in *fer/fer* mutants (Figure 4B to 4G). The severity and frequency of the dwarf phenotype correlates with the expression level of *TUN* in the *TUN(RNAi)* lines (Figure 4A). Seedlings on plates looked normal, but after seedling transfer to the soil, some plants remained small and

accumulated anthocyanins and eventually degenerated without further growth (Figure 4D). It is possible that *TUN* expression in those degenerating plants would be completely knocked-out, but expression levels could not be determined due to early lethality. These results indicate that *TUN* is necessary for normal vegetative development. However, *EVN(RNAi)* knockdown plants showed reduced *EVN* expression down to 13% of wild-type levels but no obvious vegetative phenotype was observed (Figure S9).

Taken together, downregulation of *TUN* expression does not cause complete loss of N-glycosylation

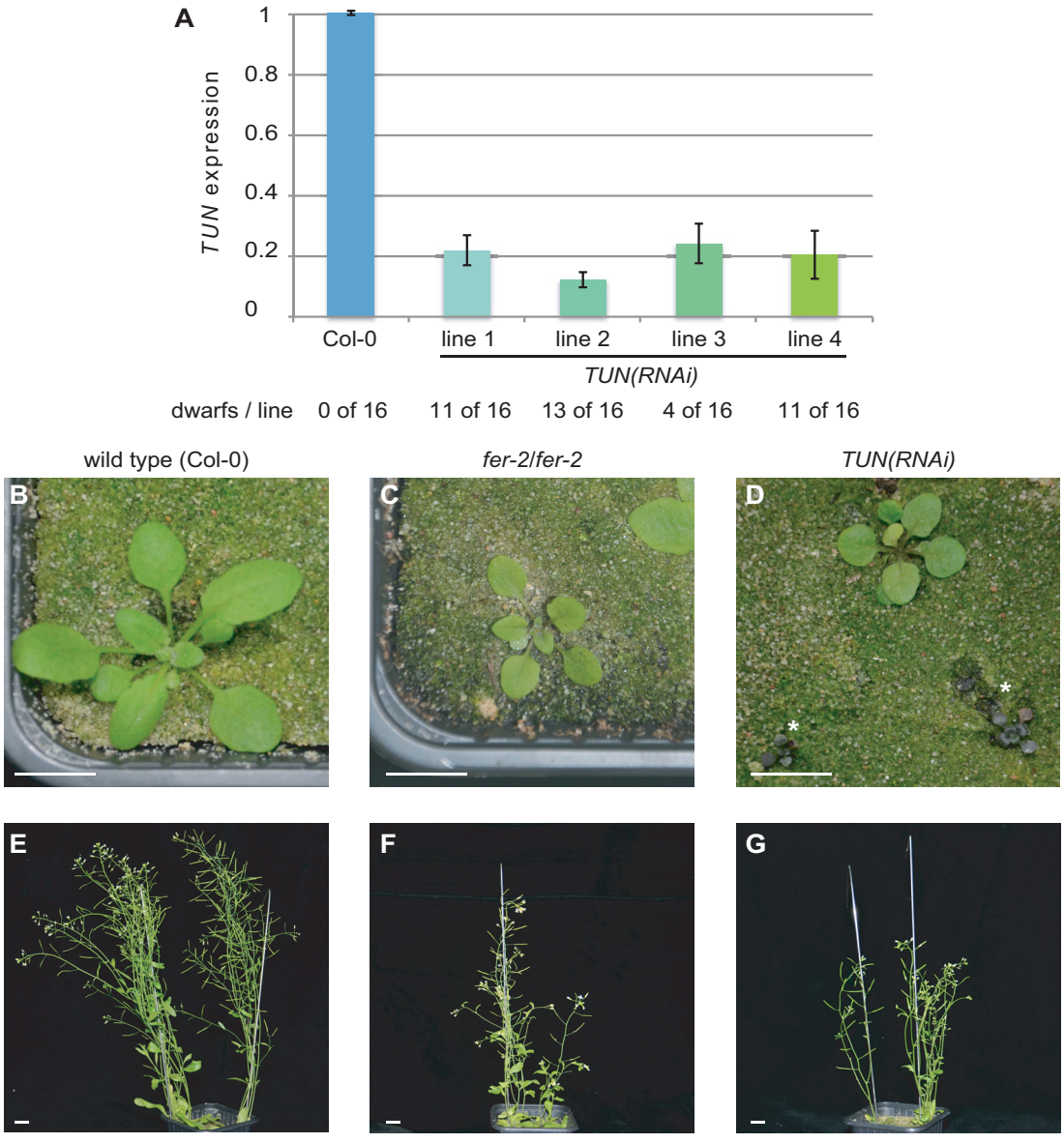

Figure 4. *TUN(RNAi)* lines show vegetative dwarf phenotype.
(A) qRT-PCR analysis of *TUN* expression in four independent *RNAi* lines. The corresponding number of dwarf individuals per line is indicated below.
(B) to **(G)** Plant size analysis of different developmental stages in wild type, *fer-2/fer-2* and *TUN(RNAi)* plants. **(B)** 30 days old wild-type seedling. **(C)** 30 days old *fer-2/fer-2* seedling. **(D)** 30 days old *TUN(RNAi)* seedlings. Asterisks indicate seedlings, which accumulate athocyanins and degenerate without further growth. **(E)** Adult wild-type plants. **(F)** Adult *fer-2/fer-2* plants. Left plant represents same developmental stage as wild-type and *TUN(RNAi)* individuals. **(G)** Adult TUN(RNAi) plant. Scale bars: 1cm.

of FER-GFP, but mis-glycosylation cannot be excluded. Moreover, TUN function is crucial for vegetative growth, but downregulation of *EVN* can be compensated in the vegetative state.

ANX1-YFP Is Absent in *tun* Mutant Pollen Grains

To investigate whether the premature PT bursting phenotype of *tun* mutant PTs is caused by alterations in the ANX1/ANX2 protein abundance and/or localization, we transformed *tun-2/TUN;qrt/qrt* mutants with *pANX1::ANX1-YFP* and additionally crossed *tun-2/TUN;qrt/qrt* to plants expressing the *pANX1::ANX1-YFP* construct. Interestingly, among 100 *tun-2/TUN* plants of the T2/F2 generation expressing *pANX1::ANX1-YFP,* no plants were found to have ANX1-YFP fluorescence in all four pollen grains of the tetrads (Figure 5). However, in wild-type segregants the *pANX1::ANX1-YFP* construct segregated normally and homozygous fluorescence could be observed (Figure 5). Thus, the *tun* mutation seems to affect ANX1-YFP production and/or stability in the male gametophyte.

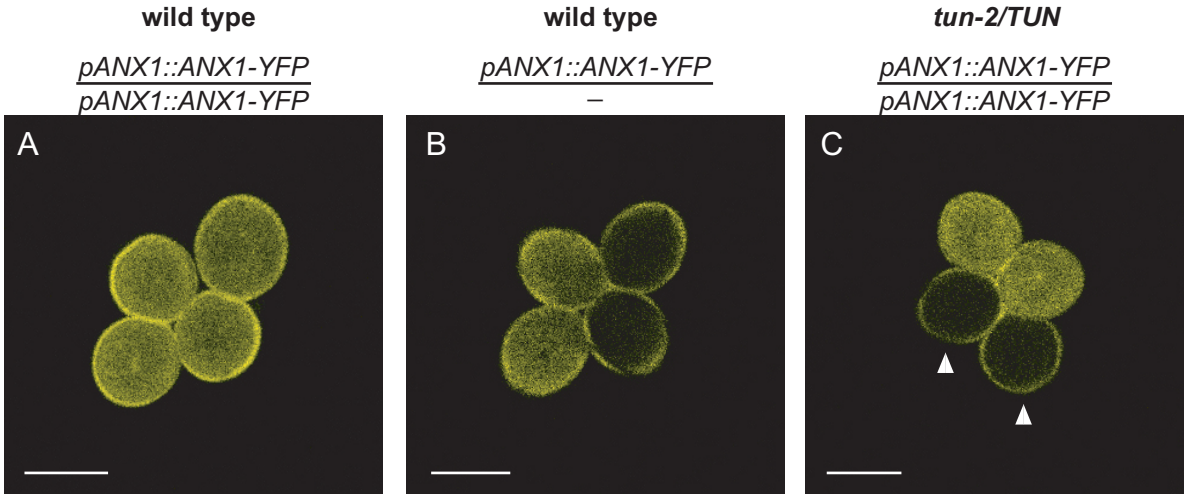

Figure 5. ANX1-YFP fluorescence is absent in *tun* mutant pollen grains.

(A) to **(C)** Confocal microscope analysis of *ANX1-YFP* expression. **(A)** *ANX1-YFP* expression in *TUN/TUN;qrt/qrt;ANX1-YFP/ANX1-YFP* (wild-type segregants homozygous for reporter). **(B)** *ANX1-YFP* expression in *TUN/TUN;qrt/qrt;ANX1-YFP/-* (wild-type segregants hemizygous for reporter). Residual fluorescence signal from the pollen coat is autofluorescence. **(C)** *ANX1-YFP* expression in *tun-2/TUN;qrt/qrt;ANX1-YFP/ANX1-YFP* mutant tetrads. Arrowheads indicate missing fluorescence in *tun* pollen grains. Yellow borders represent autofluorescence. Scale bars: 20μm.

DISCUSSION:

TUN and *EVN* Encode Two Members of the Early N-Glycosylation Pathway

In this study we identified two mutants, *tun* and *evn*, in a screen for defects in PT reception. The two mutants have similar effects on PT reception, but seem to play distinct roles during pollen development, pollen tube growth/integrity and vegetative growth. Both genes encode proteins that play putative roles during N-linked protein glycosylation, indicating that this co-translational protein modification is essential during various developmental processes.

N-linked glycosylation is an important process that affects protein folding, stability, transport and activity (reviewed in Helenius and Aebi, 2004; Varki, 1993; Skropeta, 2009). It is a multistep process starting with the assembly of an oligosaccharide, containing N-acetylglucosamine (GlcNAc), mannose (Man) and glucose (Glc), on a phosphorylated membrane-bound polyisoprenoid lipid carrier, the dolichol (reviewed in Aebi, 2013). The assembly starts on the cytosolic site and finishes on the lumenal site of the ER yielding the end product Glc_3-Man_9-$GlcNAc_2$ (reviewed in Aebi, 2013). The second step is the co-translational transfer of the oligosaccharide to an asparagine in the Asn-X-Ser/Thr sequon, where X can be any amino acid except proline (Bause, 1983). The last step is the ER-associated quality control, which ensures the proper folding of N-glycosylated proteins and subsequent exit of the ER (reviewed in Hüttner and Strasser, 2012).

EVN encodes a putative dolichol kinase, which plays an early role in the N-glycosylation pathway. The dolichol kinase in yeast, SEC59, which is an ortholog to EVN, catalyzes the cytidine-triphosphate (CTP)-dependent phosphorylation of the ER-membrane bound dolichol (Heller et al., 1992). The phosphorylated dolichol (Dol-P) serves as carrier for the assembly of the oligosaccharide on the cytosolic site of the ER and additionally, as a carrier for the monosaccharides Man and Glc in the ER lumen for GPI-anchor synthesis. In *Arabidopsis*, *EVN* is a single copy gene with described orthologs in yeast (Ferro-Novick et al., 1984), mammals (Allen et al., 1978; Rush et al., 2002) and humans (Fernandez et al., 2002). In yeast and humans, deficient dolichol kinase activity results in hypoglycosylation and subsequent lethality (Bernstein et al., 1989; Kranz et al., 2007). In fact, we never retrieved any homozygous mutant individuals for *evn*, which might be due to homozygous lethality. However, the epistatic male gametophytic lethality prohibits any conclusions regarding homozygous lethality.

TUN encodes a putative UDP-glycosyltransferase superfamily protein belonging to the Glycosyltransferase (GT) family 33, where TUN is the only member in *Arabidopsis*. The yeast ortholog *ALG1* encodes a beta-1,4 mannosyltransferase which transfers the first mannose from the GDP-D-Man substrate to the Dol-PP-$GlcNAc_2$ acceptor on the cytosolic site of the ER (Huffaker and Robbins, 1982; Couto et al., 1984). ALG1 resides in the ER membrane, forming homodimers and heterodimers with ALG2 and ALG11, respectively (Gao et al., 2004). Under non-permissive temperature conditions (37°C), temperature sensitive *alg1-1* mutants produce no mannose containing oligosaccharides (Huffaker and Robbins, 1982) leading to lethality in null mutants (Albright and Robbins, 1990). As for *evn*, no homozygous *tun* mutants were recovered, which might be caused by homozygous lethality. But again, the epistatic male gametophytic lethality prevents such a conclusion. However, the strong dwarf phenotype and dying seedlings in *TUN(RNAi)* lines supports the hypothesis that *tun* is homozygous lethal (see below).

Furthermore, both *p35S::EVN-GFP* and *p35S::TUN-GFP* fusion proteins co-localized with the *p35S::ER-dsRed* marker in transiently transformed tobacco and onion epidermis cells, respectively, suggesting similar roles for the two plant proteins compared to their yeast orthologs.

Increased Callose Deposition in the Filiform Apparatus of *evn* and *tun* Ovules

Synergid cell fate marker analysis and the proper localization of FER-, NTA-, and LRE- reporter constructs in *tun/TUN* and *evn/EVN* mutants revealed that PT overgrowth was not due to developmental defects in the synergid cells. However, in emasculated mutant siliques, 50% of the ovules displayed increased callose deposition at the filiform apparatus. In *Arabidopsis*, changes in cell wall composition in N-glycosylation mutants were reported by several independent studies (reviewed in Pattison and Amtmann, 2009). For instance, the *Arabidopsis* mutant *cytokinesis-defective* 1 (*cyt1*), which is disrupted in GDP-D-Man production, has reduced cellulose and increased callose accumulation in cell walls of heart-staged embryos (Conklin et al., 1996; Nickle and Meinke, 1998; Lukowitz et al., 2001). The same effect was seen in *peanut* (*pnt*) mutants that have defects in GPI-anchored protein biosynthesis (Gillmor et al., 2005). Under normal conditions, callose is not present in primary cell walls, but abiotic and biotic stress factors can induce callose accumulation, including defense-related responses (Nishimura et al., 2003). In *tun* and *evn* mutant siliques, no obvious upregulation of various defense-response genes has been found, indicating that callose accumulation is rather a consequence of mechanical stress (Aist, 1976) due to potential cellulose depletion as a result of deficient N-glycosylation. In *evn* and *tun* mutant ovules, further investigations are necessary to confirm decreased cellulose levels in the cell wall of the filiform apparatus. However, it is important to note that increased callose deposition in *evn* and *tun* ovules did not influence PT attraction and most likely PT reception, since all ovules attract pollen tubes and around 30% of the mutant ovules are fertilized normally.

Localization of Described Members of the Pollen Tube Reception Pathway Is not Affected in *evn* and *tun* Synergids

We showed that mutations in *EVN* and *TUN* lead to PT reception defects. Due to their protein localization to the ER it is likely that EVN and TUN are not directly mediating PT reception, but that the potentially impaired N-glycosylation pathway in mutant ovules affects other members of the PT reception pathway. To see if the already known players of the PT reception pathway are modified, the localization of translational fusions of *FER, NTA, and LRE* with fluorescent proteins was analyzed in heterozygous *evn-2/EVN* and *tun-2/TUN* siliques 2 DAE. Neither the defect of *EVN* nor the deficiency of *TUN* showed any altered localization of the three described members of the PT reception pathway. This was not surprising for NTA-GFP, which has no predicted glycosylation sites. However, LRE-Citrine was expected to be reduced or even absent in *evn* mutant ovules, since the yeast ortholog *sec59* is depleted in GPI membrane-anchored proteins (Heller et al., 1992). However, EVN and SEC59 display only 22% amino acid identity (ClustalW), hence, the roles of a dolichol kinase in *Arabidopsis* and *yeast* might not be completely conferrable.

However, protein abundance and proper protein localization does still not ensure intact protein function. *tun/TUN* heterozygous plants show the *fer*-like PT overgrowth phenotype and the *anx1/anx2*-

like premature PT bursting phenotype. Additionally, *TUN(RNAi)* lines reveal a *fer*-like vegetative dwarf phenotype. FER has nine putative N-glycosylation sites, eight of which reside on the extracellular, malectin-like domain (Lindner et al., 2012a). In *Xenopus laevis*, malectin is an ER-localized lectin, which selectively binds carbohydrates and is involved in ER-quality control of glycoproteins (Schallus et al., 2008; Galli et al., 2011). The extracellular, highly glycosylated malectin-like domain of FER suggests that its ligand contains sugar residues and that glycosylation of this domain is essential for ligand binding. However, potential deficiencies in protein glycosylation in *tun* and *evn* mutant ovules did not affect polar localization of FER-GFP to the filiform apparatus and downregulation of *TUN* did not cause complete loss of N-linked glycans of FER-GFP in *TUN(RNAi)* seedlings as revealed by protein mobility assays. However, it cannot be excluded that only some N-glycans are absent or that N-glycan composition is different. Therefore, it is possible that FER-GFP localization is unaffected, but functions like ligand binding and/or recognition and subsequent signal transduction could be reduced. This has been shown for the plant immunity leucine-rich repeat receptor-like kinase (LRR-RLK) *EF*-Tu RECEPTOR (EFR), which shows impaired ligand binding as a consequence of underglycosylation (Haweker et al., 2010).

In fact, PT reception at the filiform apparatus is an essential process to bring the male and female gametes together so that double fertilization can occur successfully. Therefore, it is crucial for the plant that PT reception can happen, even if small disturbances occur. Accordingly, it is conceivable that a "dual recognition system" exists, where the protein backbone of the receptor is required and the attached sugar residues would further enhance ligand binding, ensuring PT reception and thus increasing the chances for double fertilization even if the receptor is wrongly glycosylated. Such a dual recognition system has been described in the "domain specific model" during gamete interaction in mammals (Clark, 2010). In mammals, the glycoprotein mZP3 on the egg-cell extracellular matrix, the zona pellucida (ZP), is responsible for sperm binding (reviewed in Wassarman and Litscher, 2008). The domain specific model combines data of improved sperm binding by the glycosylated mZP3 proteins with data revealing that also unglycosylated mZP3 can bind sperm cells. Accordingly, a sperm cell protein or protein complex interacts with the glycans and/or the protein backbone of mZP3 depending on its glycosylation state and thus, the dual adhesion system ensures better sperm-egg binding but allows gamete interaction even if glycan composition is disturbed to increase the chance for fertilization (Clark, 2011). In plants, the existence of such a dual recognition system could also explain the reduced penetrance of the PT overgrowth phenotype in *tun* and *evn* ovules since the female protein component, even if not glycosylated properly, could still partially recognize the male factor. Nevertheless, it remains unknown if FER itself and/or other pathways are affected in *tun* and *evn* mutant ovules. In fact, not only receptors but also putative ligands could be wrongly glycosylated and thus show less receptor-binding affinity.

TUN(RNAi) Plants Show a Vegetative Dwarf Phenotype

N-glycosylation of proteins has been shown to be important during both embryo development and vegetative development in plants (reviewed in Pattison and Amtmann, 2009). Most reported mutants deficient in N-glycosylation are embryo lethal (*phosphomannomutase1* (*pmm1*; Hoeberichts et al., 2008); *cyt-1* (Conklin et al., 1996; Nickle and Meinke, 1998); *defective glycosylation1-2* (*dgl1-2*; Lerouxel et al., 2005); *glucosidase1 (gcs1*; Boisson et al., 2001); *knopf* (*knf*; Gillmor et al., 2002); *radial swelling3 (rsw3*; Burn et al.,

2002)), one is seedling lethal (*dgl1-1*; Lerouxel et al., 2005), and some show milder or no morphological defects (*leave wilting1* (*lew1*; Zhang et al.); *asparagine-linked glycosylation* 3-2 (*alg3-2*; Henquet et al., 2008); *saurosporine and temperature sensitive 3a and 3b* (*st3ta; stt3b*; Kelleher et al., 2003); *defender against cell death 1* (*dad1*; Wang et al., 2005); *UDP-glucose/galactose transporter* (*utr1*; Reyes et al., 2006)). In our *TUN(RNAi)* lines, we never found complete knockout plants, but a small residual activity of *TUN* always remained. However, the lower the expression was in a *TUN(RNAi)* line, the more dwarfed plants appeared. In addition, some seedlings accumulated anthocyanins early in development and degenerated without further growth. Thus, *TUN* seems to be essential during vegetative plant development potentially by mediating N-glycosylation. In contrast, *EVN(RNAi)* knockdown plants do not show an obvious vegetative phenotype but residual gene activity (at least 13%) might be sufficient for normal plant growth. Similarily, the heterozygous *lew1* mutant, which is impaired in dolichol biosynthesis, was also shown to have rather mild morphological phenotypes (Zhang et al.). As for *evn* and *tun*, no homozygous mutant *lew1* individuals were recovered suggesting that *lew1* is homozygous-lethal (Zhang et al.). Whether this lethality is sporophytic or gametophytic remains unsolved.

ANXUR1-YFP Is Absent in *tun* Pollen Grains

Interestingly, *tun/TUN* mutants do not only show the *fer*-like PT overgrowth phenotype in ovules, but also an *anx1/anx2*-like PT-bursting phenotype. ANX1 and ANX2 have seven and four potential N-glycosylation sites, respectively (Lindner et al., 2012a), whereas all four predicted glycosylation sites of ANX2 are in the extracellular malectin-like domain and are conserved in ANX1. To investigate if the ANX proteins are affected by the potentially defective glycosylation in *tun* mutant pollen grains, we analyzed ANX1-YFP fluorescence in *tun-2/TUN* pollen grains. Interestingly, we were not able to find any *tun-2/TUN* mutant plant showing homozygous ANX1-YFP fluorescence (only a maximum of 50% of all pollen grains was fluorescent). This result leads to the hypothesis that ANX1-YFP could be affected by the deficient N-glycosylation in *tun* pollen grains and is therefore degraded. Degradation could happen via the ER-associated degradation (ERAD) mechanism, which is induced when N-glycan-dependent protein folding fails (reviewed in Hüttner and Strasser, 2012). The mis-folded protein is recognized by ubiquitin protein ligases, followed by ubiquitination, retrotranslocation to the cytosol and degradation by the 26S proteasome (reviewed in Hüttner and Strasser, 2012). Specific degradation of an RLK by ERAD was shown previously: The plasma-membrane-localized LRR-RLK BRASSINOSTEROID-INSENSITIVE 1 (BRI1) contains multiple N-glycosylation sites (Li and Chory, 1997) and was shown to be a N-glycan-dependent ERAD target (Hong et al., 2008; 2009). Two mutant variants *bri1-5* and *bri1-9* retain in the ER and are degraded in a proteasome independent and dependent pathway, respectively (Hong et al., 2008; 2009).

Furthermore, since FER, NTA and LRE fusion proteins did not show any alteration in protein abundance or localization in *tun* mutant ovules, the effect on ANX1-YFP seems to be a specific effect in pollen rather than a general loss of glycosylated proteins in the plant. Specificity of ERAD has been described before for the LRR-RLKs EFR and FLAGELLIN-SENSITIVE 2 (FLS2), both involved in plant innate immunity (Li et al., 2009). Both LRR-RLKs are highly N-glycosylated PM localized proteins but mutations in two members of the ER quality control only affected EFR, but not the closely

related FLS2 (Li et al., 2009). Similarily, the closely related RLKs FER and ANX1 might both be mis-glycosylated in the *tun* mutant background, but only ANX1 and not FER is degraded via the ERAD pathway explaining the absence of ANX1-YFP but normal abundance and localization of FER-GFP.

In contrast to *TUN*, which seems to have a specific effect on PT growth/integrity, loss of *EVN* function in pollen leads to general developmental defects. So far four mutants of the N-glycosylation pathway with reduced female and/or male transmission have been described, although the reasons for reduced transmission remain elusive. The *stt3a/stt3b* double mutant of the OST complex, which is involved in co-translational N-glycan transfer, displays reduced female and male transmission (Kelleher et al., 2003). In addition, all three described mutants of the glucosidases involved in the calnexin-calreticulin protein folding cycle (*gcs1*, *knf14* and *rsw3*) show reduced female and /or male transmission (Boisson et al., 2001; Gillmor et al., 2002; Burn et al., 2002). All these described genes function much later in the glycosylation pathway than EVN and TUN, thus these two mutants are the first potential oligosaccharide assembly members showing reduced female and male transmission, due to similar female, but different male defects.

Conclusions & Future Perspectives

Taken together, we found the first evidence that protein N-glycosylation might be an important process to ensure PT reception in the synergid cells. In addition, we further support that N-glycosylation plays a crucial role during several developmental processes. The two potential members of the N-glycosylation pathway *TUN and EVN* play similar roles during PT reception in the synergid cells, but fulfill distinct functions during pollen development, pollen tube growth and vegetative development. There is no evidence that disruption of *TUN* and *EVN* affects abundance and localization of already known players of the PT reception signaling cascade in the synergid cells, however loss-of-functionality due to mis-glycosylation cannot be excluded. It is also conceivable that yet unknown co-factors or even an alternative, *FER*-independent pathway could be present and affected by *tun* and *evn*. However, in *tun* pollen grains the previously described ANX1 protein was absent, suggesting that it may be targeted by ERAD due to underglycosylation. Localization studies of other plasma membrane proteins in *tun* pollen grains and recovery studies of ANX1-YFP fluorescence after proteasome inhibitor treatment will resolve the specificity of *tun* on ANX1 and the nature of the involved degradation pathway, respectively. In tip growing PTs ANX1 and ANX2 prevent early PT bursting (Boisson-Dernier et al., 2009; Miyazaki et al., 2009). In polarly growing root hairs, FER was shown to play a similar role (Duan et al., 2010). It will be interesting to investigate if FER-GFP fluorescence is affected in the root hairs of *TUN(RNAi)* knockdown plants and/or if they show the *fer*-like root hair burst (Duan et al., 2010).

In conclusion, protein N-glycosylation seems to be an important process to mediate PT reception in the synergid cells. It is possible that plants have evolved similar mechanisms to ensure fertilization as mammals, where both sugar residue-protein and protein-protein interactions seem to act synergistically to guarantee gamete binding and thus enhance the chance for fertilization.

MATERIALS AND METHODS

Plant Material and Growth Conditions

Plant growth conditions were as previously described (Raissig et al., 2013). T-DNA insertion lines were all obtained by The European Arabidopsis Stock Center (NASC). *tun-2* corresponds to the insertion line SAIL_400_A01, *evn-2* to the insertion line SAIL_529_E06 (both lines are in the Col-0 ecotype). The *qrt1-2/qrt1-2* mutant line, published previously (Preuss et al., 1994), was a generous gift from J.F. Harper (University of Nevada, Reno). The *Lat52::DsRed* pollen line, the *pACA9::ANX1-YFP* plant line as well as the *pFER::FER-GFP* and the *pNTA::NTA-GFP* lines were previously described (Boisson-Dernier et al., 2008; 2009; Escobar-Restrepo et al., 2007; Kessler et al., 2010). Crosses were done by emasculating wild-type Col-0, *tun/TUN* and/or *evn/EVN* flower buds and pollinating with respective pollen, 2DAE.

Aniline Blue Staining

To investigate the PT overgrowth phenotype, siliques were selected around 2 days after pollination (DAP). Sepals and Petals were removed and siliques were fixed in 9:1 Ethanol:Acetic acid over night at 4°C. Aniline blue staining was described previously (Huck et al., 2003) and sample analysis was done using a Leica DM6000B epifluorescence microscope.

For callose staining of semi-thin sections, flower buds were emasculated and harvested 2 days after emasculation (DAE). Pistils were fixed in 3:1 Ethanol:Acetic acid under vacuum for 2x10min and incubated for 12 hours at 4°C. The fixative was replaced by 70% Ethanol and subsequently embedded into Paraplast X-tra embedding medium (Sigma-Aldrich), done by the embedding machine Leica ASP200 as previously described (Wuest et al., 2010). Sectioning was described before (Wuest et al., 2010), with the exception that we used 6µm thin sections. Samples were dewaxed and dehydrated after incubation for 1h at room temperature by 2x 10min Histoclear (100%), 2 x 2min EtOH (100%), followed by 2min of 80%, 60%, 30% EtOH each, 2min 0.75% NaCl and 2min H_2O treatment. Aniline blue staining was performed using 0.1% Methyl Blue (Sigma-Aldrich) and sample analysis was performed using the Leica SP5 confocal microscope.

Pollen Analysis

In vitro pollen germination was described previously (Boisson-Dernier et al., 2009). Pollen grains and tubes were imaged using the differential interfering contrast (DIC) channel of a Leica DM6000B microscope. Anthers from different stages were collected and analyzed by Alexander staining as described (Alexander, 1969). For DAPI staining anthers were fixed in 3:1 Ethanol:Acetic acid over night at 4°C and stored in 70% EtOH. For analysis 1µg/ml DAPI (4',6-diamidino-2-phenylindole) solution (0.1M sodium phosphate (pH 7), 1 mM EDTA, 0.1% Triton X-100, 1µg/ml DAPI; high grade, Sigma-Aldrich) was added and the sample was analysed using a Leica DM6000B epifluorescence microscope.

Ovule Clearing

Flower buds were emasculated and collected 2DAE, carved longitudinally on the sides and fixed in 9:1 EtOH:Acetic acid over night at 4°C. Samples were washed by an EtOH series (85%, 70%, 50%, 30%

for 30min each) and clearing solution (chloral hydrate:glycerol:water (8:1:2, w:v:v)) was added. Siliques were dissected and ovules were analyzed at the Leica DMR microscope.

β-Glucuronidase (GUS) Staining

The synergid cell GUS marker line ET2634 (Groß-Hardt et al., 2007) was crossed to *tun-1/TUN* and *evn-1/EVN* mutants, respectively. Homozygous F2 individuals were emasculated and siliques 2DAE were stained for GUS expression as previously described (Kessler et al., 2010). Stained samples were dissected and analyzed using a Leica DMR microscope.

Identification of *tun-1*, *evn-1* and *evn-3*

tun-1, *evn-1* and *evn-3* EMS-alleles were identified by SNP-ratio mapping (SRM; Lindner et al., 2012b). SNP data of *evn-1* and *evn-3* resequencing are presented in Table S1 and Table S2, respectively. Sequencing coverage for *evn-3* was only 30 reads and thus too low to identify the SNP by the segregation ratio (Figure S6). Therefore, rough mapping of an F2 mapping population was done after outcrossing *evn-3/EVN* to L*er*. A linkage was found for the marker ciw4 (70cM) on the lower arm of chromosome 3 and several candidate genes from SRM in this region were tested with Surveyor nuclease digest (see below). Primers used for gene amplification of non-causative SNPs are found in Table S3. To confirm the causative mutations in *evn-1* and *evn-3*, the SNP containing region was amplified from every sample of the sequencing pool using primers:

evn-1: 5'-TGGGCCCAACCAATATAAAG-3' and 5'-TCTCAGCCTAGGAATTGGAGA-3'

evn-3: 5'- GCCAATATGGGCCTTGTTAT-3' and 5'-TGACCATCGTGACTCAGAGC-3'

The PCR products were digested with Surveyor (Transgenomics) Cel-A nucleases according to manufacturer`s recommendations, in order to determine if the SNP was present in all mutant samples. Surveyor Gels are displayed in Figure S10.

Constructs for Stable Transformation

All PCR reactions for cloning were done using Phusion HF polymerase (NEB), Phusion HF PCR buffer and a final concentration of 2mM $MgCl_2$, 0.2mM dNTPs and 0.2-0.4mM Primer. If not mentioned otherwise we used the following, standard PCR program: 28 to 34 cycles (94°C for 15 sec, 58°C for 20 sec, and 72°C for 30-120 sec) followed by 72°C for 5min.

Gateway cloning was performed as described in (Raissig et al., 2013) and only gene-specific primers containing the first 12 base pairs of the attB sites are mentioned below.

TUN- and EVN-GFP fusions:

For Gateway cloning of *pTUN::TUN-GFP*, the complete coding sequence, without the stop codon but including a 462bp long promoter region of *TUN* (*At1g16570*) was amplified using gene-specific primers including attB Gateway sites: 5'-AAAAAGCAGGCTTAGCGTCTCACAATCTCC-3' and 5'- AGAAA GCTGGGTGTGAATCTGCAATTTGAGA-3'

For Gateway cloning of *pEVN::EVN-GFP*, the complete coding sequence without the stop codon, including a 1272bp long promoter region of *EVN* (*At3g45040*) was amplified using gene-specific primers including attB Gateway sites: 5'- AAAAAGCAGGCTCACAACAGAAGAATTATC-3' and 5'- AGAAAGCTGG

GTGCAAGCAGAGGAGTGAGTA-3'
For Gateway cloning of *p35S::TUN-GFP* and *p35EVN::EVN-GFP*, the complete coding sequence, without the stop codon was amplified by gene-specific primers including attB Gateway sites:
TUN: 5'- AAAAAGCAGGCTTAATGGGGAAAAGAGGAAGGGC-3' and 5'- AGAAAGCTGGGTG TGAATCTGCAATTTGAGA-3'
EVN: 5'- AAAAAGCAGGCTTAATGAAGACGACGGCGACG-3' and 5'- AGAAAGCTGGGTGCA AGCAGAGGAGTGAGTA-3'
PCR products were cloned via BP reaction into the pDONR207 and subsequently via LR reaction into the destination vectors (pMDC107 for native-promoter constructs and pMDC83 for 35S-promoter constructs (Curtis and Grossniklaus, 2003)) according to the manufacturer's recommendation (Invitrogen). *pTUN::TUN-GFP* and *pEVN::EVN-GFP* were transformed (see below) into *tun-2/TUN* and *evn-2/EVN* plant lines, respectively. Progeny were selected on MS plates containing 25mg/L Hygromycin to select for transformants.

LRE-Citrine fusion:
Cloning of the *pLRE::LRE-Citrine* construct was done using the Gibson cloning Master Mix from New England Biolabs (NEB) according to the manufacturer`s recommendations. This method is based on overlapping PCR products. Thus, a 779bp long promoter sequence with the predicted signal peptide from *LRE* (Capron et al., 2008) was amplified with primers containing an overhang for the vector pMDC99 (Curtis and Grossniklaus, 2003): 5'-GTGCTGCAAGGCGATTAAGTCCGTGTGCTCTGTCTGCA TT-3' and 5'- CACAGCTCCACCTCCACCTCCAGGCCGGCCTATGGAACTTGAAGAGGAGA GAGA-3'.
Citrine was amplified from the transgenic line CS36962 from the Arabidopsis Biological Recourse Center (ABRC) using gene-specific primers with overhang primers for the signal peptide of *LRE* and overhang primers for the GPI-anchor of *LRE*: 5`-GGCCGGCCTGGAGGTGGAGGTGGAGCTGTGAGCAA GGGCGAGGAGCT-3' and 5'- GGCCCCAGCGGCCGCAGCAGCACCAGCAGGATCCTTGTA CAGCTCGTCCA-3'.
The GPI-anchor of *LRE* was amplified with overhang primers for the pMDC99 vector: 5'- TGCTGG TGCTGCTGCGGCCGCTGGGGCCTCGGGTATGTCTTTTTGTTGTC-3' and 5'- AGCTCCAC CGCGGTGGCGGCCGCTCTAGAAGTCTCGCTTCTTCTTTTGT-3'.
pMDC99 was amplified with overhang primers for the *LRE* promoter and the GPI-anchor using primers: 5'-ACTTAATCGCCTTGCAGCAC-3' and 5'- TCTAGAGCGGCCGCCACCGCGG-3'.
pLRE::LRE-Citrine was transformed to *tun-2/TUN* and *evn-2/EVN* lines. Progeny were selected on MS plates containing 25mg/L Hygromycin to select for transformants.

FER-GFP/ANX1-YFP fusion:
The *pFER::FER-GFP* and *pACA::ANX1-YFP* constructs were described previously (Escobar-Restrepo et al., 2007; Boisson-Dernier et al., 2009) and were transformed into *Arabidopsis thaliana* Col-0 wild-type plants and *tun-2/TUN* mutants, respectively. Progeny were selected on MS plates containing 25mg/L Hygromycin to select for transformants.

RNAi-construct production:
For *TUN* downregulation by RNAi silencing, Exon 13 was amplified using primers with attB overhangs for Gateway cloning: 5'- AAAAAGCAGGCTCATTCAAGAACTCGTTAAAG -3' and 5'- AGAAAG CTGGGTCTGAGTGATTAAAGGTTTTGC-3'
For *EVN* downregulation, Exon 13 including the 3`UTR was amplified using primers with attB overhangs for Gateway cloning: 5'- AAAAAGCAGGCTAGAAAACGGTTGAAGGAACAGC-3' and 5'- AGAAA GCTGGGTATACGGCAATTAACAAGAGG-3'
PCR products were cloned via BP reaction in pDONR207 and subsequently via LR reaction into destination vector pHellsgate12 (Helliwell and Waterhouse, 2005) according to the manufacturer's recommendation (Invitrogen). *pFER::FER-GFP* expressing Col-0 plants (described above) were transformed using the below described transformation technique. Progeny were selected on MS plates containing 50mg/L Kanamycin and 25mg/L Hygromycin to select transformants for the silencing construct and *FER-GFP*, respectively.

Transformation Techniques
E.coli transformations were conducted using competent *E. coli* strain DH5-alpha F'I^q from NEB. For plant transformation, the destination vector was transformed into competent *Agrobacterium tumefaciens* strain GV3101 (Koncz and Schell, 1986) and *Arabidopsis thaliana* transformation was done by floral dip (Zhang et al., 2006).

Transient Expression in Onion and Tobacco Epidermis Cells
Transient onion transformation was previously described (Varagona et al., 1992). For tobacco leaf infiltration, a 5ml overnight *Agrobaterium tumefacience* strain GV3101 (Koncz and Schell, 1986) culture containing the plasmid of interest was spinned down for 15min 4000rpm (Eppendorf Centrifuge 5804R with the A-4-44 rotor) and dissolved in 2ml AS-medium (3M $MgCl_2$, 1M MES-Buffer, pH=5.6, 150mM Acetosyringone). The OD was adjusted to 0.8 using a photometer (BioRad SmartSpec3000) and different clones were mixed equally and incubated 2-4h shaking at 28°C. 3 week old *Nicotiana Benthamiana* plants were watered before infiltration and leaves were infiltrated abaxially using a standard syringe without needle. Infiltrated plants were incubated for 2-3 days and small leave pieces were analyzed using the Leica SP5 confocal microscope. The ER-marker pER-rk (mCherry) was obtained from ABRC (Nelson et al., 2007).

DNA Extraction and Genotyping
DNA was extracted as previously described (Edwards et al., 1991). T-DNA insertion lines were genotyped using three primers in one PCR reaction as follows:
The wild-type allele of *tun-2/TUN* was amplified using primers: 5'-TCCGACTCATTAGCGTCTCAC-3' and 5'-CTGGACCAAGAAAATGTCAGG-3'
The wild-type allele of *evn-2/EVN* was amplified using primers: 5'-TTCGCAGTCATGAAATGGTC-3' and 5'-TGAGAATTCCAGCAAATGGA-3'.

The T-DNA insertion was amplified using the T-DNA specific primer (LB1-Syg): 5'-GCCTTTTCAGA AATGGATAAATAGCCTTGC-3'.
After identification of the causative EMS SNPs, genotyping of *tun-1/TUN*, *evn-1/EVN* and *evn-3/EVN* was done using dCAPS primers.
For *tun-1/TUN* primers:5'-GGTTATTATCTATGAGAAATTTCATCTCACCTCACAGC-3' and 5'-GGAAAGATGGCAACAGGTTC-3' were used to amplify the gene and subsequent digest with AluI (NEB) revealed mutant individuals by cutting the mutant PCR product.
evn-1/EVN was amplified using primers: 5'-TCTCCAATTCCTAGGCTGAGAATGC-3' and 5'-TTCTCACTCTTGCTTGGGTGT-3' to amplify the gene and subsequent digest with NheI (NEB) revealed mutant individuals by cutting the mutant PCR product.
For *evn-3/EVN* genotyping primers: 5'-CGGTGGCTGTCACAGCCACCAGAAGCGAGCG-3' and 5'-GATGGCAGTGTGCTTTGTTC-3' were used to amplify the gene and subsequent digest with HhaI (NEB) revealed mutant individuals by cutting the mutant PCR product.

RNA Extraction, RT-PCR and qRT-PCR

To determine upregulation of defense-related genes in mutant siliques and residual expression of *TUN* and *EVN* in the RNAi knockdown plants, RNA from 25 emasculated *tun-1/TUN*, *evn-1/EVN*, *evn-3/EVN* and Col-0 pistils and 2-3 cauline leaves of RNAi plants and Col-0 control plants, respectively, was extracted using Trizol (Invitrogen) according to the manufacturer`s recommendations. cDNA was reverse transcribed using Oligo-dT primers and Superscript II reverse transcriptase (Invitrogen) according to the manufacturer`s recommendations.
RT-PCR analysis of defense-related genes was done using the following primers:
PR1: 5'-TCGGAGCTACGCAGAACAACT-3' and 5'-TCGGAGCTACGCAGAACAACT-3'
PDF1.2: 5'-TGGTGGAAGCACAGAAGTTG-3' and 5'-GATCCATGTTTGGCTCCTTC-3'
PR5: 5'- TCCTTGACCGGCGAGAGTT-3' and 5'- AGGAACAATTGCCCTACCACC-3'
PAL1: 5'- AACGGAGGAGGAGTGGACG-3' and 5'- CTTTCATTTGCTCCGCTGC-3'
Actin11: 5'-AACTTTCAACACTCCTGCCATG-3' and 5'-CTGCAAGGTCCAAACGCAGA-3'
Primers of *PR1*, *PR5* and *PAL1* were published in (Beckers et al., 2009). The primers of *PDF1.2* were previously described in (Qiu et al., 2008).

qRT-PCR was performed in a real-time PCR system (Applied Biosystems 7500 Fast Real-Time PCR System) using the SYBR green q-PCR mix (Applied Biosystem PCR Master Mix) according to manufacturer's recommendation. qRT-PCR of *TUN* was done using the primers : 5'-TCAGAAGAGCAACACCATTATCCC-3' and 5'-CTGCGAGCCACATTGTACGG-3'
qRT-PCR of *EVN* was done using the primers: 5'-GACCGAGCCTTATCTCCATTTGC-3' and 5'-ATGTTATTCCCGCTGCTGTTCC-3'
Expression levels were normalized against *UBIQUITIN C* (*UBC*, primers: 5'-ATGCTTGGAGTCCTGCTTGG-3' and 5'-TGCCATTGAATTGAACCCTCTC-3')

Western Blot and Deglycosylation Analysis

Protein extraction from 10days old seedlings (~400; wild type and *tun-2/TUN* containing *pFER:: FER-GFP*) was conducted by grinding them in a mixer mill and subsequently adding extraction buffer (50mM Tris pH7.5, 10mM NaCl, 0,5% Triton X-100 and a tablet of Complete Mini protease inhibitor cocktail (Roche)). Extracts were incubated on ice for 15 minutes and centrifuged for 3 minutes at 14000 rpm (Eppendorf centrifuge 5424 with a FA-45-24-11). Protein extracts were boiled at 95% with SDS loading buffer (63mM Tris-HCl (pH=6.8), 15% glycerol, 2% SDS, 0.15% bromophenol blue, 7mM DTT) and loaded on a 10% gel followed by SDS-PAGE under reducing conditions. After blotting to a PVDF membrane (Millipore Immobilon Transfer Membrane), the membrane was blocked in 5%-TBST (20mM Tris (pH=7.4), 150mM NaCl, 0.05% Tween-20), and was probed with anti-GFP B-2 antibody (Santa Cruz Biotech), washed with TBST, treated with the secondary antiboday (goat anti-mouse horseradish peroxidase-conjugated (Pierce)) and detected using chemiluminescence (SuperSignal West Dura (ThermoScientific)).

To assess protein amounts, the reducing SDS gel was stained with Coomassie Brilliant Blue R250 (Fluka) solution (0.1% Coomassie, 10% glacial acid, 40% methanol) and de-stained with destaining solution (20% methanol, 10% acetic acid).

EndoH (NEB) digestion was performed according to the manufacturer's instructions under reducing conditions.

Confocal Microscopy

Confocal microscopy was previously described (Kessler et al., 2010), with the exception that a Leica SP5 confocal microscope has been used.

ACKNOWLEDGEMENTS:

We thank Michael T. Raissig for critically reading the manuscript. This work was supported by the University of Zürich (www.uzh.ch) and grants from the Swiss National Science Foundation (www.snf.ch) to UG. The funders had no role in study design, data collection and analysis, decision to publish, or preparation of the manuscript.

AUTHORS CONTRIBUTIONS:

Conceived and designed the experiments: HL, SAK, UG. Performed the experiments: HL, LM, HSA. Interpreted the results: HL, SAK, ABD, UG. Wrote the manuscript: HL, SAK, LM, UG.

References:

Aebi, M. (2013). N-linked protein glycosylation in the ER. Biochim. Biophys. Acta **1833**: 2430–2437.

Aist, J.R. (1976). Papillae and related wound plugs of plant cells. Annu. Rev. Phytopathol. **14**: 145–163.

Albright, C.F. and Robbins, R.W. (1990). The sequence and transcript heterogeneity of the yeast gene *ALG1*, an essential mannosyltransferase involved in N-glycosylation. J. Biol. Chem. **265**: 7042–7049.

Alexander, M.P. (1969). Differential staining of aborted and nonaborted pollen. Biotech. Histochem. **44**: 117-122.

Allen, C.M., Kalin, J.R., Sack, J., and Verizzo, D. (1978). CTP-dependent dolichol phosphorylation by mammalian cell homogenates. Biochemistry **17**: 5020–5026.

Bause, E. (1983). Structural requirements of N-glycosylation of proteins. Studies with proline peptides as conformational probes. Biochem. J. **209**: 331–336.

Beale, K.M. and Johnson, M.A. (2013). Speed dating, rejection, and finding the perfect mate: advice from flowering plants. Curr. Opin. Plant Biol. **16**: 590–597.

Beckers, G.J.M., Jaskiewicz, M., Liu, Y., Underwood, W.R., He, S.Y., Zhang, S., and Conrath, U. (2009). Mitogen-activated protein kinases 3 and 6 are required for full priming of stress responses in *Arabidopsis thaliana*. Plant Cell **21**: 944–53.

Bernstein, M., Kepes, F., and Schekman, R. (1989). *Sec59* encodes a membrane protein required for core glycosylation in *Saccharomyces cerevisiae*. Mol. Cell. Biol. **9**: 1191–1199.

Boisson, M., Gomord, V., Audran, C., Berger, N., Dubreucq, B., Granier, F., Lerouge, P., Faye, L., Caboche, M., and Lepiniec, L. (2001). *Arabidopsis glucosidase I* mutants reveal a critical role of N-glycan trimming in seed development. EMBO J. **20**: 1010–1019.

Boisson-Dernier, A., Frietsch, S., Kim, T.-H., Dizon, M.B., and Schroeder, J.I. (2008). The peroxin loss-of-function mutation *abstinence by mutual consent* disrupts male-female gametophyte recognition. Curr. Biol. **18**: 63–68.

Boisson-Dernier, A., Lituiev, D.S., Nestorova, A., Franck, C.M., Thirugnanarajah, S., and Grossniklaus, U. (2013). ANXUR Receptor-Like Kinases Coordinate Cell Wall Integrity with Growth at the Pollen Tube Tip Via NADPH Oxidases. PLoS Biol **11**: e1001719.

Boisson-Dernier, A., Roy, S., Kritsas, K., Grobei, M.A., Jaciubek, M., Schroeder, J.I., and Grossniklaus, U. (2009). Disruption of the pollen-expressed *FERONIA* homologs *ANXUR1* and *ANXUR2* triggers pollen tube discharge. Development **136**: 3279–3288.

Burn, J.E., Hurley, U.A., Birch, R.J., Arioli, T., Cork, A. and Williamson, R.E. (2002). The cellulose-deficient *Arabidopsis* mutant *rsw3* is defective in a gene encoding a putative *glucosidase II*, an enzyme processing N-glycans during ER quality control. Plant J. **32**: 949-960**.**

Capron, A., Gourgues, M., Neiva, L.S., Faure, J.E., Berger, F., Pagnussat, G., Krishnan, A., Alvarez-Mejia, C., Vielle-Calzada, J.P., Lee, Y.R., Liu, B., and Sundaresan, V. (2008). Maternal Control of Male-Gamete Delivery in *Arabidopsis* Involves a Putative GPI-Anchored Protein Encoded by the *LORELEI* Gene. Plant Cell **20**: 3038–3049.

Clark, G.F. (2010). The mammalian zona pellucida: a matrix that mediates both gamete binding and immune recognition? Syst. Biol. Reprod. Med. **56**: 349-364.

Clark, G.F. (2011). Molecular models for mouse sperm-oocyte binding. Glycobiology **21**: 3–5.

Conklin, P.L., Williams, E.H., and Last, R.L. (1996). Environmental stress sensitivity of an ascorbic acid-deficient *Arabidopsis* mutant. Proc. Natl. Acad. Sci. U.S.A. **93**: 9970–9974.

Couto, J.R., Huffaker, T.C., and Robbins, P.W. (1984). Cloning and expression in *Escherichia coli* of a yeast mannosyltransferase from the asparagine-linked glycosylation pathway. J. Biol. Chem. **259**: 378–382.

Curtis, M.D. and Grossniklaus, U. (2003). A gateway cloning vector set for high-throughput functional analysis of genes *in planta*. Plant Phys. **133**: 462–469.

Dresselhaus, T. and Franklin-Tong, N. (2013). Male-Female Crosstalk during Pollen Germination, Tube Growth and Guidance, and Double Fertilization. Mol. Plant **6**: 1018–1036.

Duan, Q., Kita, D., Li, C., Cheung, A.Y., and Wu, H.-M. (2010). *FERONIA* receptor-like kinase regulates RHO GTPase signaling of root hair development. Proc. Natl. Acad. Sci. U.S.A. **107**: 17821–17826.

Edwards, K., Johnstone, C., and Thompson, C. (1991). A simple and rapid method for the preparation of plant genomic DNA for PCR analysis. Nucleic Acids Res. **19**: 1349.

Escobar-Restrepo, J.M., Huck, N., Kessler, S., Gagliardini, V., Gheyselinck, J., Yang, W.C., and Grossniklaus, U. (2007). The *FERONIA* Receptor-like Kinase Mediates Male-Female Interactions During Pollen Tube Reception. Science **317**: 656–660.

Farid, A., Malinovsky, F.G., Veit, C., Schoberer, J., Zipfel, C., and Strasser, R. (2013). Specialized Roles of the Conserved Subunit OST3/6 of the Oligosaccharyltransferase Complex in Innate Immunity and Tolerance to Abiotic Stresses. Plant Phys. **162**: 24–38.

Fernandez, F., Shridas, P., Jiang, S., Aebi, M., and Waechter, C.J. (2002). Expression and characterization of a human cDNA that complements the temperature-sensitive defect in dolichol kinase activity in the yeast *sec59-1* mutant: the enzymatic phosphorylation of dolichol and diacylglycerol are catalyzed by separate CTP-mediated kinase activities in *Saccharomyces cerevisiae*. Glycobiology **12**:

555–562.

Ferro-Novick, S., Novick, P., Field, C., and Schekman, R. (1984). Yeast secretory mutants that block the formation of active cell surface enzymes. J. Cell Biol. **98**: 35–43.

Galli, C., Bernasconi, R., Soldà, T., Calanca, V., and Molinari, M. (2011). Malectin participates in a backup glycoprotein quality control pathway in the mammalian ER. PLoS ONE **6**: e16304.

Gao, X.D., Nishikawa, A., and Dean, N. (2004). Physical interactions between the *Alg1*, *Alg2*, and *Alg11* mannosyltransferases of the endoplasmic reticulum. Glycobiology **14**: 559-570.

Gillmor, C.S., Lukowitz, W., Brininstool, G., Sedbrook, J.C., Hamann, T., Poindexter, P., and Somerville, C. (2005). Glycosylph osphatidylinositol-anchored proteins are required for cell wall synthesis and morphogenesis in *Arabidopsis*. Plant Cell **17**: 1128–1140.

Gillmor, C.S., Poindexter, P., Lorieau, J., Palcic, M.M., and Somerville, C. (2002). *Alpha-glucosidase I* is required for cellulose biosynthesis and morphogenesis in *Arabidopsis*. J. Cell Biol. **156**: 1003–1013.

Griesbeck, O., Baird, G.S., Campbell, R.E., Zacharias, D.A., and Tsien, R.Y. (2001). Reducing the environmental sensitivity of yellow fluorescent protein. Mechanism and applications. J. Biol. Chem. **276**: 29188–29194.

Groß-Hardt, R., Kägi, C., Baumann, N., Moore, J.M., Baskar, R., Gagliano, W.B., Jürgens, G., and Grossniklaus, U. (2007). *LACHESIS* restricts gametic cell fate in the female gametophyte of *Arabidopsis*. PLoS Biol **5**: e47.

Haweker, H., Rips, S., Koiwa, H., Salomon, S., Saijo, Y., Chinchilla, D., Robatzek, S., and Schaewen, von, A. (2010). Pattern Recognition Receptors Require N-Glycosylation to Mediate Plant Immunity. J. Biol. Chem. **285**: 4629–4636.

Helenius, A. and Aebi, M. (2001). Intracellular functions of N-linked glycans. Science **291**: 2364–2369.

Helenius, A. and Aebi, M. (2004). Roles of N-Linked Glycans in the Endoplasmic Reticulum. Annu. Rev. Biochem. **73**: 1019–1049.

Heller, L., Orlean, P., and Adair, W.L. (1992). *Saccharomyces cerevisiae sec59* cells are deficient in dolichol kinase activity. Proc. Natl. Acad. Sci. U.S.A. **89**: 7013–7016.

Helliwell, C.A. and Waterhouse, P.M. (2005). Constructs and methods for hairpin RNA-mediated gene silencing in plants. Meth. Enzymol. **392**: 24–35.

Henquet, M., Lehle, L., Schreuder, M., Rouwendal, G., Molthoff, J., Helsper, J., Van Der Krol, S., and Bosch, D. (2008). Identification of the gene encoding the *alpha1,3-mannosyltransferase* (*ALG3*) in *Arabidopsis* and characterization of downstream n-glycan processing. Plant Cell **20**: 1652–1664.

Hoeberichts, F.A. et al. (2008). A Temperature-sensitive mutation in the *Arabidopsis thaliana phosphomannomutase* gene disrupts protein glycosylation and triggers cell death. J. Biol. Chem. **283**: 5708–5718.

Hong, Z., Jin, H., Fitchette, A.C., Xia, Y., and Monk, A.M. (2009). Mutations of an *α1,6 mannosyltransferase* inhibit endoplasmic reticulum–associated degradation of defective brassinosteroid receptors in *Arabidopsis*. Plant Cell **21**: 3792-3802.

Hong, Z., Jin, H., Tzfira, T., and Li, J. (2008). Multiple Mechanism-Mediated Retention of a Defective Brassinosteroid Receptor in the Endoplasmic Reticulum of *Arabidopsis*. Plant Cell **20**: 3418–3429.

Huck, N., Moore, J.M., Federer, M., and Grossniklaus, U. (2003). The *Arabidopsis* mutant *feronia* disrupts the female gametophytic control of pollen tube reception. Development **130**: 2149–2159.

Huffaker, T.C. and Robbins, P.W. (1982). Temperature-sensitive yeast mutants deficient in asparagine-linked glycosylation. J. Biol. Chem. **257**: 3203–3210.

Hüttner, S. and Strasser, R. (2012). Endoplasmic reticulum-associated degradation of glycoproteins in plants. Front. Plant Sci. **3**: 67.

Kelleher, D.J., Karaoglu, D., Mandon, E.C., and Gilmore, R. (2003). Oligosaccharyltransferase isoforms that contain different catalytic STT3 subunits have distinct enzymatic properties. Mol. Cell **12**: 101–111.

Kessler, S.A., Shimosato-Asano, H., Keinath, N.F., Wuest, S.E., Ingram, G., Panstruga, R., and Grossniklaus, U. (2010). Conserved Molecular Components for Pollen Tube Reception and Fungal Invasion. Science **330**: 968–971.

Koncz, C. and Schell, J. (1986). The promoter of TL-DNA gene 5 controls the tissue-specific expression of chimaeric genes carried by a novel type of *Agrobacterium* binary vector. Mol. Gen. Genet. **204**: 383-396.

Kranz, C. et al. (2007). A defect in dolichol phosphate biosynthesis causes a new inherited disorder with death in early infancy. Am. J. Hum. Genet. **80**: 433–440.

Lerouxel, O., Mouille, G., Andème-Onzighi, C., Bruyant, M.-P., Séveno, M., Loutelier-Bourhis, C., Driouich, A., Höfte, H., and Lerouge, P. (2005). Mutants in *DEFECTIVE GLYCOSYLATION*, an *Arabidopsis* homolog of an oligosaccharyltransferase complex subunit, show protein underglycosylation and defects in cell differentiation and growth. Plant J. **42**: 455–468.

Leshem, Y., Johnson, C., and Sundaresan, V. (2013). Pollen tube entry into the synergid cell of *Arabidopsis* is observed at a site distinct from the filiform apparatus. Plant Reprod **26**: 93–99.

Leydon, A.R., Beale, K.M., Woroniecka, K., Castner, E., Chen, J., Horgan, C., Palanivelu, R., and Johnson, M.A. (2013). Three *MYB* Transcription Factors Control Pollen Tube Differentiation Required for Sperm Release. Curr. Biol. **23**: 1209–1214.

Li, H.J., Xue, Y., Jia, D.J., Wang, T., hi, D.Q., Liu, J., Cui, F., Xie, Q., Ye, D., and Yang, W.C. (2011). *POD1* Regulates Pollen Tube

Guidance in Response to Micropylar Female Signaling and Acts in Early Embryo Patterning in *Arabidopsis*. Plant Cell **23**: 3288–3302.

Li, J. and Chory, J. (1997). A putative leucine-rich repeat receptor kinase involved in brassinosteroid signal transduction. Cell **90**: 929–938.

Li, J., Zhao-Hui, C., Batoux, M., Nekrasov, V., Roux, M., Chinchilla, D., Zipfel, C., and Jones, J.D.G. (2009). Specific ER quality control components required for biogenesis of the plant innate immune receptor *EFR*. Proc. Natl. Acad. Sci. U.S.A. **106**: 15973–15978.

Li, S., Ge, F.-R., Xu, M., Zhao, X.-Y., Huang, G.-Q., Zhou, L.-Z., Wang, J.-G., Kombrink, A., McCormick, S., Zhang, X.S., and Zhang, Y. (2013). *Arabidopsis* COBRA-LIKE 10, a GPI-anchored protein, mediates directional growth of pollen tubes. Plant J. **74**: 486–497.

Liang, Y., Tan, Z.-M., Zhu, L., Niu, Q.-K., Zhou, J.-J., Li, M., Chen, L.-Q., Zhang, X.-Q., and Ye, D. (2013). *MYB97*, *MYB101* and *MYB120* Function as Male Factors That Control Pollen Tube-Synergid Interaction in *Arabidopsis thaliana* Fertilization. PLoS Genet. **9**: e1003933.

Lindner, H., Müller, L.M., Boisson-Dernier, A., and Grossniklaus, U. (2012a). *CrRLK1L* receptor-like kinases: not just another brick in the wall. Curr. Opin. Plant Biol. **15**: 659–669.

Lindner, H., Raissig, M.T., Sailer, C., Shimosato-Asano, H., Bruggmann, R., and Grossniklaus, U. (2012b). SNP-Ratio Mapping (SRM): identifying lethal alleles and mutations in complex genetic backgrounds by next-generation sequencing. Genetics **191**: 1381–1386.

Liu, J., Zhong, S., Guo, X., Hao, L., Wei, X., Huang, Q., Hou, Y., Shi, J., Wang, C., Gu, H., and Qu, L.-J. (2013). Membrane-Bound RLCKs LIP1 and LIP2 Are Essential Male Factors Controlling Male-Female Attraction in Arabidopsis. Curr. Biol. **23**: 993–998.

Lu, Y., Chanroj, S., Zulkifli, L., Johnson, M.A., Uozumi, N., Cheung, A., and Sze, H. (2011). Pollen Tubes Lacking a Pair of K+ Transporters Fail to Target Ovules in *Arabidopsis*. Plant Cell **23**: 81–93.

Lukowitz, W., Nickle, T.C., Meinke, D.W., Last, R.L., Conklin, P.L., and Somerville, C.R. (2001). *Arabidopsis cyt1* mutants are deficient in a mannose-1-phosphate guanylyltransferase and point to a requirement of N-linked glycosylation for cellulose biosynthesis. Proc. Natl. Acad. Sci. U.S.A. **98**: 2262–2267.

Michard, E., Lima, P.T., Borges, F., Silva, A.C., Portes, M.T., Carvalho, J.E., Gilliham, M., Liu, L.H., Obermeyer, G., and Feijo, J.A. (2011). Glutamate Receptor-Like Genes Form Ca2+ Channels in Pollen Tubes and Are Regulated by Pistil D-Serine. Science **332**: 434–437.

Miyazaki, S., Murata, T., Sakurai-Ozato, N., Kubo, M., Demura, T., Fukuda, H., and Hasebe, M. (2009). *ANXUR1* and *2*, Sister Genes to *FERONIA/SIRENE*, Are Male Factors for Coordinated Fertilization. Curr. Biol. **19**: 1327–1331.

Nelson, B.K., Cai, X., and Nebenführ, A. (2007). A multicolored set of *in vivo* organelle markers for co-localization studies in *Arabidopsis* and other plants. Plant J. **51**: 1126–1136.

Nickle, T.C. and Meinke, D.W. (1998). A cytokinesis-defective mutant of *Arabidopsis* (*cyt1*) characterized by embryonic lethality, incomplete cell walls, and excessive callose accumulation. Plant J. **15**: 321-332.

Nishimura, M.T., Stein, M., Hou, B.-H., Vogel, J.P., Edwards, H., and Somerville, S.C. (2003). Loss of a *callose synthase* results in salicylic acid-dependent disease resistance. Science **301**: 969–972.

Okuda, S., Tsutsui, H., Shiina, K., Sprunck, S., and Takeuchi, H. (2009). Defensin-like polypeptide LUREs are pollen tube attractants secreted from synergid cells. Nature **458**: 357-361.

Palanivelu, R. and Tsukamoto, T. (2011). Pathfinding in angiosperm reproduction: pollen tube guidance by pistils ensures successful double fertilization. Wiley Interdiscip. Rev. Dev. Biol. **1**: 96–113.

Palanivelu, R., Brass, L., Edlund, A.F., and Preuss, D. (2003). Pollen tube growth and guidance is regulated by *POP2*, an *Arabidopsis* gene that controls GABA levels. Cell **114**: 47–59.

Pattison, R.J. and Amtmann, A. (2009). N-glycan production in the endoplasmic reticulum of plants. Trends Plant Sci. **14**: 92–99.

Prado, A.M., Colaco, R., Moreno, N., Silva, A.C., and Feijo, J.A. (2008). Targeting of Pollen Tubes to Ovules Is Dependent on Nitric Oxide (NO) Signaling. Mol. Plant **1**: 703–714.

Preuss, D., Rhee, S.Y., and Davis, R.W. (1994). Tetrad analysis possible in *Arabidopsis* with mutation of the *QUARTET* (*QRT*) genes. Science **264**: 1458–1460.

Qiu, J.L., Zhou, L., Yun, B.W., Nielsen, H.B., Fiil, B.K., et al. (2008). *Arabidopsis* mitogen-activated protein kinase kinases *MKK1* and *MKK2* have overlapping functions in defense signaling mediated by *MEKK1*, *MPK4*, and *MKS1*. Plant Phys. 148: 212-222.

Raissig, M.T., Bemer, M., Baroux, C., and Grossniklaus, U. (2013). Genomic Imprinting in the *Arabidopsis* Embryo Is Partly Regulated by PRC2. PLoS Genet. **9**: e1003862.

Reyes, F., Marchant, L., Norambuena, L., Nilo, R., Silva, H., and Orellana, A. (2006). AtUTr1, a UDP-glucose/UDP-galactose transporter from *Arabidopsis thaliana*, is located in the endoplasmic reticulum and up-regulated by the unfolded protein response. J. Biol.

Chem. **281**: 9145–9151.

Rhee, S.Y., Osborne, E., Poindexter, P.D., and Somerville, C.R. (2003). Microspore separation in the *quartet 3* mutants of *Arabidopsis* is impaired by a defect in a developmentally regulated polygalacturonase required for pollen mother cell wall degradation. Plant Phys. **133**: 1170–1180.

Rotman, N., Rozier, F., Boavida, L., Dumas, C., Berger, F., and Faure, J.-E. (2003). Female control of male gamete delivery during fertilization in *Arabidopsis thaliana*. Curr. Biol. **13**: 432–436.

Rush, J.S., Cho, S.K., Jiang, S., Hofmann, S.L., and Waechter, C.J. (2002). Identification and characterization of a cDNA encoding a *dolichyl pyrophosphate phosphatase* located in the endoplasmic reticulum of mammalian cells. J. Biol. Chem. **277**: 45226–45234.

Schallus, T., Jaeckh, C., Fehér, K., Palma, A.S., Liu, Y., Simpson, J.C., Mackeen, M., Stier, G., Gibson, T.J., Feizi, T., Pieler, T., and Muhle-Goll, C. (2008). Malectin: a novel carbohydrate-binding protein of the endoplasmic reticulum and a candidate player in the early steps of protein N-glycosylation. Mol. Biol. Cell **19**: 3404–3414.

Skropeta, D. (2009). The effect of individual N-glycans on enzyme activity. Bioorg. Med. Chem. **17**: 2645–2653.

Takeuchi, H. and Higashiyama, T. (2012). A Species-Specific Cluster of Defensin-Like Genes Encodes Diffusible Pollen Tube Attractants in *Arabidopsis*. PLoS Biol **10**: e1001449.

Till, B.J., Burtner, C., Comai, L., and Henikoff, S. (2004). Mismatch cleavage by single-strand specific nucleases. Nucleic Acids Res. **32**: 2632–2641.

Varagona, M.J., Schmidt, R.J., and Raikhel, N.V. (1992). Nuclear localization signal(s) required for nuclear targeting of the maize regulatory protein Opaque-2. Plant Cell **4**: 1213–1227.

Varki, A. (1993). Biological roles of oligosaccharides: all of the theories are correct. Glycobiology **3**: 97–130.

Wang, D., Weaver, N.D., Kesarwani, M., and Dong, X. (2005). Induction of protein secretory pathway is required for systemic acquired resistance. Science **308**: 1036–1040.

Wassarman, P.M. and Litscher, E.S. (2008). Mammalian fertilization: the egg's multifunctional zona pellucida. Int. J. Dev. Biol. **52**: 665–676.

Wuest, S.E., Vijverberg, K., Schmidt, A., Weiss, M., Gheyselinck, J., Lohr, M., Wellmer, F., Rahnenführer, J., Mering, von, C., and Grossniklaus, U. (2010). *Arabidopsis* female gametophyte gene expression map reveals similarities between plant and animal gametes. Curr. Biol. **20**: 506–512.

Zhang, M., Henquet, M., Chen, Z., Zhang, H., Zhang, Y., Ren, X., Van Der Krol, S., Gonneau, M., Bosch, D., and Gong, Z. *LEW3*, encoding a putative *alpha-1,2-mannosyltransferase* (*ALG11*) in N-linked glycoprotein, plays vital roles in cell-wall biosynthesis and the abiotic stress response in *Arabidopsis thaliana*. Plant J. **60**: 983–999.

Zhang, X., Henriques, R., Lin, S.-S., Niu, Q.-W., and Chua, N.-H. (2006). *Agrobacterium*-mediated transformation of *Arabidopsis thaliana* using the floral dip method. Nat. Protoc. **1**: 641–646.

RESULTS - CHAPTER 3

Genetic Identification of *FERONIA* Interactors

Genetic Identification of *FERONIA* (*FER*) Interactors: *fer-1/fer-1* Suppressor Screen

INTRODUCTION

FER, a *Catharantus roseus* receptor-like Serine/Threonine kinase 1-like (*CrRLK1L*) subfamily member (Lindner et al., 2012) is involved in several developmental processes like PT reception in the synergid cells (Huck et al., 2003; Escobar-Restrepo et al., 2007); cell elongation in vegetative tissues (Guo et al., 2009) and polar root hair growth (Duan et al., 2010; Yu et al., 2012; Huang et al., 2013). Accordingly, *fer/fer* mutant plants show a high number of PT overgrowth and thus unfertilized ovules (Kessler et al., 2010), a severe vegetative dwarf phenotype (Guo et al., 2009; Kessler et al., 2010) and a root hair phenotype ranging from collapsed, burst to short root hairs (Guo et al., 2009). However, even though FER has a key role in several developmental processes, very little is known about interacting factors. In fact, neither a FER ligand nor any downstream targets that act in the synergids and transmit signals perceived by FER and thus accomplish PT reception, have been found yet. In addition and foremost, hardly anything is known about the role of FER during vegetative seedling growth. Even though the phenotype is severe, the genetic framework and molecular pathways interacting with FER to ensure proper vegetative growth remain elusive. Only in the root hair it is known that FER directly interacts with guanine exchange factors (ROPGEFs), which activate Rho-like GTPases (RAC/ROPs) leading to NADPH oxidase activation and ROS mediated polar growth (Duan et al., 2010; Yu et al., 2012; Huang et al., 2013). In this *fer/fer* suppressor screen, we aimed at identifying genetic interactors of FER in the gametophyte but to simplify the time consuming M1 screen for unfertilized ovules, we screened for the suppression of the vegetative phenotypes in the M2 generation. Obviously, finding gametophytic interactors would be only possible if the downstream pathways are the same in the vegetative and the gametophytic tissue. However, identification of mutants suppressing solely the vegetative phenotype but not the fertility phenotype would be desirable as well but were not our main focus.

Plant Material and Mutagenesis

Figure 1. White leaf sectors induced by EMS-mutagenesis. White sectors were counted in the M1 generation to assess the success of the mutagenesis. The arrow points to a leaf, where one half obviously bears a mutation affecting chloroplasts.

The *fer/fer* suppressor screen was conducted using the *fer-1/fer-1* allele, which shows a severe dwarf phenotype and mostly unfertilized ovules (Kessler et al., 2010). Around 0.55g (n=~27500) of *fer-1/fer-1* seeds were treated with EMS and distributed on 50 trays with soil yielding around 150 plants per tray. After three weeks in the light, 1.6% of the M1 individuals displayed white sectors on their leaves (Fig. 1), indicating that the mutagenesis had been successful (Jürgens et al., 1991). Since EMS treatment affects single cells, it was not expected to see wild type looking plants in the M1 generation, but rather dwarf plants with a wild-type-like side branch. But no obvious suppression of the *fer-1/fer-1* phenotype was observed in the M1 generation. After 8 weeks, seeds of each tray were pooled and an aliquot was germinated on big petri dishes containing MS + sucrose germination medium (for more details see Material & Methods).

Screen for Suppressors of the Dwarf Phenotype:

fer-1/fer-1 seedlings have mis-shapen, light green leaves at 7 days after germination (DAG; Kessler et al., 2010). Therefore a suppression of this seedling phenotype would be obvious already after a short time period. 12 DAG unmutagenized *fer-1/fer-1* seeds show the expected phenotype on plate (Fig. 2A), whereas control plates with *fer-1/fer-1* seeds mixed with Landsberg *erecta* (L*er*) wild-type seeds, displayed degenerating *fer-1/fer-1*- and tall and healthy wild-type seedlings (Fig. 2B). A similar pattern was expected, if a *fer*-suppressor was successfully mutated. Since one plant potentially suppressed in the *fer-1/fer-1* vegetative dwarf phenotype would result in several suppressed progeny and seeds of each tray were pooled, one would expect several suppressors with the same genotype among many more unsuppressed seedlings. Germination plates with M2 seedlings showed different patterns 12 DAG. On most plates, the majority of the seedlings degenerated, except some on the plate margin (Fig. 2C). On few plates most of the seedlings degenerated but some looked bigger and were distributed throughout the plate (Fig. 2D). All of the wild-type-like seedlings were transferred to soil (n=384 plants) and first re-screened for suppression of the vegetative phenotype. All plants were still dwarf and the suppression of the vegetative phenotype observed on plate was lost on soil. However, all candidates were additionally screened for potential suppression of the pollen tube reception phenotype: Although silique size does not necessarily correlate with the number of fertilized ovules (Shimosato-Asano & Grossniklaus, unpublished), we looked for slightly bigger siliques and counted their seed sets (Fig. 3). Siliques of 15 M2 plants were cut open and seed sets varied between 69-82% unfertilized ovules, which was similar to 83% in untreated *fer-1/fer-1* siliques. Thus, no suppressor candidate of the gametophytic or of the vegetative defect was found.

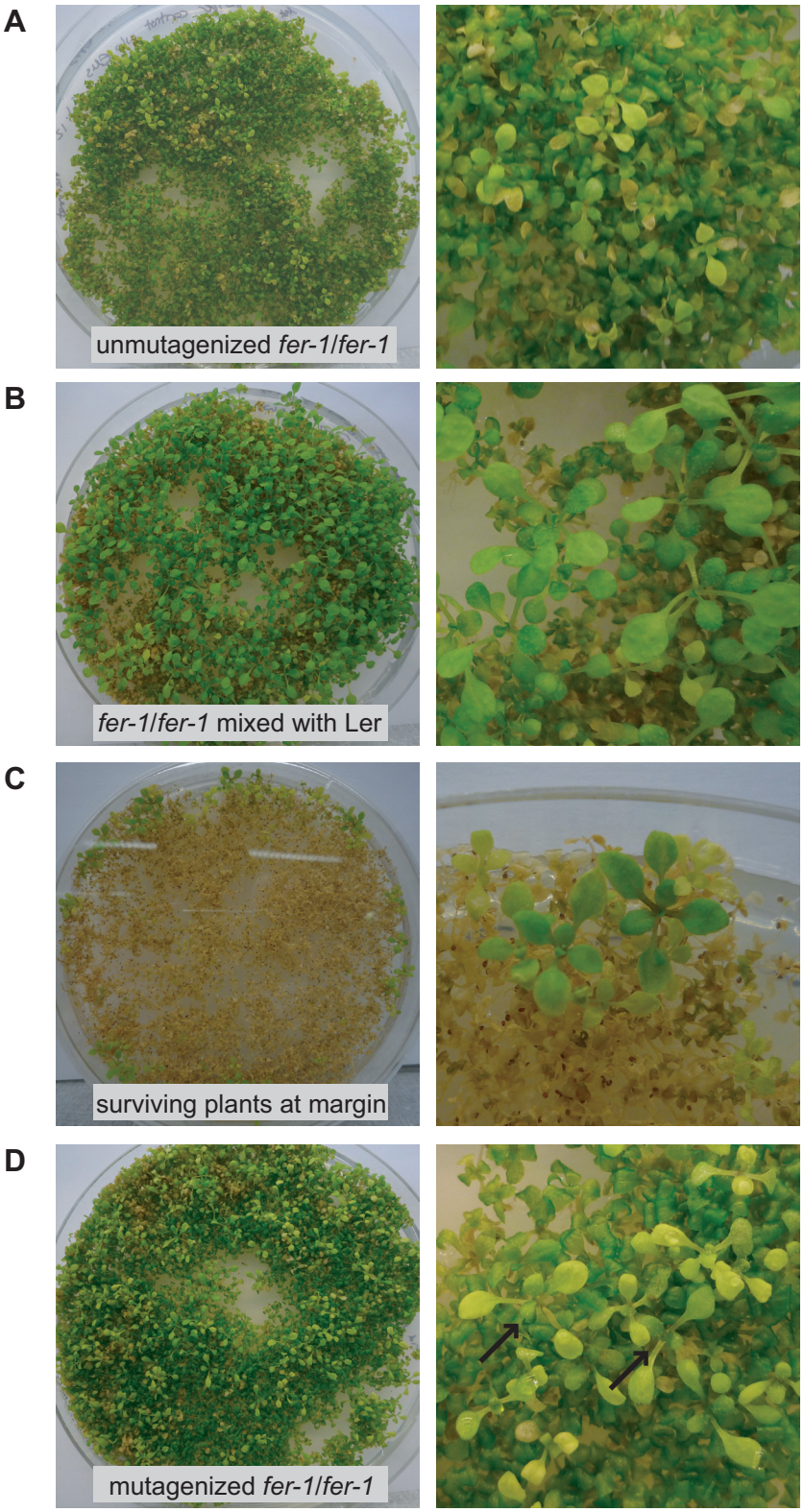

Figure 2. On-plate screen for suppressors of the *fer*-induced dwarf phenotype.
(A) Unmutagenized *fer-1/fer-1* seedlings on plate mostly degenerate and show a light-green leaf phenotype 7 days after germination (DAG). **(B)** Unmutagenized *fer-1/fer-1* seedlings mixed with wild-type L*er* seedlings. The L*er* seedlings are well-distinguishable from the degenerating *fer-1/fer-1* seedlings. **(C)** Surviving and false-positive *fer-1/fer-1* seedlings after mutagenesis at the plate margin. **(D)** Mutagenized *fer-1/fer-1* seedling plates showing seedlings that partially suppress the *fer*-induced dwarf phenotype (arrows). Those seedlings were transferred to soil and analyzed for suppressed *fer*-induced fertility defects. The left panel always depicts an overview of the whole plate, with an enlarged detail shown in the right panel.

Screen for Suppressors of the Root Hair Phenotype:

Since FER is involved in polar root hair growth (Duan et al., 2010; Yu et al., 2012; Huang et al., 2013), we additionally screened for suppression of the root hair bursting phenotype. 5 and 7 DAG, overall root length does not differ in *fer-1/fer-1* and wild-type plants. However, root hair growth was strongly decreased in *fer-1/fer-1* compared to wild type even at 5 DAG (Fig. 4A and 4B). EMS treated M2 seeds, wild-type seeds and untreated *fer-1/fer-1* seeds were put on the same plate and the root hair phenotype was determined under the binocular 5 DAG. 10 different M2 pools were each distributed on

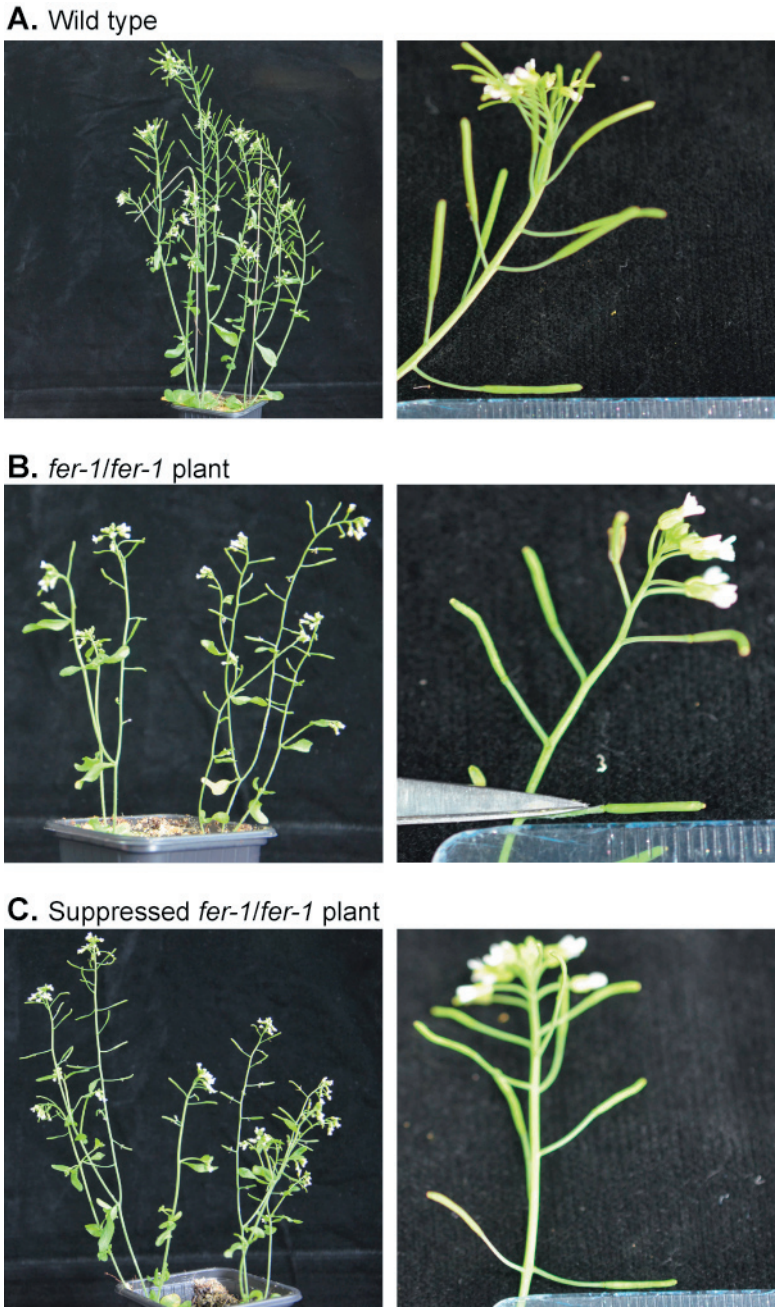

Figure 3. Plant growth habitus and silique size of potential *fer* suppressor candidates.
(A) Wild-type plant (L*er*; left panel) and normally developing silique (~15mm; right panel). **(B)** Unmutagenized *fer-1/fer-1* plant showing dwarf phenotype (left panel) and short siliques with a strongly reduced seed set (~8mm; right panel). **(C)** Potential *fer* suppressor candidate identified on plate and transferred on soil showing again the dwarf phenotype (left panel) and short siliques with a *fer*-like reduced seed set (~9mm; right panel). Note that in the overview pictures of the plants in (B) and (C) the scale is different than in (A).

2 plates and screened for suppression of the root hair burst. Although there was no clear suppression of the root phenotype even on plates, some plants seemed to have slightly more and/or longer root hairs (Fig. 4C). Those seedlings (n=16) were transplanted on soil and the vegetative and gametophytic phenotypes were determined. All plants were dwarfs and the seed sets of the 16 plants varied between 69-92% (n=1986 ovules) unfertilized ovules compared to 83% ±7.5% (n=559 ovules) in *fer-1/fer-1*- and 2.3% ± 1.4% (n=588) in L*er* controls. Thus unfortunately, no suppression of the *fer-1/fer-1* vegetative or gametophytic phenotypes was observed. In addition, the suppression of the root phenotype was not strong enough to follow it up in the next generation.

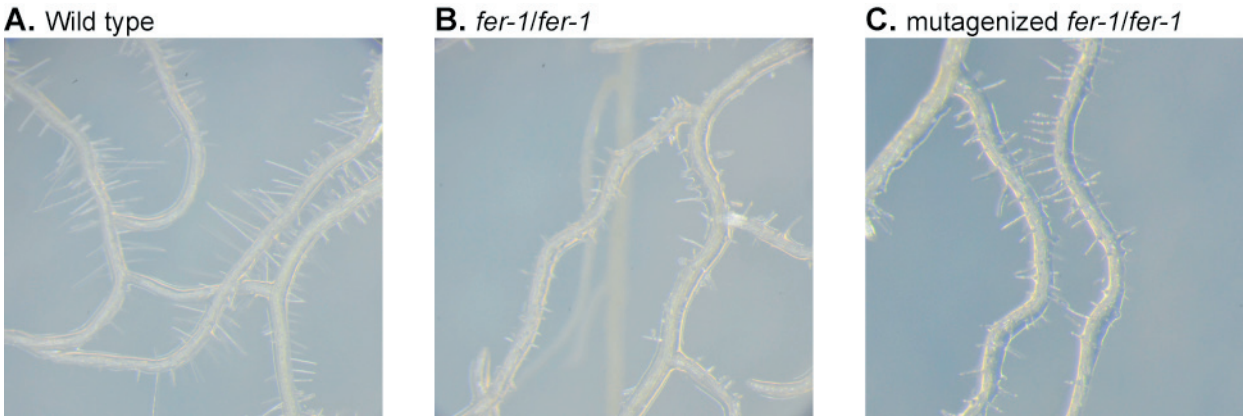

Figure 4. On-plate screen for suppressors of the *fer*-induced root hair phenotype.
(A) Wild-type roots with normal root hairs. **(B)** Unmutagenized *fer-1/fer-1* root showing clearly shorter and fewer root hairs. **(C)** Potential suppressor candidate showing partially restored root hairs. However, after transfer to soil no reduction of the *fer*-induced fertility phenotype was found.

DISCUSSION

The *fer-1/fer-1* suppressor screen yielded no potential suppressors for the vegetative and gametophytic phenotypes. It is not yet known if FER regulates both cell elongation in vegetative cells and PT reception in the synergid cells of the embryo sac via the same downstream targets. So far, the only known members of the FER regulated signaling pathway are identified for polar root hair growth. There, FER interacts with several guanine exchange factors (ROPGEFs), which activate small Rho-like GTPases (RAC/ROPs), leading to NADPH oxidase dependent ROS formation and subsequent root hair development (Duan et al., 2010; Yu et al., 2012; Huang et al., 2013). To ensure the identification of a *fer*-suppressor in the PT reception pathway, a more time consuming screening strategy would have to be conducted. In fact, screens for gametophytic factors can be conducted in the M1 generation directly since the phenotype is visible in the haploid gametophyte already in the M1. Such a suppressor screen has been done for *nta-2/nta-2* mutants (Kessler, Grossniklaus, unpublished), displaying the *fer*-like PT overgrowth phenotype in 35% of mutant ovules (Kessler et al., 2010). There, 1700 M1 plants were screened for a reduction or an increase of unfertilized ovules and subsequent aniline blue analysis determined if this number correlated with the observed PT overgrowth. Screening for *fer-1/fer-1* vegetative phenotype suppression and accompanied seed pooling of hundreds of plants, ensured a time saving strategy and increased the number of analyzed plants and, thus, potentially the success of the screen. However after pooling the seeds of hundreds of M1 plants, seed set analysis of single M2 plants is not reasonable, since in this generation numerous of progenies are segregating from one single parent individual.

In general, suppressor screens for vegetative dwarf phenotypes have been successfully conducted. *BRI1-EMS-SUPPRESSOR 1* (*BES1*) has been identified in a suppressor screen for the dwarf phenotype of *brassinosteriod-insensitive* 1-119 (*bri1-119*; Yin et al., 2002). BES1 acts downstream of BRI1 and the mutated protein is stabilized and accumulates at high levels, leading to a constitutively activated BR-response in the *bes1* suppressors. To identify *bes1*, 200.000 M2 seedlings were screened (Yin et al., 2002). Perhaps continuous screening of more *fer-1/fer-1* M2 individuals might result in the identification of a member in the FER-mediated pathway.

MATERIAL AND METHODS

Plant material and growth conditions

Plant growth conditions were as previously described (Raissig et al., 2013). For vegetative phenotype assessment on plates, seeds were grown on MS plates using 1x Murashige & Skoog (MS) salt base (Carolina Biological Supply Company) with 30mM Sucrose, pH=5.7 and 0.8% agarose. After 2-3 days of stratification in the dark at 4°C, plates were moved to a growth cabinet with constant light at 23°C.

EMS mutagenesis

In general, around 0.55g seeds were hydrated in the dark for 4 days at 4°C, then re-dried for 24h at 22°C. The seeds were immersed in a 0.2% EMS solution (Sigma-Aldrich) for ~8h (shaking). EMS solution was carefully decanted and seeds were washed 3x with 50ml H_2O and 4x 100ml H_2O. All solutions and materials were decontaminated using decontamination solution (Thioglycolic acid, Sigma-Aldrich). Seeds were put into a 50µm mesh, which was thoroughly closed, put into a funnel and washed under running water for 1h. Afterwards, the seeds were divided into 50 aliquots and directly put on soil using the "salt-n-pepper" principle: mutagenized seeds were resuspended in 50 ml water and filled in a 50 ml Falcon tube with holes in the lid and dispersed. We distributed the EMS treated seeds on 50 trays and used one extra tray of Col-0, *fer-1/fer-1* and *fer-2/fer-2* plants as controls.

Root hair analysis

Seeds were placed on MS plates (1/2 MS, 0.07 MES (pH=6), 1% sucrose, pH=5.7, 1.5% agarose) using a toothpick. After 3 days of stratification at 4°C, plates were moved to the growth cabinet in an 80% upright ankle with 16h light, 8h dark rhythm at 22°C. Root hair growth was analyzed under a binocular microscope (Leica).

References

Duan, Q., Kita, D., Li, C., Cheung, A.Y., and Wu, H.-M. (2010). *FERONIA* receptor-like kinase regulates RHO GTPase signaling of root hair development. Proc. Natl. Acad. Sci. U.S.A. **107**: 17821–17826.

Escobar-Restrepo, J.M., Huck, N., Kessler, S., Gagliardini, V., Gheyselinck, J., Yang, W.C., and Grossniklaus, U. (2007). The *FERONIA* Receptor-like Kinase Mediates Male-Female Interactions During Pollen Tube Reception. Science **317**: 656–660.

Guo, H., Li, L., Ye, H., Yu, X., Algreen, A., and Yin, Y. (2009). Three related receptor-like kinases are required for optimal cell elongation in *Arabidopsis thaliana*. Proc. Natl. Acad. Sci. U.S.A. **106**: 7648–7653.

Huang, G.Q., Li, E., Ge, F.R., Li, S., and Wang, Q. (2013). *Arabidopsis RopGEF4* and *RopGEF10* are important for *FERONIA*-mediated developmental but not environmental regulation of root hair growth. New Phytol. [Epub ahead of print]

Huck, N., Moore, J.M., Federer, M., and Grossniklaus, U. (2003). The *Arabidopsis* mutant *feronia* disrupts the female gametophytic control of pollen tube reception. Development **130**: 2149–2159.

Jürgens, G., Mayer, U., Berleth, T., and Miséra, S. (1991). Genetic analysis of pattern formation in the *Arabidopsis* embryo. Development Supplement **1**: 27–38.

Kessler, S.A., Shimosato-Asano, H., Keinath, N.F., Wuest, S.E., Ingram, G., Panstruga, R., and Grossniklaus, U. (2010). Conserved Molecular Components for Pollen Tube Reception and Fungal Invasion. Science **330**: 968–971.

Lindner, H., Müller, L.M., Boisson-Dernier, A., and Grossniklaus, U. (2012). *CrRLK1L* receptor-like kinases: not just another brick in the wall. Curr. Opin. Plant Biol. **15**: 659–669.

Yin, Y., Wang, Z.Y., Mora-Garcia, S., Li, J., Yoshida, S., Asami, T., and Chory, J. (2002). BES1 accumulates in the nucleus in response to brassinosteroids to regulate gene expression and promote stem elongation. Cell **109**: 181–191.

Yu, F. et al. (2012). *FERONIA* receptor kinase pathway suppresses abscisic acid signaling in *Arabidopsis* by activating *ABI2* phosphatase. Proc. Natl. Acad. Sci. U.S.A. **109**: 14693–14698.

RESULTS - CHAPTER 4

Functional Analysis of Related CrRLK1L Proteins

NOTE

All of Chapter 4 will be submitted with the title “Functional Analysis of Related CrRLK1L Proteins in Pollen Tube Reception” and the contributing authors Kessler SA, Lindner H, Grossniklaus U.

HL was involved in plant transformation, phenotyping for *fer* complementation including growth analysis, seed counts, aniline blue stainings of pollen tubes and confocal microscopy. SAK cloned all constructs, and was involved in plant transformation and phenotyping. HL wrote the introduction and critically read and corrected the results and the discussion. In addition, HL conceived and designed Figure 1 and Figure 2.

Supplemental Information can be found in Appendix A3.

Functional Analysis of Related CrRLK1L Proteins in Pollen Tube Reception

Sharon A. Kessler[1,2], Heike Lindner[2], and Ueli Grossniklaus[2,*]

[1] Department of Microbiology and Plant Biology, University of Oklahoma, 770 Van Vleet Oval, Norman, OK 73019, USA
[2] Institute of Plant Biology & Zürich-Basel Plant Science Center, University of Zürich, CH-8008 Zürich, Switzerland

[*] to whom correspondence should be addressed: grossnik@botinst.uzh.ch

ABSTRACT

The *Catharantus roseus* receptor-like Serine/Threonine kinase 1-like (CrRLK1L*)* subfamily of receptor-like kinases (RLK) has been implicated in a variety of developmental processes, but little is known about the structure-function relationships within this family of 17 proteins. In this study, we investigated the functional similarities and differences between three CrRLK1L members FERONIA (FER), ANXUR1 (ANX1) and HERCULES1 (HERK1) by exploring their ability to function in pollen tube reception, a process normally mediated only by FER. Domain swap analysis of these three proteins revealed that the intracellular domains are interchangeable, suggesting common downstream targets of all three CrRLK1Ls. Furthermore, we show that FER requires the intracellular domain but no kinase activity to mediate signal transduction suggesting that other kinases are involved in the FER-signal transduction cascade. Thus, the intracellular domain might be required to interact with and/or recruit yet unknown co-factors. However, the extracellular domains of FER, ANX1 and HERK1 are not interchangeable, indicating specific ligand-activation for each of these three RLK proteins.

INTRODUCTION

To accomplish double fertilization in land plants (angiosperms), the pollen lands on the stigma, hydrates and germinates to form a pollen tube (PT). This PT transports the two non-motile sperm cells through the stigma, the style and the transmitting tract. During its growth through these various female tissues the growth direction remains determined by different short- and long-range attractants (reviewed in Palanivelu and Tsukamoto, 2012; Dresselhaus and Franklin-Tong, 2013). Those attractants are also responsible for the PTs' exit from the transmitting tract and entry into the ovary. There it is guided along the funiculus of the ovule towards the micropylar end of the embedded female gametophyte, which consists of seven cells. Three antipodal cells at the chalazal pole, which degenerate eventually, the two female gametes, central cell and egg cell, and the two synergid cells at the micropylar pole. The synergid cells accomplish the last step of PT guidance towards the site of PT reception, by excreting small cysteine-rich peptides (*LURES*), which were discovered first in *Torenia fournieri* and more recently in *Arabidopsis thaliana* and *Torenia concolor* (Okuda et al., 2009; Takeuchi and Higashiyama, 2012; Kanaoka et al., 2011). PT reception happens at the filiform apparatus, a membrane-rich region at the micropylar end of the synergid cells, which is the first contact point between the male and female gametophytes. Subsequently, the PT grows beyond the filiform apparatus, enters the receptive synergid, which degenerates after PT arrival, followed by PT rupture and sperm cell release. Finally, one sperm cell fuses with the haploid egg cell to give rise to the diploid embryo and the second sperm cell fuses with the diploid central cell to form the embryo nourishing triploid endosperm.

The first evidence that PT reception is an active signaling process came from the identification of *FERONIA (FER)*, named after the Etruscan goddess of fertility (Huck et al., 2003; Escobar-Restrepo et al., 2007). *FER* encodes a Serine/Threonine receptor-like kinase (RLK) and is a member of the *Catharantus roseus receptor-like kinases1-like* (*CrRLK1L*) subfamily, which consists of 17 members (reviewed in Lindner et al., 2012). FER localizes to the plasma membrane (PM) of the filiform apparatus of the synergid cells (Escobar-Restrepo et al., 2007). *fer* mutant ovules develop normally, but remain unfertilized because the PT continues to grow inside the female gametophyte, fails to arrest its growth, and does not rupture to release the sperm cells in order to effect double fertilization (Figure 1A and 1B; Huck et al., 2003; Rotman et al., 2003; Escobar-Restrepo et al., 2007).

The two closest homologs of *FER* were named after Feronia's companion in Etruscan mythology *ANXUR1* (*ANX1*) and *ANX2* and are, in contrast to *FER*, only expressed in pollen, where they localize to the PM of the growing pollen tube tip. Whereas single *anx1* and *anx2* mutants show no phenotype, double *anx1/anx2* mutant PTs burst immediately after germination (Boisson-Dernier et al., 2009; Miyazaki et al., 2009). ANX1 and ANX2 were shown to be positive regulators of two NADPH-oxidases to systematically produce reactive oxygen species (ROS), which activate PM-localized, Ca^{2+}-permeable influx channels to sustain secretion to the PT tip and enable PT elongation (Boisson-Dernier et al., 2013). When the PT arrives at the filiform apparatus, the FER-dependent PT-reception pathway is activated and followed by the inactivation of the ANX1/2-dependent signaling cascade, leading to PT rupture, sperm release and double fertilization.

Interestingly, ANX1/2 function in tip-growing PT seems to be adopted by FER in polarly growing root hairs. There, FER acts upstream of several guanine exchange factors (ROPGEFs), activating Rho-like

GTPases (RAC/ROPs), leading to NADPH-oxidase-dependent ROS-mediated root hair development (Duan et al., 2010; Yu et al., 2012; Huang et al., 2013). Additionally, FER-RopGEF-RAC/ROP modules seem to negatively regulate abscisic acid (ABA) response and positively regulate auxin-promoted root-hair initiation and growth (Yu et al., 2012).

Furthermore it was shown that gene expression of *FER* and two other *CrRLK1L* members, *HERCULES1* (*HERK1*) and *THESEUS1* (*THE1*), are upregulated after brassinosteroid (BR) treatment in vegetative tissue. All three genes are strongly expressed in elongating cells during vegetative growth, where they localize to the PM (Guo et al., 2009). Thus, both *fer/fer* mutant plants and *the1/herk1* double mutants show a severe vegetative dwarf phenotype. Since in both mutants similar genes seem to be affected, FER, HERK1 and THE1 might act in the same pathway during cell elongation.

CrRKL1L proteins have an intracellular Serine/Threonine kinase domain (ICD) with relatively high conservation, a transmembrane domain and an extracellular domain (ECD). Boisson-Dernier et al., 2011 discovered two malectin-like domain on the ECD of some CrRLK1L proteins. However, recent domain searches predict one malectin-like domain in all CrRLK1L members (pfam.sanger.ac.uk). This malectin-like domain has limited homology to the ER-localized, carbohydrate-binding malectin protein of *Xenopus laevis* (reviewed in Boisson-Dernier et al., 2011; Schallus et al., 2008).

In this study, we investigated functional similarities and differences between three *CrRLK1L* members (FER, ANX1 and HERK1) by domain swap analysis. Full-length proteins as well as the corresponding domains of ANX1 and HERK1 replaced the ICD and ECD of FER, respectively. Furthermore, a deletion construct of the FER-kinase domain and FER proteins with loss-of-function and gain-of-function kinase domains were cloned. All constructs were expressed under the FER-promoter in *fer/FER* mutant plants, which normally show around 50% unfertilized ovules due to PT reception defects. Complementation analysis revealed common downstream signaling events but distinct ligand activation. In addition, we show that FER kinase activity is not necessary for FER function in PT reception, indicating that other kinases may play a role in the FER signal transduction cascade.

RESULTS

Domain Swap Analysis of FER and Related Proteins

The *Arabidopsis thaliana CrRLK1L* gene family has 17 members of which six have been shown to perform distinct functions (reviewed in Boisson-Dernier et al., 2011; Lindner et al., 2012). Like most RLKs, the main determinant of specificity in this protein family is predicted to be receptor-ligand interactions determined by specific amino acids in the extracellular domain (ECD). This prediction is supported by the fact that the CrRLK1L family members have highly divergent extracellular domains. However, the intracellular domain (ICD) of CrRLK1L proteins have highly-conserved Serine/Threonine kinase domains, but divergent C-terminal tails that could play a role in downstream specificity. A third

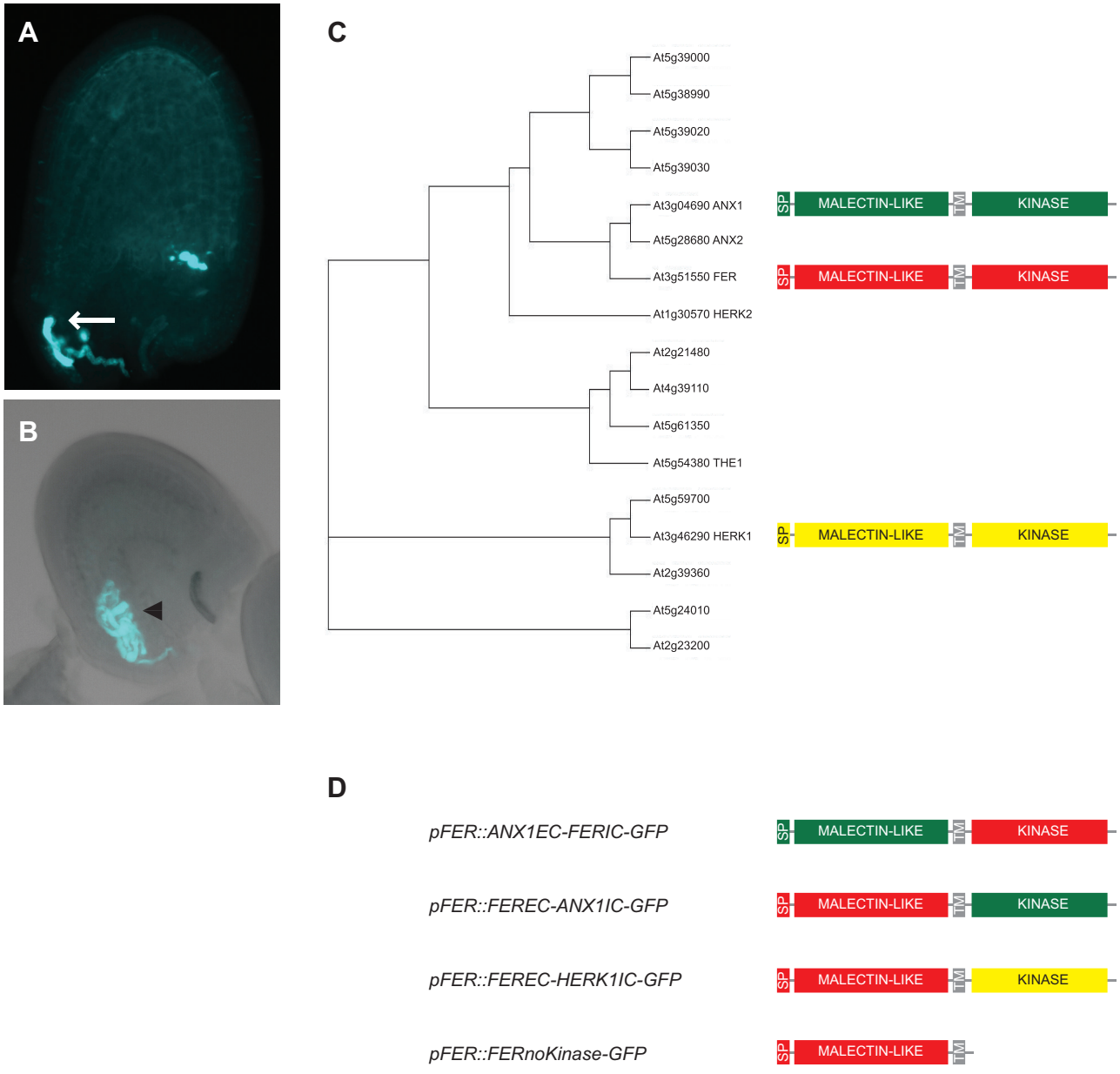

Figure 1. FERONIA is involved in PT reception and is a member of the CrRLK1L family of receptor-like kinases.
(A) Aniline blue stained ovule with normal PT reception (arrow). **(B)** Aniline blue stained *fer-1* ovule with PT overgrowth (arrowhead) in a transmission overlay. **(C)** Phylogenetic tree showing the relationships between CrRLK1L proteins. On the right side of the tree, protein models for the three investigated genes are drawn. **(D)** Chimeric and truncated proteins assessed in this study.

determinant of specificity could be the expression domain of various family members in combination with other upstream and downstream regulators. In order to determine the factors controlling CrRLK1L specificity, we tested whether closely-related (ANX1) and more distantly-related (HERK1) proteins and/or replacements of the extracellular- and intracellular domains of FER with the respective domains of ANX1 and HERK1 can complement the PT reception phenotype in *fer/FER* mutants, when expressed under control of the FER promoter.

The ANX1 and ANX2 proteins are the most closely related proteins to FER (Figure 1C). The full length ANX1 amino acid sequence shares 53% identity and 67% similarity with FER (Figure 2). The highest similarity is in the predicted intracellular domains, with 63% identity and 74% similarity. HERK1 is more distantly related, sharing 43% identity and 59% similarity over the full-length protein (Figure 2), but the HERK1 intracellular domain is almost as similar to FER as ANX1, with 58% identity and 70% similarity. As expected for related RLKs, the FER, ANX1, and HERK1 extracellular domains are less-closely related, with FER and ANX1 sharing 44% identity and 61% similarity, while FER and HERK1 share only 30% identity and 49% similarity. However, the ECDs of all three CrRLK1L proteins contain a malectin-like domain (Figure 1C; Figure 2).

We previously showed that a 1.2kb fragment upstream of *FER* drives the expression of a FER-GFP fusion protein that localizes to the filiform apparatus in synergid cells and complements the *fer* fertilization phenotype (Figure 3A; Escobar-Restrepo et al., 2007). We used the same promoter fragment to drive expression of full-length ANX1-GFP and HERK1-GFP fusion proteins in the *fer-1/FER* background. The fusion proteins were detected in the filiform apparatus for both constructs (Figure 3B and 3C), indicating that the signal sequences necessary for localization to the filiform apparatus are present in other members of the CrRLKL family. All of the primary transformants were either *FER/FER* or *fer-1/FER* and did not show significantly different numbers of unfertilized ovules compared to *FER/FER* or *fer-1/FER* control plants, respectively (Figure 4). These results indicate that full-length ANX1-GFP and HERK1-GFP constructs cannot complement the *fer-1* phenotype when they are expressed in synergid cells and that no dominant negative effects on PT reception are conferred by expressing ANX1-GFP and HERK1-GFP in synergid cells.

The failure of ANX1 and HERK1 to complement the *fer* phenotype could be due to a lack of ligand recognition, an inability to perform downstream functions, or both. In order to distinguish between these possibilities, domain swaps between ANX1 and FER were constructed and driven under the FER promoter as GFP fusions (Figure 1D). Primary transformants expressing the ANX1 extracellular domain fused to the intracellular domain of FER showed expression of the GFP fusion protein in the filiform apparatus of synergid cells in multiple transformants (Figure 3D). However, only *FER/FER* and *fer-1/FER* plants were recovered (no *fer-1/fer-1* homozygotes). The percentages of unfertilized ovules in the primary transformants were not different than FER/FER or *fer-1/FER* controls (Figure 4), indicating that the ANX1EC-FERIC-GFP fusion protein is not able to complement the *fer-1* fertilization defect and that no dominant negative effect was conferred by the ANX1 extracellular domain. Thus, the FER extracellular domain is indispensible for its function in synergid cells.

The final domain swap experiment was to exchange the FER intracellular domain with the intracellular domains of ANX1 or HERK1 and express GFP fusions under control of the FER promoter

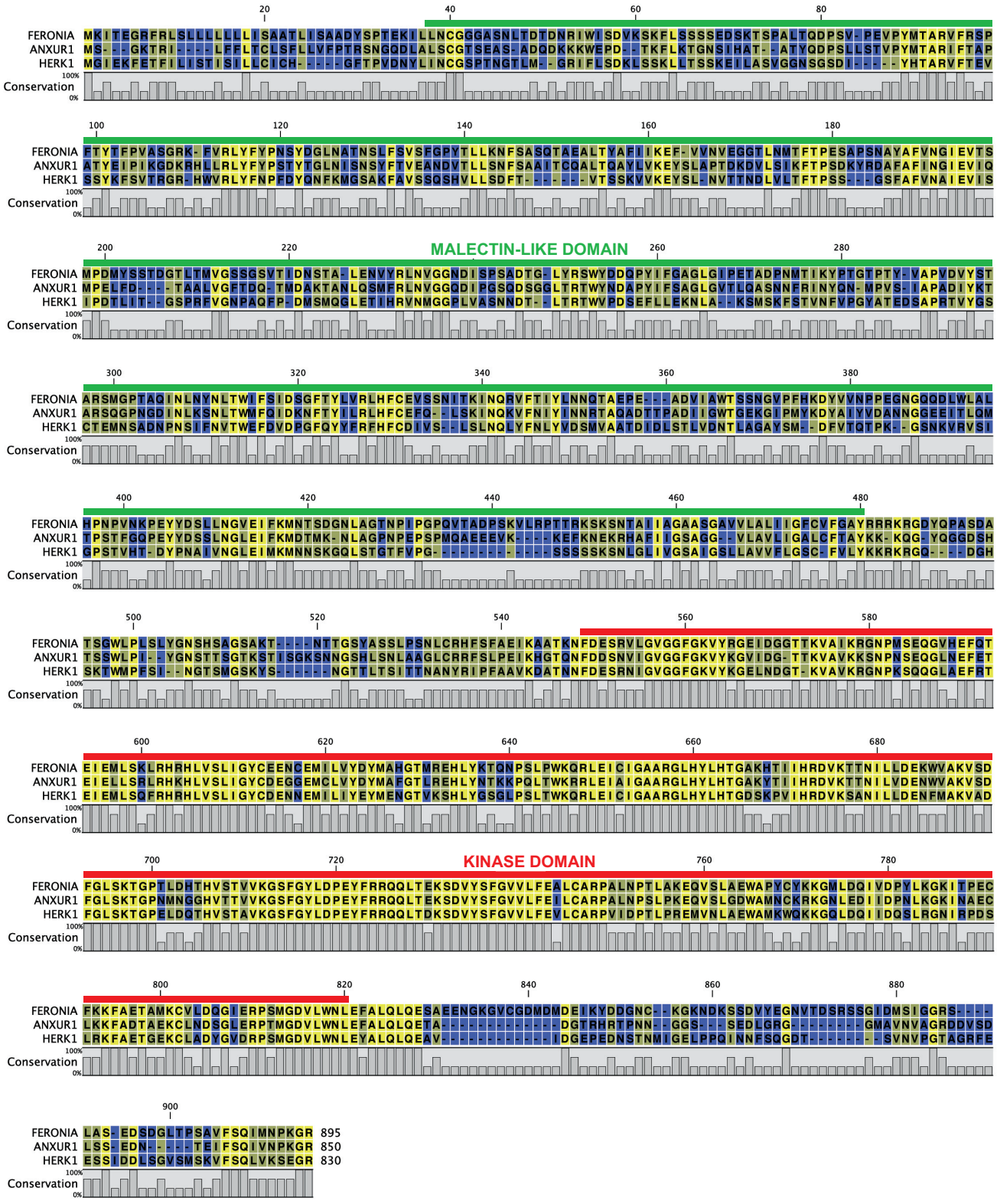

Figure 2. Protein Alignment of FER, ANX1 and HERK1.

Level of conservation is indicated by heat-map coloring (blue indicates low conservation, yellow indicates high conservation). The Malectin-like domain (in green) and the Kinase domain (in red) are indicated. Domain prediction was done using http://pfam.sanger.ac.uk/.

(Figure 1D). Both constructs were able to complement the *fer-1* phenotype. Homozygous *fer-1/fer-1* primary transformants were recovered and the percentage of unfertilized ovules was reduced by 50% in *fer-1/FER* and *fer-1/fer-1* primary transformants that were hemizygous for the complementation constructs (Figure

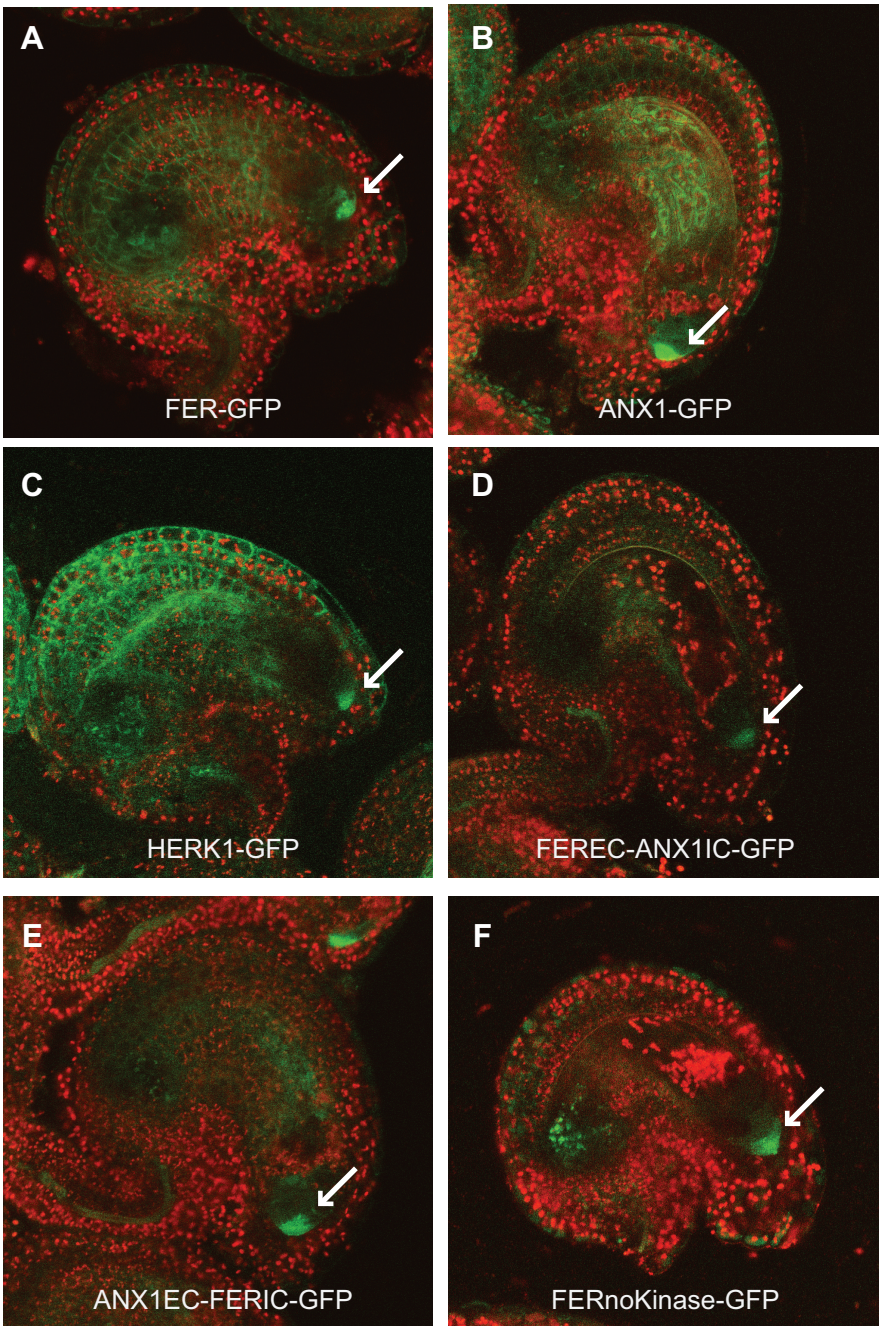

Figure 3. Representative confocal images illustrating that ANX1, HERK1, and domain swap constructs exhibit FER-like subcellular localization in the filiform apparatus of synergid cells.

For all overlayed images, GFP fusion protein signal is shown in green and chlorophyll autofluorescence is shown in red. **(A)** FER-GFP is localized to the filiform apparatus of synergid cells (arrow) and can also be detected at the periphery of sporophytic cells of the ovule. **(B)** to **(C)** Non-complementing ANX1 (B) and HERK1 (C) GFP fusions expressed under control of the FER promoter are localized at the filiform apparatus (arrow). **(D)** to **(E)** ANX1/FER domain swap constructs are localized to the filiform apparatus (arrow). **(F)** The non-complementing FERnoKinase construct is localized to the filiform apparatus (arrow).

4). These results indicate that either the intracellular domains of ANX1 and HERK1 proteins are interchangeable with the FER intracellular domain or that the intracellular domain is dispensable for FER function. In order to distinguish between these possibilities, we deleted the intracellular domain of FER in a GFP fusion construct driven by the FER promoter. The FERIC deletion construct was expressed in synergids and localized to the filiform apparatus (Figure 3F) but did not complement the *fer-1* phenotype (Figure 4), indicating that the intracellular domain is necessary for FER function in PT reception and that the ANX1 and HERK1 intracellular domains can fulfill this function when fused to the FER extracellular domain.

Functional Analysis of the FER Intracellular Domain

The intracellular domains of CrRLK1 proteins contain a typical Serine/Threonine kinase motif with a Lysine (K) at the active site and an activation loop with Serines (S) and Threonines (T) that are predicted phosphorylation sites (Figure 5A). In seedling and mature pollen phosphoproteomic studies (Nuhse et al., 2004; Mayank et al., 2012), a highly conserved peptide with a phosphorylated S corresponding to the last S in the activation loop (S701 in FER) was identified, however this peptide is highly conserved in CrRLK1 family members and could not be

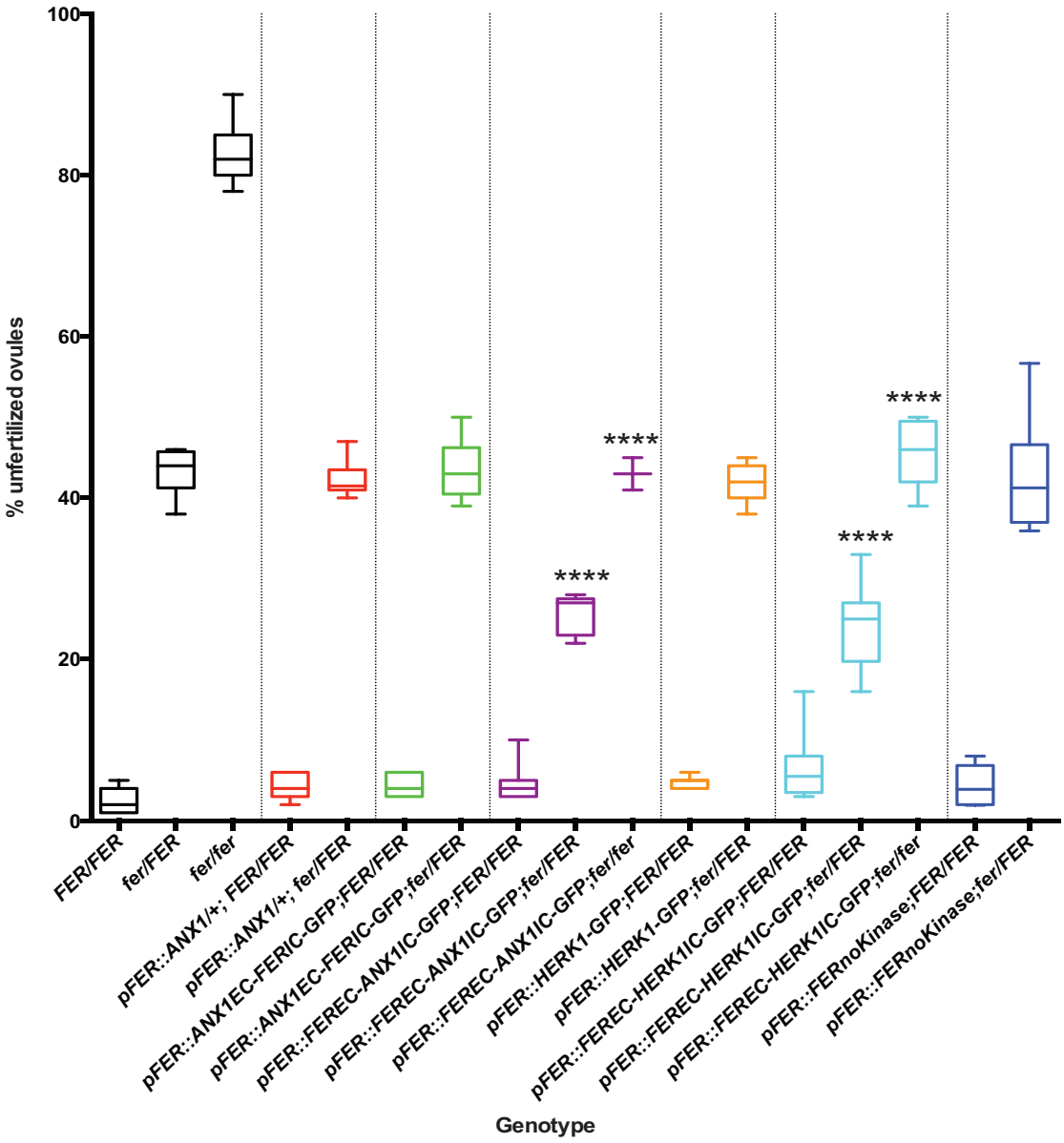

Figure 4. Complementation of the *fer-1* mutation with related CrRLK1L proteins and domains.
Box plots from complementation assays showing the percentage of unfertilized ovules for control plants and T1 transformants for each of the constructs. The FER extracellular domain is necessary for *fer-1* complementation, but the ANX1 and HERK1 intracellular domains can substitute for the FER intercellular domain in fusion with the FER extracellular domain. **** indicate lines with % unfertilized ovules significantly different than the untransformed controls of the same genotype (p-values less than 0.0001 in t-tests). At least 3 independent T1 plants (>500 ovules counted for each) were analyzed for complementing lines and at least 8 T1 plants were analyzed for non-complementing lines.

assigned to a specific protein. S695 and T696 of FER were shown to be phosphorylated in *Arabidopsis* seedlings, and the corresponding S residues were also found to be phosphorylated in HERK1 (Nuhse et al., 2004). In an *in vitro* kinase assay, the kinase domain of FER was capable of autophosphorylation (Escobar-Restrepo et al., 2007). A point mutation that changed the Lysine (K) at the active site to Arginine (R) abolished this *in vitro* kinase activity (Escobar-Restrepo et al., 2007). In order to determine if kinase activity is necessary for FER function in PT reception, a *pFER::FER-GFP* construct carrying the K-R change in the active site was transformed into *fer-1/FER* plants to check for complementation. Surprisingly, this dead kinase version of FER was able to complement the *fer-1* phenotype (Fig 4B),

indicating that kinase activity is not necessary for FER function in PT reception.

Like most kinases, FER has a predicted activation loop following the catalytic site that has Serine and Threonine residues which are targets for phosphorylation, indicating that FER function could be modulated through changes in phosphorylation states of these residues. In order to investigate this possibility, site-directed mutagenesis was used to convert the two Serine and Threonine residues (Ser695, Thr696 and Ser701) to Alanine (A) to mimic a constitutive dephosphorylated state and Aspartic Acid (D) to mimic constitutive phosphorylation. Single and double changes of these Serine- and Threonine residues had no effect on the ability of the construct to complement the *fer-1* phenotype (data not shown). Changing all three to Alanine led to production of stable FER protein that was localized in the filiform apparatus and was able to complement the *fer-1* phenotype (Figure 5B), indicating that phosphorylation of the activation loop is not necessary for FER function. In contrast, the corresponding changes to Aspartic Acid in these three Serine- and Threonine residues led to a failure to complement the *fer-1* phenotype (Fig. 5B). However, we could not recover any transformants that expressed the *pFER::FER-STS-DDD-GFP* construct in synergid cells (12 independent hygromycin-resistant primary transformants were analyzed), indicating that the STS to DDD change in the FER activation loop likely leads to protein instability.

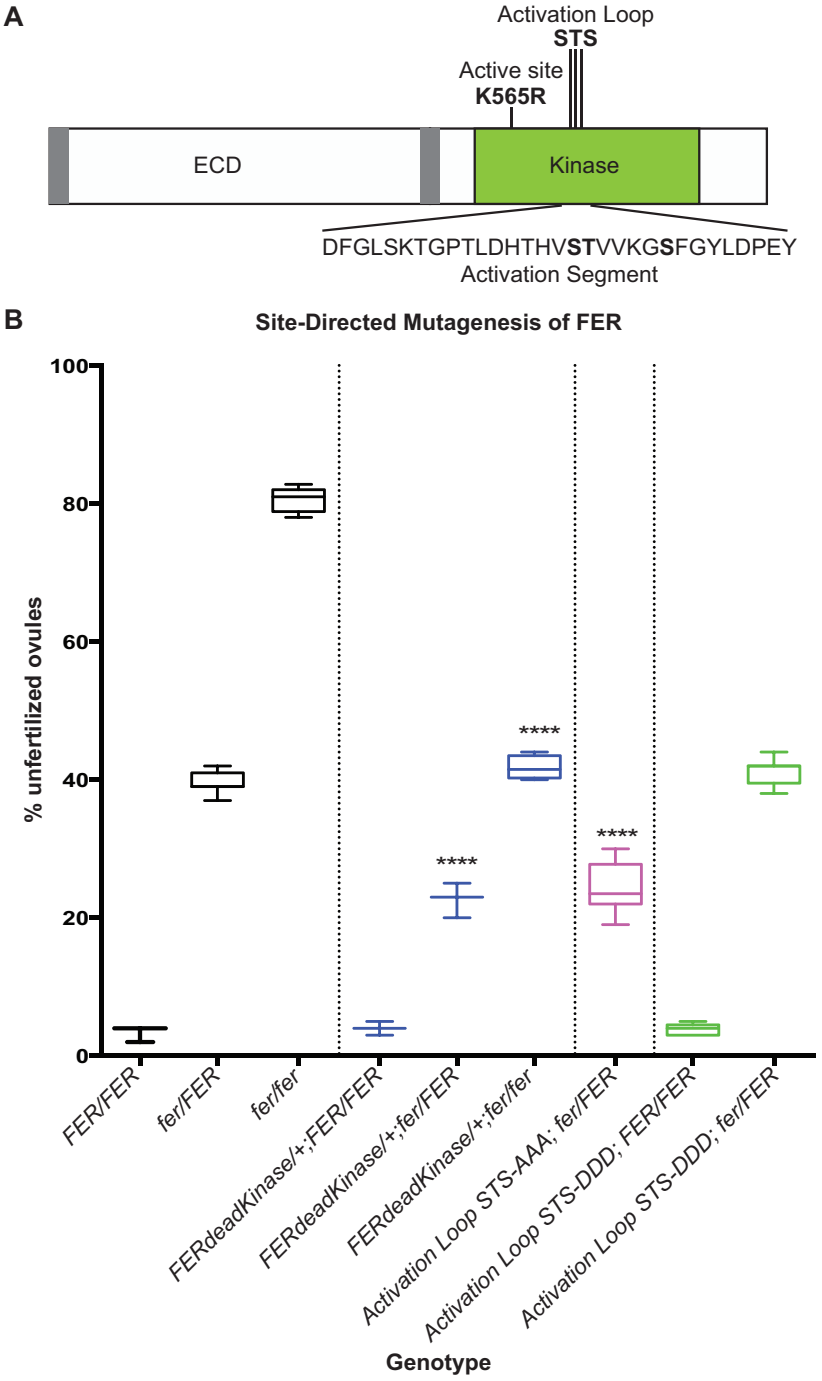

Figure 5. Site-directed mutagenesis of FER kinase domain.

(A) Diagram showing the domains of the FER protein and the positions of the mutations introduced for complementation assays. The bold S, T, and S indicate targets for mutagenesis in the activation segment. **(B)** Box plots from complementation assays showing the percentage of unfertilized ovules for control plants and T1 transformants for each of the constructs. The K565R dead kinase construct complements the *fer-1* phenotype. In the activation loop (n=5 independent T1 plants), Ala changes of the three phosphorylation sites S695, T696, and S701 (STS-AAA) have no effect on FER function (n=5 independent T1 plants), while Asp changes of the same amino acids renders the protein unstable and unable to complement the *fer-1* phenotype (n=12 independent T1 lines). **** indicate lines with % unfertilized ovules significantly different than the untransformed controls of the same genotype (p-values less than 0.0001 in t-tests).

DISCUSSION

Arabidopsis has over 400 predicted RLKs, but functions are known for relatively few of these (Shiu and Bleecker, 2003). The majority of plant RLKs are predicted to have Ser/Thr kinase activity and the largest family is the Leucine-Rich Repeat (LRR) class, the members of which have variable numbers of LRRs in their ECDs and are predicted to bind molecules such as hormones, elicitors, or peptide ligands through these protein-protein interaction domains (Dievart and Clark, 2004). The CrRLK1-like family of RLKs has 17 members, but functions have only been identified for six of the family members: FER, ANX1, ANX2, THE, HERK1, and HERK2 (reviewed in Boisson-Dernier et al., 2011; Lindner et al., 2012). The common theme in mutant phenotypes associated with *CrRLK1L* genes is cell wall sensing (Hematy and Hofte, 2008; Boisson-Dernier et al., 2011; Cheung and Wu, 2011; Lindner et al., 2012), indicating that these RLKs probably bind similar types of ligands. All of the CrRLK1L proteins contain a malectin-like domain similar to those found in the malectin protein of *Xenopus laevis* which is an endoplasmic reticulin (ER) protein involved in carbohydrate binding (Schallus et al., 2008). The presence of malectin-like domains in CrRLK1L RLKs indicates that the ligands could be either carbohydrates from the cell wall or peptide ligands with specific glycosylation patterns (Lindner et al., 2012).

ANX1 and HERK1 are not Functionally Interchangeable with FER

ANX1 and ANX2 are the most closely related proteins to FER and display a complementary expression pattern: *FER* is expressed in all tissues of the plant except for mature pollen (Escobar-Restrepo et al., 2007), while *ANX1* and *ANX2* are expressed only in pollen (Boisson-Dernier et al., 2009; Miyazaki et al., 2009). FER and ANX also perform seemingly opposite functions during pollination, with the ANX proteins maintaining pollen tube tip growth and FER causing termination of pollen tube tip growth, before pollen tube rupture and release of the two sperm cells and subsequent double fertilization can be achieved. One hypothesis for the function of FER and ANX proteins is that they compete for the same ligand, with FER binding the ligand at higher affinity at PT arrival at the synergid cells, leading to deactivation of the ANX pathway and subsequent bursting of the PT, similar to that seen in *anx1/anx2* mutants (Boisson-Dernier et al., 2009; Miyazaki et al., 2009). If this hypothesis is true, then expressing ANX1 in synergid cells should complement the *fer* phenotype, since the ANX1 ECD in the filiform apparatus would compete for the ligand at the tip of the PT. Neither our *pFER::ANX1-GFP* nor the *pFER::ANXEC-FERIC-GFP* constructs could complement the *fer-1* phenotype, indicating that ANX1 and FER probably bind different ligands and some other mechanism is responsible for inhibiting ANX signaling upon PT reception.

As expected, the more distantly related HERK1 was also not able to complement the *fer-1* phenotype when expressed in synergid cells. However, both the pFER::HERK1-GFP and pFER::ANX1-GFP fusion proteins showed very similar subcellular localization to FER-GFP in synergid cells. FER is highly concentrated in the filiform apparatus, a membrane-rich region where PTs enter at the micropylar end of the synergid cell. This localization pattern is not seen with all membrane-localized proteins in synergid cells—the ROP6C protein is evenly distributed around the synergid plasma membrane (Escobar-Restrepo et al., 2007). Our results indicate that HERK1 and ANX1 proteins contain the information needed for filiform apparatus localization when expressed in synergids, however the molecular basis for

this localization pattern remains to be determined.

The ICDs of CrRLK1 Proteins are Interchangeable

The CrRLK1L RLKs are predicted to perceive distinct ligands and transmit the signal through signal transduction cascades. Recent publications have shown that FER function in root hair elongation involves binding of guanine nucleotide exchange factors (ROPGEFs) that transduce a phosphorylation signal to a RHO GTPase (RAC/ROPs) leading to NADPH-oxidase dependent ROS production (Duan et al., 2010; Huang et al., 2013). In yeast-two-hybrid assays, the FER kinase domain can bind with at least 4 different ROPGEFs (Huang et al., 2013). This FER/GEF/ROP pathway has also been implicated in suppression of abscisic acid (ABA) signaling in roots by activating the ABI2 phosphatase (Yu et al., 2012). The ANX1 and ANX2 proteins have also been shown to be involved in NADPH-oxidase dependent ROS production during PT elongation, indicating that the same signaling pathway may be shared in tip-growing root hairs and PTs (Boisson-Dernier et al., 2013). The role of ROPGEF/RAC/ROP signal transduction in FER-mediated PT reception and in other CrRLK1L-mediated processes has yet to be determined, but our results that the ANX1 and HERK1 ICDs could complement the *fer-1* PT reception phenotype when linked to the FER ECD indicate that various members of the CrRLK1L family share common downstream signaling components.

Kinase Activity is not Necessary for FER Function

RLKs are defined by the presence of an extracellular ligand binding domain, a transmembrane domain, and an intracellular kinase domain. Most RLKs are presumed to sense a ligand and phosphorylate another protein to initiate a signal transduction cascade (Shiu and Bleecker, 2003). While FER has kinase activity *in vitro* that can be abolished by a K565R change in the active site (Escobar-Restrepo et al., 2007), the dead kinase version of FER was able to complement the PT reception phenotype when transformed into *fer-1* mutants, indicating that kinase activity is not necessary for FER function *in vivo*. While most plant RLKs that have been studied extensively require kinase activity for their functions (reviewed in Gish and Clark, 2011), a few have been reported to not require kinase function. Among these are FEI1, a Leucine-Rich Repeat (LRR) RLK involved in cell wall biosynthesis (Xu et al., 2008) and *Arabidopsis* CRINKLY4 (ACR4), a CR4-type RLK involved in epidermal development (Gifford et al., 2005). In addition, approximately 20% of the more than 400 RLKs in the *Arabidopsis thaliana* genome have amino acid substitutions in critical active sites of their kinase domains, leading to the prediction that these RLKs perform their functions without kinase activity (Castells and Casacuberta, 2007). STRUBBELIG (SUB) is one example of an RLK that lacks kinase activity in its native state (Chevalier et al., 2005). Instead of directly phosphorylating downstream components of its signal transduction cascade, FER could function as a part of a complex with another RLK that acts synergistically with FER and is thus able to complement the lack of kinase activity in the kinase dead version. Plant RLKs often occur in heterodimeric complexes. For example, in *Arabidopsis*, the BRASSINOSTEROID-INSENSITIVE 1-ASSOCIATED KINASE 1 (BAK1)/ SOMATIC EMBRYOGENESIS RECEPTOR-LIKE KINASE 3(SERK3) RLK has been shown to act in heterodimeric complexes with other LRR-RLKs such as BRASSINOSTEROID-INSENSITIVE 1 (BRI1) and FLAGILLIN-SENSITIVE 2 (FLS2) to enhance

their activity (Li et al., 2002). Like BAK1, FER has been shown to be involved in diverse developmental processes (Huck et al., 2003; Escobar-Restrepo et al., 2007; Guo et al., 2009; Deslauriers and Larsen, 2010; Duan et al., 2010; Yu et al., 2012; Huang et al., 2013). It is tempting to speculate that in some of these cases, FER also acts as a co-receptor to enhance the activity of a more "specific" receptor that transduces the received signal.

FER could also act as a scaffolding protein to bring other components such as ROPGEFs into a complex so that signal transduction can occur. In mice, the EPIDERMAL GROWTH FACTOR (EGF) family member ErbB3 has a nonfunctional kinase domain and acts in a complex with other EGF proteins with active kinase domains. Upon ligand binding, the active EGF phosphorylates ErbB3 at specific tyrosines, which then serve as docking sites for downstream targets (reviewed in Kroiher et al., 2001). FER has been shown to directly bind ROPGEF proteins that are involved in downstream signal transduction (Duan et al., 2010; Huang et al., 2013) and our data showing that the kinase domain is necessary for FER function even though kinase activity is not necessary indicates that FER may bind ROPGEFs but not be responsible for activating them by phosphorylation. It is possible that FER could act in a complex with another CrRLK1L protein or a different class of RLKs to provide a docking site for a ROPGEF that is then phosphorylated by the FER partner. Testing of this model awaits further identification of FER-interacting proteins.

Phosphorylation of the Activation Loop is Not Necessary for FER Function

X-ray crystallography experiments have shown that kinases contain an activation segment C-terminal to the catalytic domain. In many kinases, phosphorylation of residues in the activation loop of this segment determines the conformation of the loop which modulates kinase function (Nolen et al., 2004). While most structure-function studies have been done on animal kinases, site-directed mutagenesis experiments have shown that activation loop phosphorylation is important for function in some plant RLKs (Shah et al., 2001; Wang et al., 2005; Klaus-Heisen et al., 2011). The FER activation loop has two Serine and a Threonine that have been shown to be phosphorylated *in vivo* (Nuhse et al., 2004), indicating that phosphorylation of these residues may be important for conformational changes involved in FER function. Changes of these residues to Alanine to prevent phosphorylation had no effect on the ability of the protein to complement the *fer-1* phenotype, indicating that phosphorylation of the activation loop is not necessary to modulate FER function. In the converse experiment in which the phosphorylation targets were changed to Aspartic Acid to mimic constitutive phosphorylation, no transformants that expressed the transgene in synergid cells could be recovered. This result indicates that the STS-DDD conversion in the FER activation loop probably affects the stability of the protein. Whether this change in protein stability is functionally significant *in planta* remains to be determined.

Taken together, our results present the first functional evidence that the three members of the CrRLK1L subfamily FER, ANX1 and HERK1 share common downstream signaling targets, but are activated by distinct ligand interactions. Furthermore, the kinase activity of FER is not essential to execute its function indicating that FER might rather act as an important co-receptor recruiting co-factors or downstream targets to mediate signal transduction.

MATERIALS AND METHODS

Plant material and growth conditions

fer-1 plants (allele described in (Escobar-Restrepo et al., 2007)) were used for all transformations and *Landsberg erecta* was used as the wild-type control for complementation experiments. The FER-GFP line was reported in (Escobar-Restrepo et al., 2007). The *fer/fer* line was derived from the *fer-1* allele (Kessler et al., 2010). Plant growth conditions were as previously described (Huck). For transformation experiments, *fer-1* heterozygotes were selected by plating F2 seeds on MS plates supplemented with 50 mg/L kanamycin. After Agrobacterium-mediated transformation, seeds were harvested and plated on MS plates supplemented with 20 mg/L Hygromycin to select for transformants.

Fluorescence staining of pollen tubes

Aniline blue staining was performed as described previously (Huck et al., 2003). Images were captured with a Leica DM6000B epifluorescence microscope.

Domain swap and site-directed mutagenesis constructs

PCR with Phusion High Fidelity DNA Polymerase (Finnzymes, Espoo, Finland) was used to generate all constructs presented in the paper. The 2.5kb FER promoter fragment described in Escobar, et al., was used to drive expression of our GFP fusion constructs in synergid cells as well as vegetative tissues. Primers described in Table S1 were used to create overlapping fragments that were "PCR pasted" together to create fusion products with Gateway attB sites at the 5' end of the promoter and the 3' end of coding region (see table S2 for primer combinations used in each construct). These PCR products were used in BP clonase reactions to create entry clones in pDONR207 (Life Technologies) and sequenced to ensure that no undesired mutations were introduced by PCR. The resultant entry clones were used in LR reactions with pMDC111 (Curtis and Grossniklaus, 2003)to create in-frame GFP fusions in a plant binary vector. For the Kinase deletion construct, a PCR product from the 5' end of the promoter to the start of the kinase domain was amplified and cloned into pDONR207 with a BP clonase reaction. The entry clone was then used in an LR reaction with pMDC107 (identical to pMDC111 but with a different reading frame (Curtis and Grossniklaus, 2003) to create an in-frame fusion with GFP in a plant binary vector.

The site-directed mutagenesis constructs were generated by modifying the pFER::FER-GFP/pMDC111 construct that complemented the *fer-1* mutation in (Escobar-Restrepo et al., 2007). Overlapping primers (Table S3) were designed to introduce the desired nucleotide changes between the Sma1 and Xba1 restriction sites in the FER kinase domain. Restriction digests and ligations were used to replace the native fragments with the mutated PCR fragments and all constructs were sequenced to verify that the desired mutations had been introduced.

fer-1 complementation assays

The expression clones were transformed into *Agrobacterium tumefaciens* strain GV3101, and the resultant strain was used for transformation of *Arabidopsis fer-1/FER* plants using the floral dip method

(Bent, 2006). The progeny were collected and grown on MS plates containing 20 mg/L hygromycin to select transformants. Plants were grown to maturity and genotyped for the *fer-1* mutation according to Escobar, et al. Self-pollinated pistils were collected at 2-3 days after pollination and counts of fertilized vs. unfertilized ovules were performed to determine whether the constructs could complement the *fer-1* pollen tube reception phenotype. For each construct, a minimum of 3 independent T1 transformants (average 6) of each genotype (*FER/FER*, *fer-1/FER*, and *fer-1/fer-1* if possible) was used for complementation analysis and 300-500 ovules were counted for each plant. For non-complementing lines, a minimum of 8 primary transformants was analyzed for each genotype.

Confocal microscopy

For GFP analysis in order to determine the subcellular localization of complementation constructs, carpel walls were removed from mature pistils and specimens were mounted in 1M glycine, pH 9.6. They were then analyzed with a TCS SP2 confocal laser-scanning microscope (Leica, Bensheim, Germany). For GFP fusions, excitation was at 488 nm and emission was recorded from 495-525 nm. For chlorophyll autofluorescence, excitation was at 568 nm and emission was recorded from 580-650 nm. Single-focus-plane images of 1024x1024 pixels were recorded with a scan speed of 400 Hz. 3D stacks were recorded as images of 512X512 pixels, using 63X glycerol-immersion objectives and a scan speed of 200 Hz. Images were processed using Adobe Photoshop software for adjustments of brightness/contrast and image size.

References

Bent, A. (2006). *Arabidopsis thaliana* floral dip transformation method. Methods Mol Biol **343,** 87-103.

Boisson-Dernier, A., Kessler, S.A., and Grossniklaus, U. (2011). The walls have ears: the role of plant CrRLK1Ls in sensing and transducing extracellular signals. J. Exp. Bot. **62,** 1581-1591.

Boisson-Dernier, A., Lituiev, D.S., Nestorova, A., Franck, C.M., Thirugnanarajah, S., and Grossniklaus, U. (2013). ANXUR receptor-like kinases coordinate cell wall integrity with growth at the pollen tube tip via NADPH oxidases. PLoS Biol **11,** e1001719.

Boisson-Dernier, A., Roy, S., Kritsas, K., Grobei, M.A., Jaciubek, M., Schroeder, J.I., and Grossniklaus, U. (2009). Disruption of the pollen-expressed *FERONIA* homologs *ANXUR1* and *ANXUR2* triggers pollen tube discharge. Development **136,** 3279-3288.

Castells, E., and Casacuberta, J.M. (2007). Signalling through kinase-defective domains: the prevalence of atypical receptor-like kinases in plants. J Exp Bot **58,** 3503-3511.

Cheung, A.Y., and Wu, H.M. (2011). THESEUS 1, FERONIA and relatives: a family of cell wall-sensing receptor kinases? Curr Opin Plant Biol **14,** 632-641.

Chevalier, D., Batoux, M., Fulton, L., Pfister, K., Yadav, R.K., Schellenberg, M., and Schneitz, K. (2005). STRUBBELIG defines a receptor kinase-mediated signaling pathway regulating organ development in *Arabidopsis*. Proc Natl Acad Sci U S A **102,** 9074-9079.

Curtis, M.D., and Grossniklaus, U. (2003). A gateway cloning vector set for high-throughput functional analysis of genes in planta. Plant Physiol **133,** 462-469.

Deslauriers, S.D., and Larsen, P.B. (2010). FERONIA Is a Key Modulator of Brassinosteroid and Ethylene Responsiveness in *Arabidopsis* Hypocotyls. Mol Plant **3,** 626-640.

Dievart, A., and Clark, S.E. (2004). LRR-containing receptors regulating plant development and defense. Development **131,** 251-261.

Dresselhaus, T., and Franklin-Tong, N. (2013). Male-female crosstalk during pollen germination, tube growth and guidance, and double fertilization. Mol Plant **6,** 1018-1036.

Duan, Q., Kita, D., Li, C., Cheung, A.Y., and Wu, H.M. (2010). *FERONIA* receptor-like kinase regulates RHO GTPase signaling of root hair development. Proc Natl Acad Sci U S A **107,** 17821-17826.

Escobar-Restrepo, J.M., Huck, N., Kessler, S., Gagliardini, V., Gheyselinck, J., Yang, W.C., and Grossniklaus, U. (2007). The *FERONIA* receptor-like kinase mediates male-female interactions during pollen tube reception. Science **317,** 656-660.

Gifford, M.L., Robertson, F.C., Soares, D.C., and Ingram, G.C. (2005). ARABIDOPSIS CRINKLY4 function, internalization, and turnover are dependent on the extracellular crinkly repeat domain. Plant Cell **17,** 1154-1166.

Gish, L.A., and Clark, S.E. (2011). The RLK/Pelle family of kinases. Plant J **66,** 117-127.

Guo, H., Li, L., Ye, H., Yu, X., Algreen, A., and Yin, Y. (2009). Three related receptor-like kinases are required for optimal cell elongation in *Arabidopsis thaliana*. Proc Natl Acad Sci U S A **106,** 7648-7653.

Hematy, K., and Hofte, H. (2008). Novel receptor kinases involved in growth regulation. Curr Opin Plant Biol **11,** 321-328.

Huang, G.Q., Li, E., Ge, F.R., Li, S., Wang, Q., Zhang, C.Q., and Zhang, Y. (2013). *Arabidopsis* RopGEF4 and RopGEF10 are important for *FERONIA*-mediated developmental but not environmental regulation of root hair growth. New Phytol. [Epub ahead of print]

Huck, N., Moore, J.M., Federer, M., and Grossniklaus, U. (2003). The *Arabidopsis* mutant *feronia* disrupts the female gametophytic control of pollen tube reception. Development **130,** 2149-2159.

Kanaoka, M.M., Kawano, N., Matsubara, Y., Susaki, D., Okuda, S., Sasaki, N., and Higashiyama, T. (2011). Identification and characterization of *TcCRP1*, a pollen tube attractant from *Torenia concolor*. Ann. Bot. **108**: 739–747.

Kessler, S.A., Shimosato-Asano, H., Keinath, N.F., Wuest, S.E., Ingram, G., Panstruga, R., and Grossniklaus, U. (2010). Conserved molecular components for pollen tube reception and fungal invasion. Science **330,** 968-971.

Klaus-Heisen, D., Nurisso, A., Pietraszewska-Bogiel, A., Mbengue, M., Camut, S., Timmers, T., Pichereaux, C., Rossignol, M., Gadella, T.W., Imberty, A., Lefebvre, B., and Cullimore, J.V. (2011). Structure-function similarities between a plant receptor-like kinase and the human interleukin-1 receptor-associated kinase-4. J Biol Chem **286,** 11202-11210.

Kroiher, M., Miller, M.A., and Steele, R.E. (2001). Deceiving appearances: signaling by "dead" and "fractured" receptor protein-tyrosine kinases. Bioessays **23,** 69-76.

Li, J., Wen, J., Lease, K.A., Doke, J.T., Tax, F.E., and Walker, J.C. (2002). BAK1, an *Arabidopsis* LRR receptor-like protein kinase, interacts with BRI1 and modulates brassinosteroid signaling. Cell **110,** 213-222.

Lindner, H., Muller, L.M., Boisson-Dernier, A., and Grossniklaus, U. (2012). CrRLK1L receptor-like kinases: not just another brick in the wall. Curr Opin Plant Biol **15,** 659-669.

Mayank, P., Grossman, J., Wuest, S., Boisson-Dernier, A., Roschitzki, B., Nanni, P., Nuhse, T., and Grossniklaus, U. (2012). Characterization of the phosphoproteome of mature *Arabidopsis* pollen. Plant J **72,** 89-101.

Miyazaki, S., Murata, T., Sakurai-Ozato, N., Kubo, M., Demura, T., Fukuda, H., and Hasebe, M. (2009). *ANXUR1* and *2*, sister genes to *FERONIA/SIRENE*, are male factors for coordinated fertilization. Curr Biol **19,** 1327-1331.

Nolen, B., Taylor, S., and Ghosh, G. (2004). Regulation of protein kinases; controlling activity through activation segment conformation. Mol Cell **15,** 661-675.

Nuhse, T.S., Stensballe, A., Jensen, O.N., and Peck, S.C. (2004). Phosphoproteomics of the *Arabidopsis* plasma membrane and a new phosphorylation site database. Plant Cell **16,** 2394-2405.

Okuda, S., Tsutsui, H., Shiina, K., Sprunck, S., Takeuchi, H., Yui, R., Kasahara, R.D., Hamamura, Y., Mizukami, A., Susaki, D., Kawano, N., Sakakibara, T., Namiki, S., Itoh, K., Otsuka, K., Matsuzaki, M., Nozaki, H., Kuroiwa, T., Nakano, A., Kanaoka, M.M., Dresselhaus, T., Sasaki, N., and Higashiyama, T. (2009). Defensin-like polypeptide LUREs are pollen tube attractants secreted from synergid cells. Nature **458,** 357-361.

Palanivelu, R., and Tsukamoto, T. (2012). Pathfinding in angiosperm reproduction: pollen tube guidance by pistils ensures successful double fertilization. Wiley Interdiscip. Rev. Dev. Biol.**1,** 96-113.

Rotman, N., Rozier, F., Boavida, L., Dumas, C., Berger, F., and Faure, J.E. (2003). Female control of male gamete delivery during fertilization in *Arabidopsis thaliana*. Curr Biol **13,** 432-436.

Schallus, T., Jaeckh, C., Feher, K., Palma, A.S., Liu, Y., Simpson, J.C., Mackeen, M., Stier, G., Gibson, T.J., Feizi, T., Pieler, T., and Muhle-Goll, C. (2008). Malectin: a novel carbohydrate-binding protein of the endoplasmic reticulum and a candidate player in the early steps of protein N-glycosylation. Mol Biol Cell **19,** 3404-3414.

Shah, K., Vervoort, J., and de Vries, S.C. (2001). Role of threonines in the *Arabidopsis thaliana* somatic embryogenesis receptor kinase 1 activation loop in phosphorylation. J Biol Chem **276,** 41263-41269.

Shiu, S.H., and Bleecker, A.B. (2003). Expansion of the receptor-like kinase/Pelle gene family and receptor-like proteins in *Arabidopsis*. Plant Physiol **132,** 530-543.

Takeuchi, H., and Higashiyama, T. (2012). A species-specific cluster of defensin-like genes encodes diffusible pollen tube attractants in *Arabidopsis*. PLoS Biol **10,** e1001449.

Wang, X., Goshe, M.B., Soderblom, E.J., Phinney, B.S., Kuchar, J.A., Li, J., Asami, T., Yoshida, S., Huber, S.C., and Clouse, S.D. (2005). Identification and functional analysis of in vivo phosphorylation sites of the *Arabidopsis* BRASSINOSTEROID-

INSENSITIVE1 receptor kinase. Plant Cell **17,** 1685-1703.

Xu, S.L., Rahman, A., Baskin, T.I., and Kieber, J.J. (2008). Two leucine-rich repeat receptor kinases mediate signaling, linking cell wall biosynthesis and ACC synthase in *Arabidopsis*. Plant Cell **20,** 3065-3079.

Yu, F., Qian, L., Nibau, C., Duan, Q., Kita, D., Levasseur, K., Li, X., Lu, C., Li, H., Hou, C., Li, L., Buchanan, B.B., Chen, L., Cheung, A.Y., Li, D., and Luan, S. (2012). *FERONIA* receptor kinase pathway suppresses abscisic acid signaling in *Arabidopsis* by activating *ABI2* phosphatase. Proc Natl Acad Sci U S A **109,** 14693-14698.

GENERAL DISCUSSION
& FUTURE PERSPECTIVES

NOTE

In this chapter only aspects of the characterization of *TUN* and *EVN* will be discussed in more detail. Future directions and possible experiments will be suggested to obtain further insights regarding the function of *TUN* and *EVN in planta*. Chapter 3 and Chapter 4 are separately discussed within the corresponding chapters.

TUN and *EVN* Might Control Gametophyte Interaction and Development Potentially Via Protein N-Glycosylation

We identified two genes *TURAN* (*TUN*) and *EVAN* (*EVN*), which are both involved in PT reception in the synergid cells of the female gametophyte and in PT growth/integrity and pollen development, respectively. Both genes have not been characterized in plants before, but have predicted functions: *TUN* encodes an UDP-glycosyltransferase superfamily protein, whereas *EVN* encodes a dolichol kinase. Interestingly, both predicted gene functions indicate an involvement in early protein N-glycosylation on the cytosolic site of the endoplasmic reticulum (ER). Compared to yeast, relatively little is known about N-glycan biosynthesis and involved genes in this process in plants. Several members have been characterized by forward and reverse genetics and mutant analysis revealed that N-glycosylation is crucial for developmental processes such as seed, early vegetative and root development (reviewed in Pattison and Amtmann, 2009).

EVN and *TUN* have well-characterized orthologs in yeast, namely *SECRETORY 59* (*SEC59*) and *ASPARAGINE-LINKED GLYCOSYLATION 1* (*ALG1*), respectively. The yeast ortholog of *EVN*, *SEC59*, was identified in a screen for accumulation of inactive and incompletely glycosylated proteins at non-permissive temperatures (37°C; Ferro-Novick et al., 1984b). *sec59* cells were completely blocked in N-glycosylation, O-mannosylation and Glycosylphosphatidylinositol (GPI)-anchor biosynthesis (Ferro-Novick et al., 1984a; Orlean, 1990; Conzelmann et al., 1990) and the null allele *sec59-1* was not viable (Bernstein et al., 1989). These severe phenotypes occur since SEC59 catalyzes the first step of N-Glycosylation: the cytidine-triphosphate (CTP)-dependent phosphorylation of the ER-membrane-bound lipid carrier, the dolichol (Dol), on which oligosaccharide assembly takes place. *sec59* has defects in CTP-dependent dolichol kinase activity and thus in Dol-P accumulation (Heller et al., 1992). The human Dolichol Kinase (hDK1), which was identified in the human brain, showed a 30% amino acid identity to SEC59 (Figure D1A) and could complement the *sec59-1* mutant phenotypes (Fernandez et al., 2002). EVN and SEC59 proteins show 22% identity (ClustalW2; Figure D1A). Complementation analysis of the *sec59-1* mutant with *EVN* and activity measurements in yeast could give further insights of EVN function *in planta*, specifically whether EVN is able to catalyze the phosphorylation of dolichol. However, the low similarity between the plant- and the yeast orthologs might not be sufficient to exert the same function and thus complement the yeast mutant.

The yeast ortholog of TUN, *ALG1* encodes a beta-1,4 mannosyltransferase, transferring the first mannose from the GDP-D-mannose substrate to the Dol-PP-N-acetylglucosamine (GlcNAc) acceptor on the cytosolic site of the ER (Huffaker and Robbins, 1982; Couto et al., 1984). Under non-permissive temperature conditions (37°C), temperature sensitive *alg1-1* mutants synthesized mannosyl compounds at only 61% of the wild-type level and no mannose containing oligosaccharides were produced, because the first addition of mannose to $GlcNAc_2$ was abolished (Huffaker and Robbins, 1982). Furthermore, *alg1-1* null mutants were not viable under non-permissive conditions (Albright and Robbins, 1990). ALG1 and TUN proteins show in total a 35% identity (ClustalW2) and even 46% in the common glycosyltansferase (GT) 1 domain (predicted by Pfam 27.0, Figure D1B). Complementation analysis of the *alg1-1* mutant in yeast with *TUN* could give further information about comparable functions *in planta*. In fact, complementation of the *alg1-1* mutant with the *Human mannosyltransferase 1* (*Hmat-1*) has been

successful, which shows - like *TUN* - 36% protein identity to the yeast protein (Figure D1B; Takahashi et al., 2000), suggesting that even relatively low protein identity might be sufficient to exert the same function.

Interestingly, both EVN and TUN are specifically localized in the ER suggesting that they have a role in protein glycosylation reminiscent of their yeast and human orthologs. However, immunoblot band mobility assays of FER-GFP in downregulated *TUN(RNAi)* lines revealed no increased mobility due to loss of N-glycan attachment. Nevertheless, EVN and TUN could still have a role in glycosylation and defects in those genes could either alter N-glycan composition rather than abolishing it completely, or reduce the overall N-glycan amount, which might not be visible by mobility shift assays, or might just affect other proteins than FER.

In fact, several other biochemical and molecular methods have been established to investigate N-glycan composition and formation in plants: (i) mass spectrometry and immunoblot analysis against specific N-glycans, or (ii) assessing common reporters of underglycosylation using biochemical or molecular approaches. The overall N-glycan profile of glycoproteins can be determined by Matrix-assisted laser desorption ionization time-of-flight mass spectrometry (MALDI-TOF-MS; Farid et al., 2013). This method reveals the N-glycan composition and can be supported by lectin blots against specific N-glycans. In *oligosaccharyltransferase3/6-1* (*ost3/6-1*) mutants a lectin blot with Concanavalin A, which binds mainly terminal mannosyl- and glucosyl residues of glycoproteins, showed altered band mobility in the mutant (Farid et al., 2013). Reduced amounts of complex N-glycans can be determined by immunoblot analysis using anti-horseradish peroxidase (anti-HRP), which binds to certain core residues of the oligosaccharide (Wilson et al., 1998; Farid et al., 2013).

Furthermore, western blot analysis against the ER-localized glycoprotein PROTEIN DISULFIDE ISOMERASE (PDI) is used as a common reporter for underglycosylation and revealed reduced glycosylation efficiency in *alg10-1* mutants deficient in oligosaccharide assembly as hypothesized for *tun* and *evn* (Farid et al., 2011). Moreover, immunoblot analysis against GPI-anchored proteins (GAPs), like *SKU5* (Sedbrook et al., 2002), could reveal a decrease in GAPs as was shown for the *peanut* (*pnt*) mutants deficient in an ER-localized mannosyltransferase (Gillmor et al., 2005).

In addition, protein underglycosylation causes the unfolded protein response (UPR) and, thus, the upregulation of several ER-localized stress-response proteins, which was shown in N-glycosylation mutants and after chemical treatment with the N-glycosylation inhibitor tunicamycin (Koiwa, 2003). Quantitative real-time reverse transcription (qRT)-PCR analysis revealed increased levels of *BINDING PROTEIN 1* (*BiP1*) and *BiP 2*, the *CALRETICULIN 2* (*CRT2*) and *PDI5* in *ost3/6-1* mutants (Farid et al., 2013).

Furthermore, the root growth rate of N-glycosylation mutants is reduced under salt stress and seedlings are more sensitive to the protein glycosylation inhibitor tunicamycin (Zhang et al.; Farid et al., 2013). Therefore, several molecular and biochemical methods could reveal aberrant N-glycan profiles in *evn* and *tun* and thus shed light on their protein functions *in planta*. However, the fact that we cannot retrieve homozygous mutant individuals made the production of downregulated RNAi lines indispensible. Both *TUN(RNAi)* and *EVN(RNAi)* lines still have residual gene activity and it needs to be revealed how reliable a change of the glycosylation status in those lines can be detected.

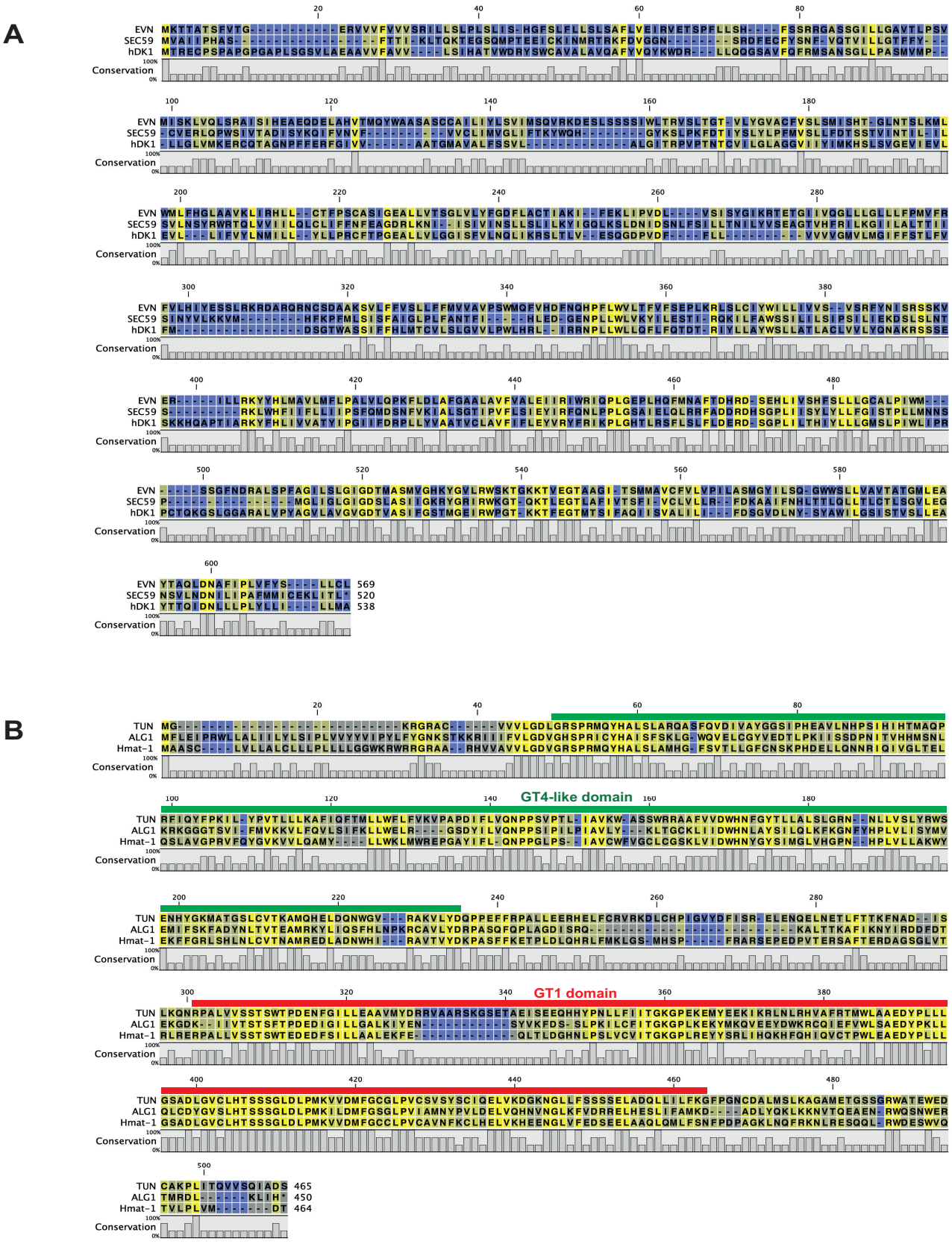

Figure D1. Protein alignment of EVN and TUN with their respective orthologs in yeast and human.

(A) Protein alignment of EVN (*Arabidopsis*), SEC59 (yeast) and hDK1 (human). Level of conservation is indicated by heat-map coloring (blue indicates low conservation, yellow indicates high conservation). Only SEC59 has a predicted Cytidylyltransferase domain (amino acids 471-596 in the alignment). **(B)** Protein alignment of TUN (*Arabidopsis*), ALG1 (yeast) and Hmat1 (human). Level of conservation is indicated by heat-map coloring (blue indicates low conservation, yellow indicates high conservation). The significant Glycosyltransferase1 (GT1) domain is indicated in red and the insignificant Glycosyltransferase4-like (GT4-like) domain in green. Domain prediction was done using http://pfam.sanger.ac.uk/.

Callose Accumulation at the Filiform Apparatus Might Be Due to Altered Cell Wall Composition But Not Causal for the Phenotype

Both *evn* and *tun* ovules display increased callose accumulation at the micropylar pole of the synergid cells 2DAE. Aberrant cell wall composition was described for *sec59* with increased chitin accumulation (Orłowski et al., 2007) and in several mutants from the ER associated N-glycosylation pathway in plants, like *cytokinesis defective 1* (*cyt1*; Conklin et al., 1996; Nickle and Meinke, 1998; Lukowitz et al., 2001), a subunit of the OST complex *defective glycosylation 1* (*dgl1*; Lerouxel et al., 2005), members from the calnexin-calreticulin cycle for proper protein folding *glucosidase 1* (*gcs1*)/*knopf 1* (*knp1*; Boisson et al., 2001; Gillmor et al., 2002) and *radial swelling 3* (*rsw3*; Burn et al., 2002). Increased callose accumulation in *cyt1* was explained by a compensatory mechanism induced by mechanical stress due to cellulose reduction (Lukowitz et al., 2001). In *evn* and *tun* ovules, the cellulose content remains to be elucidated, potentially by staining semi-thin sections with the fluorescent stain for cellulose containing structures calcofluor-white (Choi and O'Day, 1984). In addition, transmission electron microscopy (TEM) of ultra-thin sections of mutant ovules could elucidate cytological changes in the synergid cells (Huck, 2003): for example if callose accumulation influences filiform apparatus conformation or has other effects on synergid ultra structure.

However, localization of several members of the PT reception pathway (FER-GFP, NTA-GFP, LRE-Citrine) at the filiform apparatus of mutant ovules was normal giving a first indication that those proteins are not affected by callose deposition. In fact, synergid cell fate marker (ET2634) analysis revealed no differentiation defect in *evn* and *tun* ovules and all mutant ovules can attract PTs and around 30% can perceive PTs indicating that increased callose accumulation -present in all mutant ovules- at the site of PT reception was not the reason for the PT overgrowth phenotype.

Pollen Tube Burst in *tun* Might Be Due to a Direct Effect on ANX1

In vitro grown *tun* pollen tubes burst immediately after germination, a phenotype reminiscent of the *in vitro* grown *anx1/anx2* pollen tubes (Boisson-Dernier et al., 2009; Miyazaki et al., 2009). *In vivo* grown *anx1/anx2* pollen tubes germinate normally, grow longer, but hardly reach the transmitting tract of the pistil (Boisson-Dernier et al., 2009; Miyazaki et al., 2009). To assess whether *tun* mutant pollen behaves similar as *anx1/anx2* pollen tubes *in planta*, limited pollination of wild-type pistils with *tun/TUN;qrt/qrt* pollen will reveal *in vivo* growth of *tun* pollen tubes. The *quartet* (*qrt*) mutation facilitates pollen analysis of heterozygous phenotypes, because microspores fail to separate after meiosis and form tetrads of pollen grains (Rhee et al., 2003). Tetrad analysis of heterozygous mutant individuals allows the detection of pollen defects since within one tetrad, two microspores carry the wild-type and two the mutant allele of the gene of interest. By using only very little amounts of pollen from the *tun/TUN;qrt/qrt* mutant (e.g. by using an eye lash to collect pollen and distribute it on a pistil), every PT can be followed individually, revealing if in *tun/TUN;qrt/qrt* tetrads two PTs grow towards the ovules, whereas two burst prior ovule arrival.

To investigate if the burst phenotype in *tun* pollen tubes is caused by an effect on ANX proteins, we determined ANX1-YFP protein abundance/localization by fluorescence microscopy. Interestingly

among 100 *tun-2/TUN;qrt/qrt* plants, no *tun* mutant plants were found to have ANX1-YFP fluorescence in all four pollen grains of a tetrad. In contrast, the ANX1-YFP reporter segregated normally in wild-type segregants. Therefore, *tun* deficiency in pollen tubes seems to affect ANX1-YFP production and/or stability. The ANX1 protein has seven putative N-glycosylation sites (Lindner et al., 2012a). Mis-glycosylation of proteins can induce ER-associated degradation (ERAD) leading to protein degradation by the 26S proteasome in the cytosol. The plasma membrane (PM) localized leucin-rich repeat receptor-like kinase (LRR-RLK) BRASSINOSTEROID-INSENSITIVE 1 (BRI1) contains multiple N-glycosylation sites (Li and Chory, 1997) and was shown to be a N-glycan dependent ERAD target (Hong et al., 2008; 2009). Two mutant variants *bri1-5* and *bri1-9* retain in the ER and are degraded in a proteasome independent and dependent pathway, respectively (Hong et al., 2008; 2009). *bri1-5* seedling treatment with Kifunensine (Kif), an inhibitor of ER and Golgi α-1,2-mannosidases that prevents ERAD in many terminally mis-folded proteins (Tokunaga et al., 2000), increased steady state levels of bri1-5 protein and rescued the dwarf phenotype (Hong et al., 2008). However, MG132 proteasome inhibitor treatment had little effect in bri1-5 protein level. In contrast in *bri1-9*, both MG132 and Kif treatments rescued the mutant phenotypes. In *tun-2/TUN;qrt/qrt/ANX1-YFP/ANX1-YFP* plants proteasome inhibitor treatment could give further insights into the associated degradation pathway of ANX1-YFP in *tun* pollen grains. It needs to be tested, if treatment of closed flower buds will recover ANX1-YFP abundance/stability since ANX proteins might be produced before pollen maturation, or if addition of the proteasome inhibitor to pollen germination medium would even rescue the PT burst phenotype. In *Brassica napus* W1, MG132 treatment of cut flower buds has indeed been successful to disrupt the self-incompatibility response in pistils (Stone et al., 2003). On the other hand, addition of MG132 to pollen germination medium has been described for *Picea wilsonii*, and proteasome inhibitor treatment resulted in depolimerization of the PT cytoskeleton and consequently strongly altered cell wall composition and, thus, lead to reduced and delayed germination and slower PT growth rates (Sheng et al., 2006). Therefore it is not clear, if such strong phenotypic changes induced by proteasome inhibitor treatment will allow the rescue of the burst phenotype in *tun* PTs. However, another possible inhibitor that could be tested is the proteasome inhibitor syringuline A (Syl A) secreted from *Pseudomonas syringae pv. syringae* (*Pss*; Wäspi et al., 1998; Groll et al., 2008). SylA might have the advantage that it evolved to specifically target the plant proteasome pathway and is efficiently taken up by plant tissue (Hassa et al., 2000).

To investigate if ANX1-YFP is a specific target of TUN function, the abundance of other membrane-associated and glycosylated PT proteins has to be tested in *tun* PTs. ANX2 has four predicted N-glycosylation sites (Lindner et al., 2012a) and acts redundantly to ANX1 as only *anx1/anx2* double mutants show the pollen tube bursting phenotype (Boisson-Dernier et al., 2009; Miyazaki et al., 2009). This indicates that also ANX2 and, therefore, an ANX2-GFP reporter should be affected by *tun* deficiency. Furthermore, abundance/localization of ANX1/ANX2-independent PT proteins have to be investigated: LOST IN POLLEN TUBE GUIDANCE 1 (LIP1) and LIP2 are glycosylated receptor-like cytoplasmic kinases which are membrane bound via palmitoylation (Liu et al., 2013), and ACA9, which is a glycosylated, transmembrane Ca^{2+}-pump (Schiøtt et al., 2004). Fluorescence microscopy analysis of translational fusions of LIP1, LIP2 and ACA9 with fluorescent tags in *tun-2/TUN;qrt/qrt* tetrads will give further insights of the specificity of ANX1-YFP absence in *tun* mutant grains.

In principle, it is possible that the mutations in *TUN* and *EVN* cause general glycosylation defects affecting multiple glycoproteins in many different tissues. However, we believe that the mutant effect of *tun* on ANX1 is more specific. The abundance and localization of the known members of the PT reception pathway in the female gametophyte that depend on protein glycosylation, FER and LRE, is normal. In contrast, the male gametopyhte-specific factor ANX1, which has 55% amino acid identity to FER, is affected by *tun*, suggesting at least some specificity. In addition, specificity of ERAD has been described for the LRR-RLKs EF-Tu RECEPTOR (EFR) and FLAGELLIN-SENSITIVE 2 (FLS2), both involved in plant innate immunity (Li et al., 2009). Both LRR-RLKs are highly N-glycosylated PM localized proteins but mutations in two members of the ER quality control only affected EFR, but not the closely related FLS2 (Li et al., 2009).

Pollen Tube Reception Might Depend on a Dual Recognition System Involving Peptide and N-Glycan Recognition

Interestingly *tun/TUN* mutants not only show the *fer*-like PT overgrowth phenotype in the ovules but also the *fer*-like dwarf phenotype in the vegetative state. In addition, *tun* causes an *anx1/anx2*-like PT bursting phenotype. The latter might be caused by ANX1/ANX2 protein absence due to ERAD degredation (discussed above). Although ANX1 and ANX2 proteins show around 55% identity to FER, the female gametophytic and the vegetative phenotype are not caused by FER absence or complete loss of N-glycosylation in *tun/TUN* and *TUN(RNAi)* plants, respectively. FER-GFP localization in *tun* ovules seemed normal and western blot analysis of FER-GFP in *TUN(RNAi)* seedlings revealed no major differences in protein amount and protein mobility due to loss of N-linked glycans. However, it cannot be excluded that only some N-glycans are absent or that N-glycan composition is different. Therefore, it is possible that FER-GFP localization is unaffected, but functions like ligand binding and/or recognition and subsequent signal transduction could be reduced. Recently, a "domain specific model" has been proposed for sperm-egg binding in mammals (Clark, 2010), which is conducted by the glycoprotein mZP3 residing on the extracellular matrix of the oocyte, the zona pellucida (ZP). mZP3 is essential for sperm-binding and subsequent acrosome reaction in the sperm cell, leading to PM fusion and fertilization (reviewed in Wassarman and Litscher, 2008). The "domain specific model" combines results of several studies that suggested that N-glycans are important for sperm-egg binding with studies revealing that deglycosylated mZP3 proteins can compete for sperm cells and thus inhibit sperm binding to oocytes. The model explains these contradictory data by interactions of a sperm cell protein or protein complex with the glycans and/or the protein backbone of mZP3 depending on its glycosylation state (Clark, 2010). Oocytes of conditional mutants of the N-acetylglucosaminyltransferase I (GnT I) produce only high mannose glycans (Shi et al., 2004) and show 81% fewer sperm binding compared to wild-type oocytes (Hoodbhoy et al., 2005), but the strain retains 50% of wild-type fertility (Shi et al., 2004). Thus, the dual adhesion system serves as a back-up system that ensures better sperm-egg binding and increases the chance for fertilization even if receptors are mis-glycosylated (Clark, 2011). In plants, egg- and sperm cell do not get in vicinity, if prior PT reception fails. Here, recognition and acceptance happen at the first contact site between the female- and male gametophytes, namely the filiform apparatus. It is conceivable that also in plants a dual recognition system of the sugar and the protein backbone would lead to improved

PT reception and increased chances to bring both gametes together. This dual recognition system could also explain the reduced penetrance of the PT overgrowth phenotype in *tun* and *evn* ovules since the female protein component, even if not glycosylated properly, could still partly recognize the male factor. Nevertheless, it remains unknown if FER itself and/or other pathways are affected in *tun* and *evn* mutant ovules. It is even possible that a synergid derived signaling molecule is lacking a sugar residue, which is essential for triggering the complete signal transduction in the female- or male gametophyte to mediate PT reception.

The Role of *TUN* During Vegetative Development

In tip-growing pollen tubes, ANX proteins positively regulate NADPH oxidases, leading to ROS accumulation, Ca^{2+}-influx und subsequent PT elongation (Boisson-Dernier et al., 2013). In root hair, FER mediates ROS-dependent polar growth by directly interacting with guanine exchange factors (ROPGEFs), which activate Rho-like GTPases (RAC/ROPs) leading to NADPH oxidase activation and ROS production (Duan et al., 2010; Yu et al., 2012; Huang et al., 2013). Consequently, FER promotes tip growth in root hairs whereas ANX proteins mediate polar growth in pollen. Interestingly, *tun* pollen tubes burst immediately after germination and ANX1-YFP fluorescence is absent in *tun* pollen grains. Therefore, it will be interesting to analyze root hair growth in *TUN(RNAi)* lines and investigate whether FER-GFP expression is similarly affected by *TUN* knockdown in root hairs.

Additionally, we find a *fer*-like vegetative dwarf phenotype in *TUN(RNAi)* plants. The severity and frequency of this dwarf phenotype correlates with the expression level of *TUN* in the *TUN(RNAi)* lines. Complete knockout of *TUN* expression was not achieved, but several dwarfed plants degenerated without further growth, suggesting that they might express *TUN* at too low levels to survive. This indicates that *TUN* expression might be crucial for vegetative growth.

It is tempting to speculate that *TUN* deficiency affects FER function in synergid cells and during vegetative growth, since it causes the *fer*-like phenotypes in both tissues and, additionally, affects *FER*'s closest homolog in pollen tubes, ANX1. However, FER-GFP is normally abundant and normally localized in *tun* mutant ovules. In addition, mobility shift assays of FER-GFP in wild-type and *TUN(RNAi)* seedlings showed no obvious difference. However, it remains elusive whether the N-Glycan composition of FER is changed or whether the downregulation of *TUN* affects different sets of proteins in synergids and vegetative cells, leading to the described phenotypes.

In contrast, *EVN(RNAi)* lines with a residual expression of only 13% of wild-type levels, displayed no obvious vegetative phenotype. This was a bit surprising, since EVN function was essential during pollen development. So far, no complete knockouts for *EVN* expression have been identified. It is conceivable that the residual EVN function in the vegetative state is sufficient for normal plant growth and only complete loss-of-function would result in lethality.

SNP-Ratio Mapping (SRM) Requires a Sufficient Sequencing Coverage to Identify the Causal SNP in a Pool of Mutant Individuals

The development of SNP-ratio mapping (SRM) was essential for this study, since mutations in *TUN* and *EVN* do not allow the identification of homozygous mutant individuals, due to male gametophytic

defects and potential vegetative lethality (described above). SRM allows mapping of homozygous-lethal mutations or of poorly transmitted mutations and second-site modifiers in complex genetic/transgenic backgrounds. Furthermore, in contrast to other published techniques allowing the identification of causal alleles by next-generation sequencing (Schneeberger et al., 2009; Austin et al., 2011; Zuryn et al., 2010), SRM requires only few mutant individuals and only two rounds of backcrossing after the mutagenesis, making it a time saving method especially for organisms with relatively long generation times like *Arabidopsis*. At the same time, a similar method relying on segregation ratios was published for the identification of homozygous rice mutants (Abe et al., 2012). Briefly, with SRM the segregation ratios of EMS-induced single nucleotide polymorphisms (SNPs) are used to identify the causative SNP that segregates in a 1:1 ratio in a backcross population of mutant individuals versus a 1:3 ratio for unlinked SNPs in the background. In this thesis, we successfully mapped the causal SNP in three different PT reception mutants. To apply SRM on *tun-1/TUN* mutants, 50 mutant individuals were pooled and sequenced by next-generation sequencing using the SOLiD platform yielding average sequence coverage of 57 reads (Lindner et al., 2012b). Sequence coverage of 50 was calculated to be sufficient to differentiate the segregation ratios of 1:1 and 1:3 of a SNP in a pool of mutant individuals (Lindner et al., 2012b). SRM of a pool of 94 mutant individuals of *evn-1/EVN* achieved a sequence coverage of 130 reads and was sufficient to identify the causative SNP with a segregation ratio of 0.5 on the lower arm of chromosome three. This result was confirmed by PCR amplification of the mapped gene in all 94 samples and subsequent digest with nucleases cleaving single base pair mismatches in heteroduplex DNA (Till et al., 2004). The SNP was present in all but two samples, which turned out to be sampling errors (see appendix). However, SRM on a pool of 60 *evn-3/EVN* mutant samples achieved sequence coverage of only 30 reads. This coverage was too low to identify the causative SNP by visual analysis of plotted segregation ratios against their chromosomal position (described in Lindner et

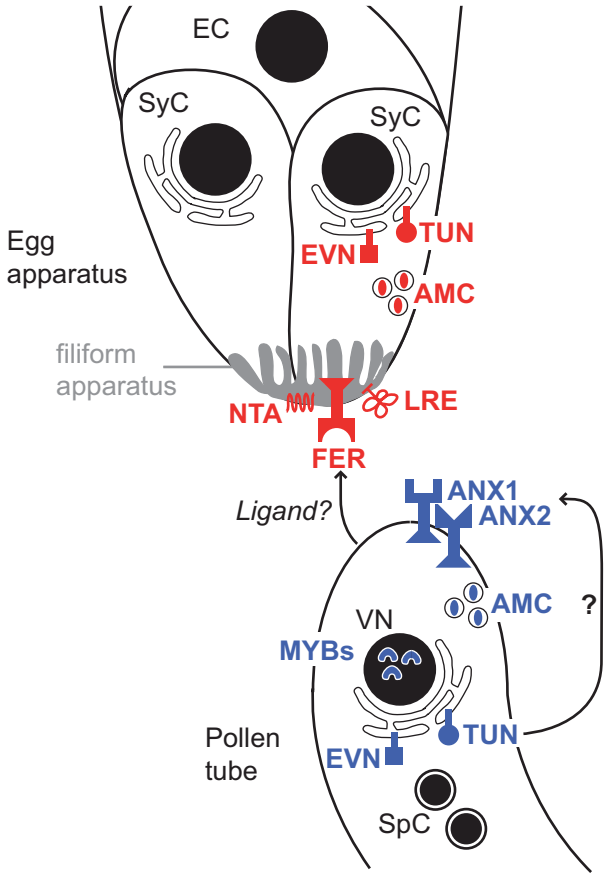

Figure D2. TUN and EVN mediate pollen tube reception in the synergids and have a role in the male gametophyte.
The two novel factors TUN and EVN are involved in the active signaling cascade in the synergids required for normal pollen tube reception. Both genes are located in the ER and might have a role in protein N-glycosylation. However, the previously identified molecular components of pollen tube reception in the synergids, FER, NTA, and LRE, are properly localized and normally abundant in *tun* or *evn*. However, whether N-glycan composition, which surely influences protein function, is normal remains unknown. In the male gametophyte, EVN is required for pollen maturation, whereas TUN is required to pollen tube growth/integrity. Interestingly, ANX1 reporters are absent in *tun* mutant pollen tubes suggesting a direct effect of TUN on ANX1, potentially via N-glycosylation. Factors targeted by EVN remain unknown. EC, egg cell; SyC, synergid cell; VN, vegetative nucleus; SpC, sperm cells.

al., 2012b). Therefore, classical rough mapping narrowed down the region of interest to the lower arm of chromosome three and PCR amplification and nuclease digest of 15 candidate genes yielded the identification of another mutant allele disrupting *EVN*. All DNA samples of the mutant pool carried this SNP, but SRM revealed a segregation ratio of only 0.3 due to the low sequence coverage. Therefore, SRM is a useful method to identify causative, heterozygous SNPs after only two rounds of backcrossing, but it requires minimal sequence coverage of 50 to yield reliable segregation ratios.

Final Conclusions

In this PhD thesis, we identified two novel genes of the PT reception pathway in the synergid cells, *TUN* and *EVN* (Figure D2). Interestingly, both described gene functions indicate potential involvement in early steps of protein N-glycosylation. Furthermore, it was shown that both genes play distinct roles in pollen, where EVN is essential for development, whereas TUN is crucial for PT growth/integrity. Although the targets of TUN and EVN in the synergids remain unknown, in PTs TUN function seems to affect the plasma membrane localized RLK ANX1 (Figure D2). Interestingly, knockdown of *TUN* additionally caused a vegetative dwarf phenotype suggesting that at least *TUN* might be an essential gene for vegetative growth. Taken together, protein N-glycosylation seems to be an important process to mediate PT reception in the synergid cells and to prevent PT burst before arrival at the receptive synergid cell and is, thus, essential for plant fertility.

References:

Abe, A. et al. (2012). Genome sequencing reveals agronomically important loci in rice using MutMap. Nat Biotechnol. **30**: 174–178.

Albright, C.F. and Robbins, R.W. (1990). The sequence and transcript heterogeneity of the yeast gene *ALG1*, an essential mannosyltransferase involved in N-glycosylation. J. Biol. Chem. **265**: 7042–7049.

Austin, R.S., Vidaurre, D., Stamatiou, G., Breit, R., Provart, N.J., Bonetta, D., Zhang, J., Fung, P., Gong, Y., Wang, P.W., McCourt, P., and Guttman, D.S. (2011). Next-generation mapping of *Arabidopsis* genes. Plant J. **67**: 715–725.

Bernstein, M., Kepes, F., and Schekman, R. (1989). *Sec59* encodes a membrane protein required for core glycosylation in *Saccharomyces cerevisiae*. Mol. Cell. Biol. **9**: 1191–1199.

Boisson, M., Gomord, V., Audran, C., Berger, N., Dubreucq, B., Granier, F., Lerouge, P., Faye, L., Caboche, M., and Lepiniec, L. (2001). *Arabidopsis glucosidase I* mutants reveal a critical role of N-glycan trimming in seed development. EMBO J. **20**: 1010–1019.

Boisson-Dernier, A., Lituiev, D.S., Nestorova, A., Franck, C.M., Thirugnanarajah, S., and Grossniklaus, U. (2013). *ANXUR* Receptor-Like Kinases Coordinate Cell Wall Integrity with Growth at the Pollen Tube Tip Via NADPH Oxidases. PLoS Biol **11**: e1001719.

Boisson-Dernier, A., Roy, S., Kritsas, K., Grobei, M.A., Jaciubek, M., Schroeder, J.I., and Grossniklaus, U. (2009). Disruption of the pollen-expressed *FERONIA* homologs *ANXUR1* and *ANXUR2* triggers pollen tube discharge. Development **136**: 3279–3288.

Burn, J.E., Hurley, U.A., Birch, R.J., Arioli, T., Cork, A. and Williamson, R.E. (2002). The cellulose-deficient *Arabidopsis* mutant *rsw3* is defective in a gene encoding a putative *glucosidase II*, an enzyme processing N-glycans during ER quality control. Plant J. **32**: 949-960**.**

Choi, A.H. and O'Day, D.H. (1984). Calcofluor staining of cellulose during microcyst differentiation in wild-type and mutant strains of *Polysphondylium pallidum*. J. Bacteriol. **157**: 291–296.

Clark, G.F. (2011). Molecular models for mouse sperm-oocyte binding. Glycobiology **21**: 3–5.

Clark, G.F. (2010). The Mammalian Zona Pellucida: A Matrix That Mediates Both Gamete Binding and Immune Recognition? Syst Biol Reprod Med **56**: 349–364.

Conklin, P.L., Williams, E.H., and Last, R.L. (1996). Environmental stress sensitivity of an ascorbic acid-deficient *Arabidopsis* mutant. Proc. Natl. Acad. Sci. U.S.A. **93**: 9970–9974.

Conzelmann, A., Fankhauser, C., and Desponds, C. (1990). Myoinositol gets incorporated into numerous membrane glycoproteins of *Saccharomyces cerevisiae*; incorporation is dependent on phosphomannomutase (*sec53*). EMBO J. **9**: 653-661.

Couto, J.R., Huffaker, T.C., and Robbins, P.W. (1984). Cloning and expression in *Escherichia coli* of a yeast mannosyltransferase from the asparagine-linked glycosylation pathway. J. Biol. Chem. **259**: 378–382.

Duan, Q., Kita, D., Li, C., Cheung, A.Y., and Wu, H.-M. (2010). *FERONIA* receptor-like kinase regulates RHO GTPase signaling of root hair development. Proc. Natl. Acad. Sci. U.S.A. **107**: 17821–17826.

Farid, A., Malinovsky, F.G., Veit, C., Schoberer, J., Zipfel, C., and Strasser, R. (2013). Specialized Roles of the Conserved Subunit OST3/6 of the Oligosaccharyltransferase Complex in Innate Immunity and Tolerance to Abiotic Stresses. Plant Phys. **162**: 24–38.

Farid, A., Pabst, M., Schoberer, J., Altmann, F., Glössl, J., and Strasser, R. (2011). *Arabidopsis thaliana alpha1,2-glucosyltransferase (ALG10)* is required for efficient N-glycosylation and leaf growth. Plant J. **68**: 314–325.

Fernandez, F., Shridas, P., Jiang, S., Aebi, M., and Waechter, C.J. (2002). Expression and characterization of a human cDNA that complements the temperature-sensitive defect in dolichol kinase activity in the yeast *sec59-1* mutant: the enzymatic phosphorylation of dolichol and diacylglycerol are catalyzed by separate CTP-mediated kinase activities in *Saccharomyces cerevisiae*. Glycobiology **12**: 555–562.

Ferro-Novick, S., Hansen, W., Schauer, I., and Schekman, R. (1984a). Genes required for completion of import of proteins into the endoplasmic reticulum in yeast. J. Cell Biol. **98**: 44–53.

Ferro-Novick, S., Novick, P., Field, C., and Schekman, R. (1984b). Yeast secretory mutants that block the formation of active cell surface enzymes. J. Cell Biol. **98**: 35–43.

Gillmor, C.S., Lukowitz, W., Brininstool, G., Sedbrook, J.C., Hamann, T., Poindexter, P., and Somerville, C. (2005). Glycosylphosphatidylinositol-anchored proteins are required for cell wall synthesis and morphogenesis in *Arabidopsis*. Plant Cell **17**: 1128–1140.

Gillmor, C.S., Poindexter, P., Lorieau, J., Palcic, M.M., and Somerville, C. (2002). *Alpha-glucosidase I* is required for cellulose biosynthesis and morphogenesis in *Arabidopsis*. J. Cell Biol. **156**: 1003–1013.

Groll, M., Schellenberg, B., Bachmann, A.S., Archer, C.R., Huber, R., Powell, T.K., Lindow, S., Kaiser, M., and Dudler, R. (2008). A plant pathogen virulence factor inhibits the eukaryotic proteasome by a novel mechanism. Nature **452**: 755–758.

Hassa, P., Granado, J., Freydl, E., Wäspi, U., and Dudler, R. (2000). Syringolin-mediated activation of the *Pir7b* esterase gene in rice cells is suppressed by phosphatase inhibitors. Mol. Plant Microbe Interact. **13**: 342–346.

Heller, L., Orlean, P., and Adair, W.L. (1992). *Saccharomyces cerevisiae sec59* cells are deficient in dolichol kinase activity. Proc. Natl. Acad. Sci. U.S.A. **89**: 7013–7016.

Hong, Z., Jin, H., Fitchette, A.C., Xia, Y., and Monk, A.M. (2009). Mutations of an *α1, 6 mannosyltransferase* inhibit endoplasmic reticulum–associated degradation of defective brassinosteroid receptors in *Arabidopsis*. Plant Cell **21**: 3792-3802.

Hong, Z., Jin, H., Tzfira, T., and Li, J. (2008). Multiple Mechanism-Mediated Retention of a Defective Brassinosteroid Receptor in the Endoplasmic Reticulum of *Arabidopsis*. Plant Cell **20**: 3418–3429.

Hoodbhoy, T., Joshi, S., Boja, E.S., Williams, S.A., Stanley, P., and Dean, J. (2005). Human sperm do not bind to rat zonae pellucidae despite the presence of four homologous glycoproteins. J. Biol. Chem. **280**: 12721–12731.

Huang, G.Q., Li, E., Ge, F.R., Li, S., and Wang, Q. (2013). *Arabidopsis RopGEF4* and *RopGEF10* are important for *FERONIA*-mediated developmental but not environmental regulation of root hair growth. New Phyt. [Epub ahead of print]

Huck, N. (2003). The female control of male behaviour in sexual plant reproduction : characterization of the female

gametophytic mutant *feronia* in *Arabidopsis thaliana*. PhD Thesis.

Huffaker, T.C. and Robbins, P.W. (1982). Temperature-sensitive yeast mutants deficient in asparagine-linked glycosylation. J. Biol. Chem. **257**: 3203–3210.

Koiwa, H. (2003). The STT3a Subunit Isoform of the *Arabidopsis* Oligosaccharyltransferase Controls Adaptive Responses to Salt/Osmotic Stress. Plant Cell **15**: 2273–2284.

Lerouxel, O., Mouille, G., Andème-Onzighi, C., Bruyant, M.-P., Séveno, M., Loutelier-Bourhis, C., Driouich, A., Höfte, H., and Lerouge, P. (2005). Mutants in *DEFECTIVE GLYCOSYLATION*, an *Arabidopsis* homolog of an olig osaccharyltransferase complex subunit, show protein underglycosylation and defects in cell differentiation and growth. Plant J. **42**: 455–468.

Li, J. and Chory, J. (1997). A putative leucine-rich repeat receptor kinase involved in brassinosteroid signal transduction. Cell **90**: 929–938.

Li, J., Zhao-Hui, C., Batoux, M., Nekrasov, V., Roux, M., Chinchilla, D., Zipfel, C., and Jones, J.D.G. (2009). Specific ER quality control components required for biogenesis of the plant innate immune receptor EFR. Proc. Natl. Acad. Sci. U.S.A. **106**: 15973–15978.

Lindner, H., Müller, L.M., Boisson-Dernier, A., and Grossniklaus, U. (2012a). *CrRLK1L* receptor-like kinases: not just another brick in the wall. Curr. Opin. Plant Biol. **15**: 659–669.

Lindner, H., Raissig, M.T., Sailer, C., Shimosato-Asano, H., Bruggmann, R., and Grossniklaus, U. (2012b). SNP-Ratio Mapping (SRM): identifying lethal alleles and mutations in complex genetic backgrounds by next-generation sequencing. Genetics **191**: 1381–1386.

Liu, J., Zhong, S., Guo, X., Hao, L., Wei, X., Huang, Q., Hou, Y., Shi, J., Wang, C., Gu, H., and Qu, L.-J. (2013). Membrane-Bound RLCKs LIP1 and LIP2 Are Essential Male Factors Controlling Male-Female Attraction in Arabidopsis. Curr. Biol. **23**: 993–998.

Lukowitz, W., Nickle, T.C., Meinke, D.W., Last, R.L., Conklin, P.L., and Somerville, C.R. (2001). *Arabidopsis cyt1* mutants are deficient in a *mannose-1-phosphate guanylyltransferase* and point to a requirement of N-linked glycosylation for cellulose biosynthesis. Proc. Natl. Acad. Sci. U.S.A. **98**: 2262–2267.

Miyazaki, S., Murata, T., Sakurai-Ozato, N., Kubo, M., Demura, T., Fukuda, H., and Hasebe, M. (2009). *ANXUR1* and *2*, Sister Genes to *FERONIA/SIRENE*, Are Male Factors for Coordinated Fertilization. Curr. Biol. **19**: 1327–1331.

Nickle, T.C. and Meinke, D.W. (1998). A cytokinesis-defective mutant of *Arabidopsis* (*cyt1*) characterized by embryonic lethality, incomplete cell walls, and excessive callose accumulation. Plant J. **15**: 321-332.

Orlean, P. (1990). *Dolichol phosphate mannose synthase* is required *in vivo* for glycosyl phosphatidylinositol membrane anchoring, O mannosylation, and N glycosylation of protein in *Saccharomyces cerevisiae*. Mol. Cell. Biol. **10**: 5796–5805.

Orłowski, J., Machula, K., Janik, A., Zdebska, E., and Palamarczyk, G. (2007). Dissecting the role of dolichol in cell wall assembly in the yeast mutants impaired in early glycosylation reactions. Yeast **24**: 239–252.

Pattison, R.J. and Amtmann, A. (2009). N-glycan production in the endoplasmic reticulum of plants. Trends Plant Sci. **14**: 92–99.

Rhee, S.Y., Osborne, E., Poindexter, P.D., and Somerville, C.R. (2003). Microspore separation in the *quartet 3* mutants of *Arabidopsis* is impaired by a defect in a developmentally regulated polygalacturonase required for pollen mother cell wall degradation. Plant Phys. **133**: 1170–1180.

Schiøtt, M., Romanowsky, S.M., Baekgaard, L., Jakobsen, M.K., Palmgren, M.G., and Harper, J.F. (2004). A plant plasma membrane Ca2+ pump is required for normal pollen tube growth and fertilization. Proc. Natl. Acad. Sci. U.S.A. **101**: 9502–9507.

Schneeberger, K., Ossowski, S., Lanz, C., Juul, T., Petersen, A.H., Nielsen, K.L., Jørgensen, J.-E., Weigel, D., and Andersen, S.U. (2009). SHOREmap: simultaneous mapping and mutation identification by deep sequencing. Nat Meth **6**: 550–551.

Sedbrook, J.C., Carroll, K.L., Hung, K.F., Masson, P.H., and Somerville, C.R. (2002). The *Arabidopsis SKU5* gene encodes an extracellular glycosyl phosphatidylinositol-anchored glycoprotein involved in directional root growth. Plant Cell **14**: 1635–1648.

Sheng, X., Hu, Z., Lu, H., Wang, X., Baluska, F., Samaj, J., and Lin, J. (2006). Roles of the Ubiquitin/Proteasome

Pathway in Pollen Tube Growth with Emphasis on MG132-Induced Alterations in Ultrastructure, Cytoskeleton, and Cell Wall Components. Plant Phys. **141**: 1578–1590.

Shi, S., Williams, S.A., Seppo, A., Kurniawan, H., Chen, W., Ye, Z., Marth, J.D., and Stanley, P. (2004). Inactivation of the *Mgat1* gene in oocytes impairs oogenesis, but embryos lacking complex and hybrid N-glycans develop and implant. Mol. Cell. Biol. **24**: 9920–9929.

Stone, S.L., Anderson, E.M., Mullen, R.T., and Goring, D.R. (2003). ARC1 is an E3 ubiquitin ligase and promotes the ubiquitination of proteins during the rejection of self-incompatible *Brassica* pollen. Plant Cell **15**: 885–898.

Takahashi, T., Honda, R., and Nishikawa, Y. (2000). Cloning of the human cDNA which can complement the defect of the yeast mannosyltransferase I-deficient mutant *alg1*. Glycobiology **10**: 321–327.

Till, B.J., Burtner, C., Comai, L., and Henikoff, S. (2004). Mismatch cleavage by single-strand specific nucleases. Nucleic Acids Res. **32**: 2632–2641.

Tokunaga, F., Brostrom, C., Koide, T., and Arvan, P. (2000). Endoplasmic reticulum (ER)-associated degradation of misfolded N-linked glycoproteins is suppressed upon inhibition of ER mannosidase I. J. Biol. Chem. **275**: 40757–40764.

Wassarman, P.M. and Litscher, E.S. (2008). Mammalian fertilization: the egg's multifunctional zona pellucida. Int. J. Dev. Biol. **52**: 665–676.

Wäspi, U., Misteli, B., Hasslacher, M., Jandrositz, A., Kohlwein, S.D., Schwab, H., and Dudler, R. (1998). The defense-related rice gene *Pir7b* encodes an alpha/beta hydrolase fold protein exhibiting esterase activity towards naphthol AS-esters. Eur. J. Biochem. **254**: 32–37.

Wilson, I.B., Harthill, J.E., Mullin, N.P., Ashford, D.A., and Altmann, F. (1998). Core alpha1,3-fucose is a key part of the epitope recognized by antibodies reacting against plant N-linked oligosaccharides and is present in a wide variety of plant extracts. Glycobiology **8**: 651–661.

Yu, F. et al. (2012). *FERONIA* receptor kinase pathway suppresses abscisic acid signaling in *Arabidopsis* by activating *ABI2* phosphatase. Proc. Natl. Acad. Sci. U.S.A. **109**: 14693–14698.

Zhang, M., Henquet, M., Chen, Z., Zhang, H., Zhang, Y., Ren, X., Van Der Krol, S., Gonneau, M., Bosch, D., and Gong, Z. *LEW3*, encoding a putative alpha-1,2-mannosyltransferase (*ALG11*) in N-linked glycoprotein, plays vital roles in cell-wall biosynthesis and the abiotic stress response in *Arabidopsis thaliana*. Plant J. **60**: 983–999.

Zuryn, S., Le Gras, S., Jamet, K., and Jarriault, S. (2010). A strategy for direct mapping and identification of mutations by whole-genome sequencing. Genetics **186**: 427–430.

APPENDIX

APPENDIX A1:

GENETICS

Supporting Information
http://www.genetics.org/content/suppl/2012/05/26/genetics.112.141341.DC1

SNP-Ratio Mapping (SRM): Identifying Lethal Alleles and Mutations in Complex Genetic Backgrounds by Next-Generation Sequencing

Heike Lindner, Michael T. Raissig, Christian Sailer, Hiroko Shimosato-Asano, Rémy Bruggmann, and Ueli Grossniklaus

DOI: 10.1534/genetics.112.141341

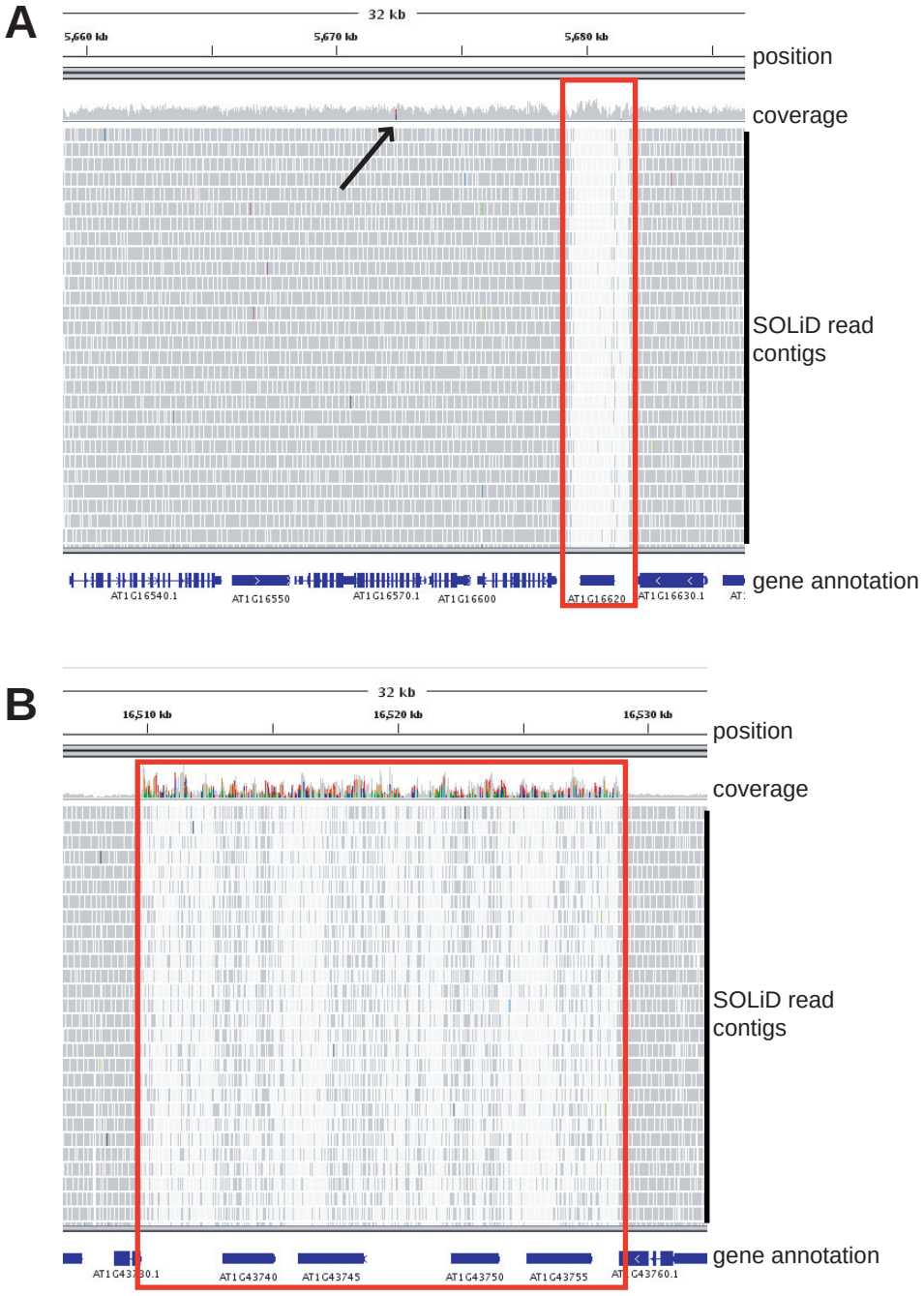

Figure S1 Integrative Genomics Viewer (www.broadinstitute.org/igv/) screenshots of mapped reads around the causative SNP in *At1g16570* (A) and in a transposable element gene region on chromosome I (B). (A) The causative SNP (arrow) is in a region with high qualitiy reads (dark grey colored contigs) but the transposable element gene *At1g16620* is only covered by low mapping quality reads (light grey colored contigs, red box). (B) The transposable element genes *At1g43740* until *At1g43755* (red box) are mainly covered by low quality reads (light grey contigs). As a consequence, the SNP density is very high, indicated as colored bars in the coverage plot on top.

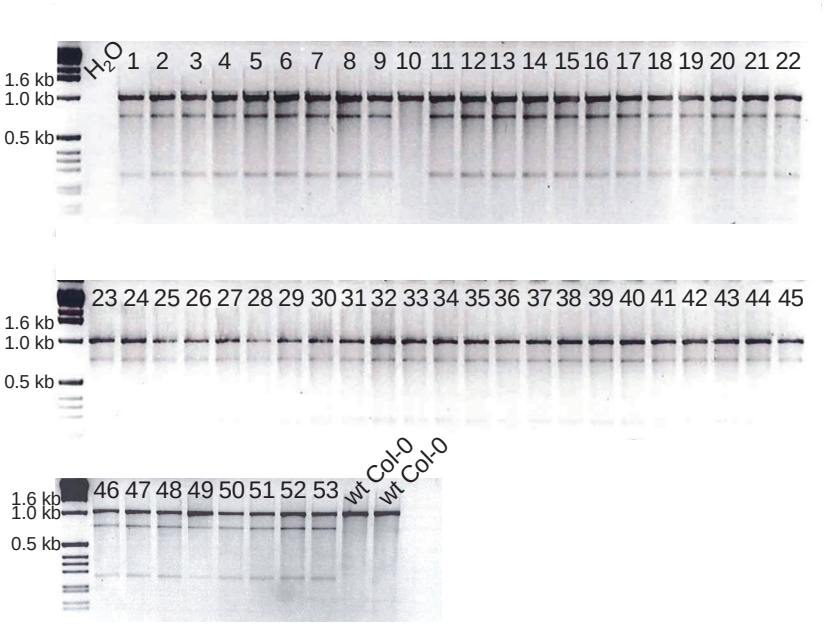

Figure S2 SURVEYOR™ nuclease digest of sequenced samples. The SNP region of the *At1g16570* gene was amplified from each of the 53 DNA samples that had been pooled for sequencing, two Col-0 controls and a H_2O control. PCR products were digested with the SURVEYOR™ nuclease cleaving single base pair mismatches in heteroduplex DNA (TILL et al. 2004). The undigested wild-type band is 989 bp, whereas any sample containing the SNP displays an undigested band at 989 bp and the digestion products at 719 bp and 217 bp. Individual 10, showing a wild type band only, was a sampling mistake (see text).

File S1

Supporting Methods

Plant material:

0.23g Col-0 seeds with the *Lat52::GFP* reporter were treated with 0.15% ethane methyl sulfonate (EMS) for 8h. M1 plants were grown as previously described (HUCK et al. 2003). For screening, siliques of 1800 M1 plants were collected 2 days after pollination and prepared for aniline blue staining of callose in pollen tubes (HUCK et al. 2003). Images were captured with a Leica DM6000B epifluorescence microscope. One line with high penetrance of the pollen tube overgrowth phenotype was backcrossed twice to the Col-0 wild-type accession, using the wild-type line (Col-0) as pollen donor.

Preparation of genomic DNA and SOLiD sequencing:

Genomic DNA was extracted with a QIAGEN DNeasy Plant Mini Kit from 53 BC2 individuals displaying the mutant phenotype. By mixing DNA in equimolar concentrations, a fragment library was produced using the SOLiD Fragment Library Construction kit (Applied Biosystems). 1 µg of genomic DNA was fragmented to a size range of 100–150 bp with the use of a Covaris S2 (Covaris) and analyzed on an Agilent Bioanalyzer 2100 DNA Chip 7500. Fragments were end-repaired using polishing enzymes and ligated with barcoded adapters in the presence of T4 DNA Ligase. The ligated DNA was size selected to approximately 200bp using AMPure beads XP (Agencourt). This product was nick translated and amplified by PCR with primers complementary to the sequence of the SOLiD 4 adaptors. After quality control on an Agilent Bioanalyzer DNA Chip 1000 the libraries were pooled and used for e-PCR based on a concentration of 0.5pM. Approximately one half of a SOLiD 4 sequencing slide (Applied Biosystems) was used.

Sequence data analysis:

The paired end (50x35bp) sequence reads from SOLiD platform were mapped to the *Arabidopsis thaliana* genome assembly TAIR version 10 (ftp.arabidopsis.org/home/tair/Sequences/whole_chromosomes/) using Bioscope version 1.3.1 (default settings) from Applied Biosystems (Life Technologies, Carlsbad, CA, USA). After mapping, the SNPs were called by using the DiBayes algorithm (Life Technologies, Carlsbad, CA, USA) with high and medium stringency settings. The obtained SNPs were classified into intronic, intergenic, coding (synonymous and non-synonymous amino acid substitutions) and splice-site variants with a custom software pipeline.

Statistical identification of causative SNP candidates

The results of the sequence data analysis were tabulated in the following structure: chromosome, position on the chromosome in bp, number of reference counts (reads), number of variant counts, zygosity (either “homozygous” or “heterozygous”). The table in this structure was loaded into R as tab-delimitated text file. To identify the 1:1 segregating

SNPs the dataset was filtered in 3 steps: First, all homozygous reads were removed. Second, all reads with a coverage less than 50-fold were removed (see Table S1). Third, F~Binomial (H_0: Π = 0.5; H_A: Π ≠ 0.5) was calculated for each SNP. All SNPs with α < 0.05 and α > 0.95 were removed. This resulted in a list of 1:1 segregating SNPs (n=118).

SNPs neighboring the causative SNP are genetically linked and thus follow an expected pattern of co-segregation. The expected pattern of co-segregation of two neighboring SNPs on each side of each 1:1 segregating SNP was calculated. This was done with the complete dataset of heterozygous SNP without filtering for low and high coverage in 3 steps:

- First, the genetic distance (in cM) between the SNPs was calculated by dividing the physical distance (bp) between the SNPs by the mean physical distance per cM (357,042 bp/cM). The mean genetic distance was calculated using the physical map and the most recent, sex-specific genetic map of *Arabidopsis thaliana* (TAIR version 10 (www.arabidopsis.org); GIRAUT et al. 2011). In *Arabidopsis*, dramatic differences between male and female meiosis have been found (genetic map length: male=575cM, female=332cM) and since we crossed the mutants always as females, the female genetic map length was used here. However, we obtained the same results using the overall mean genetic distance of 1cM per 198,556 bp (i.e. combined male and female recombination rates: genetic map length=597cM; LISTER AND DEAN, 1993). Since the mean physical distance in bp per cM can be estimated for most organisms used in genetic research, this procedure is generally applicable. If more accurate combined genetic and physical maps are available, local recombination rates could be integrated into this procedure.
- Second, the expected number of variant reads for a 1:1 class SNP was calculated by dividing the number of total reads (coverage) per SNP by two (diploid organism).
- Third, the expected number of variant reads for each neighboring and co-segregating SNP was calculated according to the genetic distance between the SNPs based on the mean physical distance per cM. This was done for each of the two neighboring SNPs on each side of the 1:1 segregating SNP.

To test which SNPs differ from the expected pattern of co-segregation, a χ^2 goodness of fit test was applied. The calculated expected number of variant reads was subtracted from the observed number of variant reads and this value was squared, followed by division with the calculated expected number of variant reads. This was done for each of the 2 neighboring SNPs on each side of the 1:1 segregating SNP, giving 5 χ^2-values, which were summed up (for α < 0.05 and df = 4, χ^2 = 9.49; en.wikipedia.org/wiki/Chi-squared_distribution). All SNPs with a χ^2 > 9.49 were discarded, because they differed significantly from the genetic expectations.

The R-script is available as an extra file (File S2) and can be downloaded at http:/

Confirmation of mutation:

The SNP region of the *At1g16570* gene was amplified from each of the 53 DNA samples, that had been pooled for sequencing, two Col-0 controls and a H_2O control with the primers 5`-CTTTTGATCTTGCAGCCACA-3`and 5`-

ACGTGCAGCGTTTGTTGTAG-3 and ExTaq Polymerase (TaKaRa) in a standard PCR reaction. PCR products were digested with the SURVEYOR nuclease cleaving single base pair mismatches in heteroduplex DNA (TILL et al. 2004). The undigested wild-type band was at 989 bp, whereas any sample containing the SNP displayed an undigested band at 989 bp and the digestion products at 719 bp and 217 bp. In addition an independent T-DNA line disrupting the identified gene was analyzed (SAIL_400_A01) and showed the same pollen tube overgrowth phenotype as the EMS allele (Figure 2).

Supporting references:

HUCK, N., J. M. MOORE, M. FEDERER, U. GROSSNIKLAUS, 2003 The Arabidopsis mutant feronia disrupts the female gametophytic control of pollen tube reception. Development **130:** 2149-2159

GIRAUT, L., M. FALQUE, J. DROUAUD, L. PEREIRA, O.C. MARTIN, C. MÉZARD, 2011 Genome-wide crossover distribution in Arabidopsis thaliana meiosis reveals sex-specific patterns along chromosomes. Plos Genet. **7:** e1002354

LISTER, C. AND C. DEAN, 1993 Recombinant inbred lines for mapping RFLP and phenotypic markers in Arabidopsis thaliana. Plant J. **4:** 745-750.

R DEVELOPMENTAL CORE TEAM, R: A language and environment for statistical computing. Vienna.

TILL, B. J., C. BURTNER, L. COMAI AND S. HENIKOFF, 2004 Mismatch cleavage by single-strand specific nucleases. Nucleic Acids Res. **32:** 2632-2641

Table S1 Simulation of a binomial distribution to determine the minimal sequencing coverage needed to differentiate a 1:1 from a 3:1 segregation of SNPs.

n	x	α F(1:1)	β 1-F(1:3)
20	5	0.0207	0.3828
30	10	0.0494	0.1057
40	14	0.0403	0.0544
50	18	0.0325	0.0287
60	23	0.0462	0.0075

Simulation of a binomial distribution to determine the minimal sequencing coverage needed to differentiate a 1:1 from a 3:1 segregation of SNPs, with 1st (α) and 2nd class (β) mistakes being <0.05. Π – values for H_0: Π = 0.5; H_A: Π= 0.25. The optimum is found at a sample size of 50. α = F~Binomial; β = 1-F~Binomial; n = sequence coverage; x = highest occurence of variant SNP to reject H0.

Table S2 Overview of the SNP data after mapping the reads to the *Arabidopsis thaliana* genome

Total SNPs	**2337**
homozygous	521
heterozygous	1816
non-synonymous	122
synonymous	69
mean coverage of heterozygous SNPs	**57.3**

SNPs were called by using the DiBayes algorithm with high stringency settings and analyzed with a custom software pipeline.

Table S3 SNP data of the resequenced EMS-mutagenized genome of *tun-1* (Col-0 accession).

All data presented has been obtained using the DiBayes algorithm for SNP calling with high stringency setting. The data is presented in a separate Excel file and available for download at http://www.genetics.org/content/suppl/2012/05/26/genetics.112.141341.DC1.

Table S4 Overview of the ten remaining 1:1 class candidate SNPs after χ^2 goodness of fit test for an expected pattern of co-segregation

chromosome	position	coverage	ratio	χ^2	cM (covered by the linkage group)
1	4891806	54	0.44	9.27	6.831
1	***5672441***	***68***	***0.49***	***7.29***	***4.673***
1	15198294	84	0.42	4.47	0.009
1	17143759	78	0.55	9.42	0.001
2	4905462	74	0.46	4.86	0.011
2	4905990	55	0.42	4.79	0.013
3	13191694	65	0.42	8.67	0.004
3	13191833	71	0.48	8.81	0.008
4	4003316	94	0.52	7.92	0.004
5	12012845	58	0.53	5.21	0.001

To test which SNPs differ from the expected pattern of co-segregation in a linkage group (five neighboring SNPs), a χ^2 goodness of fit test was applied (for $\alpha < 0.05$ and df = 4, $\chi^2 = 9.49$; en.wikipedia.org/wiki/Chi-squared_distribution). All SNPs with a $\chi^2 > 9.49$ were discarded (n=108), because they differ significantly from the genetic expectations, whereas all 10 SNPs with a $\chi^2 < 9.49$ have been kept and are shown in the above table. The line in bold and italic corresponds to the *tun-1* SNP.

APPENDIX A2: Supplemental Information to Chapter 2 „*TURAN* and *EVAN* Mediate Pollen Tube Reception in the Synergid Cells but Play Distinct Roles in the Male Gametophyte“

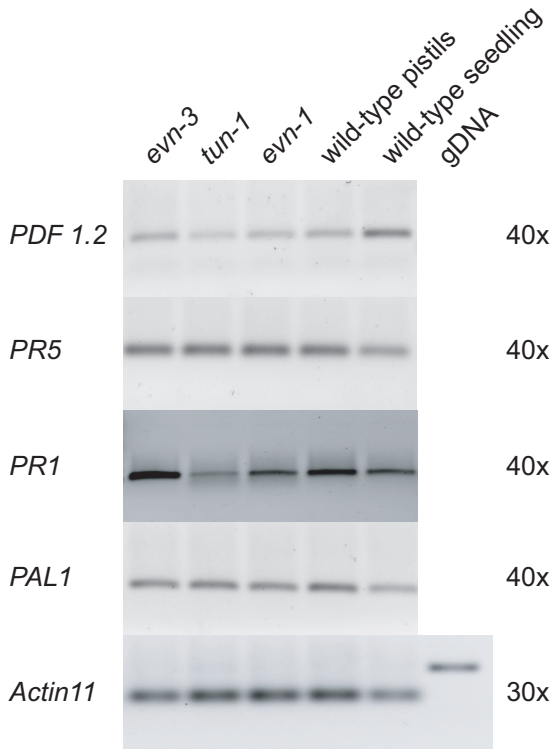

Figure S1. Callose deposition in *tun* and *evn* ovules is not due to upregulated plant defense response.
RT-PCR of *PLANT DEFENSIN1.2* (*PDF1.2*), involved in jasmonate-dependent plant defense response, *PATHOGENESIS RELATED PROTEIN1* (*PR1*), involved in systemic acquired resistance, *PR5* and *PHENYLALANINE AMMONIA-LYASE1* (*PAL1*) involved in salicylic acid response, in *evn-1/EVN, tun-1/TUN, evn-3/EVN* and wild-type pistils 2DAE and in a seedling control. Numbers on the right indicate number of amplification cycles. *ACTIN11* serves as expression control.

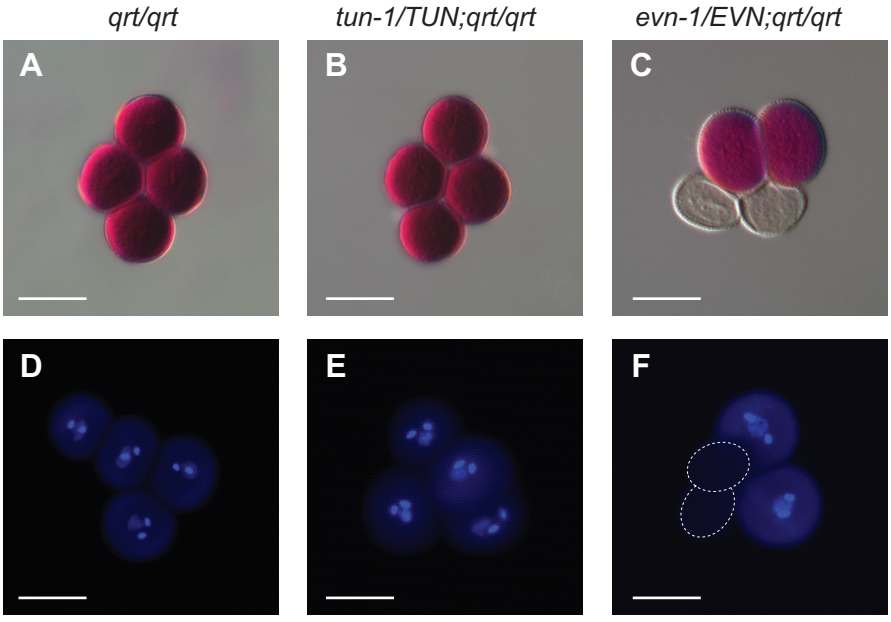

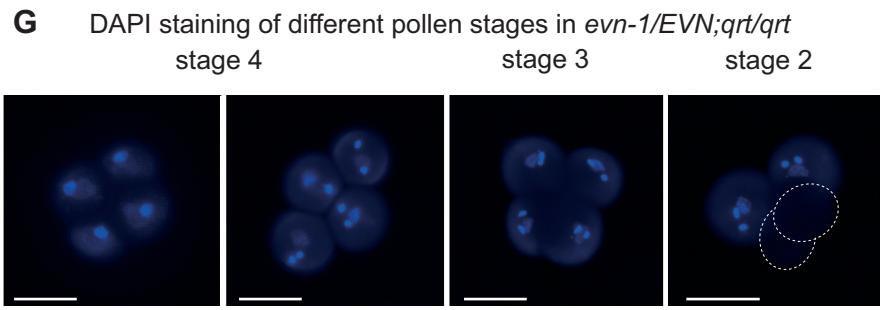

Figure S2. Alexander staining and DAPI staining reveals different pollen phenotypes in *tun* and *evn* mutant pollen grains.
(A) Alexander staining of mature *qrt/qrt* control pollen. **(B)** Alexander staining of mature *tun-1/TUN;qrt/qrt* mutant pollen tetrads. **(C)** Alexander staining of mature *evn-1/EVN;qrt/qrt* mutant pollen tetrads. **(D)** DAPI staining of DNA in mature *qrt/qrt* control tetrads. **(E)** DAPI staining of DNA in mature *tun-1/TUN;qrt/qrt* mutant tetrads. **(F)** DAPI staining of DNA in mature *evn-1/EVN;qrt/qrt* mutant tetrads. **(G)** DAPI staining of DNA in stage 4 (bi-cellular/early tri-cellular pollen), in stage 3 (tri-cellular pollen), and in stage 2 (late tri-cellular/early mature pollen) *evn-1/EVN;qrt/qrt* mutant tetrads. Scale bars: 20µm.

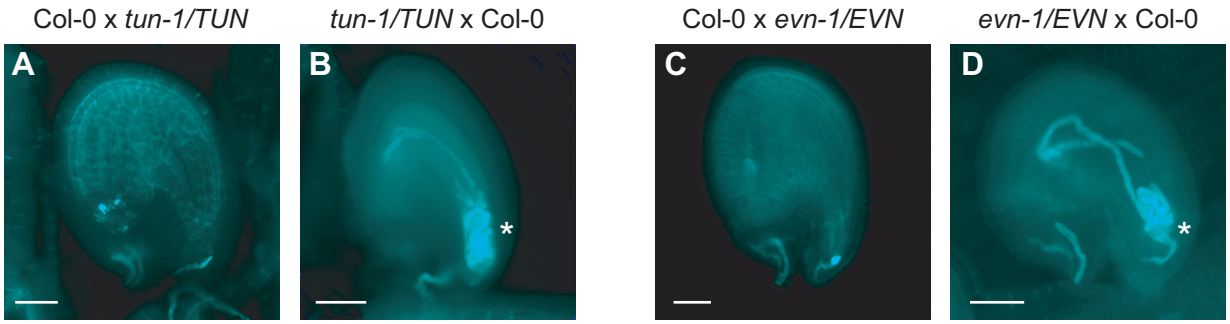

Figure S3. Reciprocal crosses reveal the PT overgrowth phenotype to be caused by a female gametophytic defect.

(A) to **(D)** Aniline blue staining of callose in PT- and ovule cell walls 2DAP. **(A)** Col-0 ovule pollinated with *tun-1/TUN* pollen. **(B)** *tun*-1 mutant ovule pollinated with Col-0 pollen. **(C)** Col-0 ovule pollinated with *evn-1/EVN* pollen. **(D)** *evn*-1 mutant ovule pollinated with Col-0 pollen. Asterisks indicate PT overgrowth phenotype. Scale bars: 20μm.

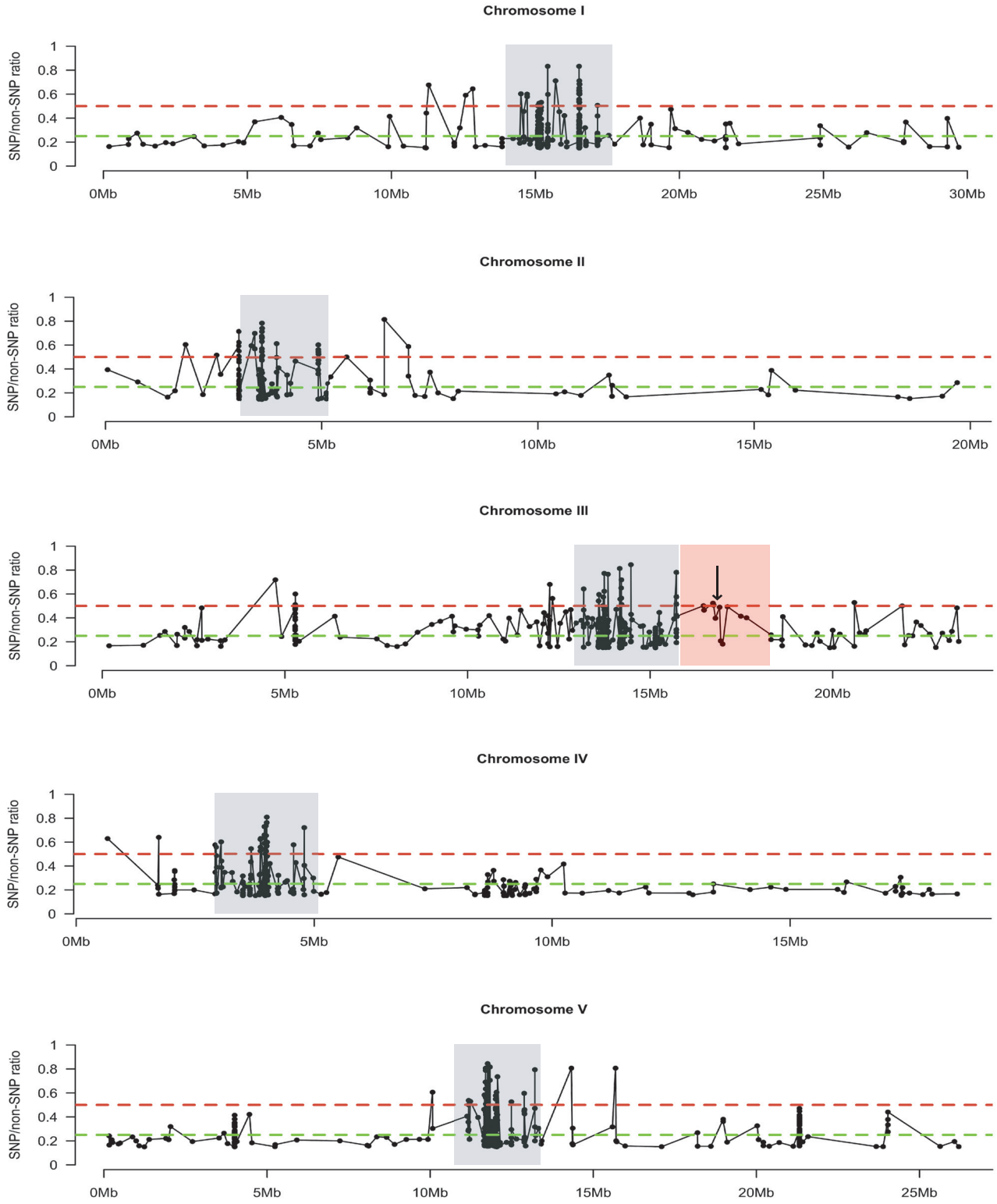

Figure S4. The causative EMS-mutation in *evn-1* localizes to the lower arm of chromosome III and disrupts the gene *At3g45040*.

Ratios of heterozygous SNPs plotted against their chromosomal position. The red dashed line indicates the ratio at 0.5, where the causative SNP is expected. The green dashed line marks the ratio at 0.25, where the unlinked SNPs should locate. The red box indicates the linked and selected region on the lower arm of chromosome III around *At3g45040*. Grey boxes mark centromeric regions. Arrow indicates causative SNP with a segregation ratio of 0.5 in a pool of mutant individuals. Segregation ratio was reliable due to the high sequence coverage of 130 reads.

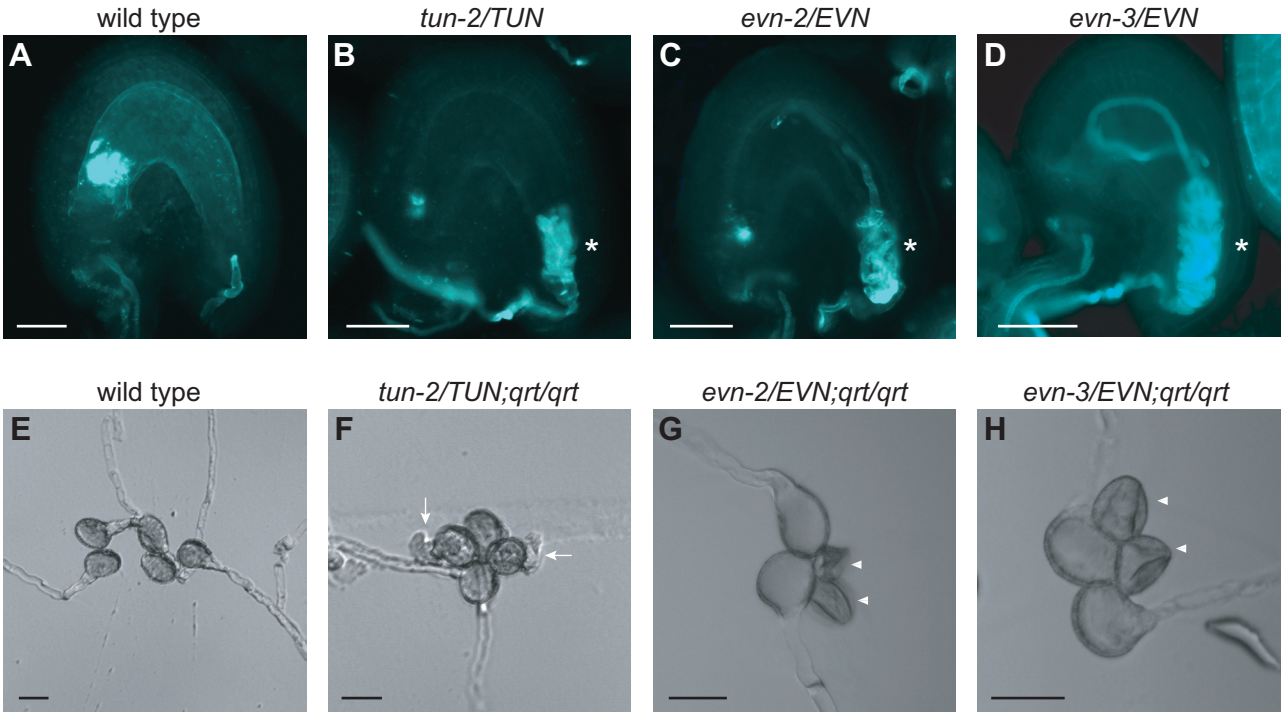

Figure S5. Additional alleles confirm female and male gametophytic phenotypes.

(A) to **(D)** Aniline blue staining of callose in PT cell walls 2 DAP. **(A)** Normal PT reception in a wild-type ovule. **(B)** PT overgrowth in a *tun-2* mutant ovule. **(C)** PT overgrowth in an *evn-2* mutant ovule. **(D)** PT overgrowth in an *evn-3* mutant ovule. Asterisks mark PT overgrowth phenotype.

(E) to **(H)** *In vitro* pollen germination analysis. **(E)** Normal pollen germination of wild-type pollen. **(F)** PT burst phenotype of *tun-2/TUN;qrt/qrt* pollen. Arrows indicate PT bursting. **(G)** Degenerated pollen phenotype in *evn-2/EVN;qrt/qrt*. **(H)** Degenerated pollen phenotype in *evn-3/EVN;qrt/qrt*. Arrowheads indicate degenerated pollen. Scale bars: 20μm.

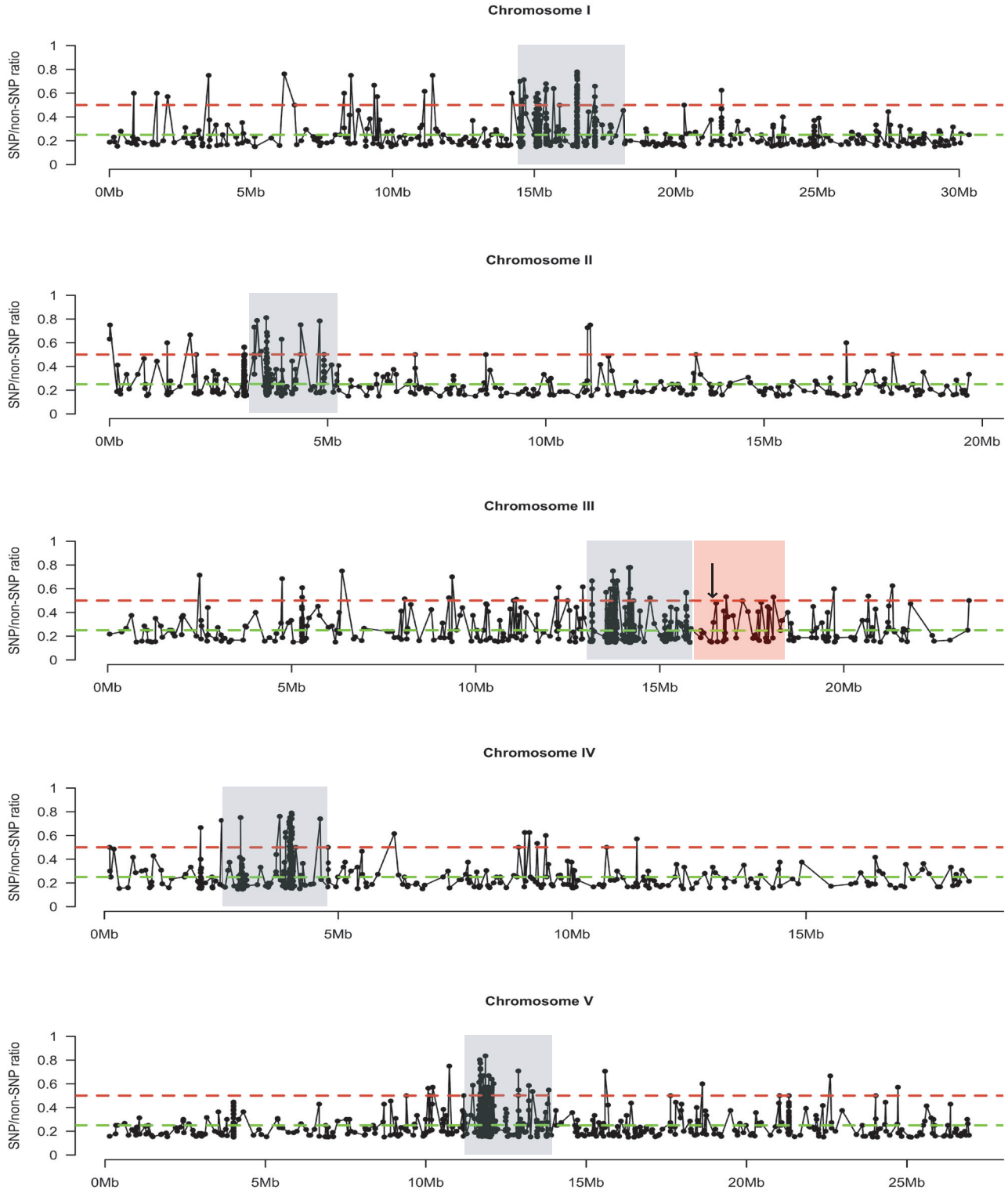

Figure S6. The causative EMS-mutation in *evn-3* localizes to the lower arm of chromosome III and disrupts the gene *At3g45040.*

Ratios of heterozygous SNPs plotted against their chromosomal position. The red dashed line indicates the ratio at 0.5, where the causative SNP is expected. The green dashed line marks the ratio at 0.25, where the unlinked SNPs should locate. The red box indicates the linked and selected region on the lower arm of chromosome III around *At3g45040*. Grey boxes mark centromeric regions. Arrow indicates causative SNP with a segregation ratio of 0.3 in a pool of mutant individuals. The too low segregation ratio was due to poor sequence coverage (see Material and Methods).

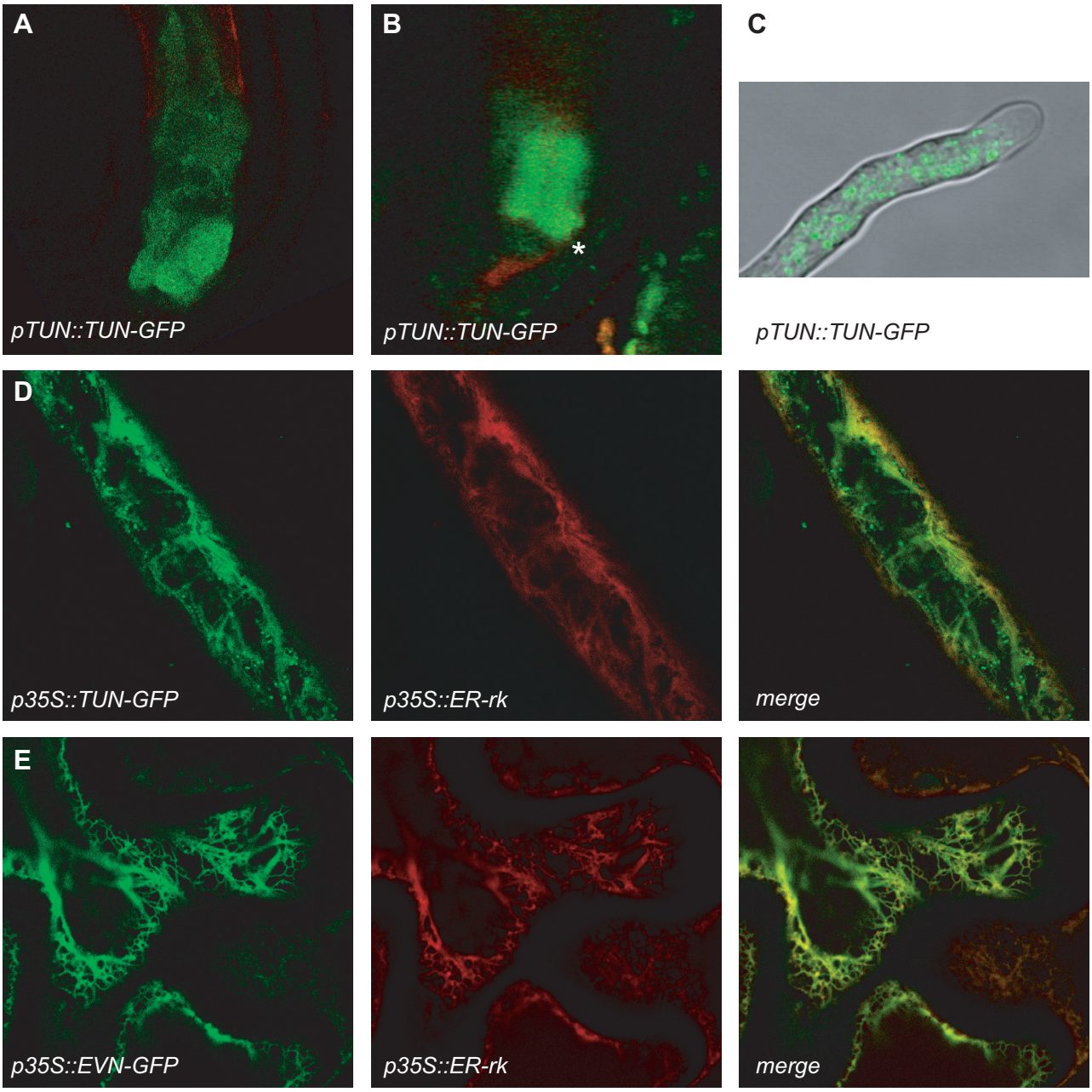

Figure S7. TUN-GFP and EVN-GFP translational fusions locate to the ER.
(A) to **(E)** Confocal microscope analysis of fluorescent labeled proteins. **(A)** *pTUN::TUN-GFP* expression in synergid cells 2DAE. **(B)** *pTUN::TUN-GFP* expression 8 hours after pollination with dsRed-labeled pollen. Asterisk marks site of pollen tube entry. **(C)** *pTUN::TUN-GFP* expression in a PT. **(D)** *p35S::TUN-GFP* (left panel) and *p35S::ER-rk* (middle panel) in transiently transformed onion epidermis cells and merge of both channels (right panel). **(E)** *p35S::EVN-GFP* (left panel) and *p35S::ER-rk* (middle panel) in transiently transformed tobacco epidermis cells and merge of both channels (right panel).

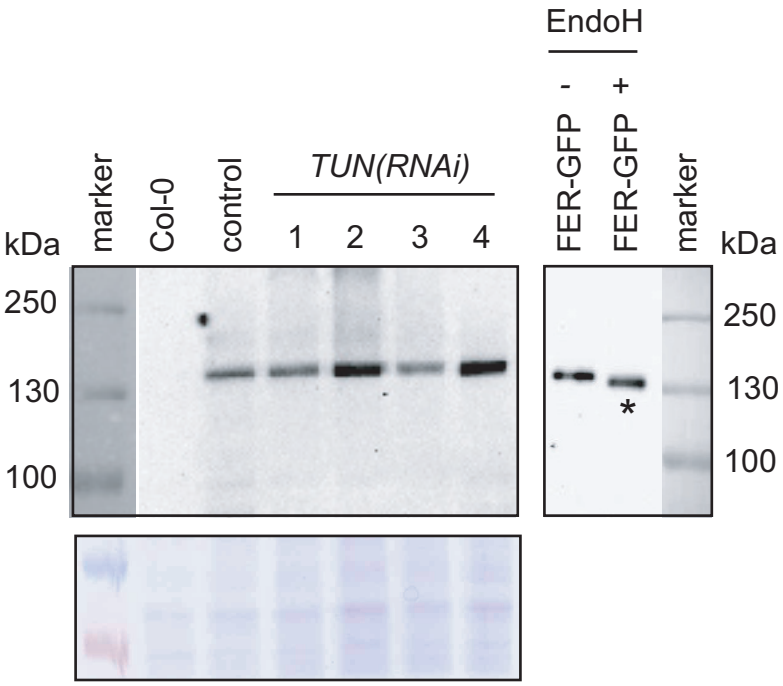

Figure S8. FER-GFP in *RNAi(TUN)* lines is not deglycosylated.
Western blot analysis of FER-GFP protein from control and *TUN(RNAi)* seedlings using an antibody against GFP. Coomassie-stained SDS-PAGE (bottom) serves as control for loaded protein amounts. Asterisk marks completely N-deglycosylated FER-GFP after treatment of the protein extract with the deglycosylase EndoH.

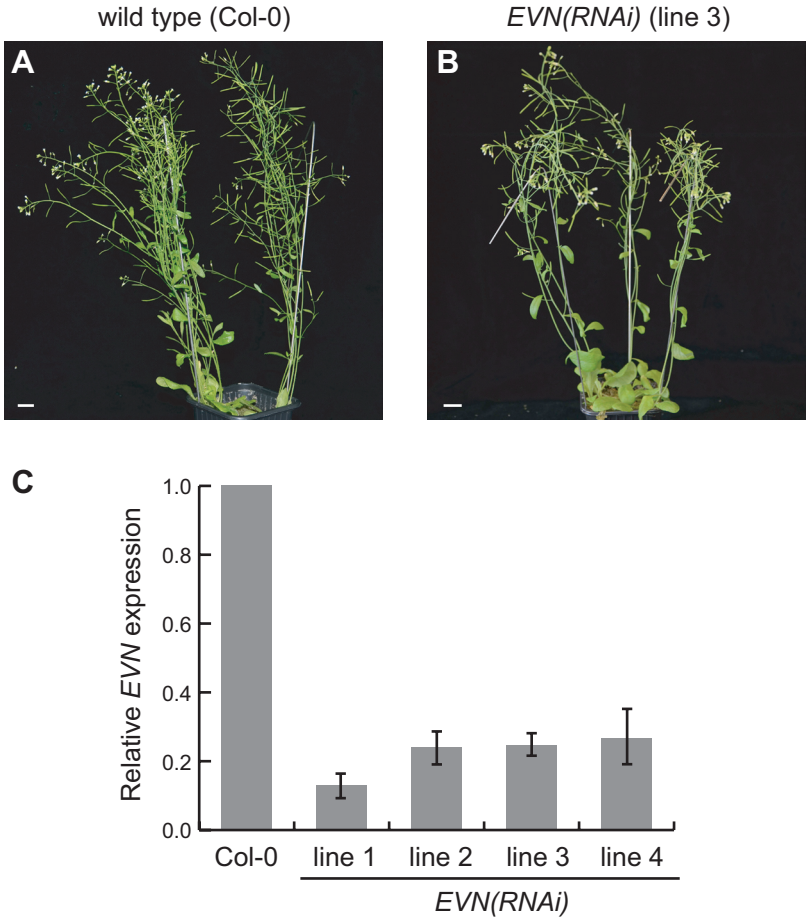

Figure S9. *EVN(RNAi)* do not show aberrant vegetative growth.
(A) Adult wild-type plants. **(B)** Adult *EVN(RNAi)* plants with downregulated *EVN* expression (line 3). **(C)** qRT-PCR analysis of *EVN* expression in four independent *RNAi* lines.

A. Surveyor assay for *AT3G45040* in the *evn-1* SRM mutant sequencing population

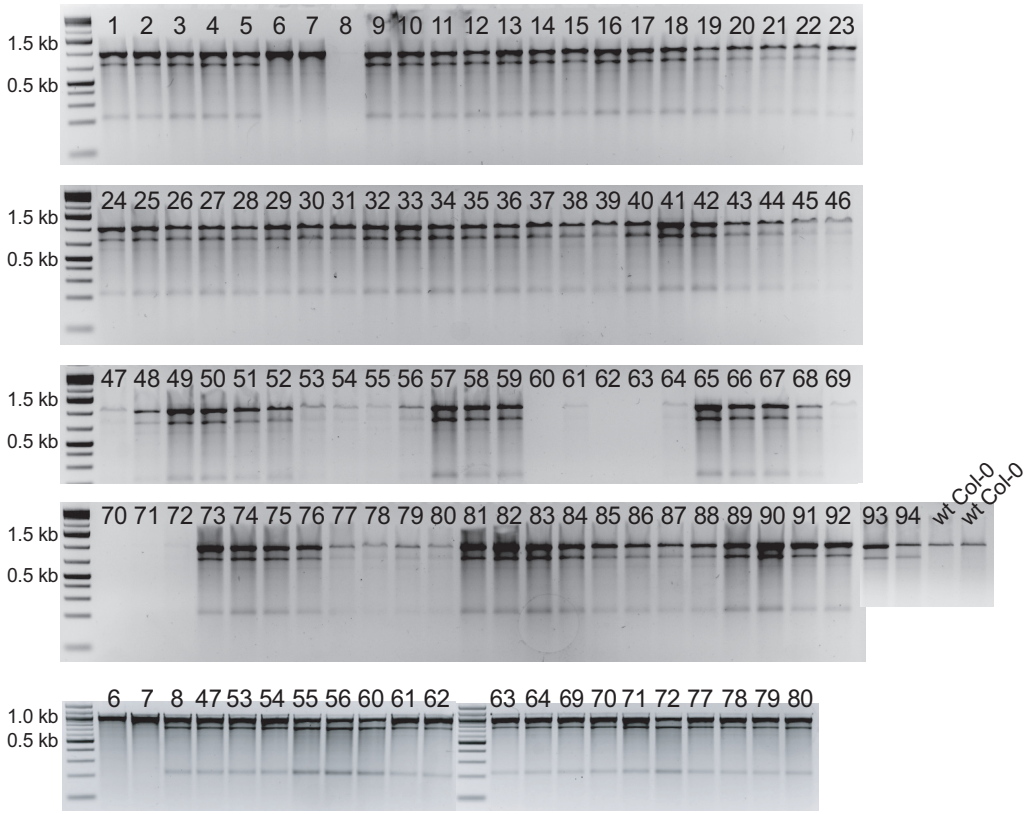

B. Surveyor assay for *AT3G45040* in the *evn-3* SRM mutant sequencing population

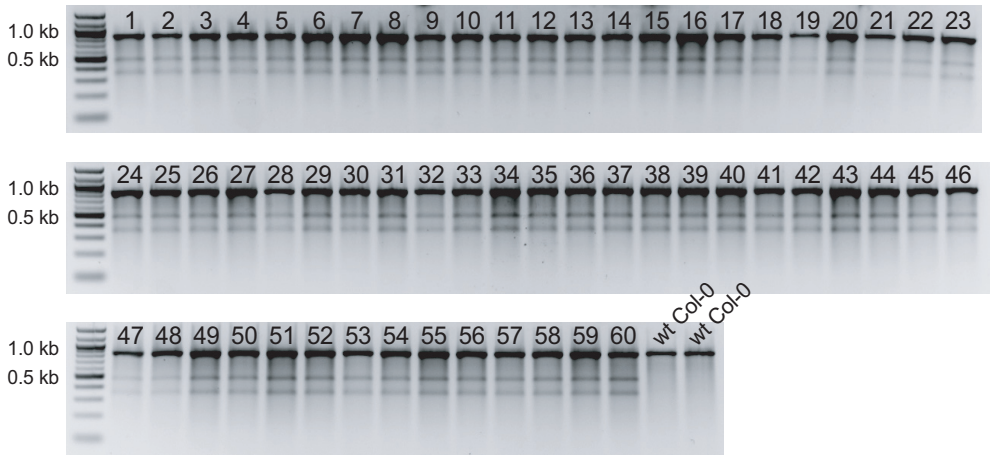

Figure S10. Surveyor nuclease digest of sequenced samples of *evn-1* and *evn-3*.
The SNP region of the *At3g45040* gene was amplified from each of the 94 and 60 DNA samples that had been pooled for sequencing from *evn-1* and *evn-3*, respectively, and two Col-0 controls. PCR products were digested with the SURVEYOR™ nuclease cleaving single base pair mismatches in heteroduplex DNA (Till et al., 2004). In *evn-1*, the undigested wild-type band is 1000 bp, whereas any sample containing the SNP displays an undigested band at 1000 bp and two digestion products at around 800 bp and around 200 bp. Individuals 6 and 7, showing a wild-type band only, were proven to be sampling mistakes. In *evn-3*, the undigested wild-type band is 900 bp, whereas any sample containing the SNP displays an undigested band at 900 bp and two digestion products at around 500 bp and around 400 bp. Results for *tun-1* have been published previously (Lindner et al., 2012b).

Table S1. SNP data of the resequenced EMS-mutagenized genome of *evn-1* (Col-0 accession)
All data presented has been obtained using the DiBayes algorithm for SNP calling with the highest stringency setting (Lindner et al., 2012). The data is presented in a separate Excel file available for download at https://www.dropbox.com/sh/755in1zt9dgspv2/4puwKtgfVP?n=195652504

Table S2. SNP data of the resequenced EMS-mutagenized genome of *evn-3* (Col-0 accession)
All data presented has been obtained using the DiBayes algorithm for SNP calling with the highest stringency setting (Lindner et al., 2012). The data is presented in a separate Excel file available for download at https://www.dropbox.com/sh/755in1zt9dgspv2/4puwKtgfVP?n=195652504

Table S3. Primers amplifying *evn-3*-linked genes carrying a non-causative EMS-SNPs for Surveyor analysis.

At3G56230 (ratio 0.43):
Forward 5'-CTTGGAGCGTTATGGCGTAT-3'
Reverse 5'-TGCACCACAATGCCATCTAT-3'

At3G59020 (ratio 0.47):
Forward 5'-GCCATAAGCTGCACATGAGA-3'
Reverse 5'-GGTTTGTGCCAAAACTTGGT-3'

AT3G58410 (ratio 0.24):
Forward 5'-CTGATCAAACCAGCGATGTG-3'
Reverse 5'-AAGTCACGAGGGACAAATGC-3'

At3G51570 (ratio 0.19):
Forward 5'-GCTCACATTGTCCTCAGCAA-3'
Reverse 5'-GATTTGGTGGAAGCTTTGGA-3'

At3G52320 (ratio 0.31) :
Forward 5'-TGCGTGACCAGTTCTCAAAG-3'
Reverse 5'-CTTGTGAGAGCCGCAACATA-3'

At3G55690 (ratio 0.54):
Forward 5'-GGGCAGGAATTACGGATTTT-3'
Reverse 5'-TATTTCCGGGGAAGGAAAAC-3'

At3G52660 (ratio 0.16):
Forward 5'-CCTCCACATGGTTCAGAGGT-3'
Reverse 5'-AGCCGAAGAATCTCCTCCTC-3'

At3G55640 (ratio 0.33):
Forward 5'-ACGAGGCTTCACGGATATTG-3'
Reverse 5'-CAAGAAAGCAAAAGGCCAAC-3'

At3G57290 (ratio 0.32):
Forward 5'-GGTTTAACGGCGATGAAAAA-3'
Reverse 5'-CAAGAGCGTCAGCTTTACCC-3'

At3G57310 (ratio 0.27):
Forward 5'-TGATGCAGATTTCATTGTTGG-3'
Reverse 5'-TCTTTGAATTTCTGCAAGTCTGA-3'

At3G43180 (ratio 0.16):
Forward 5'-AAAGCGATGTGGGAACAAAG-3'
Reverse 5'-GCTCAAGCTGTTCCTCTTGC-3'

At3G45630 (ratio 0.41):
Forward 5'-AACCATTTTGACTGCCAAGC-3'
Reverse 5'-GTTGCATGGATGGGGATAAC-3'

At3G45850 (ratio 0.37):
Forward 5'-TAGCTTTCTTCCCGCTCTCA-3'
Reverse 5'-TTCGAAACATTCGCATGAAC-3'

At3G48090 (ratio 0.5):
Forward 5'-ATCGCTGGCTTGAGAAGTGT-3'
Reverse 5'-ACAAGGAAGAAGCAGGAGCA-3'

APPENDIX A3: Supplemental Information to Chapter 4 „Functional Analysis of Related CrRLK1L Proteins in Pollen Tube Reception“

Supplemental Table 1: Primers used to generate complementation constructs

Primer name	Sequence
SKpromFER-attB1	ggggacaagtttgtacaaaaaagcaggctggtaagcttcgatttaagcg
promFER-R	cgatcaagagcacttctccg
FERIC-F	gctattattgcaggcgcagc
attB2FERIC-R	ggggaccactttgtacaagaaagctgggtacgtccctttggattcatgatc
FEREC-R	cgtattgcttttcgatttcct
ANX1FER-F	cggagaagtgctcttgatcgatgagcgggaaaactcggattc
ANX1FER-R	actggctgcgcctgcaataatagcgtgtctcttttcgttcttg
FERANX1-F	aggaaatcgaaaagcaatacggctttcatcattggttcggc
attB2ANX1-R	ggggaccactttgtacaagaaagctgggttcgtcctttgggatttacaatc
HERK1FER-F	cggagaagtgctcttgatcgatgggtattgaaaagtttgaaac
HERK1FER-R	actggctgcgcctgcaataatagcccgagattactcttactgc
FERHERK1-F	aggaaatcgaaaagcaatacgttgattgtaggttcagccat
attB2HERK1-R	ggggaccactttgtacaagaaagctgggttcttccttcagatttcaccag
SKFER-17FattB1	aaaaagcaggcttcggtaagcttcgatttaagcg
SKFER-15RattB2	agaaagctgggtgaccaccaacaccaagcacc

Supplemental Table 2: Primer combinations used for fusion constructs

Construct	**Primers**
pFER::ANX1-GFP;	SKpromFER-attB1, promFER-R, ANX1FER-F, attB2ANX1-R
pFER::HERK1-GFP;	SKpromFER-attB1, promFER-R, HERK1FER-F, attB2HERK1-R
pFER::ANX1ecFERic-GFP;	SKpromFER-attB1, promFER-R, ANX1FER-F, ANX1FER-R, FERIC-F, attB2FERIC-R
pFER::FERecANX1ic-GFP;	SKpromFER-attB1, FEREC-R, FERANX1-F, attB2ANX1-R
***pFER::FERecHERK1ic-GFP*;**	SKpromFER-attB1, FEREC-R, FERHERK1-F, attB2HERK1-R
pFER::FERnoKinase-GFP;	SKFER-17FattB1, SKFER-15RattB2

Table 3: Primers used for site-directed mutagenesis

SKFER-5F	tcacgaattccgggtgcttggtgttgg
SKFER-6R	tcacggatccacagaacatctcccattg
SKferS695DFor	gtagacacagttgtgaaaggaag
SKferS695DRev	tcacaactgtgtctacgtgtgtgtggtctagtg
SKferS695Afor	gtagccacagttgtgaaaggaag
SKferS695Arev	tcacaactgtggctacgtgtgtgtggtctagtg
SKferT696Dfor	gtaagcgatgttgtgaaaggaag
SKferT696Drev	tcacaacatcgcttacgtgtgtgtggtctagtg
SKferT696Afor	gtaagcgcagttgtgaaaggaag
SKferT696Arev	tcacaactgcgcttacgtgtgtgtggtctagtg
SKferSTDDfor	gtagacgatgttgtgaaaggaag
SKferSTDDrev	tcacaacatcgtctacgtgtgtgtggtctagtg
SKferSTAAfor	gtagccgcagttgtgaaaggaag
SKferSTAArev	tcacaactgcggctacgtgtgtgtggtctagtg
SKferS701Dfor	gagatttcggttatcttgacccag
SKferS701Drev	gataaccgaaatctcctttcacaactgtgcttac
SKferS701Afor	gagctttcggttatcttgacccag
SKferS701Arev	gataaccgaaagctcctttcacaactgtgcttac
SKferSTSDDDfor	gttgtgaaaggagatttcgg
SKferSTSDDDrev	atctcctttcacaacatcgtctacg
SKferSTSAAAfor	gttgtgaaaggagctttcgg
SKferSTSAAArev	agctcctttcacaactgcggctacg

APPENDIX A4: Vector maps (of constructs used in Chapter 2)

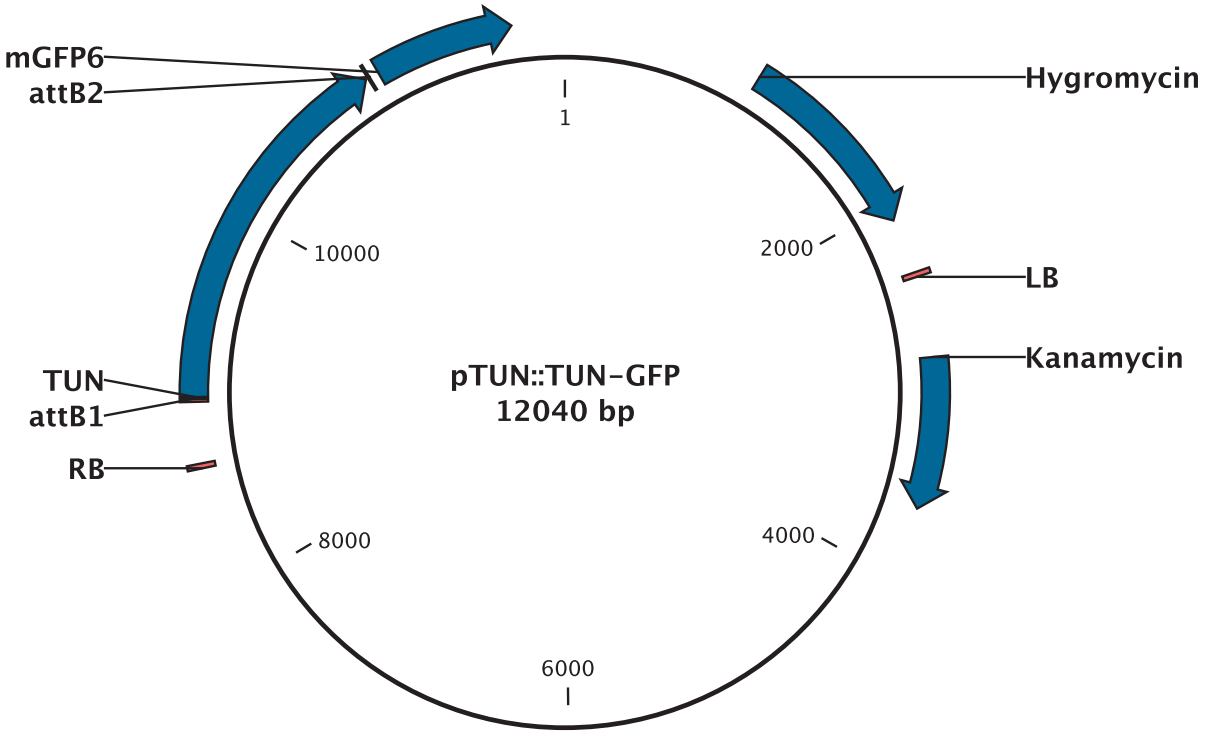

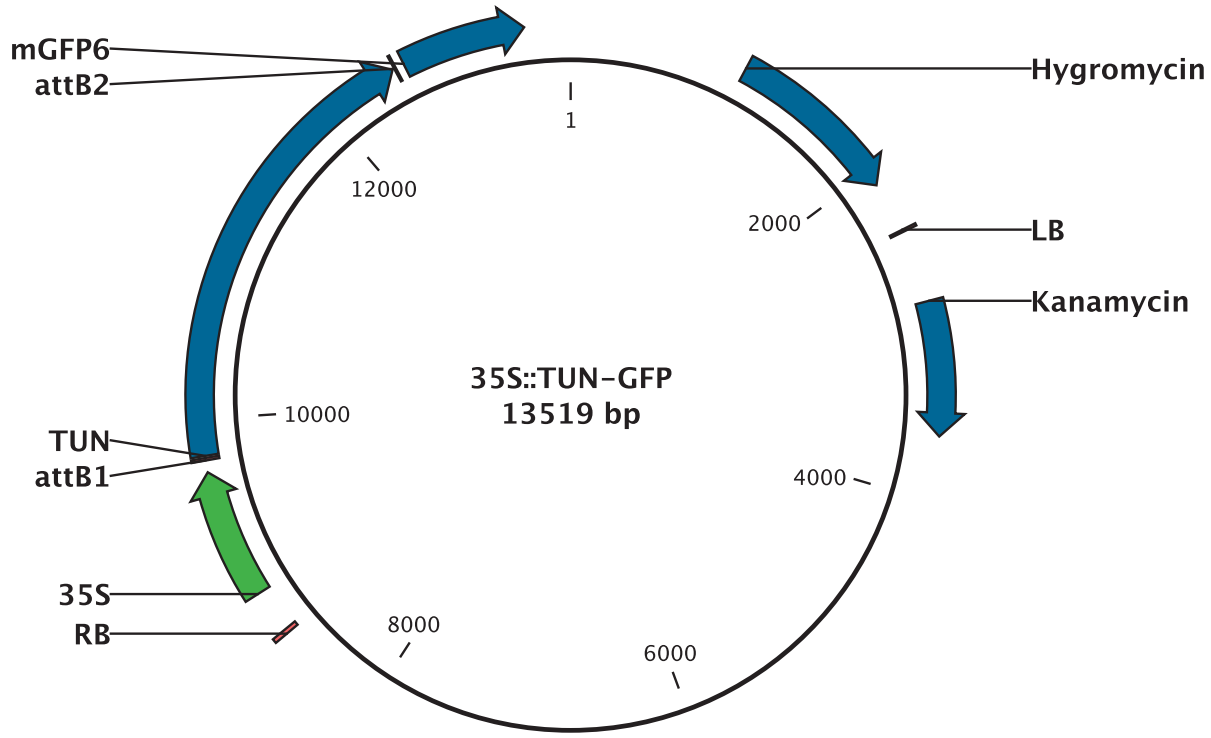

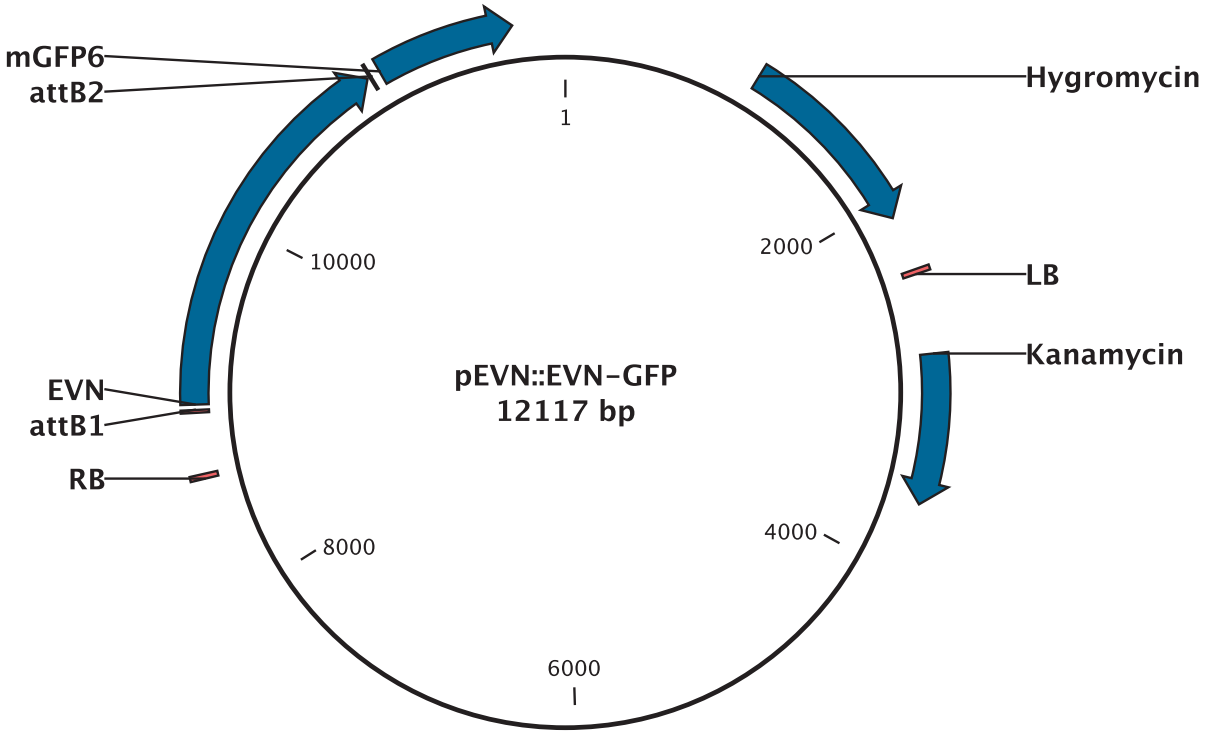
mGFP6
attB2
Hygromycin
1
2000
LB
10000
Kanamycin
pEVN::EVN-GFP
12117 bp
EVN
attB1
RB
8000
4000
6000

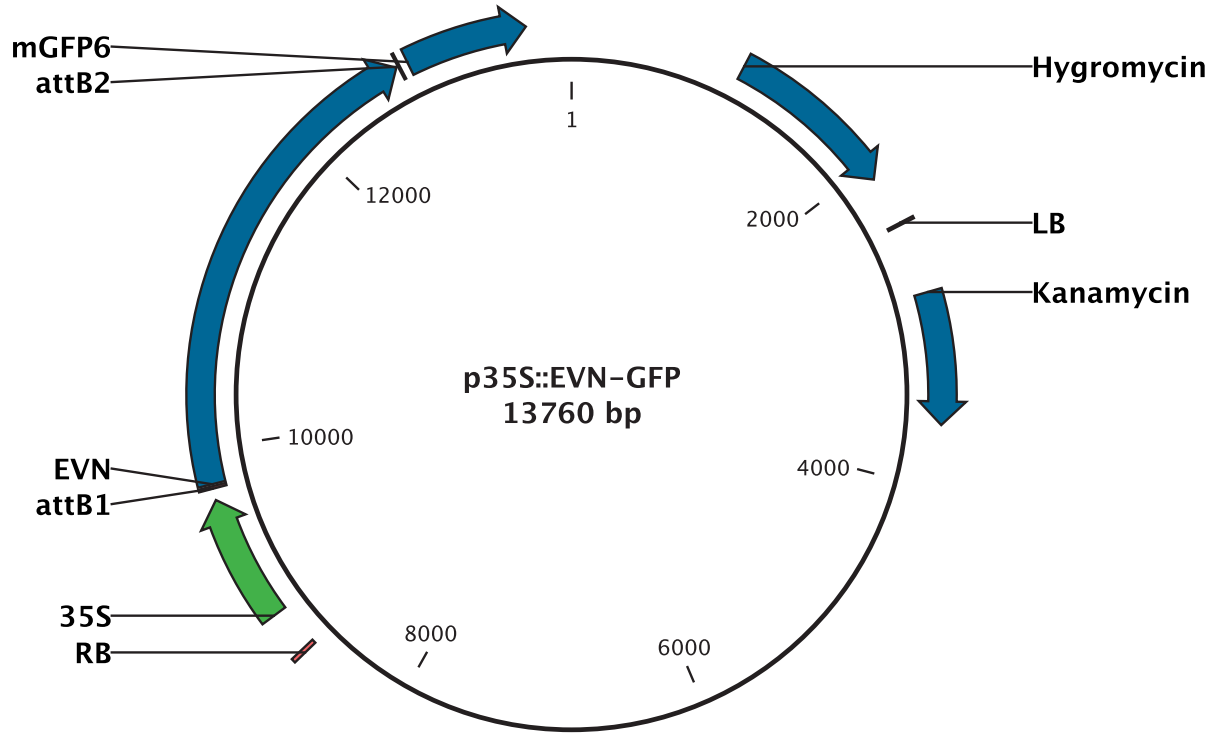
mGFP6
attB2
Hygromycin
1
12000
2000
LB
Kanamycin
p35S::EVN-GFP
13760 bp
10000
EVN
attB1
4000
35S
RB
8000
6000

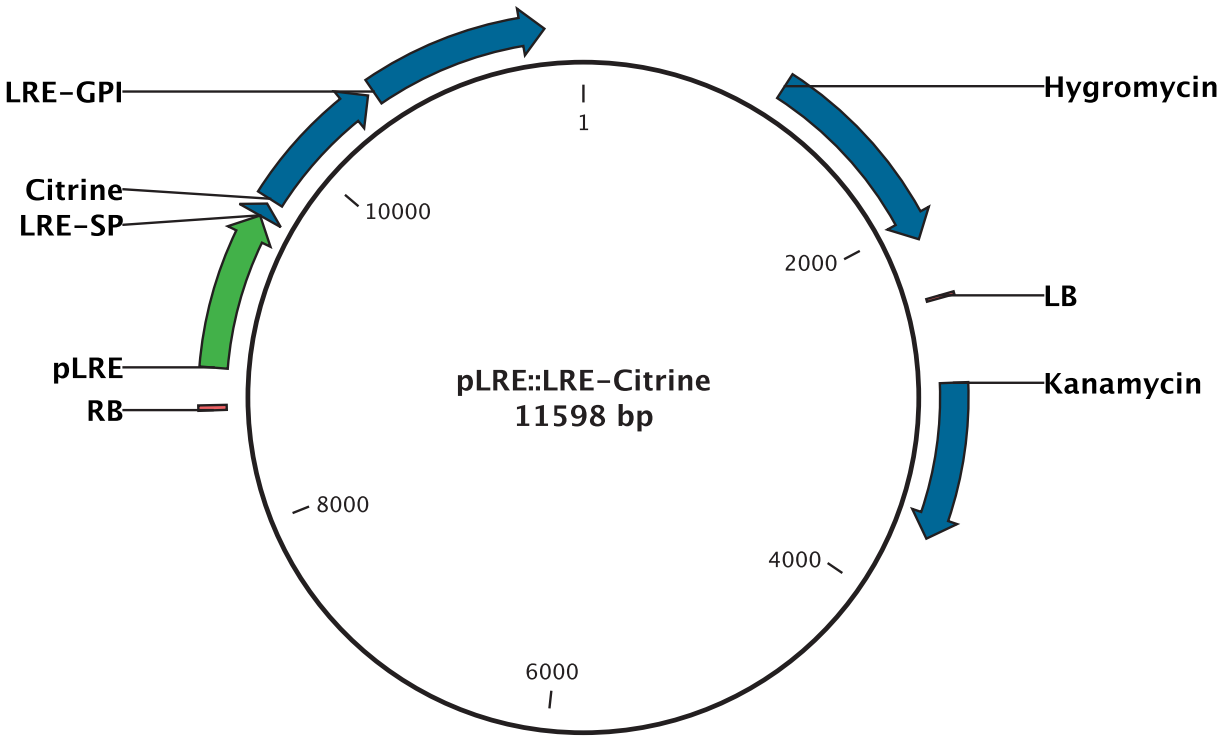
LRE-GPI
Citrine
LRE-SP
pLRE
RB
Hygromycin
LB
Kanamycin
1
2000
4000
6000
8000
10000
pLRE::LRE-Citrine
11598 bp

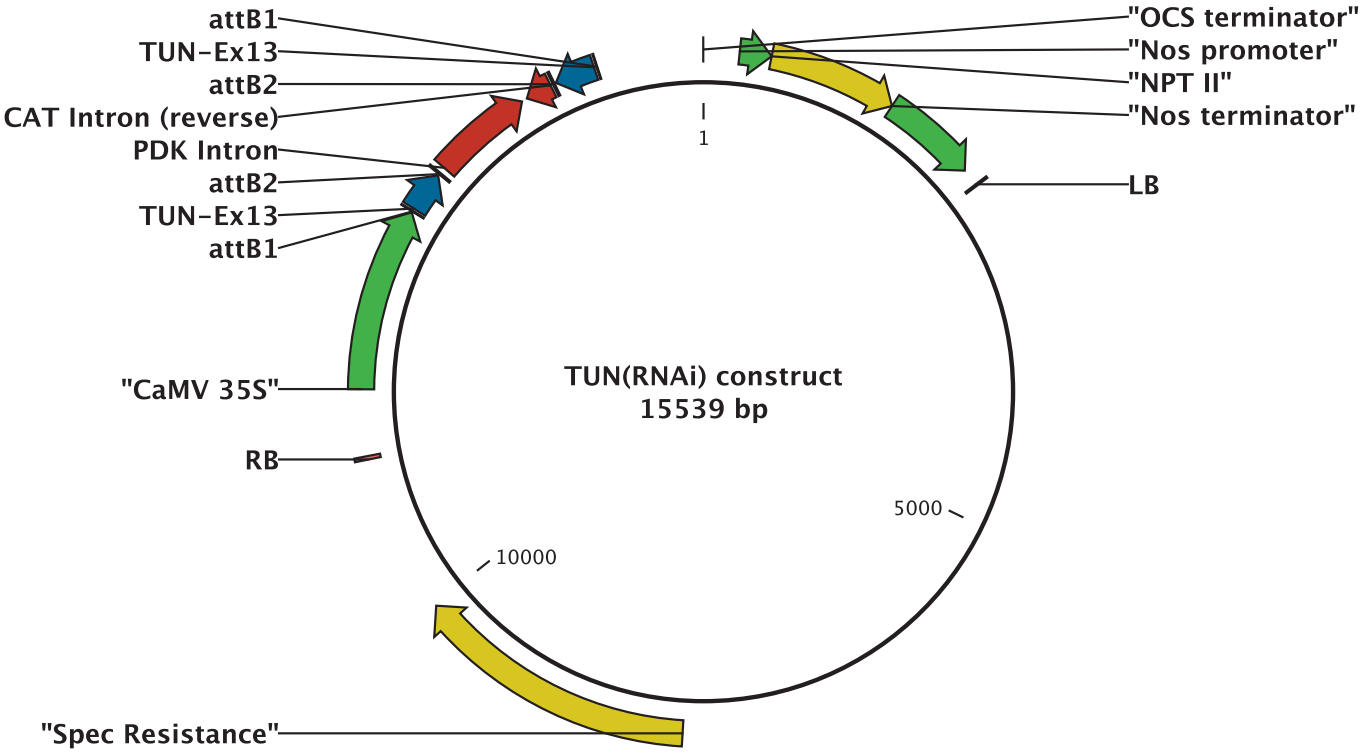
attB1
TUN-Ex13
attB2
CAT Intron (reverse)
PDK Intron
attB2
TUN-Ex13
attB1
"CaMV 35S"
RB
"Spec Resistance"
"OCS terminator"
"Nos promoter"
"NPT II"
"Nos terminator"
LB
1
5000
10000
TUN(RNAi) construct
15539 bp

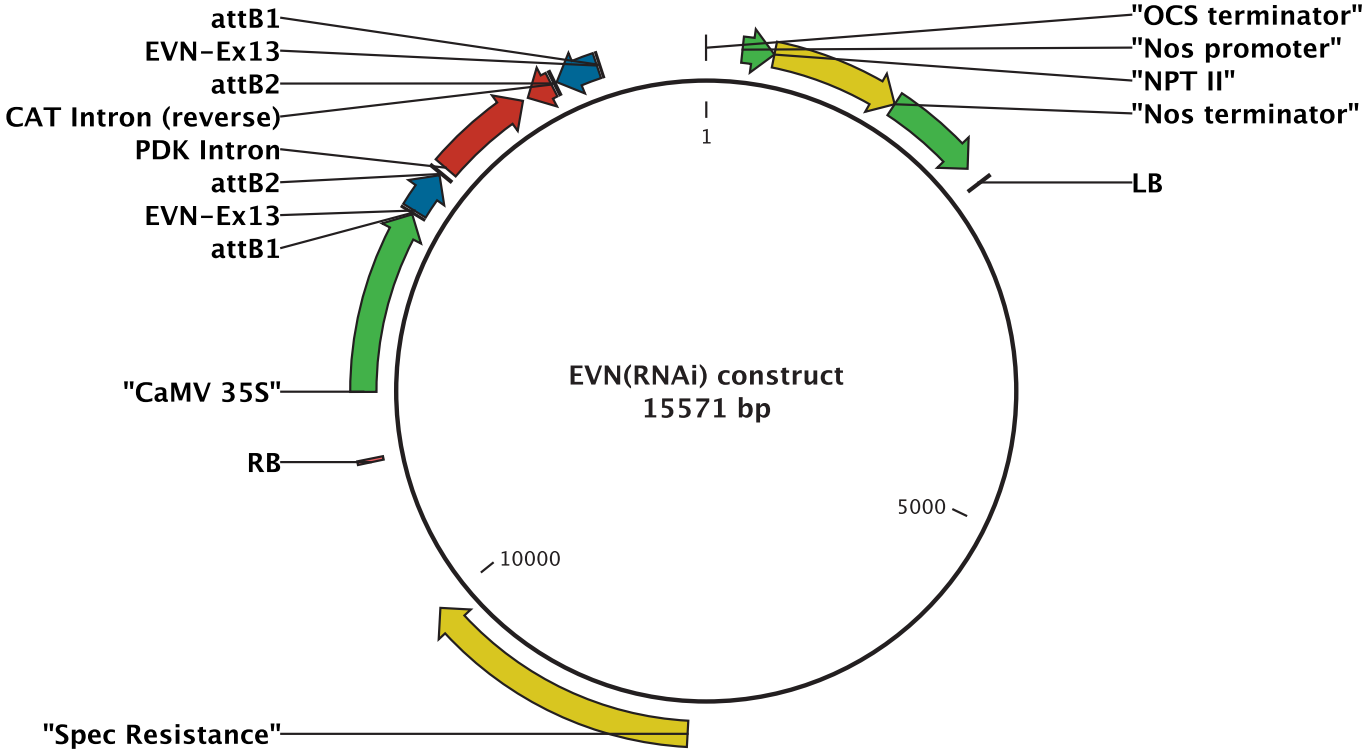
attB1
EVN-Ex13
attB2
CAT Intron (reverse)
PDK Intron
attB2
EVN-Ex13
attB1
"CaMV 35S"
RB
"Spec Resistance"
"OCS terminator"
"Nos promoter"
"NPT II"
"Nos terminator"
LB
1
5000
10000
EVN(RNAi) construct
15571 bp